

Research Programme of the Research Fund for Coal and Steel
Steel RTD

*Project carried out with a financial grant of the
Research Programme of the Research Fund for Coal and Steel*

Final Report

Technical Report No: 6

Period of Reference: 01/07/04 – 30/06/07

Technical Group: TGS8 “Steel products and applications for buildings, construction and industry”

ROBUSTNESS - Robust structures by joint ductility

Contract Number: RFS-CR-04046

Contractors: Institute of Structural Design, University of Stuttgart, Germany
Institute of Mechanics and Civil Engineering, M & S Department,
University of Liège, Belgium
Arcelor Profil Luxembourg S.A.-Research, Product Department
Structural, Luxembourg
PSP Technologies GmbH, Engineering Service Company,
Germany
Department of Mechanical and Structural Engineering, University
of Trento, Italy

Location: see separate list

Co-ordinator: Institute of Structural Design, University of Stuttgart, Germany

Authors: as given in the introductions

Commencement Date: 01/07/04

Completion Date: 30/06/07

Locations of the project partners:

Institute of Structural Design
Universität Stuttgart (USTUTT)
Pfaffenwaldring 7
70569 Stuttgart
Germany

Institute of Mechanics and Civil Engineering, M & S Department
University of Liège (ULg)
1 Chemin des Chevreuils
4000 Liège 1
Belgium

Arcelor Profil Luxembourg S.A.-Research
Product Department Structural
Rue de Luxembourg 66
4009 Esch-sur-Alzette
Luxembourg

PSP – Prof. Sedlacek & Partner (PSP)
Technologien im Bauwesen GmbH
Pauwelsstraße 19
52074 Aachen
Germany

Department of Mechanical and Structural Engineering
Università degli Studi di Trento (UNITRENTO)
Via Mesiano 77
38050 Trento
Italy

DISTRIBUTION LIST

Members of the technical group TGS8:

CM	LG. CAJOT	Arcelor Profil Luxembourg S.A.
----	-----------	--------------------------------

Reimbursed:

A. KÄHÖNEN	OUTOKUMPU, Sverige
------------	--------------------

A. KARAMANOS	MSRS, Greece
--------------	--------------

A. KLIMPEL	SUT, Poland
------------	-------------

J. KOUHI	FCSA, Finland
----------	---------------

J.K. KRISTENSEN	FORCE, Denmark
-----------------	----------------

H. LINGER	BOEHLER, Austria
-----------	------------------

J. ORDIERES MERE	UNIV RIOJA, Spain
------------------	-------------------

W. SALVATORE	UNIV PISA, Italia
--------------	-------------------

G. SEDLACEK	RWTH, Germany
-------------	---------------

Not reimbursed:

A. BANNISTER	CORUS UK, United Kingdom
--------------	--------------------------

T. BRAINE-BONNAIRE	ARCELOR, France
--------------------	-----------------

G. DEMOFONTI	CSM, Italia
--------------	-------------

A. FERNANDES	UNIV PORTO, Portugal
--------------	----------------------

TABLE OF CONTENTS

	Page
1 Introduction	21
2 Systematic analysis of existing data	23
2.1 General	23
2.2 Basic guiding principles to robustness and common work	24
2.2.1 Preventing the progressive collapse: the strategies	24
2.2.2 Structural robustness and codes	25
2.2.3 The European approach to robustness	25
2.2.4 Ductility: a strategy to achieve robustness	28
2.2.5 Beam-to-column joint modelling: the component method	29
2.3 Database overview	30
2.4 Conclusions	32
3 Concepts and strategies	33
3.1 General	33
3.2 Different strategies to achieve robustness	34
3.3 Investigations on the event “Loss of a column”	36
3.4 Investigations on the event “Loss of a bracing”	38
3.5 Investigation on the event “Fire”	39
3.6 Investigation on the event “Earthquake”	40
3.7 Conclusions	41
4 Experiments and evaluation	42
4.1 General	42
4.2 Concept in view of the event “Loss of a column”	43
4.3 Substructure test	43
4.3.1 General	43
4.3.2 Design of an “actual” composite building according to Eurocode 4 recommendations	44
4.3.2.1 Introduction	44
4.3.2.2 Design of the structural members	44
4.3.2.3 Design of the structural joints subjected to hogging bending moments	45
4.3.2.4 Verification of the internal main frame modelled with the predicted joint properties	47
4.3.2.5 Conclusions	48
4.3.3 Extracted substructure tested at Liège University	48
4.3.3.1 Introduction	48
4.3.3.2 Substructure geometric layout	49
4.3.3.3 Reinforcement and stud layouts of the substructure	49
4.3.3.4 Joint and column base configurations within the substructure	50
4.3.3.5 Simulation of the lateral restraint during the test	50
4.3.3.6 Conclusions	51
4.3.4 Substructure test results	52
4.3.4.1 Introduction	52
4.3.4.2 Characterisation of the constitutive materials	52
4.3.4.3 Geometrical measurements	53
4.3.4.4 Description of the load path during the test	53
4.3.4.5 Test equipments	54
4.3.4.6 Substructure test results	56
4.3.5 Conclusions	62

4.4	Joint tests	62
4.4.1	General	62
4.4.2	Composite joint tests	63
4.4.2.1	General	63
4.4.2.2	Design and dimensions of the joint test specimens	64
4.4.2.3	Test setup	65
4.4.2.4	Material characteristics	65
4.4.2.5	Properties of the joints	66
4.4.2.6	Results of the joints under pure bending exposure	67
4.4.2.7	Results of the M-N-interaction	69
4.4.2.8	Conclusions	73
4.4.3	Steel joint tests	73
4.4.3.1	General	73
4.4.3.2	Design and dimensions of the steel joint test specimens	74
4.4.3.3	Test setup	74
4.4.3.4	Material characteristics	75
4.4.3.5	Test results	75
4.4.3.6	Evaluation of the test results	79
4.4.3.7	Conclusions	81
4.5	Component tests	82
4.5.1	General	82
4.5.2	Experimental study on concrete specimens	82
4.5.2.1	General	82
4.5.2.2	Layout of the specimens	83
4.5.2.3	The tests	84
4.5.2.4	Material properties	85
4.5.2.5	Test results	85
4.5.2.6	Tension stiffening effect	88
4.5.2.7	Conclusions	89
4.5.3	Experimental tests on T-stubs	90
4.5.3.1	General	90
4.5.3.2	Layout of the specimen	90
4.5.3.3	T-stub tests under tension	91
4.5.3.4	T-stub tests under axial and shear force	92
4.5.3.5	Material properties	92
4.5.3.6	Test results of the tension tests	93
4.5.3.7	Test results of the tests under tension and shear force	94
4.5.3.8	Conclusions	95
4.5.4	Test on the connection	96
4.5.4.1	General	96
4.5.4.2	Layout of the specimens	97
4.5.4.3	The tests	97
4.5.4.4	Test results	98
4.5.4.5	Conclusions	100
4.6	Summary and conclusions of the experimental results	101
5	Numerical and analytical studies	103
5.1	General	103
5.2	Validation of the numerical tools	103
5.2.1	Introduction	103
5.2.2	Validation of FINELG with the experimental tests	103
5.2.3	Benchmarking of other software - loss of a column	105
5.2.3.1	General	105
5.2.3.2	Description of the structure benchmark model 3	105
5.2.3.3	Results	105
5.2.4	Benchmarking of other software - loss of a bracing	106
5.2.4.1	General	106
5.2.4.2	Description of the structure benchmark model 2	106
5.2.4.3	Results	106
5.2.5	Conclusions	107

5.3	Investigations on the event “Loss of a column”	107
5.3.1	Introduction	107
5.3.2	Numerical studies of 2D and 3D structures	108
5.3.2.1	Introduction	108
5.3.2.2	Investigations on a 2D-system	108
5.3.2.3	Investigation on a 3D-system	114
5.3.3	Numerical studies of the simplified substructure	117
5.3.3.1	General	117
5.3.3.2	Validation of the simplified substructure modelling	119
5.3.3.3	Parametrical studies on the simplified substructure	122
5.3.4	Development of analytical methods to predict the development of the membrane forces	127
5.3.4.1	Introduction	127
5.3.4.2	Analytical prediction of the M-N interaction resistance curve of composite joints	127
5.3.4.3	Analytical procedure to predict the development of the membrane forces in a structure	133
5.3.4.4	Conclusions	134
5.4	Investigations on the event “Loss of a bracing”	134
5.4.1	General	134
5.4.2	Dimensions and properties of the car park frame	135
5.4.3	Applied loads at the car park	136
5.4.4	Procedure of the numerical simulation	137
5.4.5	Numerical simulations for “Loss of a bracing”	138
5.4.5.1	Calculation of the undamaged frame structure	138
5.4.5.2	Calculation for “Loss of a bracing”	138
5.4.6	Further parametrical studies for the car park frame	140
5.4.6.1	Introduction	140
5.4.6.2	Examination of the car park as pure sway-frame	140
5.4.6.3	Examination of different joint characteristics for the car park frame	142
5.4.6.4	Examination of the size of the column profile	143
5.4.7	Conclusions	143
5.5	Investigation on the event “Fire”	143
5.6	Investigation on the event “Earthquake”	145
6	<i>Design requirements and design criteria</i>	147
6.1	General	147
6.2	Conclusions for the event “Loss of a column”	148
6.3	Conclusions for the event “Loss of a bracing”	149
6.4	Conclusions for the event “Fire”	150
6.5	Conclusions for the event “Earthquake”	151
7	<i>Summary</i>	154
8	<i>Outlook</i>	158

ABSTRACT

In view of recent disasters and their immense economical and human consequences more and more focus is given not only on the safety of structures - to reduce the risk for the life of people by collapse even under exceptional loading – but on minimizing the disastrous results and to enable a quick rebuilding and reuse. One crucial mean to achieve this aim is the design of redundant robust structures. Robustness prevents the collapse of the total structure when only parts of the structure are damaged or destroyed. To avoid progressive failure, redundant structures with inherent sufficient ductile behaviour allowing deformations when a local failure occurs, have to be built. Redundancy can be achieved by allowing force redistribution within a structural system. Therefore the single sections and joints have to be especially designed and optimized, not necessarily requiring additional fabrication costs. But until now no specific rules for robustness by ductile joints exist. The aim of the present project is to define general requirements for ductile joints as part of a structural system subjected to exceptional unforeseen loading.

FINAL SUMMARY

Objectives of the project

The objective of this project is to encourage and to promote the wider use of composite and steel frames by increasing the robustness of structures. This will be achieved by using the inherent advantage of steel, designing especially highly ductile structures. The four main objectives of robust design may be summarized:

- Prevent progressive failure caused by local damage
- Reduce risk of life by collapse under exceptional loads
- Minimise disastrous results
- Enable quick rebuilding and reuse

A progressive failure of the whole structure can be prevented by robust design. Robustness ensures structural safety by preventing the collapse of the total structure when only one part of the structure is damaged or destroyed. This can be achieved by enabling the joints to provide large rotations, so that membrane forces can be activated allowing a redistribution of internal forces. Thus an adaptive structure is created which keeps sufficient strength even under exceptional loading and large deformations. By increasing deformations joints are subjected to increased tensile forces, while bending moment exposure of the joints decreases or is even inversed. Within the research project various experimental investigations are made on the behaviour of the joints under large deformations and combined loading of bending and tension, including a full scale test of a substructure, a number of joint tests and numerous component tests. To derive robustness requirements, different structural systems subjected to exceptional events are numerically investigated in order to see how the structures work when part of the structure is destroyed as well as how and how far redistribution takes place. So the project aim has been creating redundant structures allowing for moment and force redistribution

- by defining requirements for ductile joints and sections
- by developing new ductile joint solutions

Comparison of initially planned activities and work accomplished

The work of this project closely followed the original work plan and the distribution of work according to the different work packages was kept. The partners made only minor adjustments in order to better achieve the objectives of the project with regard to the numerical investigations. The following adjustments were thoroughly discussed and agreed on during the coordination meetings:

The Work Package 2 “Requirements” has been recognized as key for directing the project. So all the other activities refer to the aims defined by Work Package 2 and have oriented their investigations in order to derive the necessary requirements at least for a certain choice of structural systems. Thus the decision was to prolong that WP for the whole project runtime.

As it was recognized that there were not just two types of calculations “simplified and sophisticated” system calculations, but a cascade of different levels of sophistication already at an early stage the decision was taken to merge Work Package 3 and Work Package 6 due to the close interrelation. So also in this report the work packages are presented as one unit leading to conclusions which at the end allowed us to develop more detailed design criteria.

Description of activities and discussion

During the project runtime extensive investigations were carried out and presented to the partners at the six coordination meetings for discussion. The intermediate results were reported regularly in the

technical reports. It should be mentioned that nearly all partners had the opportunity to attend the experimental substructure test which was carried out at University of Liège in September 2006.

An Access database has been created which collects and analysis literature regarding the questions of accidents, exceptional loading, progressive collapse, requirements. This will serve also for future research and discussion.

Extensive experimental investigations on the behaviour of joint ductility and resistance as well as on the behaviour of numerous components (steel, concrete and composite) were carried out to be able to define requirements for robust design. Thereby a data bank is created the relevance of which goes far beyond the single aims of this project but may form the preformed basis of future efficient and robust joint design.

Further on an additional highlight should be mentioned: The experiments on components, joints and the substructure have been organised in a very consequent way to allow already experimentally building a full chain of recognitions: The same material, the same components, the same loadings were applied, so that the results of all single tests strongly support each other.

The aim of investigations presented here is not so much that it allows already to list design criteria in general for all events and cases which may be thought of but that for a choice of events and especially for the event “Loss of a column” as a prototype an in-depth strategy has been developed and realized up to practical design requirements that now may be followed by similar investigations on further events that are characteristic for exceptional scenarios. The concept or strategy developed with this project may thus serve as model guide.

Conclusions

This section summarises in short the conclusions which have been drawn at the end of each main chapter.

Firstly the investigations for the exceptional event “Loss of a column” are addressed. An extensive experimental test program including a substructure test, a number of joint tests and numerous component tests which have been based on each other were performed by different partners. All tests were successfully finalized. In the substructure test it was possible to observe the development of the catenary action within the frame and its effects on the joints. In particular, a very good ductility of the joints was achieved with a maximum observed rotation of 190 mrad. The composite joint tests aimed on the characterization of the behaviour of these joints under sagging and hogging bending moment with and without tension force and to obtain the M-N-interaction resistance curve. The steel joint tests aimed at the investigation of the membrane effect in the endplate depending on the endplate thickness and the bolt arrangement. The joint tests confirmed the findings of the substructure test, e.g. the very good ductility of the joints. In particular it was demonstrated that only ductile components were activated to pass from the behaviour under pure bending to the behaviour under pure tensile load. The component tests analyzed each component which was part of the substructure and the joint configuration. These tests gave information about the influence of each component on the global behaviour of the joint and, in particular, the component tests highlighted the effects of the development of the membrane forces within the components in bending or the highly ductile tension bar in the concrete slab. General criteria, derived from the experimental tests, to improve the deformation capacity of single components are given in § 4.6.

The experimental tests had an additional task by validating the numerical tools. Numerical investigations were performed on the tested substructure in order to compare the numerical prediction to the experimental results. From this comparison, the difficulty to model the actual behaviour of joints subjected to combined bending moments and axial loads was illustrated. However, it was shown that it is possible to model the behaviour of the joints with equivalent double-T beams if the developed membrane forces within the structure are not too important.

Furthermore the numerical simulations for the event “Loss of a column” included a benchmark study at a steel frame building to validate the different softwares used by different partners involved in the numerical calculations. The results of the different softwares were in good agreement and in the following numerical analyses for 2D and 3D structure have been performed including extensive parametrical studies which subsequently permitted to observe the redistribution of the loads within the

structure and to have an idea on the requested ductility as a consequence of the event “Loss of a column” at the structural element level. Besides the numerical simulations have contributed to develop, simplified analytical methods to predict the response of a framed structure caused by the “Loss of a column”. Through 2D numerical analyses, it was shown that it is possible to simulate very accurately the response of a structure through the proposed substructure. In addition, parametrical studies on the substructure were conducted so as to identify the parameters to be included in the developed analytical procedures. The developed analytical procedure is able to estimate the M-N interaction resistance curve of composite joints. Through comparisons to the results of the experimental test performed on the substructure composite joint in isolation, it was shown that the developed method permits to obtain a very accurate prediction of the composite joint behaviour when subjected to combined bending moments and tensile loads. With the so-obtained substructure response, it is then possible, knowing the maximum concentrated load Q to be supported by the system (what is possible with the analytical procedures presented in the PhD thesis of Luu Nguyen Nam Hai [88]), to predict the maximum vertical displacement associated to the considered column loss (as illustrated in Figure 6-2) and, as a result, the requested rotation capacity at the joint level. This analytical procedure is also included in more details in the design handbook [34].

Secondly investigations for the event “Loss of a bracing in a car park” have been carried out. These investigations were limited to numerical simulations only. At first a benchmark study was performed to validate the different softwares of the different partners and the results of the various softwares corresponded very well. Next the “Loss of a diagonal bracing” in the bottom storey was simulated at a 2D composite framed structure with partial-strength joints. Afterwards parametrical studies were executed to investigate the influence of joint characteristics and properties of the structural members to the collapse resistance and to the redistribution behaviour within the structure. An important finding of these numerical calculations was that the collapse resistance of the car park frame was decisively depending on the bearing capacity of the chosen column profile. The remaining stiff panel effect of the undamaged bracings in the upper storeys still provides a frame effect and in addition the moment resistance of the semi-rigid joints also creates a moment resisting frame where the resulting rotation requirements for the joints are not extremely high. A crucial aim of the numerical simulations was in addition to determine requirements for the joints which allow for redistributions of loads within the structure when “Loss of a bracing” occurs and avoid premature joint failure. First minimum requirements for the joints concerning the ductility have been determined by the numerical studies and are presented in the corresponding chapter.

For the event “Fire” two states have to be differentiated. On one hand localised fire influences only local structural members leading to local failure of members like loss of a column or a bracing. So the local fire may be translated e.g. to the event “Loss of a column” or “Loss of a bracing”. This has been shown for a given example. At the other hand a fully engulfed fire is no more a problem of robustness of structure but a problem of global fire resistance of the building which has to be designed in an independent “hot” design.

For the exceptional event “Earthquake” investigations were concentrated to collect and to check the most important codes and standards worldwide concerning provisions ensuring a structural ductile behaviour. Thereby main focus was given to connection requirements of steel as well as of concrete structures. But it have to kept in mind that the different nature of the actions associated with seismic events or an accidental actions and the consequent different structural behaviour doesn’t allow the extension of the available seismic detailing rules also to robustness without further studies. Certainly, the rules provided by seismic codes may be an interesting reference because the knowledge in seismic design is built up of decades of research in basic principals.

Exploitation and impact of the research results

As a result of the research work first basics in the field of robustness have been developed. By summarizing the state-of-the-art concerning robustness strategies implemented in standards all over the world a large data base has been installed. The numerical and experimental work results in first design requirements which have to be provided by the structural members and joints. So possible improvements could be pointed out. Meanwhile within Europe and other parts of the world an intensive discussion on “ROBUSTNESS” has started. Two COST initiatives COST C26 “Urban Habitat Constructions under catastrophic Events” which deals with exceptional loading and COST TU06001

“Robustness” which deals with robustness including the aspects of safety and reliability have recently started. The members of this research group have brought the results of this project into these COST actions. The action underline the current need of investigations in this field. The advantage of the research done in this project is that it is application oriented and thus may direct the general discussion in a more practical direction aiming at the rules and recommendations which can be realized. As also codified rules are started to be developed in Europe (...Draft Model Code) as well as in USA and Canada it is of high importance to bring in the experience of this research work. As in this project the different national background of each partner how to apply and interpret Eurocode rules was brought together and general knowledge has been collected it will also facilitate the harmonisation and implementation of Eurocode rules. Especially the possibilities and restrictions of the new design provisions need to be highlighted with regard to the conceptual design of robust structures.

Within this project more than fifteen background documents were created which add substantial knowledge to the results presented in the Final Report. They are contained on the CD attached to the Final Report. During the project runtime doctoral, master and diploma thesis [7], [17], [35], [57], [85], [86], [88], [90], [104] have been successfully accomplished and the basis has been set for more to be finalised in the near future. System calculations have been thoroughly compared to each other on the basis of benchmark models and lead to a method of deriving parameters from one level of sophistication to another, in order to come to powerful simplified design equations.

- Within the frame of Cost C26 a contribution has been made to the Workshop in Prague in March 2007 presented in [26]. In addition several internal Cost presentations have supported the discussions.
- In the frame of Cost TU 0601 a presentation as well as paper [27] was given during the workshop in Zurich in February 2008.
- The discussion about robustness with US Experts was intensified during an internal workshop held in Liège in February 2007.
- Several papers are announced for future conferences e.g. Cost C26 Midterm conference in Malta in October 2008, Connections in Steel Structures [15], EUROSTEEL 2008 [16], PhD Symposium 2008 [28].
- Besides that, the following publications are in direct relation with this project: [1], [2], [3], [4] [13], [14], [18], [19], [20].

First ideas about a continuation and extension of the research work by a future European research project have been developed. Based on the concept applied in this project and on the results achieved further structures and scenarios have to be investigated. They may finally lead to the definition of a robustness index for any structure which allows the owner to decide on the level of safety and redundancy he wants to apply. The results of this project form the basis to quantify this level and build a precondition of such an innovative future approach.

List of figures

Figure 2-1: Design strategies for accidental load adopted by EN 1991-1-7.....	27
Figure 2-2: Horizontal ties to be adopted for consequences classes 2a and 2b.....	28
Figure 2-3: Component model for beam-to-column joint	29
Figure 2-4: Typical report for category ‘B’ documents [5].....	32
Figure 3-1: Specific local resistance.....	34
Figure 3-2: Alternate load path by redistribution of internal forces.....	34
Figure 3-3: Global strategy followed within this project	35
Figure 3-4: Loss of a column in a residential or office building frame.....	36

Figure 3-5: Development of the catenary action in the structure – illustration in an “applied load/beam deflection” curve.	36
Figure 3-6: Actual loading in the joint or in the beam end section until failure.....	36
Figure 3-7: Undamaged car park frame.....	38
Figure 3-8: Damaged frame structure.....	38
Figure 3-9: Procedure followed for the analysis of BM 2.....	38
Figure 3-10: Localised fire.....	39
Figure 3-11: Fully engulfed fire.....	39
Figure 4-1: Experiments form a unique chain.....	42
Figure 4-2: From the actual composite building to the tested substructure.....	43
Figure 4-3: 3D view of the designed building and representation of the main frames.....	44
Figure 4-4: Static scheme considered for the main frame design.....	44
Figure 4-5: Slab cross section.....	45
Figure 4-6: Composite beam cross section.....	45
Figure 4-7: Distribution of the studs along the composite beam length.....	45
Figure 4-8: External steel joint configuration.....	45
Figure 4-9: Geometrical properties of the end-plate.....	45
Figure 4-10: Internal composite joint configuration.....	46
Figure 4-11: Comparison of behavioural curves for different types of failure modes.....	47
Figure 4-12: Examples of considered load cases.....	48
Figure 4-13: Deformed shape at collapse and load multiplier-deflection curve obtained through the non-linear analysis.....	48
Figure 4-14: From the actual frame to the tested substructure.....	49
Figure 4-15: Reinforcement and stud layouts.....	50
Figure 4-16: Column support and hinge at the external joints.....	50
Figure 4-17: Lateral restraint influencing the catenary action.....	51
Figure 4-18: Possible positions of column loss for the computation of “K”.....	51
Figure 4-19: Symmetric response of the tested substructure.....	51
Figure 4-20: Detailed drawing of the substructure test configuration.....	51
Figure 4-21: Evolution of the concrete resistance in compression with time.....	52
Figure 4-22: Column at the middle simulated by two locked jacks.....	53
Figure 4-23: Application of a vertical load with two vertical jacks.....	54
Figure 4-24: Horizontal restraint simulated by horizontal hollow jacks.....	54
Figure 4-25: Displacement transducers.....	55
Figure 4-26: Rotational transducers.....	55
Figure 4-27: Strain gauges at the IPE140 bottom flange.....	55
Figure 4-28: Vertical load at the middle vs. vertical displacement curve.....	56
Figure 4-29: Accentuated cracks in the vicinity of the external composite joints at the formation of the beam plastic mechanism.....	56
Figure 4-30: Yielding of steel component at the external and internal composite joints.....	57

Figure 4-31: Concrete splitting at the internal composite joint	57
Figure 4-32: Horizontal displacement vs. horizontal load at the hollow jacks curves	57
Figure 4-33: Collapse of the longitudinal rebars in the vicinity of the external composite joints at point “D” of Figure 4.31	58
Figure 4-34: Yielding spread in the steel components of the external composite joints	58
Figure 4-35: State of the internal composite joint at point “D” of Figure 4-28	58
Figure 4-36: Deformation of the specimen at point “E” of Figure 4-28 and horizontal displacement of the specimen at point “E” of Figure 4-28	58
Figure 4-37: External composite joints at the end of the test	59
Figure 4-38: Internal composite joints at the end of the test	59
Figure 4-39: Cracks in the welds between the IPE140 profile and the end-plate	60
Figure 4-40: Rotation of the internal and external composite joints	60
Figure 4-41: Evolution of the stresses in the bottom flange at position A (see Figure 4-27)	61
Figure 4-42: Evolution of the stresses in the bottom flange at position B (see Figure 4-27)	61
Figure 4-43: Evolution of the stresses in the bottom flange at position C (see Figure 4-27)	61
Figure 4-44: Distribution of the cracks in the concrete slab	62
Figure 4-45: Stage I: Service conditions	63
Figure 4-46: Stage II: Column failure	63
Figure 4-47: Stage III: Membrane state	63
Figure 4-48: Steel beam IPE 140 with the arrangement of the shear studs	64
Figure 4-49: Cross-section	65
Figure 4-50: Layout of the test specimen	65
Figure 4-51: Load step 1 (corresponds to stage II Figure 4-46)	65
Figure 4-52: Load step 2 (corresponds to stage III Figure 4-47)	65
Figure 4-53: Geometrical properties of the endplate	66
Figure 4-54: Geometrical dimensions of the composite joint	66
Figure 4-55: Crack distribution in the distance of the stirrups	67
Figure 4-56: Two big cracks at the corner of the column profile	67
Figure 4-57: M-phi-curves for the “pure” joint rotation	68
Figure 4-58: Crack distribution and deformation behaviour for sagging moment	68
Figure 4-59: Crumbling of the concrete in column section	68
Figure 4-60: Bearing reactions for the first state of the loading procedure	69
Figure 4-61: Bearing reactions for the second state of the loading procedure(hogging)	69
Figure 4-62: Computed M-N-curves of the composite joint tests	69
Figure 4-63: Test specimen V1 after failure under M-N exposure (hogging)	70
Figure 4-64: Test specimen V4 after failure under M-N exposure (sagging)	71
Figure 4-65: Arrangement of strain gauges on rebars for test V1	71
Figure 4-66: Arrangement of strain gauges on IPE 140 for tests V1-V5	71
Figure 4-67: Stress Distribution V2 (Pos. A)	72
Figure 4-68: Stress Distribution V2 (Pos. B)	72

Figure 4-69: Stress Distribution V5 (Pos. A)	72
Figure 4-70: Stress Distribution V5 (Pos. B)	72
Figure 4-71: Unexpected brittle bolt failure in previous test conducted in Stuttgart [83].....	73
Figure 4-72: Overview of the test specimens S1- S6	74
Figure 4-73: View on the test setup.....	75
Figure 4-74: Development of the endplate deformation of test S1	76
Figure 4-75: Development of the endplate deformation of test S3	76
Figure 4-76: Development of the endplate deformation of test S4	76
Figure 4-77: Development of the endplate deformation of test S6	76
Figure 4-78: Moment-phi curves of S1-S4.....	78
Figure 4-79: Moment-phi curves of S1-S5-S6	78
Figure 4-80: Check of the rotation capacity and the component deformations of test S1	79
Figure 4-81: Check of the rotation capacity and the component deformations of test S4.....	79
Figure 4-82: Transducer arrangement of T-stub test 6bab	80
Figure 4-83: Measured curves of the T-stubs 6bab, 6bb, 6bc	80
Figure 4-84: validation of the numerical model	81
Figure 4-85: Comparison of deformed shape: experimental - numerical	81
Figure 4-86: Localisation of membrane effects within the endplate	81
Figure 4-87: Geometrical configuration for specimens RCSL (measures in mm).....	83
Figure 4-88: Geometrical configuration for specimens RCRR (measures in mm)	84
Figure 4-89: Transducers set-up for specimen RCSL	84
Figure 4-90: Transducers set-up for specimen RCRR.....	84
Figure 4-91: Results of the tensile tests on rebars.	85
Figure 4-92: Crack path for specimen RCSL	86
Figure 4-93: Crack path for specimen RCRR	86
Figure 4-94: Overall response of specimen RCSL5 (gage length 2687mm).....	87
Figure 4-95: Overall response of specimen RCRR1-2 (gage length 2175 mm).....	87
Figure 4-96: Transducers response (gage length 300 mm)	88
Figure 4-97: Effect of reinforcement ratio (gage length 2175 mm)	88
Figure 4-98: Comparison between concrete specimens and rebars depending on maximum strain of rebars	89
Figure 4-99: Comparison between concrete specimens and rebars depending on strength ratio of rebars	90
Figure 4-100: Joint configurations. (measures in mm).....	91
Figure 4-101: Typical transducers' set-up for tension tests on T-stubs.....	92
Figure 4-102: Testing apparatus and transducers' set-up for tests on T-stubs under axial and shear force.	92
Figure 4-103: Bolts' and flange deformations (on the left) and N-V domain (on the right) for column T-stub specimens of length 256mm.	95
Figure 4-104: Test on the complete joint – Initial beam-to-actuator angle of 20°	97

Figure 4-105: Test's results for end-plate T-stub on rigid support.....	98
Figure 4-106: Comparison between end-plate T-stub on column and on rigid support.....	98
Figure 4-107: Comparison between connection on rigid support and T-stub responses.....	99
Figure 4-108: Contour map at collapse for connection on rigid support.....	99
Figure 4-109: Comparison between connection on rigid support and on the column.....	100
Figure 5-1: Comparison of the M-N interaction curves – hogging moment	104
Figure 5-2: Comparison of the M-N interaction curves – sagging moment.....	104
Figure 5-3: Comparison between the numerical predictions and the experimental results	105
Figure 5-4: Comparison of collapse analysis of benchmark model 3	106
Figure 5-5: Comparison of collapse analysis of benchmark model 2	107
Figure 5-6: Denotation code of columns	108
Figure 5-7: M- ϕ interaction of loss a column C-0.....	111
Figure 5-8: M-N interaction of loss a column C-0	112
Figure 5-9: M-N interaction of loss a column C-0	113
Figure 5-10: 3-D structure and denotation	115
Figure 5-11: Top view on the collapsed structure (93 % of column failure C-0- γ simulated); illustrated with a deformation scale factor of 100.....	116
Figure 5-12: Middle frame of the global 3-D structure	116
Figure 5-13: Front view and top view of the reduced model of the beam 6 and beam 6.1.	117
Figure 5-14: Mises-stresses after the second step of the calculation (displacement + compression); illustrated with deformation scale factor 2	117
Figure 5-15: Distribution of the membrane forces developing in the directly affected part	118
Figure 5-16: Extracted subsystem	118
Figure 5-17: Global model	119
Figure 5-18: Affected beams of the global model.....	119
Figure 5-19: Simplified substructure.....	119
Figure 5-20: Global model	120
Figure 5-21: Spring force-displacement curves.....	120
Figure 5-22: Simplification of the spring behaviour	120
Figure 5-23: Loads of the upper and the lower column during collapse simulation	121
Figure 5-24: Resulting loads acting on the substructure	121
Figure 5-25: Deformation of the global model and the substructure.....	122
Figure 5-26: The eleven levels of the parametric study	124
Figure 5-27: Variation of K – Results for “Level 1” subsystem – Mid-span deflection vs. applied load curve	126
Figure 5-28: Variation of A – Results for “Level 1” subsystem with K = 3000kN/m– Mid-span deflection vs. applied load c	126
Figure 5-29: Variation of I – Results for “Level 9” subsystem with K = 3000kN/m– Mid-span deflection vs. applied load curve.....	126
Figure 5-30: Comparison between the analytical prediction and the experimental results – hogging moment.....	129

Figure 5-31: Deformation of the end-plate and the column flange at the end of the bending test	129
Figure 5-32 Comparison between the component method prediction and the experimental test result	130
Figure 5-33 Comparison between the component method prediction and the experimental test result	131
Figure 5-34 Comparison of the resistance interaction curves	131
Figure 5-35 Distribution of the loads within the bolt rows at point A and point E of Figure 114	132
Figure 5-36 Substructure to be investigated and definition of the main parameters	133
Figure 5-37 Comparison between the analytical predictions and the experimental result	134
Figure 5-38: Main dimensions and loads of the main frame	135
Figure 5-39: Main dimension of the structure in transversal direction	135
Figure 5-40: Cross-sections of the members	135
Figure 5-41: Cross-section of the composite beam over total length	135
Figure 5-42: Dead Load	136
Figure 5-43: Wind Load	136
Figure 5-44: Calculation of the fully functional structure	137
Figure 5-45: Calculation of the damaged structure	137
Figure 5-46: Analysis of the limit load factors of the damaged system (horizontal load)	138
Figure 5-47: Analysis of the limit load factors of the damaged system (vertical load).....	138
Figure 5-48: Comparison of the normal force diagram in the columns (damaged system)	139
Figure 5-49: Comparison of the M-N-interaction in the columns (damaged system).....	139
Figure 5-50: Location of the calculated Φ_j in Table 5-10	140
Figure 5-51: Required joint rotation inner composite joint.....	140
Figure 5-52: Required joint rotation external steel joint	140
Figure 5-53: Joint rotations extract of a composite sway-frame with partial-strength joints	141
Figure 5-54: Moment distribution extract of a composite sway-frame with partial-strength joints.....	141
Figure 5-55: Development of plastic panel mechanism of sway frames with semi-rigid joints	142
Figure 5-56: Influence of the capacity M_{pl} of the joint to the limit load factor	142
Figure 5-57: Influence of the capacity M_{pl} of the joint to the limit load factor	142
Figure 5-58: Influence of the column profile to the limit load factor.....	143
Figure 5-59: Transpolis-General view.....	144
Figure 5-60: Transpolis-Detail	144
Figure 5-61: Thermal analysis - Beam HD400x314	144
Figure 5-62: Thermal analysis - Column HD400x551	144
Figure 5-63: Loading of the structure (Transpolis).....	144
Figure 5-64: Geometry of the structural system.....	145
Figure 5-65: Deformation of the Structure after 1920 seconds of fire	145
Figure 5-66: Deformation of the structure after 7200 seconds of fire.....	145
Figure 5-67: Vertical displacement of the node	145
Figure 6-1: Determination of required and available joint rotation e.g. for loss of a column	147

Figure 6-2 Analytical prediction of the simplified subsystem response and determination of the maximum deflection associated to the maximum load to be supported.....	149
Figure 6-3: Fully engulfed fire	151
Figure 6-4: Localised fire	151
Figure 6-5: Detailing rules for seismic rebars in interior and exterior joints	152
Figure 6-6: Coupling beam framing into a wall (on the left) and beam-to-column connection (on the right).....	153

List of tables

Table 4-1: Mechanical properties of the external steel joints.....	46
Table 4-2: Mechanical properties of the internal composite joints	46
Table 4-3: Bearing capacities of the joints (hogging moment) acc. EC 4 Part 1-1	66
Table 4-4: Bearing capacities of the joints (sagging moment) acc. EC 4 Part 1-1	67
Table 4-5: Overview about the bearing capacity of the steel joints tests	77
Table 4-6: Comparison of the bearing capacities and rotations of the joints S1-S5-S6	78
Table 4-7: Comparison of the bearing capacities and deformations of the T-stub tests 6bab-6bb-6bc ..	80
Table 4-8: Test results for reinforced concrete specimens	86
Table 4-9: Comparison between deformation capacities of concrete specimens and of bare rebars.	88
Table 4-10: Test results for the CS joint.	93
Table 4-11: Test results for the SJ joints.....	94
Table 4-12: Test's results for column T-stub specimens under axial and shear force.....	96
Table 4-13: Test's results for the connection on rigid support.....	99
Table 4-14: Test's results for the complete joints.	100
Table 4-15: Requirements for joint components to ensure a ductile joint behaviour.....	102
Table 5-1: "Collapse" factor.....	109
Table 5-2: Load case combinations.....	113
Table 5-3: Internal loads and deformations under different loads when the simulation of loss of column C-0 was completed.	114
Table 5-4: Main properties of the studied levels	125
Table 5-5: Key values obtained experimentally and through the new prediction approach.....	129
Table 5-6: Key values obtained experimentally and through the new prediction approach.....	130
Table 5-7: Resistance of the composite beams and composite joints.....	136
Table 5-8: Comparison of the limit load factors of the undamaged system.....	138
Table 5-9: Comparison of the limit load factors of the damaged system.....	139
Table 5-10: Joint rotations at the inner and external joints just before collapse of the frame	139

List of references

Own references (as outcome of the project)

- [1] BALDASSINO, N., ZANDONINI, R.: Experimental Study on the Behaviour of Steel and Concrete Joint Components in Large Displacement Field, Proceedings of the 2AESE 2007-

- Second International Conference on Advances in Experimental Structural Engineering, Vol. 1, Shanghai, China, 4-6 December, Tongji University, pp. 73-81, 2007.
- [2] BALDASSINO, N., ZANDONINI, R.: Component Tests for Characterisation of Composite Steel-Concrete Joints, Proceedings of the SEMC 2007-Recent Developments in Structural Engineering, Mechanics and Computations, vol. 1, Cape Town, South Africa, 10-12 September, Millpress Science Publishers, pp. 1127-1132, 2007.
- [3] BALDASSINO, N., SEEMA, ZANDONINI, R.: Alcune Considerazioni sulla Robustezza Strutturale. Atti XXI Congresso C.T.A., Catania, Italia, 1-3 Ottobre 2007, Dario Flaccovio Editore, pp. 17-24, 2007.
- [4] BALDASSINO, N., ZANDONINI, R.: Comportamento di collegamenti in strutture composte soggette a carichi eccezionali, Atti del convegno Sperimentazione su materiali e strutture, Venezia, Italia, 6-7 dicembre, Dca-IUAV, pp. 337-346, 2006.
- [5] BALDASSINO, N., SEEMA, ZANDONINI, R.: Database on Robust Systems, Document N°: Robustness - Report - TRENTO - 001- June 2007
- [6] BALDASSINO, N., ZANDONINI, R.: Experimental Tests on Steel and Concrete Beam-to-Column Joint Components, Internal report for the RFCS project RFS-CR-04046 “Robust structures by joint ductility”, Document N°:ROBUSTNESS-Report-TRENTO-002, University of Trento, 2007.
- [7] CORSI, S.: Giunti trave-colonna in acciaio in grandi spostamenti, Master Thesis, in Italian, Università degli Studi di Trento, 2006.
- [8] DEMONCEAU, J.F.; JASPART J.P.: Predesign of the substructure to be tested at the University of Liège. Internal report for the RFCS project RFS-CR-04046 “Robust structures by joint ductility”, Document N°:ROBUSTNESS-Report-ULg-001, Liège University, January 2006
- [9] DEMONCEAU, J.F.; JASPART J.P.: From the actual composite building to the tested substructure. Internal report for the RFCS project RFS-CR-04046 “Robust structures by joint ductility”, Document N°:ROBUSTNESS-Report-ULg-002, Liège University, January 2006
- [10] DEMONCEAU, J.F.; JASPART J.P.: Loss of a column in an office or residential building frame – First investigations of the steel “two-beams” system. Internal report for the RFCS project RFS-CR-04046 “Robust structures by joint ductility”, Document N°:ROBUSTNESS-Report-ULg-003, Liège University, May 2006
- [11] DEMONCEAU, J.F.; JASPART J.P.: Experimental test simulating the loss of a column in a composite building – Liège University. Internal report for the RFCS project RFS-CR-04046 “Robust structures by joint ductility”, Document N°:ROBUSTNESS-Report-ULg-004, Liège University, September 2006
- [12] DEMONCEAU, J.F.; JASPART, J.P.: Detailed drawings of the substructure to be tested in Liège. Internal report for the RFCS project RFS-CR-04046 “Robust structures by joint ductility”, Document N°:ROBUSTNESS-Report-ULg-005, Liège University, January 2006
- [13] DEMONCEAU, J.F.; LUU, H.N.N.; JASPART, J.P.: Recent investigations on the behaviour of buildings after the loss of a column, ICMS conference, Poiana Brasov, September 20 – 22, 2006.
- [14] DEMONCEAU, J.F.; JASPART, J.P.: Experimental investigations on the behaviour of a composite frame after the loss of a column, ICSAS 2007, 6th International Conference on Steel and Aluminium Structures, Oxford, July 24 – 27, 2007.
- [15] DEMONCEAU, J.F.; JASPART, J.P.: Robustness of structures – behaviour of composite joints, International Workshop on Connections in Steel Structures 2008, Chicago, 23 – 25 June 2008 (Abstract accepted)
- [16] DEMONCEAU, J.F.; JASPART, J.P.: Development of membrane effects in frame beams: experimental and analytical investigations, EUROSTEEL 2008 “5th International conference on Steel and Composite Structures”, 3 – 5 September 2008 (Abstract accepted).

-
- [17] HOIER, A.: Modellierung eines geschraubten Stahlknotenanschlusses mit Finiten Elementen. Diploma Thesis, Universität Stuttgart, Mitteilung des Instituts für Konstruktion und Entwurf Nr. 2007-8X, 2007 (in German)
- [18] JASPART, J.P.; DEMONCEAU, J.F.; LUU, H.N.N.: Numerical, analytical and experimental investigations on the response of steel and composite buildings further the loss of a column, Colloquium on structural design of constructions subjected to exceptional or accidental actions, Brussels, Belgium, 9 April 2008.
- [19] JASPART, J.P.; DEMONCEAU, J.F.: Contribution to the derivation of robustness requirements for steel and composite structures, ICASS 2007 “Advances in steel structures”, 5 – 7 December 2007, Singapore.
- [20] KUHLMANN, U.; JASPART, J.-P.; VASSART, O.; WEYNAND, K.; ZANDONINI, R.: Robust structures by joint ductility. Proceedings of IABSE Symposium Budapest 2006, Vol. 92, 2006
- [21] KUHLMANN, U.; RÖLLE, L.: Experimental tests on composite joints with biaxial loading –test results. Internal report for the RFCS project RFS-CR-04046 “Robust structures by joint ductility”, Document N°: ROBUSTNESS-Report-USTUTT-001, 2007
- [22] KUHLMANN, U.; RÖLLE, L.: Evaluation of the experimental tests on composite joints under biaxial loading. Internal report for the RFCS project RFS-CR-04046 “Robust structures by joint ductility”, Document N°: ROBUSTNESS-Report-USTUTT-002, 2007
- [23] KUHLMANN, U.; RÖLLE, L.: Experimental tests on steel joints and evaluation of the test results. Internal report for the RFCS project RFS-CR-04046 “Robust structures by joint ductility”, Document N°: ROBUSTNESS-Report-USTUTT-003, 2007
- [24] KUHLMANN, U.; RÖLLE, L.: Numerical Simulation of the event “Loss of a bracing in a car park”. Internal report for the RFCS project RFS-CR-04046 “Robust structures by joint ductility”, Document N°: ROBUSTNESS-Report-USTUTT-004, 2007
- [25] KUHLMANN, U.; RÖLLE, L.: Numerical investigations for benchmark model 1 “Loss of a column in an office building”. Internal report for the RFCS project RFS-CR-04046 “Robust structures by joint ductility”, Document N°: ROBUSTNESS-Report-USTUTT-005, 2007
- [26] KUHLMANN, U.; RÖLLE, L.; JASPART, J.-P.; DEMONCEAU, J.-F.: Robustness-Robust structures by joint ductility. Proceedings of COST C 26 Workshop Prague, 2007
- [27] KUHLMANN, U.; RÖLLE, L.: Redundant and Robust Frame Structures by Joint Ductility. COST TU 0601 Workshop Zurich, February 2008
- [28] RÖLLE, L.: Redundant and Robust Frame Structures by Joint Ductility. 7th fib International PhD Symposium in Civil Engineering Stuttgart, September 2008 (Abstract accepted)
- [29] ROBUSTNESS/ALL-01: RFS-CR-04046 Six-monthly technical report. Reporting period 07/2004-12/2004.
- [30] ROBUSTNESS/ALL-02: RFS-CR-04046. Six-monthly technical report. Reporting period 01/2005-06/2005.
- [31] ROBUSTNESS/ALL-03: RFS-CR-04046. Mid-term technical report. Reporting period 07/2005-12/2005.
- [32] ROBUSTNESS/ALL-04: RFS-CR-04046. Six-monthly technical report. Reporting period 01/2006-06/2006.
- [33] ROBUSTNESS/ALL-05: RFS-CR-04046. Six-monthly technical report. Reporting period 07/2006-12/2006.
- [34] ROBUSTNESS: RFS-CR-04046. Design Guidance. Document N°: ROBUSTNESS-Handbook-001, 2007
- [35] STEFANI, M.: Tension stiffening in elementi in cemento armato in regime di grandi spostamenti, Master Thesis, In Italian, Università degli Studi di Trento, 2006.
-

- [36] WEYNAND, K.; ZILLER, C.; BUSSE, E.; LENDERING, M.: System Calibration - Benchmark model 3, Internal report for the RFCS project RFS-CR-04046 “Robust structures by joint ductility”, Document N°: ROBUSTNESS-Report-PSP-001, Aachen 2007
- [37] WEYNAND, K.; ZILLER, C.; BUSSE, E.; LENDERING, M.: Parametric studies “Loss of a column”, Internal report for the RFCS project RFS-CR-04046 “Robust structures by joint ductility”, Document N°: ROBUSTNESS-Report-PSP-002, Aachen 2007
- [38] WEYNAND, K.; ZILLER, C.; BUSSE, E.; LENDERING, M.: Calibration of the simplified substructure, Internal report for the RFCS project RFS-CR-04046 “Robust structures by joint ductility”, Document N°: ROBUSTNESS-Report-PSP-003, Aachen 2007

Other references

- [39] ABAQUS/CAE, User’s manual Version 6.5 Documentation, ©ABAQUS, Inc. 2004.
- [40] ANSYS User’s manual. ANSYS Mechanical Solutions Release 11.0, 2007
- [41] AGARWAL, J.; ENGLAND, J.; BLOCKLEY, J. and D.: Vulnerability Analysis of Structures, Structural Engineering International, IABSE, Vol. 16 (2), pp. 124-128, 2006
- [42] AHMED, B.; LI, T.Q.; NETHERCOT, D.A.: Design of Composite Fin-plate and Angle Cleated Connections. Journal of Constructional Steel research. vol. 41(1). pp. 1-29, January 1997.
- [43] ANDERSON, D.: Composite steel-concrete joints in frames for buildings: Design provisions. COST C1 – Semi-rigid behaviour of civil engineering structural connections, Luxembourg, 1999.
- [44] AS/NZS 1170.0: 2002: “Structural design actions–General principles”, Standards Australia, Standards New Zealand, 2002 Edition.
- [45] AS/NZS 1170.0 Supplement 1: 2002 “Structural design actions–General principles–Commentary”. Standards Australia, Standards New Zealand, 2002 Edition.
- [46] BANIOTOPOULOS C.C. & WALD F, (eds) (2000). The Paramount Role of Joints onto the Reliable Response of Structures, NATO Science Series. Dordrecht. Kluwer Academic Publishers.
- [47] BENUSSI, F.; NETHERCOT, D. A.; ZANDONINI, R.: Experimental Behaviour of Semi-Rigid Connections in Frames”, The 3rd Int. Workshop on Connections in Steel Structures, Trento, Italy, 1995.
- [48] Building Regulations. Approved Document A. The building regulations 1991. Structure 1992 Edition.
- [49] Building Regulations 2000 – Approved Document A – Structures, Approved Document A – Amendments 2004 – The Stationary Office, 2004.
- [50] BURSI, O.S.: Elastic-Plastic Modelling of Structural Fasteners for Steel Bracing Connections. Journal of Constructional Steel Research. vol. 30 (1), pp. 13-38, 1994.
- [51] BURSI, O.S.; FERRARIO, F.; FONTANARI, V.: Non-linear Analysis of the Low-cycle Fracture Behaviour of Isolated T-Stub Connections. Computer and Structures. vol. 80 (27-30). pp. 2333-2360, 2002.
- [52] CERFONTAINE, F.: Study of the interaction between bending moment and normal force in bolted joints. PhD Thesis. Université de Liège, 2004
- [53] CORLEY, W.G.: Lessons learned on Improving Resistance of Buildings to Terrorist Attacks, Journal of Performance of Constructed Facilities, Vol. 18 (2), pp. 68-78, 2004.
- [54] CORLEY, W.G.: Applicability of Seismic Design in Mitigating Progressive Collapse, Proc. of Workshop on Prevention of Progressive Collapse Multihazard Mitigation, Council of National Institute of Building Sciences, U.S.A., 10-12 July, 2002.

-
- [55] Council of National Institute of Building Sciences, Washington DC (2003). “Prevention of progressive Collapse”. Report on the July 2002 National Workshop and Recommendations for future efforts, multi-hazard mitigation.
- [56] COSSFIRE. RFCS Contract N°: RFSR-CT-2006-00028. Connections of steel and composite structures under natural fire conditions. Runtime Periode 07/2006 – 06/2009
- [57] DEMONCEAU, J.F.: Steel and composite building frames: sway response under conventional loading and development of membrane effects in beams further to an exceptional event. PhD thesis. University of Liège, June 2008.
- [58] DONALD, O.D. (2002). “Review of Existing Guidelines and Provisions Related to Progressive Collapse”. Proc. of Workshop on Prevention of Progressive Collapse Multihazard Mitigation. Council of National Institute of Building Sciences, U.S.A..10-12 July.
- [59] ECCS Document N° 111. ECCS Model Code on fire engineering. Technical Committee 3. Brussels 2001
- [60] ECCS Document N°109. Design of composite joints for buildings. ECCS Technical Committee 11. Brussels 1999
- [61] ECCS Document N°96. Design handbook for braced composite steel-concrete buildings according to Eurocode 4. Profilearbed Recherches, Brussels 2000
- [62] ELLINGWOOD, B. R.; DUSENBERRY, D. O. (2005). “Building Design for Abnormal Loads and Progressive Collapse”. Computer-Aided Civil and Infrastructure Engineering. Vol. 20.
- [63] EN 1990: Eurocode – Basis of Structural Design, CEN European Committee for Standardization, April 2002.
- [64] EN 1991-1-1: Eurocode 1 – Actions on structures – Part 1-1 General Actions – Densities, Self-weight, Imposed loads for Buildings, CEN, 2002
- [65] EN 1991-1-4: Eurocode 1 - Actions on structures - Part 1-4: General actions, Wind actions; German version EN 1991-1-4:2005
- [66] EN 1991-1-7: Eurocode 1 – Actions on structures – Part 1-7: General Actions - Accidental actions due to impact and explosions, CEN, 2002
- [67] EN 1992-1-1: Eurocode 2 – Design of Concrete Structures – Part 1-1: General Rules for buildings. CEN, 2004.
- [68] EN 1993-1-1: Eurocode 3 - Design of Steel Structures - Part 1-1: General Rules and Rules for Buildings. CEN, 2005
- [69] EN 1993-1-8: Eurocode 3 - Design of Steel Structures - Part 1-8: Design of joints. CEN, 2005
- [70] EN 1994-1-1: Eurocode 4 - Design of Composite steel and concrete Structures - Part 1-1: General Rules and Rules for Buildings. CEN, 2004
- [71] EN 1998-1: Eurocode 8 - Design of Structures for Earthquake Resistance, Part 1: General rules, seismic actions and rules for buildings. CEN, 2005
- [72] FAELLA, C.; PILUSO, V.; RIZZANO, G.: Structural Steel Semirigid Connections: Theory, Design and Software, CRC Press LLC, Boca Raton, 2000.
- [73] FINELG user’s manual: Non-linear finite element analysis software. Version 8.2, July 1999
- [74] FRANSSEN, J.-M., PROGRAM SAFIR, Ver. 1.3, User’s Manual, Universite de Liege, Institut du Genie Civil, Service Ponts et Charpentes, December 1996.
- [75] GARCIA, E.M.; DAVISON, B.; TYAS, A.: Analysis of the response of Structural Bolts subjected to rapid rates of loading, Proceedings of the 4th European Conference on Steel and Composite Structures. vol. C. Maastricht, The Netherlands, 8 th-10th June 2005.
- [76] GERARDY, J. C.; SCHLEICH, J. B.: Semi-rigid action in steel frame structures, Commission of the European Communities: technical steel research, Report EUR 14427 EN, 1992.
-

-
- [77] GHOBARAH, A.; OSMAN, A.; KOROL, M.: Behaviour of Extended End-plate Connections under Cyclic Loading. Engineering Structures. vol. 12(1). pp. 15-27, January 1990.
- [78] GRIFFITHS, H.; PUGSLEY, A.; SAUNDERS, O.: Report of the Inquiry into the Collapse of Flats at Ronan Point Canning Town, Her Majesty's Stationery Office, London (UK), 1968.
- [79] HUBER, G.; KRONENBERGER, H.J.; WEYNAND, K. (1998). "Representation of Joints in the Analysis of Structural Systems". Proc. COST CI Conference on Semi Rigid Connections. Liege, September.
- [80] JASPART, J.P.: Etude de la Semi-Rigidite des Noeuds Poutre-Colonne et son Influence sur la Resistance et la Stabilité des Ossatures en Acier, Ph.D. Thesis, University of Liege, Belgium, 1991.
- [81] JASPART, J. P.; STEENHUIS, M.; ANDERSON, D., (1998). "Characterisation of the Joint properties by means of the Component Method". Proc. COST CI Conference on Semi Rigid Connections. Liege. September.
- [82] KRAUTHAMMER, T.; HALL, R. L.; WOODSON, S. C.; AYLOT, J. T.; HAYES, J. R., (2002). "Development of Progressive Collapse Analysis Procedure and Condition Assessment for Structures". Proc. of Workshop on Prevention of Progressive Collapse Multihazard Mitigation. Council of National Institute of Building Sciences. U.S.A..10-12 July.
- [83] KUHLMANN, U.; SCHÄFER, M.: Innovative verschiebbliche Verbundrahmen mit teiltragfähigen Verbundknoten. Schlussbericht, Research Project by order of the Studiengesellschaft Stahlanwendung e.V., Nr. P505 (2003).
- [84] LAHMEYER, J. Untersuchung an verschiebblichen Verbundrahmenelementen mit teiltragfähigen Knoten. Diploma thesis. Universität Stuttgart, Mitteilung des Institutes für Konstruktion und Entwurf 2003-5X (2003)
- [85] LE CHUYEN, N. K.: Analytical prediction of the lateral restraint influencing the development of the membraner forces. Master Thesis. Université de Liège, 2005
- [86] LEROY, R.: Evaluation of the rotation capacity of joints in steel and composite structures. Diploma Thesis. Université de Liège, 2005
- [87] LIU, R., DAVISON, J. B., TYAS A. (2005). "A study of Progressive Collapse in Multistorey Buildings". Proc. of the 2005 Structures Congress and Forensic Engineering symposium, New York.
- [88] LUU, N. N. H.: Structural response of steel and composite building frames further to an impact leading to the loss of a column. PhD thesis presented at the University of Liège, August 2008.
- [89] MAES, M. A.; FRITZSONS, K. E.; GLOWIENKA, S.: Structural Robustness in the Light of Risk and Consequence Analysis, Structural Engineering International, Vol. 16 (2), pp. 101-107, May 2006.
- [90] MARECHAL, D.: Evaluation of the rotation capacity of joints in steel structures. Diploma Thesis. Université de Liège, 2004
- [91] MAZZOLANI, F.M.; PILUSO, V.: Theory and Design of Seismic Resistant Steel Frames, E&FN SPON, an Imprint of Chapman & Hall, London, 1996.
- [92] Model Code 1990, Bulletin d'information n 213/214, CEB-FIP, Thomas Telford, London, 1993.
- [93] MOORE, D. B.: The UK and European Regulations for Accidental Actions, Proc. of Workshop on Prevention of Progressive Collapse Multihazard Mitigation, Council of National Institute of Building Sciences, 10-12 July, 2002.
- [94] PRECIOUS. RFCS Contract N°: RFSR-CT-2003-00034. Prefabricated composite beam-to-concrete filled tube or partially reinforced-concrete-encased column connections for severe seismic and fire loadings. Runtime Periode 09/2003 – 08/2006
- [95] PUHALI, R.; SMOTLAK, I.; ZANDONINI, R.: Semi-Rigid Composite Action: Experimental Analysis and a Suitable Model. Journal of Constructional Steel Research, vol. 15 (1/2), pp. 121-151, 1990.
-

-
- [96] SCHÄFER, M.: Zum Rotationsnachweis teiltragfähigen Verbundknoten in verschieblichen Verbundrahmen. Dissertation. Universität Stuttgart, Mitteilung des Institutes für Konstruktion und Entwurf Nr. 2005-1, (2005)
- [97] SEDLACEK, G.; WEYNAND, K.; KLINGHAMMER, R.; HÜLLER, V.: Typisierte Anschlüsse im Stahlhochbau. Deutscher Stahlbau-Verband DSTV Stahlbau Verlag- und Service GmbH. “. Auflage 2 (Band 2), November 2002.
- [98] Seismic Provisions for Structural Steel Buildings. Part 1: Provisions, American Society of Civil Engineers (AISC), 2002 Edition.
- [99] Seismic Provisions for Structural Steel Buildings. Part 2: Commentary, American Society of Civil Engineers (AISC), 2002 Edition.
- [100] SOFISTIK user’s manual Star 2, Non-linear frame system analysis software. Version 14.13, 2005
- [101] STAROSSEK, U.: Progressive Collapse of Structures: Nomenclature and Procedure, Structural Engineering International, IABSE, Vol. 16 (2), pp. 113-117, 2006.
- [102] STEENHUIS, C.M., HERWIJNEN Van F, SNIJDER, H.H. (2000). “Safety Concepts for Ductility of Joints”. International AISC/ECCS workshop on Connections in Steel Structures IV. Roanoke. October 22-25.
- [103] SWANSON, J.A.; LEON, R.T.: Bolted Steel Connections: Tests on T-Stub Components. Journal of Structural Engineering, Vol. 126(1). pp. 50-56, 2000.
- [104] TRONG TRI, N.: Analytical study of cantenary action in beams further to the accidental loss of a column in a steel building frame. Master Thesis. Université de Liège, 2006
- [105] VLASSIS, A.G.; IZZUDIN, B.A.; ELGHAZOULI A.Y.; NETHERCOT, D.A.: Design Oriented Approach for Progressive Collapse Assessment of Steel Framed Buildings, Structural Engineering International, IABSE, Vol. 16 (2), pp. 129-136, 2006.
- [106] www.connectionprogram.com
- [107] ZOETEMEIJER, P.: A design method for the tension side of statically loaded, bolted beam-to-column connections, Heron Stevin-Laboratory, vol. 20 (1), The Netherlands, pp.3-59, 1974.
- [108] ZOETEMEIJER, P.: “Summary of the Research on Bolted Beam to Column Connections”. Delft University of Technology, Faculty of Civil Engineering. Stevin Laboratory report 6-90-02 (1990).

1 INTRODUCTION

Depending on the public or commercial relevance of buildings today it is no longer sufficient for engineers to consider only basic design criteria for planning of structural framework. For a first time after the collapse of Ronan Point Building in London 1968 a design for robustness and against progressive collapse was required and these achieved scientists' attraction. Some research even led to however very limited recommendations and even codified rules in UK but which was not wider spread at global level. Since the terrorist attack of September 11, 2001 this area has gained momentum and the researches are focussing on the maximum amount of public and structural safety within the sphere of economic and time constraint. Engineers are increasingly being required to consider progressive collapse mitigation as additional design criteria. Therefore it ought to avoid that local initial damage due to impact, explosion, etc. causes a progressive collapse. That means the structure has to be designed in such a way that initial damage of a structural member does not lead to global collapse of the structural system. There are different design approaches to achieve the mitigation of progressive collapse. One method of achieving this goal effectively is to utilize the redundancy approach (or alternate load path method). This redundancy approach is well suitable for structural steel buildings with inherent sufficient ductile material behaviour allowing deformations when local failure occurs. Therefore the single sections and joints have to be especially designed and optimized. Special focus has to be given to the joint configuration and design in particular by using semi-rigid joints.

The aim of this project has been to carry out extensive experimental and theoretical investigations on the behaviour of steel and composite joints in framed structures to derive robustness requirements in order to develop good practice recommendations. Practically speaking many exceptional events and structures could be considered, but only few have been chosen as model cases within this project.

Special focus is given to:

- Loss of a column
- Loss of a bracing
- Fire
- Earthquake

For the 4 different events different strategies have been followed: An in-depth investigation including also a substructure test was performed for the event "Loss of a column". For the event "Loss of a bracing" the investigations were only based on numerical studies. The event "Fire" could be reduced to a local failure of a member such as "Loss of a column" or "Loss of a bracing" in case of a localised fire, for more global events reference has been made to other investigations. For the event "Earthquake" a review has been made of existing rules and recommendations and a summary of them relevant for robustness is given.

In more detail the work has been performed on the following topics:

- Systematic analysis of accidents and the resulting behaviour of structures to find out weak points of the structure and to define conditions for robust structures as well as collection and review of existing experimental and analytical work related to ultimate strength and ductility. (WP1, WP2)
- Experimental investigations for a high number of joint components subjected to bending and tension stresses, as well as combined bending and tension stress. (WP4, WP5)
- Experimental investigations for composite joints under biaxial loading to determine the M-N-behaviour and resistance. (WP4, WP5)
- Experimental investigations for steel joints in realistic dimensions to identify failure dependencies (WP4, WP5)
- Experimental investigation for a substructure test in order to simulate the exceptional event "Loss of a column". (WP4, WP5)

- Numerical and analytical investigations for steel framed structures concerning the event “Loss of one or more columns”. (WP2, WP3&6)
- Numerical and analytical investigations for a composite car park frame in regard to the event “Loss of a diagonal bracing”. (WP2, WP3&6)
- Developing of simplified design criteria for specific cases of exceptional events (WP7)

The results are presented in 4 main topics concerning:

- Concepts and strategy
- Experiments and evaluation
- Numerical and analytical studies
- Design requirements and design criteria

At the end of each chapter a summary is given in which conclusions are presented and recommendations are summarized. Design guidelines in a separate handbook [34] are the outcome for each of the addressed events. Main focus given within the handbook is the analytical tool to determine requirements for joints caused by “Loss of a column”. Design examples illustrate the outcome for the various addressed events inside each of relevant chapters.

2 SYSTEMATIC ANALYSIS OF EXISTING DATA

2.1 General

The general principles of structural design prescribe that a structure have to be designed and executed in such a way to possess adequate levels of structural resistance, serviceability and durability. To satisfy these requirements actual design strategies follow a local level approach which consists in design/check of single structural elements against specified limit states which can occur during the intended life of the structure. Recent structural collapses due to local damages caused by accidental actions pointed out the inadequacy of this design approach, which doesn't take into account the fact that structural safety depend also on the interaction among structural elements and hence on the effects that local damages can induce on the whole structure. The effects of local damages become important if the structure is not robust: local damages can activate chain reactions which could result in the partial or complete collapse of the structure. To prevent progressive collapse, structural design should consider all possible sources of collapse initiation and evaluate the related system response by means of non-linear dynamic analysis in the time domain. Difficulties from the computational point of view and inability to foresee all possible scenarios, induce to develop design criteria able more to mitigate than prevent damages [101], [41]. The aim of a rational design criterion against accidental loads is the design of robust structures, such as the damage is not disproportionate to the causes.

Studies and researches on robustness started in the '60, allowed at individuating the general strategies to prevent the progressive collapse. The interest of the scientific community in this particular field increased after the structural collapses recently happened as a consequence of terrorist attacks [53], [78]. These events pointed out the need of additional studies aimed at the definition of specific design criteria for structural robustness.

Starting from these general assumptions the main aim of the first package was to collect data and information available in literature about the main topics related to the research project. Primarily the attention was focused on robustness and on the way to achieve robustness. In addition because the research project focuses on steel and concrete composite structures, and in particular on the joint ductility as a strategy to prevent the progressive collapse, data were collected also about these specific topics. Summarising the following subjects was considered:

- Structural behaviour in case of accidental loading conditions;
- Causes of progressive collapse;
- Requirements to achieve robustness;
- Structural behaviour of steel frames, beams and joints;
- Structural behaviour of steel and concrete composite frames, beams and joints.

The documents were classified on the basis of the subject and organically collected in a data base (ACCESS database).

The wide data collected on different topics make difficult to produce an exhaustive summary. In the following the attention is focused on the subject of this research i.e. robustness and in particular to the strategies to prevent the progressive collapse. Due to the particular strategies selected to achieve structural robustness the main concept concerning ductility and in particular the beam-to-column joint ductility are considered. Finally a general overview to the contents of the database is presented.

2.2 Basic guiding principles to robustness and common work

2.2.1 Preventing the progressive collapse: the strategies

The word “robustness” is adopted with different meanings in different field of science and technology such as control theory, statistical inference, quality control, product development, design optimization,and in civil engineering [89]. In this last field there is not an unanimous agreement on the significance of this word which is often used as a synonymous of stability, ductility, reserve of resistance or redundancy. EN 1991-1-7 [66] defines robustness as “the ability of a structure to withstand events like fire, explosions, impact or the consequences of human error, without being damaged to an extent disproportionate to the original cause”. Following this approach robustness is considered as structural properties which is independent of the possible causes/events. If the dependence on the events is considered it is more appropriate to talk of collapse resistance [101].

The distinction between robustness and collapse resistance allows to identify different strategies of analysis and design which are based on the identifiability of the events, on the probability of occurrence of the accidental actions, on the effects of these actions/events, on the structural response and finally on the consequences of the failure. The aforementioned factors can be simply summarised as level of risk. By considering the level of risk, the strategies of prevention can be classified in two categories:

- Structural requirements aimed at ensuring a minimum level of structural robustness. This goal can be achieved by the adoption of prescriptive design and detailing rules producing a minimum level of strength, continuity and ductility in elements and connections. Additional structural resources can arise by the adoption of tying requirements, bridging techniques and the design of key elements. This approach is generally adopted in case of low levels of risk.
- Structural design by considering a set of hazards scenario each of them characterised by intensity and location of the action and consequent state of damage. The solutions consist in the design of redundant structures and/or of structural elements so as to avoid the activation of chain reaction (performance-based design). The techniques consist of event control, design of alternative load paths and key elements, compartmentalisation.

The general definition of probability of collapse allows a clear understanding of the design strategies to prevent progressive collapse. By considering an accidental action (H_i), the probability of progressive collapse can be expressed as:

$$p(F) = p(F/D \cap H_i) \cdot p(D/H_i) \cdot p(H_i) \quad (2.1)$$

where:

- $p(H_i)$ probability of occurrence of the action H_i ;
- $p(D|H_i)$ probability of the local damage D as a consequence of the action H_i ;
- $p(F|D \cap H_i)$ failure probability as a consequence of the local damage D caused by the action H_i .

The probability of collapse can be reduced by decreasing the values of the terms on the right hand side of equation (2.1). As a consequence, the strategies of prevention can operate on three different levels:

- on the events (event control method) limiting the probability associated to the event H_i ;
- on the local damage (selecting appropriate structural typologies not very sensitive to damage, strengthen vital structural elements) limiting the probability of a local damage D due to the accidental action H_i . This approach is known as specific local resistance method (SLR);
- on the progressive collapse (redundant structures, alternative load paths) limiting the failure probability due to the local damage D caused by the accidental action H_i , approach known as alternate path method (AP).

The event control method can be classified as non-structural approach. The remaining methods which operate on the local damage and on the progressive collapse are classifiable as structural approaches

because directly related to the structure. Direct and indirect method can be adopted. The direct methods consist in the design of structural elements and components against accidental actions and on the check of the ability of the structure to bridge over notional removed structural elements. The indirect methods operate at level of progressive collapse through the provision of minimum levels of strength, continuity and ductility.

Difficulties in taking into account all the potential accidental actions make impracticable the use of equation (2.1). In case of a low level of risk the design approach to prevent progressive collapse can be simplified through the adoption of design strategies not directly related to the event/action. In this case the equation (2.1) becomes [62]:

$$p(F) = p(F/D) \bullet p(D) \quad (2.2)$$

In this case the design strategies consist in the adoption of the alternate load paths aimed at avoiding the spreading of the local damage.

2.2.2 Structural robustness and codes

The first design rules concerning progressive collapse were based on the results of the studies and researches performed after the collapse of the Ronan Point [78]. The concept of structural design to be performed so as the damage is not disproportionate to the causes was introduced by the Building Regulation published in United Kingdom in 1976. Afterwards in the Approved Document A the general concepts concerning robustness were converted in design requirements which were based on tying prescriptions, alternative load paths able to bridge over the local damages and the design of key elements. The strategies of prevention were then adopted, modified and integrated by the codes for the design of steel, masonry and reinforced concrete structures. The extensive use of such a design prescriptions and the analysis of the behaviour of structures designed in accordance to those rules in case of accidental actions resulted in updating of the documents up to the last version of the Approved Document A published in 2004 [49].

In the United States the general concepts about the progressive collapse were first introduced in the document ANSI A.58.1 published in 1972. These concepts were extensively updated and then incorporated in the 1982 version, and in the document ASCE-7. As in the United Kingdom, also in USA the general concepts on robustness were incorporated in the main codes for structural design. A great contribution to this topic was provided by the work of American government Agencies (ed es) Interagency Security Committee (ISC), General Services Administration (GSA), Department of Defense (DoD), Federal Emergency Management Agency (FEMA)) which promoted specific studies and researches. Similarly to United Kingdom and United States, other countries (Canada, Australia e New Zealand,) established specific design prescriptions.

British studies and standards, the first in providing criteria for the design of robust structures, were the referee for the most part of the structural design codes which adopted the same design philosophy and the same methodological approach. This occurs also in the Eurocode 1 and in particular in EN 1991-1-7 [66] which refer to the design in case of accidental actions. Despite Document A [49] and EN 1991-1-7 [66] utilize the same approaches; the last one document proposes a wider and systematic analysis of the accidental actions and of the relative techniques of analysis [93].

2.2.3 The European approach to robustness

The approach to robustness adopted by EN 1991-1-7 [66] is based on the design criteria provided by EN 1990 [63] which states that “a structure shall be designed and executed in such a way that it will not be damaged by extent such as explosion, impact and consequences of human errors to an extent disproportionate to the original causes”. To design the structure following this criterion means to limit the probability of failure to an acceptable extent by means of structural measures which are economically justifiable and sustainable. In structural design a question to be solved is to establish if or when the structure shall be designed against accidental loads. At this aim, a reliable parameter of judgment is the impact the collapse would produce on the society, evaluated by considering the consequences on people, on the economy and on the environment. The approach followed by EN 1991-

1-7 [66] consists in classifying the structures in classes of consequences. Three classes (CC) are considered:

- CC1: low consequence of failure;
- CC2: medium consequence of failure;
- CC3: high consequence of failure.

Moreover EN 1991-1-7 [66] shared CC2 in two subclasses named respectively CC2a and CC2b. The belonging to one of the aforementioned classes depends on the building type and occupancy. For each of these classes the following strategies of prevention are prescribed:

- CC1: no specific consideration is necessary for accidental actions except to ensure that the robustness and stability rules given in EN 1990 to EN1999, as applicable, are met;
- CC2: depending upon the specific circumstances of the structure, a simplified analysis by static equivalent action models may be adopted or prescriptive design/detailing rules may be applied;
- CC3: an examination of the specific case should be carried out to determine the level of reliability and the depth of structural analyses required. This may require a risk analysis to be carried out and the use of refined methods such as dynamic analyses, non-linear models and interaction between the load and the structure.

The choice of the strategy of prevention is also influenced by the peculiarities of the accidental actions. By considering the unforeseen ability of the events and the practical impossibility to define “a priori” all the possible scenarios, EN 1991-1-7 [66] distinguishes the accidental actions in identified and unidentified actions (Figure 2-1). The probability of occurrence of the action, the consequences of the damage, the possibility of the adoption of measures of prevention and the level of the acceptable risk allows classifying an action as identifiable or unidentifiable. Disregarding fire and earthquake actions, which are considered in specific parts of the Eurocodes, EN 1991-1-7 [66] takes into consideration as identified accidental the impact (from road vehicle, forklift trucks, trains, ships, hard landing of helicopters on roofs) and the internal explosions. For these actions appropriate models to describe the actions and operative criteria in case of risk analysis are provided. The strategy of prevention to be adopted can be summarised as (Figure 2-1):

Event control:

- preventing the action from occurring;
- reduction of the probability of occurrence of the accidental action to an acceptable level;
- reduction of the magnitude of the action through structural measures;

Protection measures of protection so as to limit the effects of the accidental actions.

Structural measures:

- design of structural members which allow the survival of the structure;
- selection of materials and design of structural members characterised by sufficient ductility so as to absorb strain energy without reaching the collapse;
- design of redundant structures allowing the load transfer through alternative load paths.

The most appropriate measures depend on the peculiarities of the actions (intensity, way to act, on the structural performances and on the consequences of the collapse).

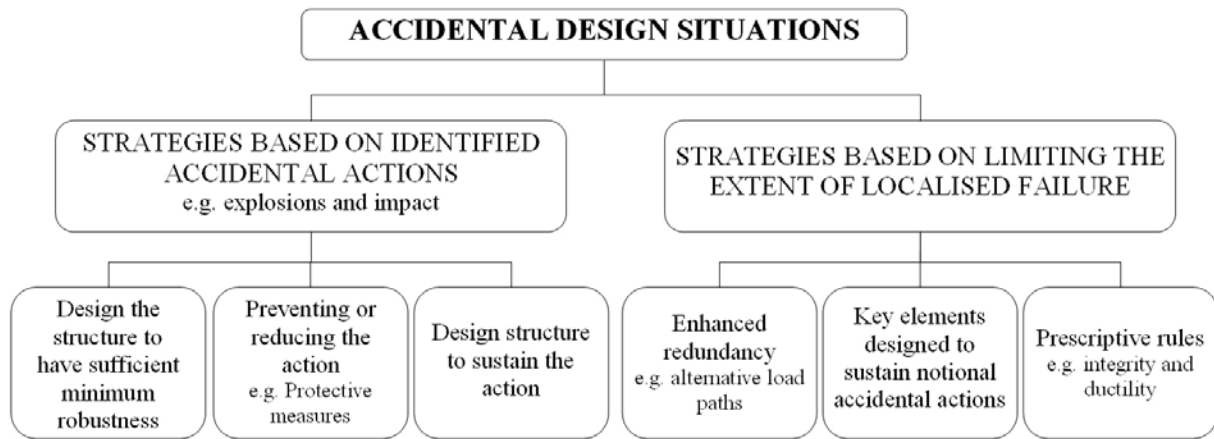


Figure 2-1: Design strategies for accidental load adopted by EN 1991-1-7

In case of unidentified accidental actions, the prevention strategies are selected with the aim to provide the structure of a sufficient robustness to survive for a period sufficient to facilitate the safe evacuation and rescue of personnel from the building and its surroundings. At this aim the design strategies provided by EN 1991-1-7 [66] are (Figure 2-1)

- design of key structural elements with respect an unidentified accidental action A_d (for building it is suggested $A_d = 34 \text{ kN/m}^2$);
- structural design so as a localised damage does not endanger the stability of the structure or of part of it;
- adoption of prescriptive design rules so that to provide a sufficient robustness to the structure.

These general concepts are specialised by considering the consequence classes as:

CC1: structural design following the criteria prescribed by Eurocodes 0-9;

CC2a: design strategies as for CC1 and use of horizontal ties in framed structures (Figure 2-2) or anchorages of suspended floor to walls for load-bearing wall construction;

CC2b: design strategies as for CC1, use of horizontal ties together with vertical ties in all the supporting columns and walls (Figure 2-2). Alternatively to the last provisions, in case of the removal of each supporting column and each beam supporting a column or any nominal section of load-bearing wall the structural stability should not be compromised and any local damage does not exceed a fixed limit;

CC3: systematic risk analysis of the structures should be performed taking into account foreseeable and unforeseeable hazards. The design strategies to be adopted could be structural (structural design against suitable action levels, alternative load paths) or non structural (reduction of the occurrence of the actions, limiting the intensity of the events and of the related consequences).

It should be mentioned that specific design criteria are provided only for consequences classes 2a and 2b. The main goal of this requirement is to guarantee a minimum level of robustness to the structure so as to allow the development of alternative load path in case of the collapse of a vertical bearing element. For consequence class 3, EN 1991-1-7 [66] indicates possible strategies of prevention to be specialized to the particular scenarios. The risk analysis for the consequence classes 3 (CC3) could be performed at a qualitative level or if, the problem requires a more detailed analyses, in a quantitative way. In this case the adoption of preventive measures is strictly dependent on the adoption of an acceptable level of risk. If the analysis suggests the need of prevention measures, the possible strategies consist in:

- mitigation of the events by means of structural or non-structural measures;
- controlled evolution of the event;
- design of the structures so as to guarantee reserves of resistance, robustness and redundancy;
- reduction of the magnitude of the damage by controlled failures.

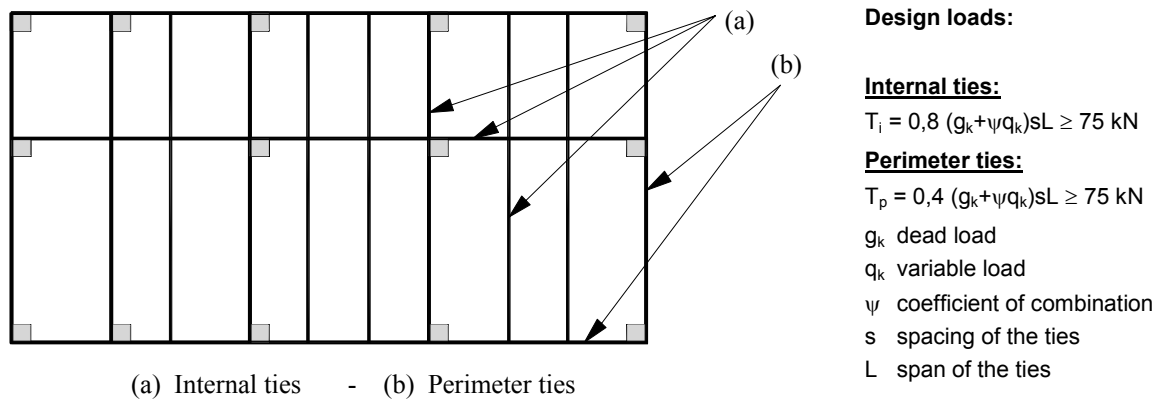


Figure 2-2: Horizontal ties to be adopted for consequences classes 2a and 2b

2.2.4 Ductility: a strategy to achieve robustness

The review of literature concerning robustness highlighted that the ductility of joints can be considered an economic and effective strategy to prevent the spreading of localized damages caused by accidental actions [87], [105]. An appropriate joint behaviour allows the structure to bridge over notional removed structural elements finding a new stable configuration. The achievement of a ductile behaviour of joint involves both material properties and the functioning of the structural system. Despite steel is known as ductile material, this characteristic alone is not sufficient for steel or steel and concrete composite structures to be defined (by default) as ductile ones. Ductility in literature is used with different meanings and in different contexts: e.g. that for the material itself (in terms of elongation), for a cross section (in terms of curvature), for a connection (in terms of deformation), for a complete joint (in terms of rotation), etc.

Ductility is defined as the ability of the structure/structural member/material to undergo large deformations after initial yielding without any significant reduction in strength. From the structural point of view a complete understanding and fulfilment of “required ductility” and “available ductility” is a key step which accompanies several advantages for the system. To avoid brittle damages and to dissipate more energy with less damage are the major advantages that are achieved with careful design of a ductile system. Ductility in a system can be achieved by enabling the joints to provide large rotations, so that membrane forces in the members can be activated allowing a redistribution of internal forces [72]. Following this approach an adaptive structure can be created with sufficient strength reserve even under exceptional load allows large deformations. By increasing deformations, joints are subjected to increase in tensile forces, while bending moment exposure decreases or is even inversed.

Research till date has exploited ductility as an essential tool for systems subjected to seismic forces [91]. This has resulted in seismic design standards where, ductility requirements for joints are formulated in terms of deemed to satisfy rules i.e. provided that certain design requirements are met, the joint may be assumed to behave sufficiently ductile to ensure a safe structural behaviour. The different natures of the seismic action and those which can arise in case of a progressive collapse need an investigation to check if the ductility provisions for seismic purposes are also adequate for robustness. Studies have shown that the adoption of seismic detailing can result in a significant reduction of the damage due to blast. The analyses carried out on the Murrah Federal Building in Oklahoma City collapsed due to a terrorist bombing showed that if it had been designed accordingly to the more recent seismic design provisions the damage would have been substantially reduced from a minimum of 50 % to a maximum of 80 % depending on the seismic structural measures adopted [54]. Studies about the nature of occurrence and the effects of the more common accidental actions such as blasts overpressures, impacts and fire loads were developed in the recent past. As a result, appropriate models aiming at reproducing the actions were developed and in case of fire ‘ad hoc’ design recommendations were produced. A detailed view about the art of study related to fire and seismic actions is presented in § 3.5 and § 3.6 of this document. In between of accidental actions a variety of scenarios are possible some of them a priori not identifiable. The development of adequate structural requirements able to

avoid the progressive collapse requires numerical and experimental analysis aiming at analysing the structural response and hence the structural requirements.

2.2.5 Beam-to-column joint modelling: the component method

In analysis of framed structures the modelling of the joint behaviour plays a central role [81], [76], [60], [47], [43]. The local deformations which take place in the joint area greatly influence the distribution of the internal forces between the structural elements, the global stability and the displacements due to vertical and horizontal loads. This effect can be properly reproduced by an accurate representation of the joint behaviour. Studies and researchers recently developed allowed the development of simplified and reliable models aiming at simulating the behaviour of the joints, which can be simply implemented in most of the programs of structural analysis. With reference to the beam-to-column connection the main sources of deformations are related to the flexural deformation of the connection and to the shear deformability of the column web. These deformations result in a relative rotation between beam and column. As a consequence the behaviour of joint can simply be represented by a moment-rotation (M - Φ) relationship. The accuracy in modelling the beam-to-column joint behaviour is depended on the type of global analysis to be performed. Different approaches in modelling the beam-to-column joints can be adopted, i.e. empirical, analytical, mechanical, finite elements and experimental approach [72].

Mechanical models, the spring models, are based on the simulation of the joint/connection by using a set of “active components” which can potentially be sources of deformations and possible fracture (Figure 2-3).

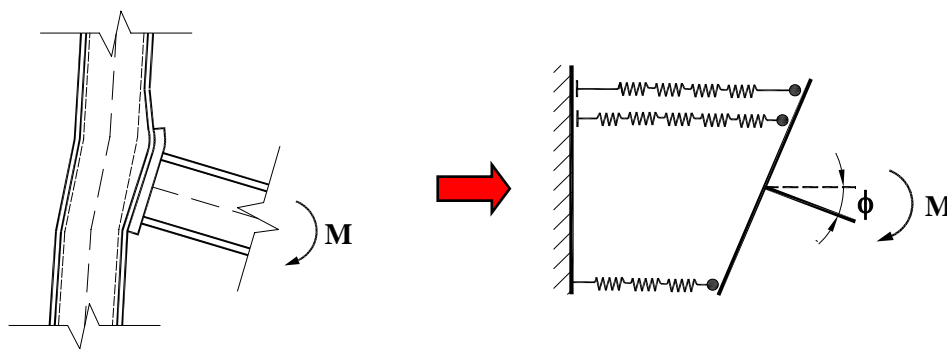


Figure 2-3: Component model for beam-to-column joint

EN 1993-1-8 [69] codifies the so-called component method for predicting the behaviour of beam-to-column and base joints. Focusing the attention on the beam-to-column joint the procedure to evaluate the moment-rotation curve of requires the following steps [81], [79]:

- Identification of the active component of the beam-to-column joint;
- Evaluation of the force-displacement relationship of the basic components;
- Assembly of the components by evaluating the moment-rotation curve of the whole joint.

The constitutive law of the joint components can be derived from experimental test, numerical simulation or analytical methods. The component method is codified by EN 1993-1-8 [69] with reference to three connection typologies: fully welded connection, end-plate connection and top and seat angle connection. However, the component approach is sufficiently general to deal with any beam-to-column joint by decomposing into the relevant components. Furthermore, different levels of accuracy can be adopted to predict the force-displacement curve for each of the components.

The knowledge of the plastic rotation capacity of the beam-to-column joints is of primarily importance in designing moment-resisting frame to be used for seismic resistant frames. Ductility is also a strategy for preventing progressive collapse. Many reviews of the experimental data were performed aiming at identifying the parameters which affect the plastic joint capacity deformation. The main results of the analysis pointed out the key role played by the beam depth, and by the plastic deformation of the joint components at the beam flange level. Generally, the weakest joint component governing the joint flexural resistance is also the main source of plastic deformation capacity. In bolted beam-to-column

connections the column flange in bending, the end plate in bending and the angle in bending are the weakest joint components. Following the procedure suggested by EN 1993-1-8 [69] the behaviour of these joint components can be suitably modelled as equivalent T-stubs. The prediction of the load-displacement curve of bolted T-stubs up to collapse, would allow the prediction of the main source of plastic deformation capacity of the joints. For design purposes, bolted connections can achieve sufficient rotation capacity provided that the end plate is a ‘weak link’ relative to the bolts. In order to meet the ductility requirements, it has to be ensured that the required joint rotation is less or equal to the available joint rotation and the main component to support the joint rotation is the thin end plate deformation.

2.3 Database overview

As mentioned at the beginning of this chapter, with the aim to improve the knowledge about robustness and about the behaviour of steel and concrete composite structures, data of literature were collected on these subjects:

- structural behaviour in case of accidental loading conditions;
- causes of progressive collapse;
- requirements to achieve robustness;
- structural behaviour of steel frames, beams and joints;
- structural behaviour of steel and concrete composite frames, beams and joints.

The documents are divided into two main categories (categories A and B):

- category A: documents like codes, standards, thesis, books and recommendations which contents cannot be summarized in a report format.
- category B: documents like papers or research report, which can be briefly summarized. For each of them a short report (Figure 2-4) was prepared for quick view of the document.

Documents in category B were divided in three subcategories depending of their contents:

EXTREME LOADING:

- contains the documents related to the causes, analysis, findings and recommendations related to abnormal loading scenarios, progressive collapse cases, events as explosion, impact loading and fire;

STEEL STRUCTURES AND COMPONENTS:

- contains documents related behaviour of steel structures, components and joints. In between the available literature attention was focused on strength and ductility requirements.

STEEL AND CONCRETE COMPOSITE STRUCTURES AND COMPONENTS:

- contains documents related to behaviour of composite structures, components and joints. Documents are focused on beam-to column connections and column base connections. Both the experimental and the FE modelling aspects are covered.

A total of 181 documents were considered: 51 documents belong to category A and 130 to category B. A complete list of the documents is included on the CD in the Annex A in [5].

With the aim to facilitate the data search the documents were included in a database prepared with ‘Microsoft Access’. This particular program was selected because of its popularity and its flexibility of usage. The documents in category A were listed in a table labelled as “Detailed Documents” which contains:

- Identification number;
- Title;
- Authors;

- Kind of document (i.e. ECCS document, FEMA document,)
- Document details (for books: number of volume and year, etc.);
- Document link (if the file version is available).

The documents in category B were collected in a table format and catalogued by considering:

- Identification number;
- Title;
- Authors;
- Kind of document (paper, book, research report, PhD thesis, etc.);
- Document detail (for papers: name of the journal, for books: printer and/or editor, etc.);
- Additional document details (for journals and books: number of volume and year, etc.);
- Subject of the paper;
- Kind of subject (behaviour, modelling, experimental, FE analysis);
- Keywords (maximum 5);
- Report link (for documents in category B);
- Document link (if the file version is available).

The database allows making a quick search by considering one or more of the parameters, considered to catalogue the documents. At this aim, the ‘Subject’ was introduced to make the search plan easy and general for the user. In addition with the help of ‘kind of subject’ the user can select in more restrictive way the documents of his interest by considering the behavioural, modelling, experimental and finite elemental aspects. ‘Keywords’ make the search even more particular, narrowing down the targeted documents. Every precaution was taken in choosing the keywords so that search is effective. For this the keywords are defined to avoid any confusion. The complete list of keywords with their definitions is included on CD in the Annex B [5] to this document. For an easy use, even the keywords are divided into three categories as for the documents:

- Extreme Loading;
- Steel structures and Components;
- Composite structures and components;

For each of the categories mentioned above, the keywords have been further subdivided as:

- Description of the type of structure/ joint/component;
- Testing;
- Subject dealt with;
- Analysis/ Design methods;
- Final products.

The ACCESS database is installed on the project website so as to be available to other project partners and for the general access.

Paper No. : **EL_1.1**

The Oklahoma City Bombing: Summary and Recommendations for Multihazard Mitigation

Corley, W. G.; Mlakar, P. F.; Sozen, M. A.; Thornton, C. H.

Journal of Performance of Constructed Facilities, August 1998, pp. 100-112(13).

Summary :

This paper presents the investigation and analysis of the damage that occurred in the Murrah building as a result of the blast caused by a large truck bomb. The purpose of the investigation were to review damage caused by the blast, to determine the failure mechanism of the building and to review the engineering strategies for reducing such damage to new and existing buildings. Specifically mitigation of wind, bombing and earthquake effects were considered.

Keywords :

Collapse Mechanism, Compartmentalized Construction, Dual System, Mitigation, Redundancy.

Key Results :

- Loss reduction techniques should be formed and utilized to prevent a bad situation from getting worse i.e. to prevent progressive collapse. Redundancy is the key design feature for the prevention of progressive collapse.
- Compartmentalized construction, special moment frames and dual systems provide the mass and toughness necessary to reduce the effects of extreme overloads on buildings. Consequently, it is recommended that these structural systems be considered where a significant risk of seismic behaviour and/ or blast damage exists.
- The above mentioned techniques are cost effective with respect to ordinary moment frame construction as the difference is approximately 1-2 % of the total construction cost.

Figure 2-4: Typical report for category 'B' documents [5]

2.4 Conclusions

The systematic collection of existing data provides on one hand information on construction and design of robust structures with ductile joints. On the other hand guiding principles concerning strategies for progressive collapse, definitions and approaches of robustness and ductility were developed by thorough analysis of the literature and existing data forming the basis of the common project work. As a special outcome going beyond the direct purpose within the project a database was established. This may also serve for future research on this topic.

3 CONCEPTS AND STRATEGIES

3.1 General

In EN 1990 [63] Basis of Structural Design the following is demanded:

(4)P A structure shall be designed and executed in such a way that it will not be damaged by events such as:

- *Explosion,*
- *Impact, and*
- *the consequences of human errors, to an extent disproportionate to the original cause.*

However in contrast to design rules for ultimate, serviceability and durability limit states only these general requirements and very few detailed rules exist. An example of more detailed but very specific rules are the rules in UK Codes of Practice and in EN 1991-1-7 Accidental Actions [66]:

Following measures:

- *Introduce vertical ties,*
- *Design key elements for a recommended accidental design action $A_d = 34 \text{ kN/m}^2$*
- *Ensure that upon the notional removal of a supporting column, wall section or beam the damage does not exceed 15% of the floor in each of 2 adjacent stories*

Nothing is said about necessary deformation requirements and what kind of event should really be prevented by these measures. So though recent incidents show the high relevance and importance of robust design and many structures such as power plants, banking, finance and healthcare office buildings are key elements of modern infrastructure a clear stringent concept of design is completely missing according to requirements as well as realization.

Structures are designed for “normal” loading situation with high probability but not sufficiently reliable for unforeseen and catastrophic events. Extreme or catastrophic events such as fire, earthquake or explosion are events of low probability but sometimes disastrous consequences. They are partially covered by design rules for accidental loading situation but not for all structures and areas and not for all possible load levels. The same is true also for the “normal” load cases: they also may become an exceptional loading if the load level exceeds what has been foreseen during normal design. So this project deals with exceptional loading events defined as accidental loads not taken into account in the normal design.

However it does not specify the detailed loading cases like fire etc as such, but focus is given to the structural consequences of these events. So due to fire, explosion or earthquake a single member of a structure such as a column may fail and if the member is a key-element of the structure this may lead to a progressive collapse understood as extensive structural failure initiated by local structural damage. To prevent progressive collapse structural integrity or the ability of a structure to remain stable even if one part is destroyed by an exceptional event is asked for. Robustness as major project aim is understood as a way to achieve structural integrity in unforeseen cases.

There are different strategies to achieve robustness which will be explained in more detail in the following including the solutions chosen in the frame of this project. It has to be pointed out that at that moment it is impossible to come already to general requirements for all cases and events to be thought of but that a choice had to be made between some model cases called scenarios. Also for them the solutions chosen do not achieve the same degree of completeness and feasibility. But considering the lack of knowledge and information on start of the project a good deal of progress in practical design has been achieved and a model concept for future investigations been developed. For the following scenarios the possible structural failures have been studied in more details:

- Loss of a column in an office or residential building frame

- Loss of a bracing in a car park frame
- Unexpected earthquake
- Unexpected fire

The investigations on these different load scenarios comprise the following issues:

- Study structural failure mechanism
- Identify load paths
- Study behaviour of structural elements (members and joints)
- Identify structural systems allowing for redistribution
- Develop requirements for ductility of members and joints

One another innovative aspect should also be pointed: Ductility or the ability to undergo large deformation without losing strength has been recognized as crucial for robust design. This is a characteristic feature of structural members and joints of which the importance has so far not sufficiently be realised in everyday design. And also in this respect important expertise and improvements could be achieved.

3.2 Different strategies to achieve robustness

There are various approaches to achieve robustness in dependence on the consequence class or the peculiarity of the accidental design situation, see § 2.2.3 especially Figure 2-1.

One strategy to achieve robustness is to integrate all possible exceptional loads in the design process in itself; for sure this will lead to non-economic structures and, by definition, the probability to predict all the possible exceptional events, the intensity of the resulting actions and the part of the structure which would be affected is seen to be “exceptionally” low (probabilistic optimisation approach).

Another strategy is to derive requirements that a structure should fulfil in addition to those directly resulting from the normal design process and which would provide a certain robustness to the structure, i.e. an ability to resist locally the exceptional loads and ensure a structural integrity to the structure, at least for the time needed to safe lives and protect the direct environment. Obviously the objective could never be to resist to any exceptional event, whatever the intensity of the resultant actions and the importance of the structural part directly affected. The so called “Direct design methods” aim at the enhancement of reliability against local initial failure (local resistance method) or at a mitigation of progressive damage due to local failure (alternate load path method). For both strategies it is important to identify so-called key-elements. A key-element refers to one or more load bearing members (or sections of a load-bearing structure) that correspond in an initial failure and where the loss of this element may cause, if there are no provisions, a disproportionate collapse.

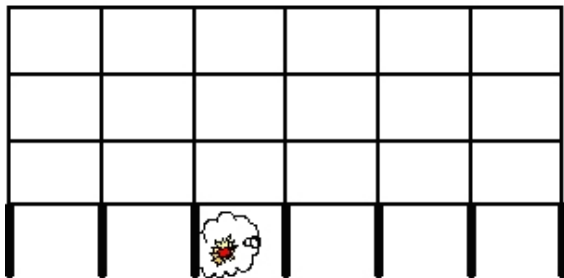


Figure 3-1: Specific local resistance

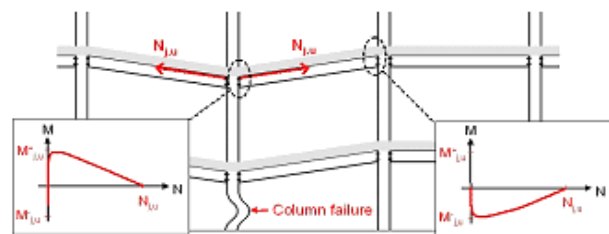


Figure 3-2: Alternate load path by redistribution of internal forces

The strategy “specific local resistance” is focused to the identified key-elements. The failure safety of these key-elements is increased. This is realized by providing a specific local resistance of these key-components of the structure using e.g. a design for accidental actions leading to achieve an over-strength in comparison to the usual design level. As example designing a column to sustain explosion or

blast loading (see Figure 3-1). But total safety against local failure is hardly realizable and in the most cases expensive as well.

The strategy “alternate load paths” allows local failure because of the redundancy of the load-bearing structure and a possible redistribution of internal forces to the undamaged part of the structure. For the design method of alternate load paths the structural system is designed by simulating the loss of single members and verifying that the remaining structure is still stable. There are different types of structural systems to provide alternate load paths. One alternative is by install strengthening of one floor above the danger spot to allow a hang-back of the loads above the damaged member without any significant deformations of the structure. This might be realized with bracings in one floor or with a strong support beam above the spot of damage.

Another alternative to get alternate load paths is the activation of membrane effects within the structural members, for example the activation of a catenary action within a frame structure and the transition from bending state to pure tension exposure (see Figure 3-2). For this special focus has to be given to the ductility of members and joints.

In the present project the alternate load path method by activation of membrane forces is mainly followed.

The robustness is required from the structural system not directly affected by the exceptional event (to avoid the local destruction of the structural element where the event occurs being often not possible). In this process, the ability to redistribute plastically extra forces resulting from the exceptional event is of high importance. This requires from all the structural elements and from the constitutive joints a high degree of plastic deformability under combined bending, shear, or axial forces.

As a general procedure to derive robustness requirements, different structural systems subjected to exceptional events are numerically investigated in order to see how the structures work when part of the structure is destroyed as well as how and how far redistribution takes place. From these first numerical investigations, few situations related to the destruction of various structural parts (one column, two columns, one beam, ...) are identified.

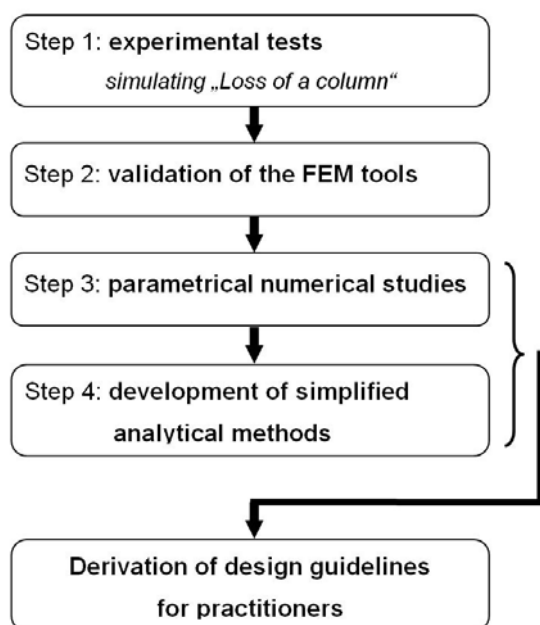


Figure 3-3: Global strategy followed within this project

member such as “loss of a column” or “loss of a bracing” in case of a localised fire, for more global events reference has been made to other investigations.

As a second way especially for the event “earthquake” recommendations are collected and summarized particularly for non-engineered structures that allow for a certain degree of redundancy or over-strength

One of these, the event “loss of a column”, has been tested experimentally (see Chapter 4.2); this allows validating the numerical tools used for the numerical and analytical studies.

Finally, parametrical studies are carried out numerically for the selected events and robustness requirements are derived.

In Figure 3-3 the strategy followed for the event “Loss of a column” is described.

For the event “loss of a bracing” no experimental investigations were performed, but similar to the procedure described before design guidelines were derived based on systematic numerical studies.

The event “fire” could mainly be reduced to a local failure of a

of crucial elements without deriving the details from refined calculations. This procedure follows more the strategy of “direct strength design”.

3.3 Investigations on the event “Loss of a column”

At first, before a column loss, the joints and the beams are mainly subjected to bending moments and shear forces. When the column loses its carrying capacity further to an impact (Figure 3-4), catenary action develops in the beams (as illustrated in Figure 3-5); axial forces increase (because of loads transferred by the column stub located just over the impacted one) until the joint or the beam reaches a full plastic state (under moment and axial forces). The beam takes large transverse displacements and axial forces increase further while bending moments decrease; this loading path and the evolution of the bending moment and axial force in the joint (or in the beam) are qualitatively illustrated in Figure 3-6.

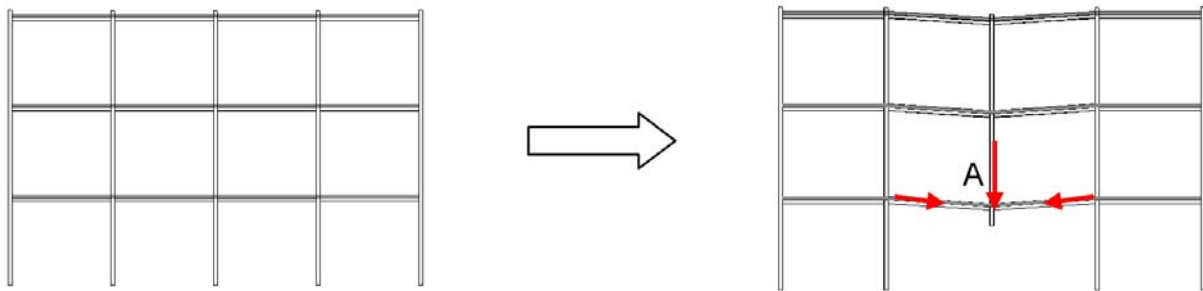


Figure 3-4: Loss of a column in a residential or office building frame

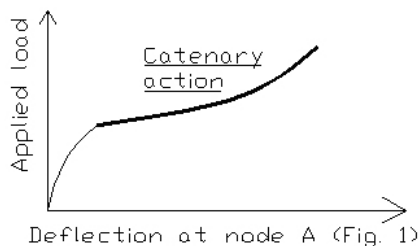


Figure 3-5: Development of the catenary action in the structure – illustration in an “applied load/beam deflection” curve.

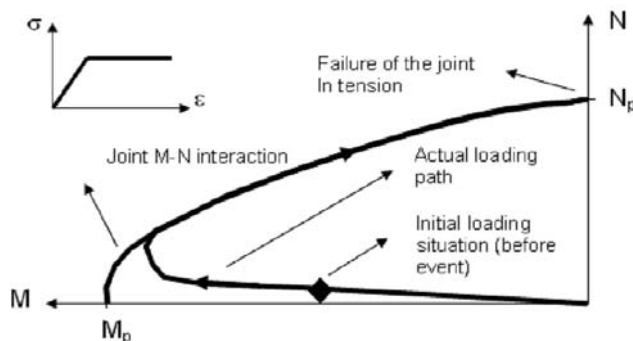


Figure 3-6: Actual loading in the joint or in the beam end section until failure.

At the end, the joints and the beams work mainly in tension. If the transverse forces applied to the beam (loads acting on the beam itself and loads from the upper storeys) is such that the axial force N in the

beams or in the joints remains lower than N_p , the system has a sufficient robustness to face the event; if not, a lack of robustness has to be contemplated.

The scope of the project is to reach robustness through joint ductility. So, the frames under consideration possess partial-strength and semi-rigid beam-to-column joints; the “weak” elements when catenary actions develop are therefore the joints.

The loss of a column can be associated to different types of exceptional actions: explosion, impact of a vehicle, etc.. Under some of these exceptional actions, dynamic effects may play an important role; within the present project, it is assumed that the action associated to the column loss does not induce significant dynamic effects. So, the performed investigations are based on static approaches.

These investigations on the event “Loss of a column” are fully in line with the global strategy defined in Figure 3-3.

In a first step, an experimental campaign has been carried out in different laboratories; three types of experimental tests have been performed:

- Test on a substructure at the University of Liège to simulate the loss of a column in a composite frame. The objective was to observe the development of the membrane forces and their effect on the structural beam-to-column joint behaviour.
- Tests in isolation on the substructure composite joints at the University of Stuttgart. These joints have been subjected to combined axial loads and bending moments; the objective was to characterise the behaviour of the joints met in the substructure.
- Tests on the substructure joint components at the University of Trento in order to characterise each components met in the substructure joints.

All the steel profiles and components were delivered by Arcelor Profil Luxembourg s.a. All the steel elements tested in the different laboratories came from the same production and the same rolling to be able to compare the obtained results. The performed experimental tests and the main results are presented in § 4.

Then, in a second step, the numerical tools used within the project have been validated through comparisons to the experimental test results and/or through benchmark studies. The validation is presented in § 5.2.

In step 3, parametrical studies have been performed with the so-validated tools to investigate the behaviour of buildings further to the loss of a column. Firstly, numerical investigations have been performed at PSP on 2D and 3D building frames; these studies are presented in § 5.3.2. Then a simplified substructure modelling able to simulate the global behaviour of a frame has been defined and validated through numerical investigations (§ 5.3.3.2). Finally, parametrical studies have been performed in § 5.3.3.3 on the simplified substructure modelling so as to identify the parameters to be included in the developed analytical procedures. Within these studies, braced/unbraced and sway/non-sway buildings have been considered.

In the last step, analytical procedures have been developed at the University of Liège to predict the development of the membrane forces in the simplified substructure. Also, as a key parameter to be taken into account is the M-N interaction appearing in the joints, an analytical method has been developed and validated to predict the response of composite joints subjected to bending moments and axial loads; the developed method is based on the method developed in the PhD thesis of Frederic Cerfontaine [52] dedicated to the behaviour of steel joints subjected to M-N. All these developments are presented in § 5.3.4.

In § 6.2, general conclusions are given concerning all the investigations performed on the exceptional action “Loss of a column in a composite or steel building frame”.

3.4 Investigations on the event “Loss of a bracing”

A steel or composite frame building can be designed as non-sway frame or sway frame structure. A typical car park frame structure e.g. usually is a braced frame construction that means a non-sway frame structure as shown in Figure 3-7. The composite joints are assumed as semi-rigid ones. But for the basic design of the car park frame they are only dimensioned for internal forces due to vertical loading. Additional internal forces resulting from lateral loading are transferred by the bracing so joints and members have no explicit design for this additional stress. “Loss of a bracing” (Figure 3-8) means an exceptional load case because additional internal forces due to lateral loads have to be transferred suddenly by members and joints and furthermore second order effects cause additional stresses.

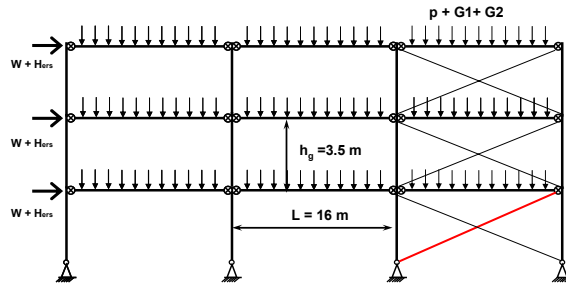


Figure 3-7: Undamaged car park frame

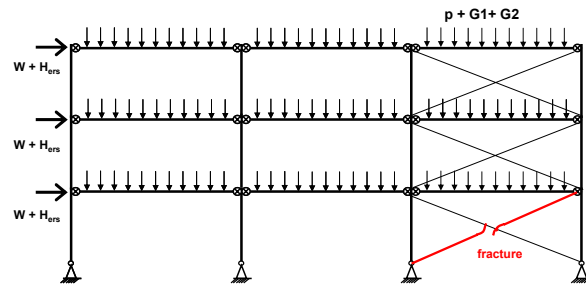


Figure 3-8: Damaged frame structure

In comparison to the investigation of the event “loss of a column” in § 3.3 no experimental tests have been executed for the event “Loss of a bracing”. For this exceptional event only numerical studies were performed to explain the global behaviour of framed composite structure when local failure of a bracing occurs and determines the remaining bearing capacity of the damaged structure. The value of robustness is reflected by the global behaviour when modifying the initial structure. The calculations were executed by the University of Liege and the University of Stuttgart, see § 5.4. The main aim of the numerical simulations of the event “loss of a bracing” in a car park frame was to study the redistribution of the internal forces within the structure when fracture of a bracing happened and to derive the resulting requirements for the members and joints. Another aspect is to see how the failure mode of the global structure changes and which members are mostly influencing the limit load factor. It was assumed that the event loss of a diagonal bracing happened in the bottom storey, because the utilization of the bracing in the bottom storey is maximal. For the car park frame it has also been decided to use a composite structure and not a pure steel frame because in practice the executed car park frames are mainly composite structures.

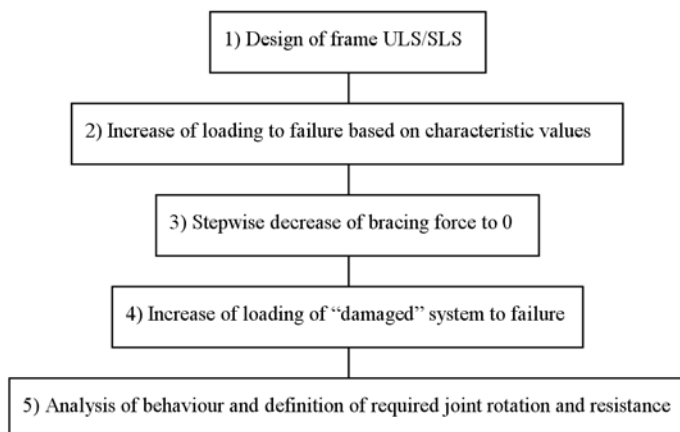


Figure 3-9: Procedure followed for the analysis of BM 2

For the numerical simulation of loss of bracing two different Finite Element softwares have been used. First they have been validated which is presented in § 5.2.4 then the event loss of bracing and further parametrical studies for the framed composite structure have been investigated, see § 5.4. The procedure followed for the numerical calculations of the event “Loss of a bracing” in a car park frame structure are shown in Figure 3-9.

Conclusions are summarized in § 6.3.

3.5 Investigation on the event “Fire”

Concerning the robustness of steel structures in case of fire, some events may happen but may be “translated” into more basic events.

A localised fire for example of a pallets of paper in an office building can locally increase the fire load. If this fire remains localised, only one or two members may be affected by the fire (see Figure 3-10).

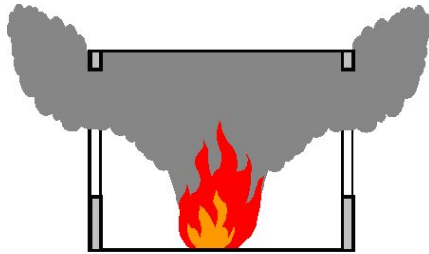


Figure 3-10: Localised fire

So in the case of a localised fire, the event “fire” may be translated for example in:

- loss of a column in an office or residential building frame;
- loss of a beam in an office or residential building frame;
- loss of a column in an industrial portal frame;
- loss of a bracing in an industrial portal frame;
- loss of a bracing in a car park;

depending on the position of the fire and the nature of the building. Investigations are concentrated on the case of localised fire, so in § 5.6 an example calculation of a real structure is given showing that such a reduction to one of the basic events, in this case the event “loss of a column”, is possible.

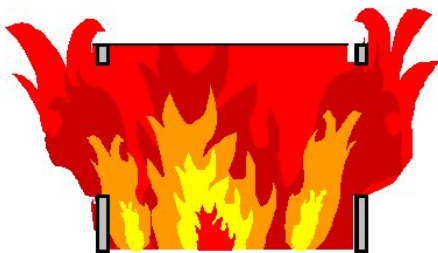


Figure 3-11: Fully engulfed fire

If the fire does not remain localised and grows until reaching the flash-over (see Figure 3-11), the problem is no more a problem of Robustness of structure but a problem of global fire resistance of the building.

Details for fire engineering are given e.g. in ECCS N° 111 [59] and also various experimental works have been carried out on the behaviour of steel connections for steel and composite structures under standard fire conditions around Europe. Here is referred to two running RFCS projects which are related to connections under fire. PRECIOUS [94] studies the residual fire resistance of some composite connections after they have been submitted to a seismic loading. COSSFIRE [56] seeks to obtain a

better understanding about connections and to develop simple design rules for Eurocode application on connections of steel structures.

3.6 Investigation on the event “Earthquake”

The design of structures under seismic loading condition received a great attention from researchers all over the world due to the huge consequences that events produce in terms of economic and human losses. Studies and researchers were activated resulting in the development of specific design criteria for the reliable structural design. The more recent design approach for seismic design provide the designers with the criteria for selecting appropriate structural systems and designing structural and non structural components so that for specified levels of earthquake intensity the structural damage will be constrained within given limits.

Despite seismic actions may be considered as accidental events and hence in the range of actions considered within this research project, the reason of this investigation is due to the central role that ductility has in seismic design: a reliable approach against seismic action requires in fact ductility, strength and stiffness to be considered at the same importance level.

The behaviour of a building during an earthquake is a shaking problem. The seismic action of the ground damage the structure by internally generated inertial forces caused by the vibration of the building mass. In order to estimate the ability of different structural systems of withstanding a ground motion event it is essentially to consider their overall tendency to dissipate the amount of energy transferred to them by the earthquake. The forms the structures can respond to and dissipate the energy input can be classified as elastic, hysteretic, kinetic and damping.

The capacity of structural systems to resist seismic actions is mainly achieved by dissipating energy through ductile behaviour of its members, connections and/or other “ad hoc” elements. For a structural system, ductility is quantified as its ability to undergo large deformations after initial yielding without any significant reduction in strength. Hence, by “introducing” ductility into a structural system several advantages go hand in hand such as to avoid brittle failures so increasing the escaping time, a limitation of damage (and of subsequent retrofitting costs) etc. Seismic analysis of structures requires the evaluation of the ductility capacity and the computation of the ductility demand associated with the strongest possible design earthquake. Therefore ductility has been widely investigated in case of seismic design, and this knowledge may be extended to robust design of structures.

The seismic ductile design forms a two step process aimed at ensuring that:

- a ductile performance of the structure is achieved;
- it is sustained through the damaging process.

Referring to the first step, it has to be said that steel and steel and concrete composite structures need to be designed as ductile by establishing an identifiable chain of events to occur during an earthquake. Within this aim, some ductile links are envisaged in the structure whereas the others are assumed to be brittle and therefore over-designed in comparison to the ductile ones (over-strength and capacity design concepts). Specific members are detailed for inelastic behaviour and all the other elements are protected against any cases that could cause failure. Plastic hinges regions within the structure are identified and designed to have dependable strength and ductility, brittle components not suited for stable energy dissipation are protected. In other word, ductility of the structural system is initiated by establishing a Hierarchy of resistance. In several world-wide Standards and Codes, the sustainability of the ductile behaviour of the structural system is guaranteed by the adoption of simple rules aiming to the prevention of the early buckling or failing of the elements, joints and their components commonly known as detailing design.

Taking into consideration the importance of ductility with regards to seismic design as well as for robust design, it seemed appropriate to collect the seismic codes from different countries and analyze them and derive rules applicable to robust design. The AISC [98], [99], the AS/NZS 1170.0 [44], [45] and finally EN 1998-1 [71] were considered. The seismic codes were thoroughly analyzed by considering different aspects i.e. the general criteria proposed to model the seismic actions, the structural design approach to prevent seismic collapse with particular reference to the steel and steel and

concrete composite structures. The main results of the comparison are presented in sections § 5.6 and § 6.5.

3.7 Conclusions

Aside of general ideas on strategies to follow to achieve robustness of structures by structural measures, such as ductile joints for chosen events, different conceptual ideas have been explained as the basis of investigations.

For the event “loss of a column” a full in-depth strategy has been developed. The strategy is presented in Figure 3-3. On the basis of experimental tests and numerical simulations a simplified analytical tool has been derived which allows the engineer to determine joint requirements. These practical design requirements can be calculated by means of an analytical method. The development of the analytical method is described in § 5.3.4 and the procedure of the analytical method is illustrated in the design guidelines [34].

For the event “loss of a bracing” no experimental investigations were performed, but similar to the procedure described before design guidelines were derived based on systematic numerical studies, see also Figure 3-9.

The event “fire” could be reduced to a local failure of a member such as “loss of a column” or “loss of a bracing” in case of a localised fire, for more global events reference has been made to other investigations.

For the event “earthquake” the procedure follows more the strategy of “direct strength design”: recommendations are collected and summarized particularly for non-engineered structures that allow for a certain degree of redundancy or over-strength of crucial elements without deriving the details from refined calculations.

That now may be followed for by similar investigations on further events that are characteristic for exceptional scenarios.

4 EXPERIMENTS AND EVALUATION

4.1 General

Aside of the numerical investigations a lot of focus is given to the experimental tests which have been performed by three of the partners, in Trento, Stuttgart and Liège. From the very first meeting of the project it has been planned to focus the experimental work on the investigation of one exceptional event. Because it involves a lot of time to conduct such a large series of tests coordinated by three partners, an investigation of more events within the duration of the project would not have been feasible and realistic. So all tests performed are related to the exceptional event “loss of a column”. For further exceptional events like “loss of a bracing”, fire and earthquake links and references to other research projects related to these topics are given in the corresponding chapters.

Much effort has been devoted to the definition and the realisation of the testing set-up relative to the testing programmes planned in Trento (tests on components in isolation), Stuttgart (tests on joints in isolation) and in Liège (test on substructure). The tests in Trento should inform about the behaviour of all single components used in the joint and substructure tests. The tests in Stuttgart should allow to indicate how the selected joints behave when subjected to bending and axial forces and undergo a certain load history and the Liège test interpreted, on the basis of the results of the Stuttgart tests has been used to understand how the structure behaves after the loss of a column and to calibrate the FEM tools used in the numerical studies.

Also the test approaches required focused attention on the coordination of the testing programme between the partners. So the adjustment of the various tests was very important (Figure 4-1). It was agreed that the experiments should be a unique chain. This means the joints tested in Stuttgart are part of the substructure test conducted in Liège, as well as the component tests of Trento include all components which are relevant within the joint and substructure tests. Therefore profiles and plates were used of one rolling. The reinforcement for the testing bodies has been ordered together using reinforcement bars of one rolling for each diameter and the same geometry was chosen.

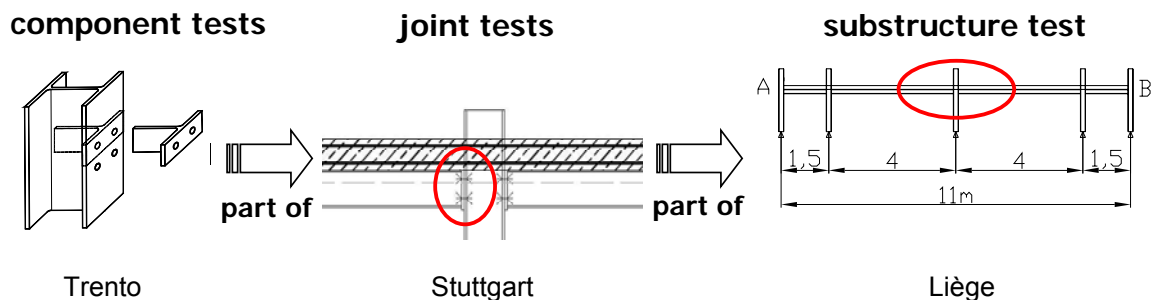


Figure 4-1: Experiments form a unique chain

The component tests inform about the deformation of each single component under uniaxial as well as under biaxial loading. The joint tests shown as result the moment-rotation curves as well as the moment-normal force curves of the test specimens. The substructure test reflects the behaviour of a “whole” structural system when loss of a column occurs. So the component tests are very important to understand and explain phenomena happened in the joint tests and substructure test. And the composite joint tests contribute to identify the M- ϕ and M-N behaviour of the joints for hogging moment as well as for sagging moment and with these findings the numerical tools for recalculation of the substructure test could be calibrated.

As already mentioned the main aim of the present project is to define general requirements for ductile joints as part of a structural system subjected to exceptional loading and to develop simplified design criteria for ductile joint solutions to allow the designer to satisfy the general requirement for robustness expressed in EC 3. The experimental test results on joint components, joints and a whole substructure build also the basis for the system calculation on sophisticated level.

4.2 Concept in view of the event “Loss of a column”

To define the substructure properties, an “actual” composite building has been designed at Liège University according to the EN 1994-1-1 [70] recommendations, so under “normal” loading conditions (i.e. loads recommended in EN 1991-1-1 [64] for office buildings); this actual building is used as Benchmark model 1 in § 5.2 to validate Finite-Element software. Special focus has to be given by extracting a substructure from the actual frame described with dimensions in order to respect the dimensions of the testing floor in the laboratory but also to exhibit a similar behaviour than of the actual frame. The development from the actual frame to the tested substructure is illustrated in Figure 4-2.

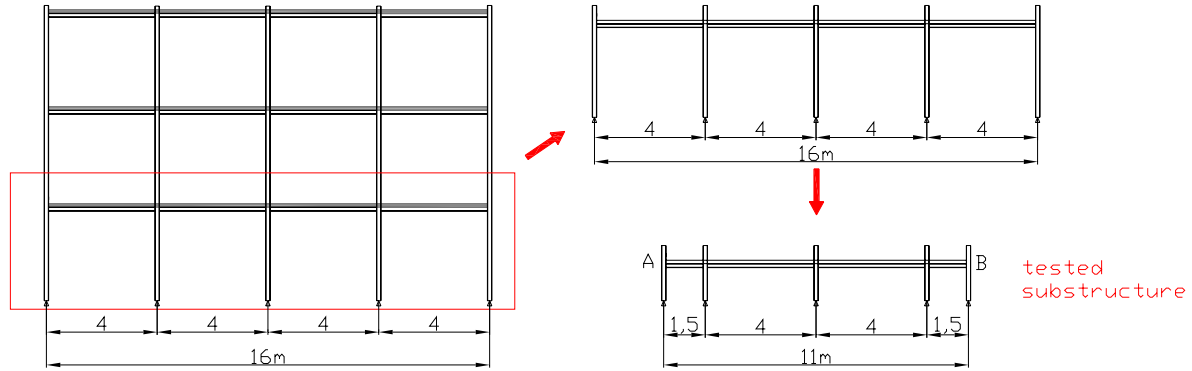


Figure 4-2: From the actual composite building to the tested substructure

4.3 Substructure test

4.3.1 General

The present section introduces the experimental test performed at Liège University (Argenco Department) on a composite substructure simulating the loss of a column in a composite frame. The section is organised as follows:

- In a first step, an “actual” composite building is designed according to the recommendation of EC4 [70], so under “normal” loading conditions (i.e. loads recommended in Eurocode 1 [64] for office buildings) with the aim to obtain realistic dimensions for the structure to be tested; the designed building is presented in § 4.3.2
- As it is not possible to test a full 2-D actual composite frame within the project, a substructure has been extracted from the actual building described in § 4.3.2; the extracted substructure has been designed so as to respect the dimensions of the testing slab but also to exhibit a similar behaviour as the one which would be observed in the actual frame. The extracted substructure is described in details in § 4.3.3.
- Finally, the accomplishment of the test as well as the test results are presented in § 4.3.4, putting into sight the main observations.

More detailed information may be found in the relevant background documents [8], [9], [11], [12].

4.3.2 Design of an “actual” composite building according to Eurocode 4 recommendations

4.3.2.1 Introduction

As said in § 4.3.1, an “actual” composite building is first designed in agreement with the recommendations of Eurocode 4 [70] under “normal” loading. The general layout of the building which is considered with one of its main frame is presented in Figure 4-3.

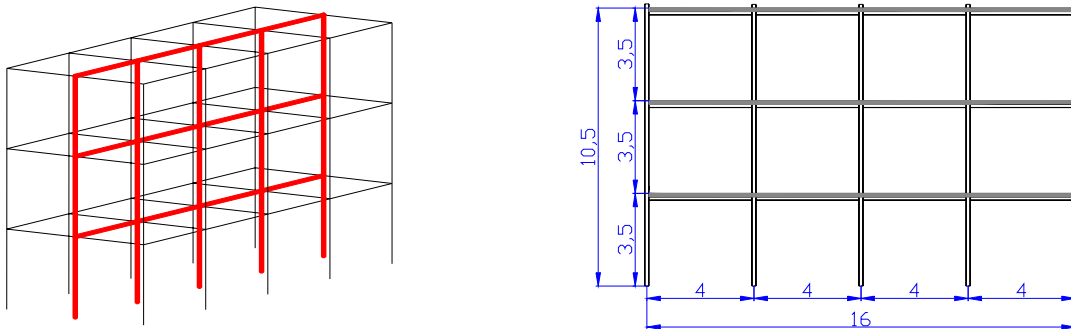


Figure 4-3: 3D view of the designed building and representation of the main frames

The building is composed of three main frames with a space of 3 m between them. The main frames are four bays – three storeys ones with a total width of 16 m (bay span = 4 m) and a total height of 10.5 m (storey height = 3,5 m). The loads which have been considered for the design of the structural elements are the following:

- the self-weight;
- a permanent load of 2 kN/m²;
- an imposed load of 3 kN/m² (load recommended for office building in Eurocode 1 [64]).

The main frames are assumed to be braced and the column bases to be perfect hinges. In a first approach, the external joints are assumed to be fully pinned and the internal ones to be fully rigid; the validity of these assumptions will be checked later on in § 4.3.2.3 presenting the joint design. The static scheme considered for the main frame design is presented in Figure 4-14.

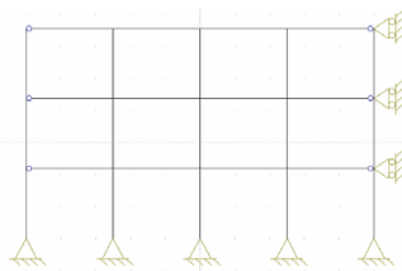


Figure 4-4: Static scheme considered for the main frame design

4.3.2.2 Design of the structural members

The design of the main frame at the middle of the building is given with details in [11] and [26]; according of the latter design, the following structural members have been defined:

- The slab is a reinforced concrete one with a thickness of 120 mm and made of a C25/30 concrete ($f_{ck} = 25 \text{ N/mm}^2$); it has been designed according to the rules given in Eurocode 2 [67].

The reinforcement is composed of two meshes: one place at the top with 10mm rebars space of 200 mm and one place at the bottom with 10mm rebars space of 150 mm. The steel grade for these rebars is S500C (high ductility rebars with $f_{sk} = 450 \text{ N/mm}^2$) and the cover is equal to 25 mm. The cross section of the slab is presented in Figure 4-5.

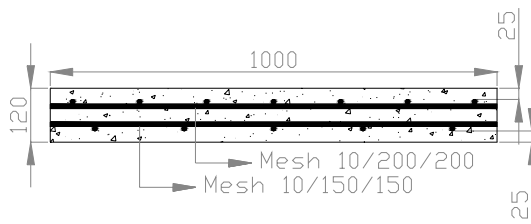


Figure 4-5: Slab cross section

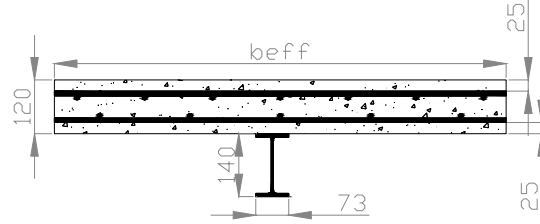


Figure 4-6: Composite beam cross section

- The beams are composite ones (upper flange of the profile connected to the concrete slab); they have been designed according to the rules of Eurocode 4 [70]. The steel part of the beam is an IPE140 profile with a S355 steel grade ($f_{yk} = 355 \text{ N/mm}^2$); the composite beam cross section is presented in Figure 4-6. A full connection between the profile and the concrete part has been designed; the number of studs (Nelson studs with a diameter equal to 16 mm and a height of 75 mm – $f_u = 450 \text{ N/mm}^2$) needed to ensure this full connection is presented in Figure 4-7.
- The columns are steel ones; they have been designed according to the rules given in Eurocode 3 [68]. The profile is an HEA160 one with a S355 steel grade.

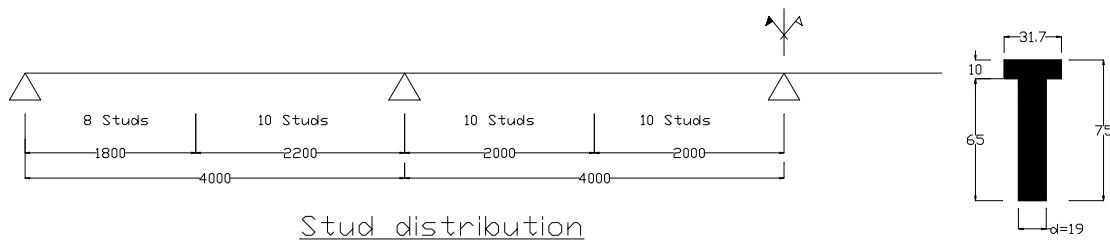


Figure 4-7: Distribution of the studs along the composite beam length

4.3.2.3 Design of the structural joints subjected to hogging bending moments

For the external joints, it is assumed that the concrete slab is stopped in front of the external columns (see Figure 4-8); so, these joints are steel ones.

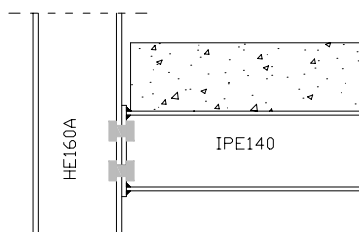


Figure 4-8: External steel joint configuration

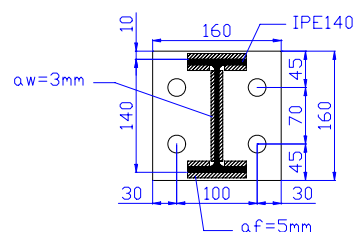


Figure 4-9: Geometrical properties of the end-plate

The joint properties have been chosen so as to ensure a ductile behaviour of the joint at failure and that, with account of the overstrength effects. To achieve this goal, only ductile components are activated at failure. The selected external joint configuration is a flush-end plate bolted joint one. Figure 4-9 presents the geometrical properties of the end-plate.

The bolts are M20 8.8 ones. The end-plate thickness is equal to 8 mm. The steel grade for all the steel components of the joint is S355 with a possible overstrength of 35 % (value proposed in EC8 [71] for seismic design) which corresponds to $f_{y,overstrength} = 480 \text{ N/mm}^2$.

Different states have been considered in the joint design so as to be sure that, even if overstrength occurs in some components, the joint still have a ductile mode of failure. The joint mechanical properties with no overstrength are given in Table 4-1. The latter have been computed through the software CoP [106] and which is in full agreement with the Eurocode 3 recommendations [69].

Table 4-1: Mechanical properties of the external steel joints

	Overstrength	$M_{pl,Rd}$ [kNm]	$M_{el,Rd}$ [kNm]	Failure mode	V_{Rd} [kN]	$S_{j,ini}$ [kNm/rad]
<i>Initial state</i>	No overstrength	15,1	10,1	End-plate in bending	134,4	970

The initial stiffness of the external joints is equal to 970 kNm/rad; the latter is higher than $0.5EI_b/L = 890 \text{ kNm/rad}$ (EI_b is the uncracked flexural stiffness of the composite cross-section of the beam and L is the span of the beam), which is the upper limit under which a joint can be assumed as pinned. So, the assumption of pinned external joints in the actual composite building design is not validated. A computation of one main frame modelled with the predicted properties of the joints has been performed and the internal forces have been compared to the resistance of the joint; the obtained results are presented in § 4.3.2.4.

The steel components of the internal composite joints have the same configuration than the one used for the external steel joints presented in the previous section. A representation of one internal composite joint is given in Figure 4-10.

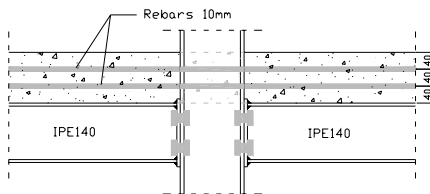


Figure 4-10: Internal composite joint configuration

The mechanical properties of this joint configuration have been computed according to the procedure described in [39] which is in agreement with the Eurocode 4 recommendations [70]. The mechanical properties of the internal composite joints are summarised in Table 4-2 (assuming that the internal joint is symmetrically loaded, i.e. the transformation coefficient β for the column web panel in shear is assumed to be equal to 0).

Table 4-2: Mechanical properties of the internal composite joints

	Overstrength	$M_{pl,Rd}$ [kNm]	$M_{el,Rd}$ [kNm]	Failure mode	V_{Rd} [kN]	$S_{j,ini}$ [kNm/rad]
<i>Initial state</i>	No overstrength	39,8	26,5	Beam flange in compression	134,4	7541

The initial stiffness of the internal joints is equal to 7541 kNm/rad; the latter is lower than $8EI_b/L = 14240 \text{ kNm/rad}$, which is the lower limit above which a joint can be assumed as rigid. So, the assumption of fully-rigid internal joints in the actual composite building design is not validated. A computation of one main frame modelled with the predicted properties of the joints has been performed

and the internal forces have been compared to the resistance of the joint; the obtained results are presented in § 4.3.2.4.

From the previous results, it can be concluded that all the structural joints are semi-rigid and partially resistant. The external steel joint failure is associated to components in tension while the internal composite joint failure to components in compression. It is due to the fact that, in the composite joint configuration, an additional component, which is the reinforcement in tension, is activated; so, the total resistance of the components in tension is increased.

All the failure modes for the two joint configurations are ductile ones, even if overstrength in some components occurs. Nevertheless, there is a difference in the post-limit behaviour of the two joints; indeed, the failure modes are associated in one hand to a component in compression and, in the other hand, to a component in tension. This difference is explained here below:

- For a joint with a failure associated to a component in compression: when $M_{pl,Rd}$ is reached, the joint can not sustain this bending moment (no plateau in the behavioural curve) and the bending moment at the joint level decreases progressively.
- For a joint with a failure associated to a component in tension: when $M_{pl,Rd}$ is reached, the joint can keep this bending moment (plateau in the behavioural curve).

This phenomenon is illustrated in Figure 4-11.

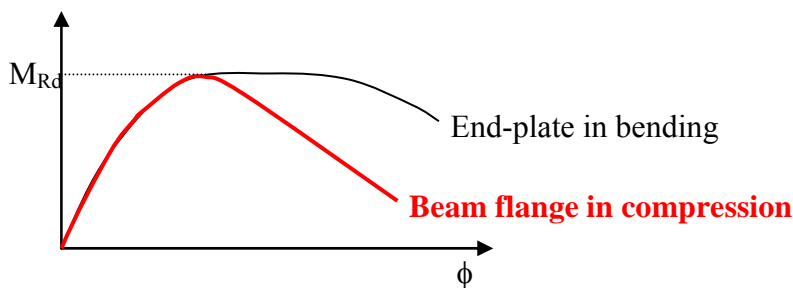


Figure 4-11: Comparison of behavioural curves for different types of failure modes

In the present case, to ensure a good behaviour of the joint under exceptional loading, it is not necessary to keep the bending moment in the post-limit stage. Indeed, to have robustness, only ductility is requested. The rotation capacity of the joint must be sufficient so as to permit to pass from a behaviour of the joints in bending to a behaviour of the joints in tension (associated to the development of membrane forces within the composite beam). In addition, when the joint will work in tension, the fact that the failure in bending is associated to a component in compression can have a positive effect. Indeed, if the failure in bending is associated to a component in tension, an important part of the resistance in tension is already “eaten” when the joint then works in tension; so, if the resistance is associated to a component in compression, the reserve of resistance in tension is bigger.

4.3.2.4 Verification of the internal main frame modelled with the predicted joint properties

According to the joint properties computed in the previous paragraph, an elastic cracked analysis is performed through the software OSSA2D (elastic linear software developed at Liège University – Argenco Department) on the internal main frame (see Figure 4-4). Different load cases are considered; some examples are presented in Figure 4-12.

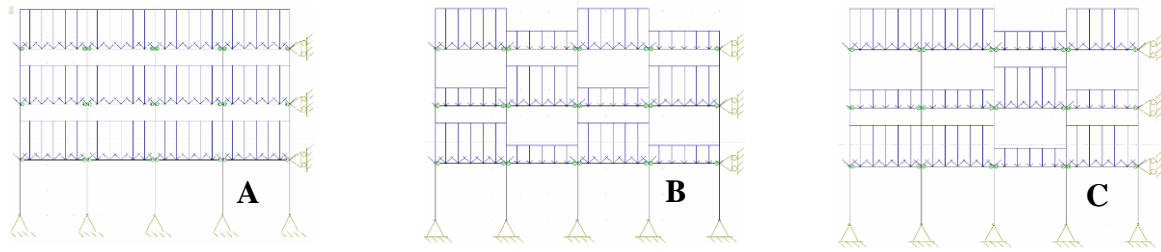


Figure 4-12: Examples of considered load cases

The stiffness of the joints introduced in the modelling is equal to $S_{j,ini}/2$ as recommended in the Eurocodes for an elastic linear analysis. The extreme internal forces which are obtained through this analysis for the different load cases are always smaller than the resistant forces of the structural elements.

A full non-linear analysis has also been performed through the homemade FEM software FINELG [73] validated (for “normal” loading) in § 5.1. The joints and the steel materials have been modelled with elastic-perfectly plastic behavioural curves; the concrete has been modelled with a parabolic curve with tension stiffening. The mechanical properties which have been introduced are the characteristic ones; the loads are the design ones with all the spans are fully loaded (load case A in Figure 4-12).

Through this analysis, the collapse of the frame occurs with the formation of a beam plastic mechanism in the external composite right beam at the second storey for a load multiplier equal to 1.68. Figure 4-13 gives the deformation of the frame at collapse and the load multiplier of the design loads vs. deflection curve at mid-span of the external right beam at the second storey.

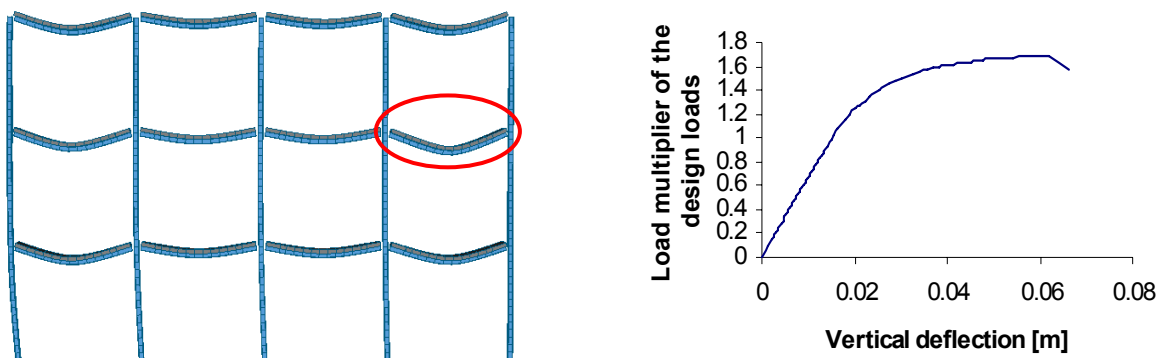


Figure 4-13: Deformed shape at collapse and load multiplier-deflection curve obtained through the non-linear analysis

4.3.2.5 Conclusions

Through the presented design, a three storeys - four bays composite frame has been defined; all the structural members (i.e. the composite beams, the steel columns and the composite joints) have been designed in agreement with the Eurocodes. The joints have been designed so as to be partial-strength ones with ductile modes of collapse (taken into account of the possible material overstrength). In the next section, a substructure to be tested in the Argenco laboratory (Liège University) is isolated from this “actual” building.

4.3.3 Extracted substructure tested at Liège University

4.3.3.1 Introduction

According to the laboratory facilities, it was not possible to test the full actual composite frame previously described. So, a substructure had to be extracted from the latter; this substructure is designed so as to respect the laboratory facilities and to exhibit behaviour as close as possible to the actual frame

one. In the present paragraph, the extracted substructure is described, putting into sight the main modifications according to the actual building.

4.3.3.2 Substructure geometric layout

To perform the test, the bottom storey is isolated from the actual building (see Figure 4-14). According to the reaction slab dimensions in the laboratory, it is not possible to have a width of 16 m for the substructure (which is the width of the actual building). So, it is decided to reduce the width of the external spans as illustrated in Figure 4-14. Also, the width for the concrete slab of the substructure has to be fixed; the chosen width is equal to 500 mm (see Figure 4-15). This width has been fixed so as to be sure that, during the loading, the distribution of the stresses within the concrete will be as close as possible to an uniform distribution; 500 mm is the value of the effective width of the concrete slab in the actual building for the hogging moment zone (according to the recommendation of EC 4 [70]).

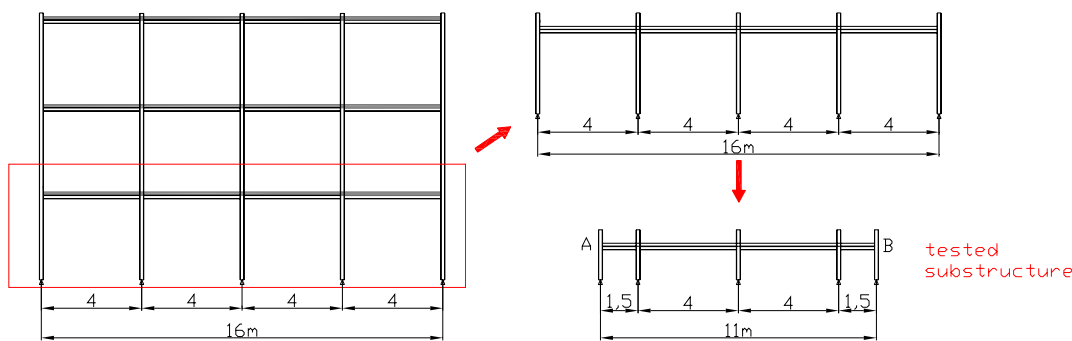


Figure 4-14: From the actual frame to the tested substructure

4.3.3.3 Reinforcement and stud layouts of the substructure

First, it has been agreed to use six 8 mm rebars for the longitudinal reinforcement (151 mm^2) instead of four 10 mm ones (157 mm^2), which are the rebars included within the 500 mm width in the actual building (see § 4.3.2). The scope of this modification is to increase the probability to have a distribution of small cracks along the slab during the loading instead of having big cracks which have to be avoided from the ductility point of view. For the transversal rebars, 10 mm rebars are used as illustrated in Figure 4-15.

Secondly, the layout of the headed studs and the reinforcement has been chosen in a way that a tension band can develop in the concrete slab, with an especially high ductile behaviour. Therefore the distance between the first stud and the face of the column flange is increased compared to standard layout while the amount of reinforcement within this area is kept constant (see Figure 4-15); this type of layout has already been investigated in a previous project conducted by Kuhlmann/Schäfer [83] and showed good results. Also, it has been decided to use studs with a diameter of 19 mm instead of studs with a diameter of 16 mm which permits to limit the number of stud to ensure a full connection (23 studs in the internal composite beam instead of 28 – see Figure 4-7).

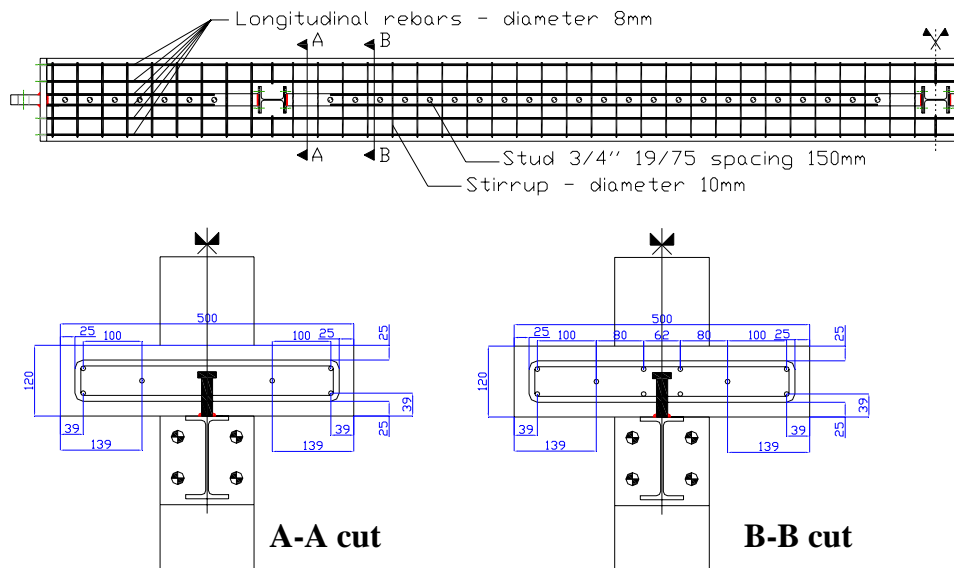


Figure 4-15: Reinforcement and stud layouts

4.3.3.4 Joint and column base configurations within the substructure

At the column bases, actual hinges are placed with the column supports presented in Figure 4-16; teflon elements are put between the pin and the column support so as to limit the friction between these two elements during the loading.



Figure 4-16: Column support and hinge at the external joints

The composite joint configuration in the substructure is the same than the one in the actual building. However, for the joints between the external beams and the external columns (Beam A and Column A respectively in Figure 4-20), it has been decided to place actual hinges (as shown in Figure 4-16) instead of the actual external joint (see Figure 4-8) so as to limit the number of parameters which could influence the response of the internal beams under investigation during the test (Beam B in Figure 4-20).

4.3.3.5 Simulation of the lateral restraint during the test

As previously mentioned, the tested substructure is defined so as to exhibit a behaviour as close as possible to the actual frame one. By isolating the substructure from the actual frame, reducing the length of the external spans and placing actual hinges at the external joints, a key element is modified: the lateral restraint “K” coming from the “undamaged” frame elements and influencing the development of the catenary action which is under investigation, as illustrated in Figure 4-17.

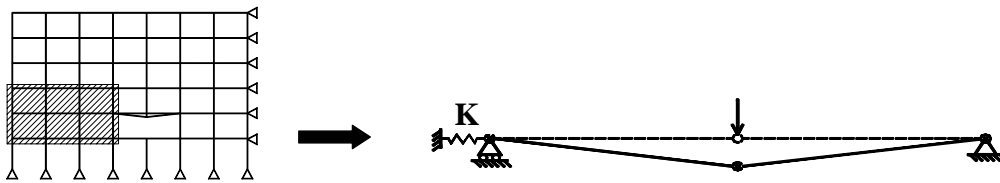
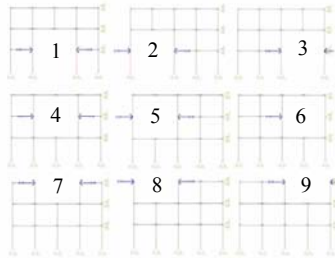


Figure 4-17: Lateral restraint influencing the catenary action

Different values of the lateral restraint “K” have been computed for the actual frame, each “K” value corresponding to different positions of the column loss, as illustrated in Figure 4-18. The computed values for “K” have been obtained through an elastic linear analysis performed with the homemade software OSSA2D.



K_1 [kN/m]	1639	K_4 [kN/m]	2041	K_7 [kN/m]	556
K_2 [kN/m]	794	K_5 [kN/m]	870	K_8 [kN/m]	138
K_3 [kN/m]	2564	K_6 [kN/m]	3333	K_9 [kN/m]	1010

Figure 4-18: Possible positions of column loss for the computation of “K”

For the test, lateral restraints are placed each side of the substructure (see point A and B in Figure 4-14) so as to replace the restraints released by the modifications; the scope of placing them each side of the substructure is to induce a “symmetric” response of the substructure during the test (see Figure 4-19) which facilitates the application of the loads and the measurements.

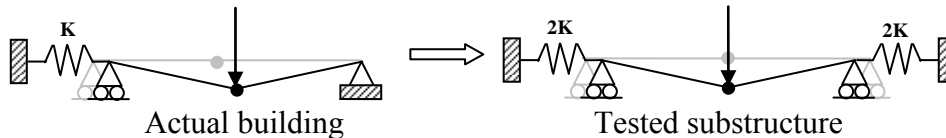


Figure 4-19: Symmetric response of the tested substructure

In practice, these restraints are brought by two horizontal jacks (see Figure 4-20) which are calibrated so as to exhibit a restraint close to the actual one corresponding to the loss of the column at the position 1 (K_1 in Figure 4-18); the restraint is assumed to be elastic from the beginning to the end of the test.

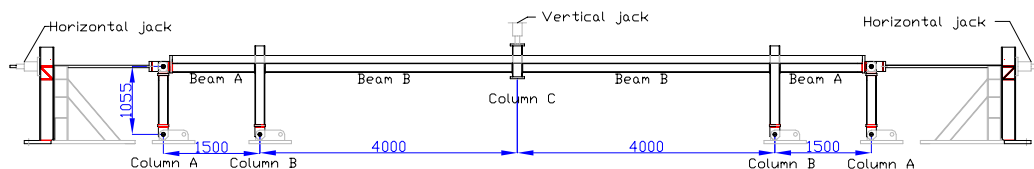


Figure 4-20: Detailed drawing of the substructure test configuration

4.3.3.6 Conclusions

This section describes the substructure extracted from the actual building (designed in the previous section) to be tested at the laboratory of Liège University. Some modifications have been done to pass from the actual frame to the tested substructure so as to respect the laboratory facilities and to facilitate the interpretation of the results; all these modifications have been described and justified in the present chapter. With the so-defined substructure, drawings were prepared and sent to PARE (Profil Arbed Research Establishment) for the fabrication; the latter are given with all the geometrical details in [12].

In the next section, the performance of the substructure test is described and the obtained results are presented.

4.3.4 Substructure test results

4.3.4.1 Introduction

The test accomplishment and the obtained results are described in the present section, see also [11]. The section is divided as follows:

- first, annex tests aiming at characterising the properties of the constitutive materials are presented in § 4.3.4.2;
- then, so as to have the actual geometrical properties of the specimen, measurements have been made on the main elements of the substructure; these measurements are explained in § 4.3.4.3;
- in § 4.3.4.4, the loading path of the test is then described;
- the test equipment of the tested substructure is presented in § 4.3.4.5;
- finally, the test results are given in details in § 4.3.4.6.

4.3.4.2 Characterisation of the constitutive materials

In order to be able to compare the obtained results from the different laboratory, it was decided that all the steel members used for the different tests should come from the same production and rolling. So, the mechanical properties of the steel materials used for the substructure are the ones presented for the joint tests in § 4.4.2.4.

For the concrete slab, twelve tests on cube and four on cylinder were performed. With the cubes, tests in compression at different days (3 cube tests at day 7, 14, 28 and the day of the test (day 72)) were performed to see the evolution of the concrete resistance as presented in Figure 4-21; also, the equivalent resistances which would have been obtained on cylinder (= characteristic value f_{ck}) have been computed according the Eurocode 2 rules [67]. Also, tests in compression have been performed on two cylinders the day of the test and are reported in Figure 4-21; the cylinder resistances computed from the cube resistances are in good agreement with the cylinder test results.

One splitting tensile test was performed the day of the substructure test on a cylinder to obtain the tensile resistance of the concrete; the obtained value from this test is 3.14 Mpa for the tensile resistance. In parallel, one test on the last cylinder was performed to obtain the value of the elastic modulus of the concrete; the obtained value from this test is 26046 Mpa for the elastic modulus. This latter value seems to be small according to the value proposed in Eurocode 2 [67] for C25/30 concrete ($E_{cm} = 31000$ MPa).

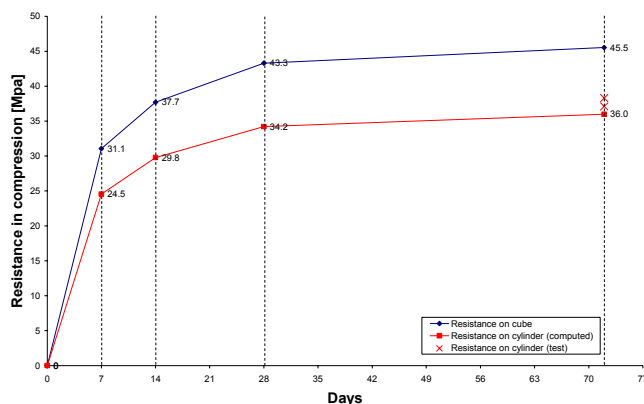


Figure 4-21: Evolution of the concrete resistance in compression with time

4.3.4.3 Geometrical measurements

The scope of the geometrical measurements is to obtain the actual geometrical properties of the constitutive elements of the substructure. The main measurements which have been made deal with the actual dimensions of the IPE140 and HEA160 profiles, the end-plates, the structural members and the substructure in global. Also, the actual position of the rebars in the vicinity of the composite joints have been measured. All these measurements are reported in [11]. The latters have been compared to the dimensions reported on the drawings sent to PARE for the production of the substructure elements [12]; there are all in good agreements.

4.3.4.4 Description of the load path during the test

In the present section, the loading path followed during the test is described. All the actions applied on the substructure have been applied “statically” (i.e. progressive removal of the column), which means that the dynamic aspects of the impact action and of the column loss itself have not been taken into account. It is justified here after:

- One objective of the performed test is to observe the “physic” phenomena linked to the loss of a column in a frame. So, that is why it was decided to remove progressively the column so as to be able to observe all these phenomena.
- Another reason is that the final aim of the test is to validate our numerical tools so as to perform parametrical numerical studies (see § 5.2). To reach this goal, it was needed to be able to measure all the displacements, rotations, loads and strains which was only possible with a progressive removal of the column.

The load path during the test is as follows:

- The substructure is first preloaded with an uniformly distributed load on the internal beams to simulate the reaction of the concrete slab on the main frame in the actual building (see Figure 4-22); during this preloading, two locked jack are placed at the middle of the substructure to simulate the presence of the column, as illustrated in Figure 4-22. In practice, the uniformly distributed load is applied with steel plates and concrete blocks, as shown in Figure 4-22, which represent a total load of 6 kN/m; also, L shape profiles are placed so as to maintain the steel plates and the concrete blocks at their place when big deflection will occur (see Figure 4-22). The 6kN/m load is smaller than the one to be considered for the ULS verifications under the accidental combination of actions ($\cong 10$ kN/m); however, it is the maximum load that can be “safely” applied in the laboratory during the test.

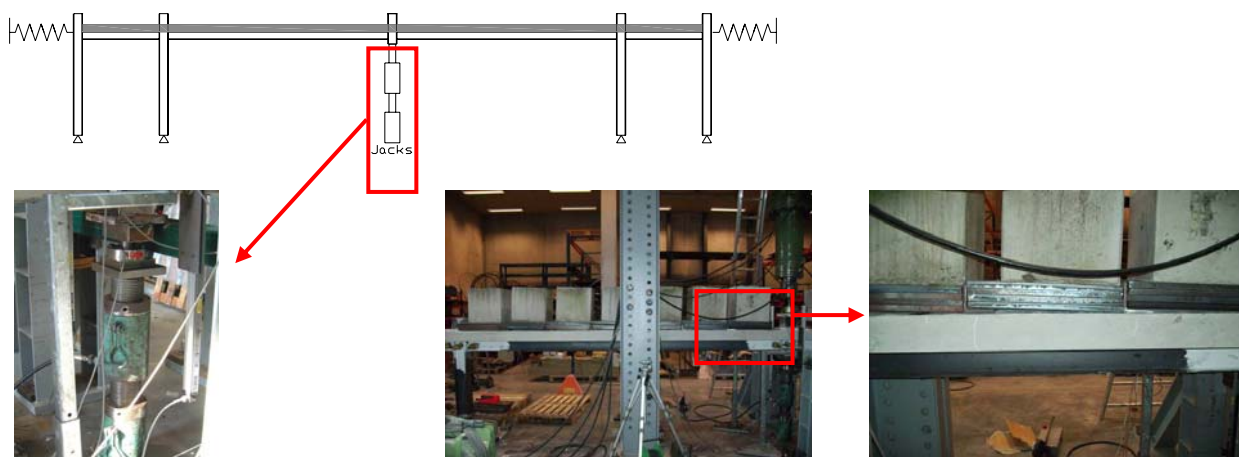


Figure 4-22: Column at the middle simulated by two locked jacks

- In a second step, the support brought by the jacks is progressively removed by unlocking the jack; when the latter are removed, the free deflection of the system is observed. The further step is to apply a vertical force with two jacks on the column thus further deformation will occur (see Figure 4-23).

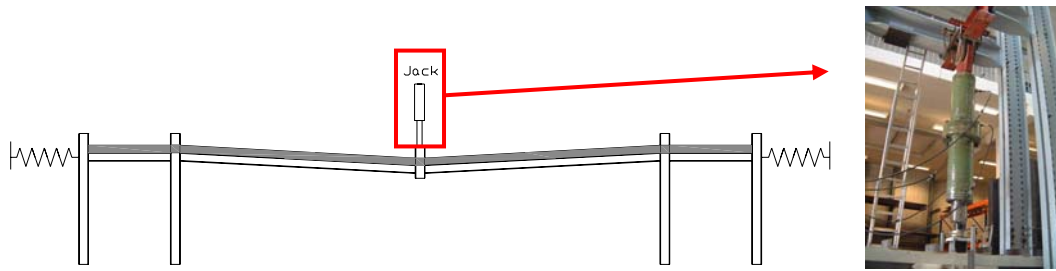


Figure 4-23: Application of a vertical load with two vertical jacks

As explained in § 4.3.3.5, the substructure is laterally restrained with two horizontal jacks to simulate an elastic linear restraint. The system used to simulate this lateral restraint is presented in Figure 4-24.

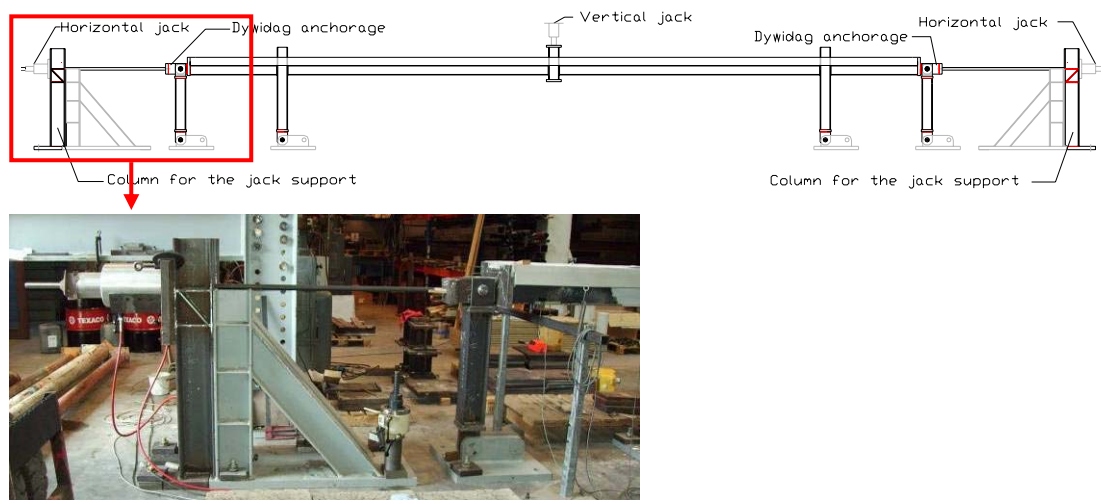


Figure 4-24: Horizontal restraint simulated by horizontal hollow jacks

4.3.4.5 Test equipments

To simulate the presence of the middle column, two screw jacks (displacement controlled) are placed (see Figure 4-22); these jacks permit to be “mechanically” blocked during the application of the uniformly distributed loads. Then, for the application of the vertical load until collapse, two hydraulic jacks (displacement controlled) are placed in tandem (see Figure 4-23) so as to have a maximum displacement capacity of 800 mm. Finally, the lateral restraint is simulated each side of the substructure by hollow jacks (see Figure 4-24) with a displacement capacity of 200 mm (displacement controlled). The applied loads at these jacks are measured through load cells.

Four displacement transducers are placed: two at the middle of the substructure to measure the vertical displacement and one each side of the substructure to measure the horizontal displacement. The displacement transducers are presented in Figure 4-25. Also, rotational transducers are placed in the vicinity of the joint as shown in Figure 4-26.

Four strain gauges have been glued on the bottom flange of the IPE140 profile at three different places (the two external ones (A and C) at 500 mm from the adjacent column and the internal one (B) at the middle) as illustrated in Figure 4-27. The objective with these strain gauges is to have a rough estimation on how the strains (and the stresses) evaluate in the bottom flange during the test.

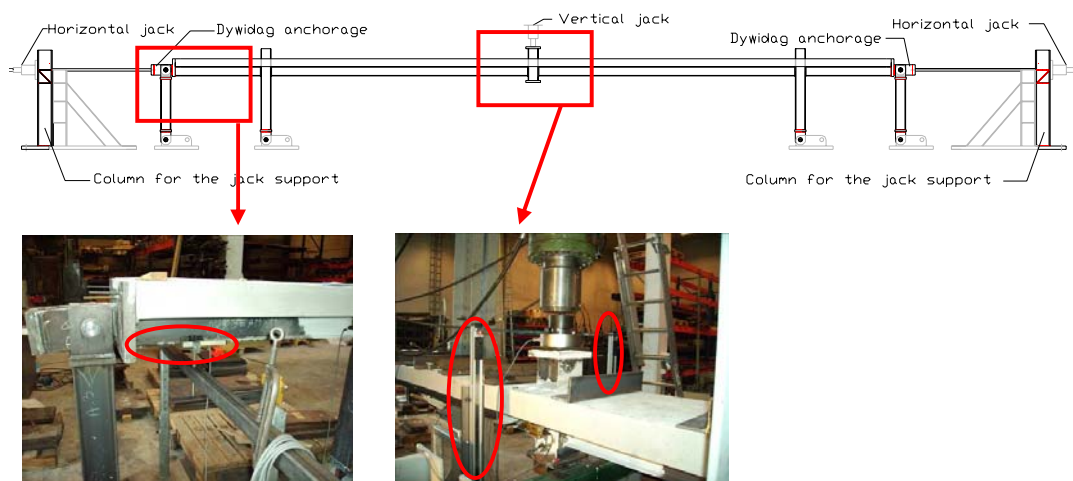


Figure 4-25: Displacement transducers

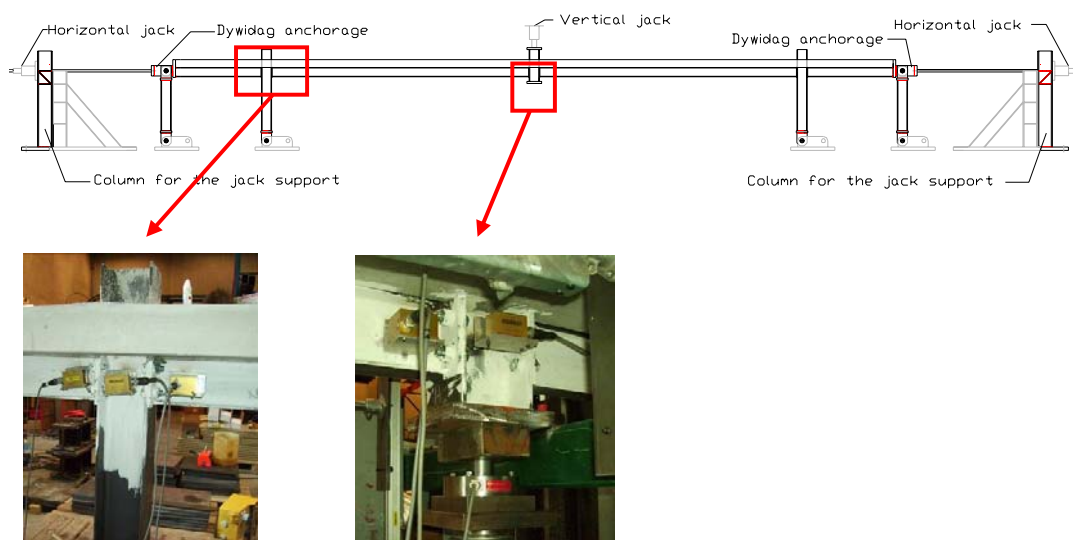


Figure 4-26: Rotational transducers

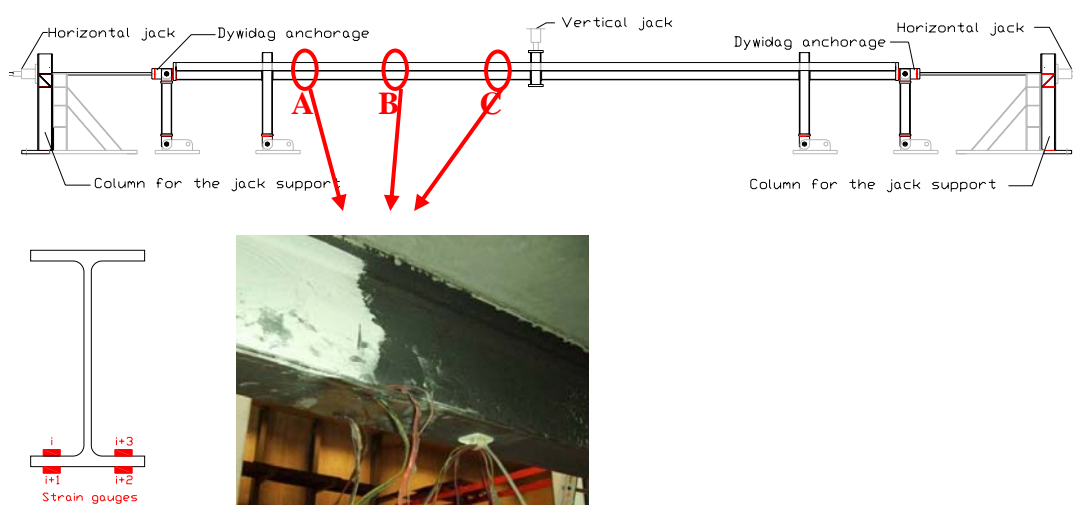


Figure 4-27: Strain gauges at the IPE140 bottom flange

4.3.4.6 Substructure test results

As explained in § 4.3.4.4, a uniformly distributed load is first applied on the substructure with steel plates and concrete blocks. After the application of the latter, first small cracks are already observed in the concrete slab in the vicinity of the external composite joints. After the application of the uniform load, the jacks at the middle are unlocked and progressively removed. The system is completely released, i.e. the applied load at the jacks is equal to 0, when a deflection of 29 mm is reached. At this stage, the width of the cracks at the vicinity of the external joints is bigger and first steel yielding are observed in the column web panel of the internal composite joint.

This first step of the test is illustrated by the part “OA” of the curve presented in Figure 4-28 representing the evolution of the vertical load at the middle of the structure according to the vertical displacement. The vertical reaction which was associated to the uniformly distributed load and to the self-weight of the substructure is equal to 33.5kN (value of the load at point “O”). From Figure 4-28, it can be seen that the structure still be in the elastic range when “A” is reached.

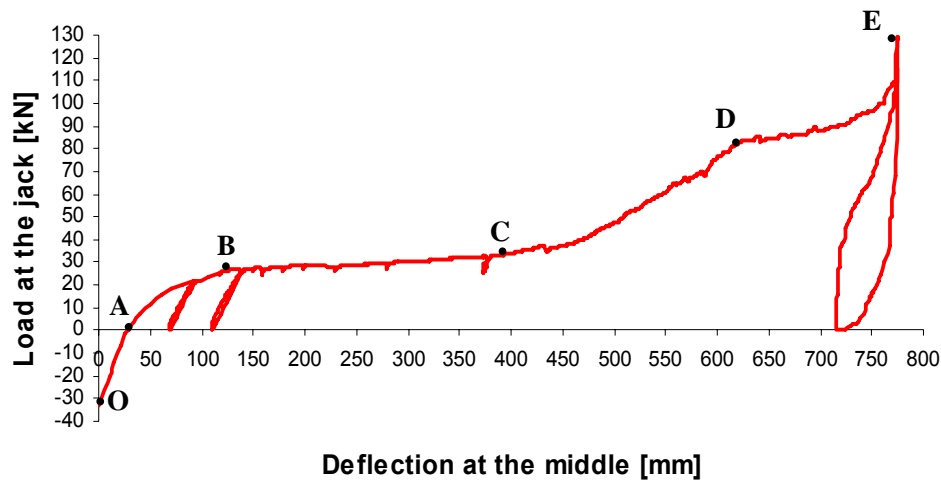


Figure 4-28: Vertical load at the middle vs. vertical displacement curve

Then, as previously mentioned, a vertical load is progressively applied until collapse of the tested specimen. During this stage, two “unloading-reloading” are performed at the beginning of the loading as illustrated in Figure 4-28. From point “A” to “B”, the substructure enters in the yielding stage to finally form a beam plastic mechanism at point “B” with formation of the plastic hinges at the joint level. During this stage, the cracks in the vicinity of the external composite joints are more pronounced (see Figure 4-29) and yielding of some steel components of the joints is observed (column web and beam flange in compression – see Figure 4-30). Also, for the internal composite joint, a detachment between the end-plate and the column flange is observed, as illustrated in Figure 4-30. From point “B” to “C” in Figure 4-28, a plateau is observed which means that the vertical displacements increase for a constant vertical applied load (equal to 30 kN). During this stage, the concrete cracks in the vicinity of the external composite joints continue to develop and yielding spreads in the steel components. One important observation is that the concrete in the vicinity of the internal composite joint splits in compression as illustrated in Figure 4-31.



Figure 4-29: Accentuated cracks in the vicinity of the external composite joints at the formation of the beam plastic mechanism



Figure 4-30: Yielding of steel component at the external and internal composite joints

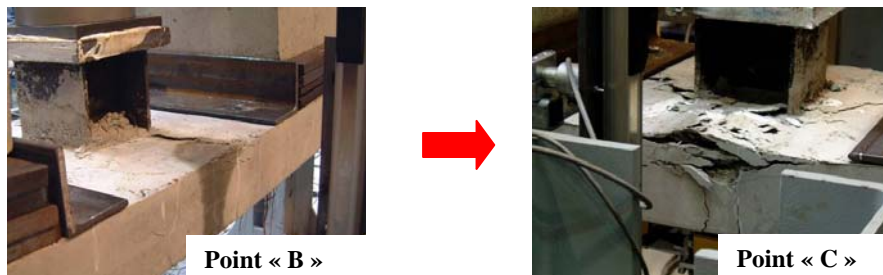


Figure 4-31: Concrete splitting at the internal composite joint

Figure 4-32 gives the horizontal displacements according the horizontal loads at the hollow jacks placed each side of the specimen (see Figure 4-24). As previously mentioned (see § 4.3.3.5), these jacks have been calibrated so as to exhibit a linear elastic behaviour; it is confirmed by the curves presented in Figure 4-32 where the theoretical curve to which the jacks have been calibrated is reflected.

The horizontal jacks begin to be significantly activated at point “C” in Figure 4-28; at this point, membranar forces begin to develop as confirm by the shape of the curve part “CD” in Figure 4-28. At point “D”, the longitudinal rebars in the vicinity of the external composite joints completely collapse (see Figure 4-33) and the external joints work as steel ones. The yielding also spreads in the different components of the internal and external composite joints as illustrated in Figure 4-34 and Figure 4-35. At point “D”, a loss of stiffness is observed in Figure 4-28 which is linked to the loss of the longitudinal rebars in the vicinity of the external joints; indeed, when these rebars are lost, the tensile stiffness of the external joints decreases, phenomenon which affects the development of the membrane forces.

However, it can be observed that the loss of the slab rebars do not affect the loading capacity of the substructure; indeed, after point D, the substructure still be able to support additional vertical loads applied by the vertical jacks at the middle as illustrated by part “DE” of the curve presented in Figure 4-28. This phenomenon can be explained by the fact that, if the vertical displacement at the load application point is kept constant, the membrane forces in the beams are reduced when the axial stiffness is reduced (through the collapse of the rebars). So, if the steel components of the joint are able to support alone, i.e. without the steel rebars, the reduced membrane forces the system can continue to support additional loads; obviously, the remaining steel components have to be sufficiently ductile to support the additional rotation.

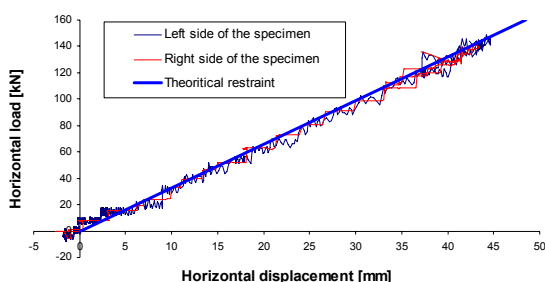


Figure 4-32: Horizontal displacement vs. horizontal load at the hollow jacks curves



Figure 4-33: Collapse of the longitudinal rebars in the vicinity of the external composite joints at point “D” of Figure 4.31



Figure 4-34: Yielding spread in the steel components of the external composite joints



Figure 4-35: State of the internal composite joint at point “D” of Figure 4-28

At the end of the test, a maximum vertical displacement of 775 mm is reached for an applied vertical load of 114 kN; the deformation of the specimen at this stage is presented in Figure 4-36. The maximum horizontal displacement at each side of the structure is equal to 45 mm for a horizontal load of 147 kN; the observed horizontal displacement is illustrated in Figure 4-36.



Figure 4-36: Deformation of the specimen at point “E” of Figure 4-28 and horizontal displacement of the specimen at point “E” of Figure 4-28

At the end of the test, all the joint components of the internal and external composite joints suffer of big deformations and yielding as illustrated in Figure 4-37 and Figure 4-38 (where the damage concrete has been removed). In particular:

- For the external composite joints: yielding of the column web in compression, the beam flange and web in compression, the column flange in bending.
- For the internal composite joints: yielding of the column web in tension (Luders bands) associated to the membrane forces, column flange in bending, beam flange and web in tension.

The test was stopped with the apparition of cracks at the bottom weld between the IPE140 profile and the end-plate at the internal composite joint (Figure 4-39).

The evolution of the joint rotations according to the applied load is given in Figure 4-40; in the “joint rotation”, only the rotation associated to the web panel in shear and the connection in bending are taken into account.

At the end of the test, the maximum joint rotations are equal to 11° (192 mrad) and to 9.5° (166 mrad) for the internal and external composite joints respectively. It can be observed in Figure 4-40 that:

- The behaviours of the internal and external composite joints are much closed.
- The joint rotations are mainly associated to the rotation of the yielded connections, what was already illustrated through the previous figures.
- The beam plastic mechanism develops with formation of plastic hinges in the joints.

From the maximum rotation values observed at the end of the test, it can be concluded that the joints exhibited a very ductile behaviour with a very high rotation capacity, as expected. Also, through these observations, it is confirmed that, even if the collapse mode under hogging bending moment is associated to the component “beam flange in compression”, the ductility of the joint is sufficient to develop the catenary action, as predicted in § 4.3.2.3.



Figure 4-37: External composite joints at the end of the test



Figure 4-38: Internal composite joints at the end of the test



Figure 4-39: Cracks in the welds between the IPE140 profile and the end-plate

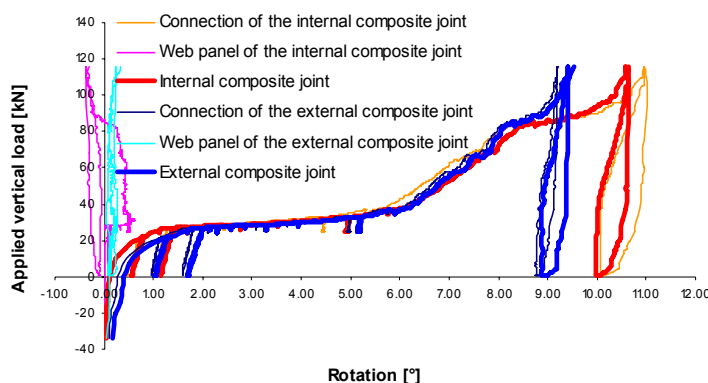


Figure 4-40: Rotation of the internal and external composite joints

As mentioned in § 4.3.4.5, the evolution of the stresses (through strain gauges) was registered. The obtained results are presented from Figure 4-41 to Figure 4-43; the position of the strain gauges at the specimen and in the cross-sections is presented in Figure 4-27. From these results, interesting observations can be made:

- The initial stresses which are observed are linked to the applied permanent loads. Indeed, the curves which are reported begin with the removal of the column at the middle; so, at the beginning of the curves, the permanent loads have already been applied.
- From the strain gauges at the left of the beam (position A in Figure 4-27), it can be seen that the bottom flange is in compression but, when the plastic mechanism is formed (for a vertical load of about 30 kN), the compression stresses decrease with the development of the membrane forces. At the end of the test, the stresses are close to 0.
- The bottom flange at the middle of the beam (position B in Figure 4-27) is in tension all along the loading and still in the elastic range. It seems that a problem occurred for the gauge 5 during the test; this gauge will not be taken into account for further investigations.
- At the right side of the beam (position C in Figure 4-27), close to the internal composite joint, the bottom flange is in tension and, after the formation of the beam plastic mechanism, the latter yields with the development of the membrane forces (stresses close to 400 MPa which is the actual elastic limit of the IPE140 flange).
- In all the gauge measurements, it can be observed that the stains (and the stresses) are affected by the collapse of the rebars at the external composite joints (for an applied vertical load of about 90 kN).

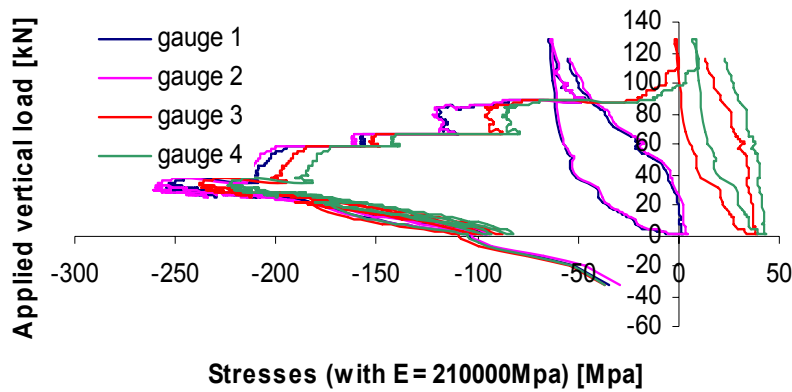


Figure 4-41: Evolution of the stresses in the bottom flange at position A (see Figure 4-27)

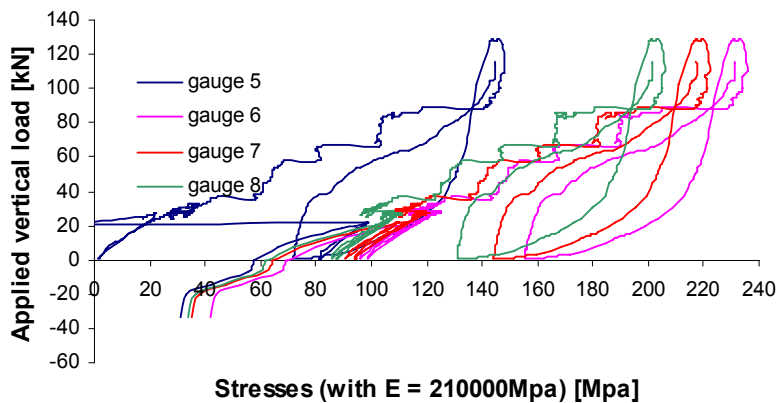


Figure 4-42: Evolution of the stresses in the bottom flange at position B (see Figure 4-27)

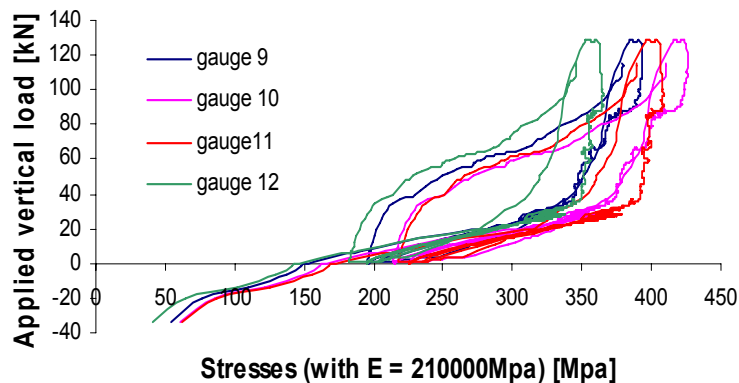


Figure 4-43: Evolution of the stresses in the bottom flange at position C (see Figure 4-27)

After the test, the steel plates and the concrete blocks were removed so as to see the disposition of the cracks along the concrete slab. As shown in Figure 4-44, only two big cracks appeared in the vicinity of the external composite joints what was not expected. Indeed, as mentioned in § 4.3.3.3, the studs layout (see Figure 4-15) was fixed in agreement with the recommendation of a previous project [83] so as to have a good distribution of the cracks in the zone without studs; according to the presented results, the recommendation can not be validated. The apparition of one big crack in the vicinity of the joint is associated to the fact that, even if the composite joints are composed of flush end-plates, the latter are extended in the concrete slab (see Figure 4-10); so, when the end-plates deform, a crack is easily initiated by the part embedded in the concrete.

However, the joints exhibited a very ductile behaviour during the test although to have one big crack is not the best situation from the ductility point of view.

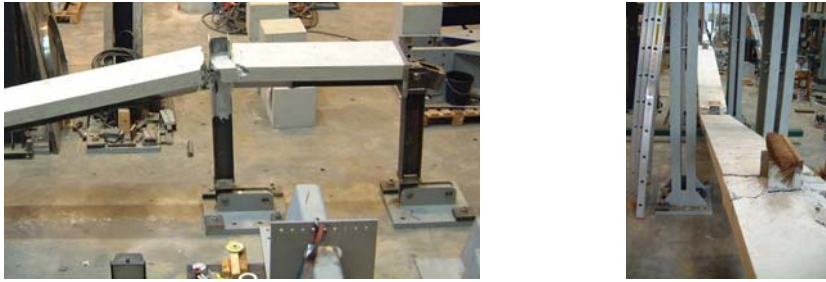


Figure 4-44: Distribution of the cracks in the concrete slab

4.3.5 Conclusions

The objective of the performed test that was to simulate the loss of a column in a composite frame to observe the development of the membrane forces in the structure after the loss of the column and the effects of these forces on the joint response.

The tested specimen was extracted from an actual building designed in agreement with Eurocode 4 recommendations and that, for normal loading, i.e. design loads recommended in Eurocode 1 without account of the exceptional loading “loss of a column”. The tested specimen and the test configuration were defined so as to observe a behavioural response as close as possible to the one that the actual would have exhibited.

The main measurements which were registered are the vertical displacements at the column loss level, the rotations of the main joints and the horizontal displacements and forces appearing at the specimen extremities.

The performed test was successful and all the phenomena under investigations were registered. Indeed, the development of the catenary action in the system was observed and the registered curves confirmed the development of membrane forces in the beams. Also, the composite joints loaded by combined tensile forces and bending moments exhibited a ductile behaviour as expected.

The results obtained through this test is used later on to validate the numerical tools (§ 5.2) and the developed analytical model in § 5.3.4.

4.4 Joint tests

4.4.1 General

The joint tests realized at the University of Stuttgart can be subdivided into two main series: One series on composite joints with dimensions and design related to the substructure test in Liège, and a second series bending tests on pure steel joints. The tests on composite joints mainly investigate the behaviour of the joints under combined loading. Special focus is given to the load path. Main aim of the composite joint tests performed in Stuttgart is to analyze the joint response under biaxial loading. Especially the M-phi-curve and the M-N-interaction of the joints are investigated. These both characteristic data of a joint express the strength and ductility of a joint and point to the possibility to activate additional membrane forces. Due to the fact that membrane forces can be activated allowing a redistribution of internal forces, additional bearing capacity of the structure could be achieved.

In the following figures the investigated scenario within the composite test series is illustrated.

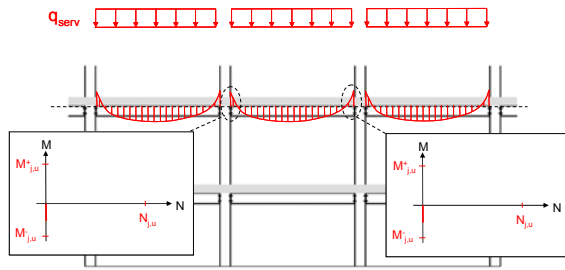


Figure 4-45: Stage I: Service conditions

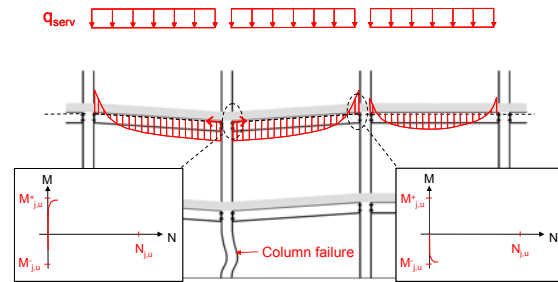


Figure 4-46: Stage II: Column failure

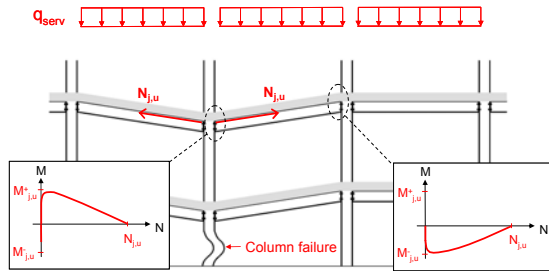


Figure 4-47: Stage III: Membrane state

The illustration in Figure 4-45 to Figure 4-47 show the theoretical behaviour of the frame structure when loss of a column occurs and what happens in the joints directly influenced. In the undamaged structure the joints are only stressed by bending. When column failure takes place large deformations within the structure appear

The aim of the pure steel joint tests on large IPE 500 profiles with thin endplates is to analyse the ductility of steel joints and their main components bolts in tension and endplate in bending. In previous tests conducted in Stuttgart by Kuhlmann/Schäfer [83] brittle failure of the bolts had been observed although the ductility criterion according to EN 1993-1-8 [69] was not violated. It is assumed that the brittle bolt failure occurred due to bending exposure of the bolts as well as additional bearing effects in the endplate by membrane conditions. This bending exposure seems to depend on the distance between the flange and the web of the beam on one hand and the bolt on the other side. To receive more reliable criteria these tests with varied endplate thickness and bolt distances were conducted. A strong dependency of the failure mode results from the behaviour of the single components.

4.4.2 Composite joint tests

4.4.2.1 General

As explained for the substructure test in § 4.3.3 two different situations exist: a hogging bending moment for the first inner joint in Figure 4-45 to Figure 4-47 which undergoes an increase of the bending moment as well as an additional membrane force action and a sagging moment with a combined tension force at the inner joint where the loss of the column occurred. To investigate this five composite joints under combined loading have been tested, three joints under negative (hogging) moment and two joints under positive (sagging) moment. The first of each group has been stressed until M_u in order to evaluate the actual hogging and sagging bending capacity. For the following tests the joints were exposed to a change from pure bending moment to combined bending and tension. For the specimens under combined loading the vertical jack was stopped at $\approx 0.95 M_u$ to ensure that all components are still serviceable when starting the horizontal loading. The dimensions as well as the used profiles for the joint configuration are given in Figure 4-48 to Figure 4-50 and follow the chosen sections of the sub-structure test. For both types of composite joint tests, for hogging moment as well as sagging moment tests, special care has been taken of the loading procedure, see Figure 4-51 and Figure

4-52. At the first stage, see Figure 4-51, by increasing force and deformation by the vertical hydraulic jack a moment just below the ultimate moment of the joint $M_{j,u}$ was applied to the testing specimens. Then the vertical jack was arrested in order to keep the rotation of the joint as presented in Figure 4-52. Then by the horizontal hydraulic jack a tensile force was applied on the testing body, leading to a biaxial loading of the specimen. The tensile force was increased until collapse of the joint. The arrangement of the transducers at the composite joints was chosen in order to measure all components of the joints which contribute to the rotation capacity of the joint and to determine the single load deformation behaviour of the relevant components.

The most important outcome of the joint tests is the moment-rotation curves as well as the M-N-interaction behaviour. Both are needed later to compare and calibrate the joint behaviour which is given by the numerical simulations. For more detailed information about the composite joint tests see [21], [22].

4.4.2.2 Design and dimensions of the joint test specimens

The cross section of the composite joint given in Figure 4-49 was chosen according to the substructure test in Liège, using the same materials. The steel connection consists of a 160 x 160 mm endplate with a thickness of 8 mm of steel grade S355. The bolts were M20 bolts of grade 8.8. The concrete slab had a thickness of 12 cm and a width of 50 cm. To get very ductile joints the component „reinforcement in tension“ had been performed analogous to the tests of Kuhlmann/Schäfer [83]. The layout of the shear studs had been chosen in the way that the distance between the column profile and the first shear stud was much more than conventionally (see Figure 4-50). Highly ductile reinforcement (B 450 C) with a very large expansion length and great hardening factor $f_u/f_y > 1.3$ was arranged. Also the expansion length in the column section of the concrete slab was increased. Instead of using diameter 10 mm it had been agreed to use diameter 8 mm for the longitudinal bars and diameter 10 mm for the transversal ones. The amount of reinforcement had also been slightly adjusted in order to make sure that a ductile failure mode in the concrete slab would occur. The aim of this special modification of the component “reinforcement in tension” was to have a lot of small cracks instead of having only a few big cracks. By increasing the distance of the crack distribution at both sides of the column and control at the same time the crack width the expansion of the tension bar in the concrete slab might be increased. But the development of a tension band in the concrete slab depends also very much on the actual material properties.

The concrete slab was intentionally designed only with a width of 50 cm to limit the number of parameters which could influence the component “reinforcement in tension”.

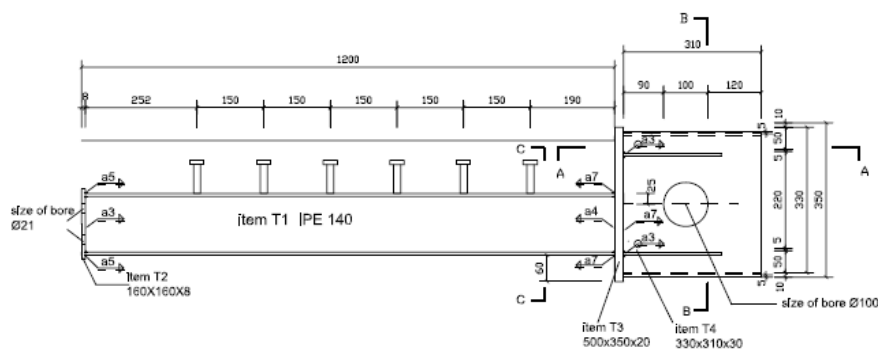


Figure 4-48: Steel beam IPE 140 with the arrangement of the shear studs

In Figure 4-48 the workshop drawing of the steel beam belonging to the composite joint illustrates all dimensions and distances of the single members as well as the load application point for horizontal loading at the end of the beam.

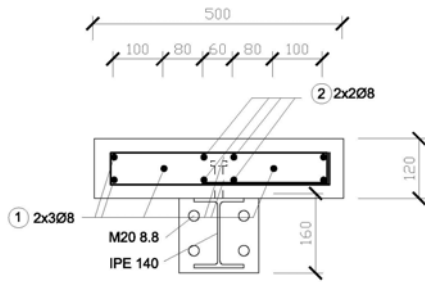


Figure 4-49: Cross-section

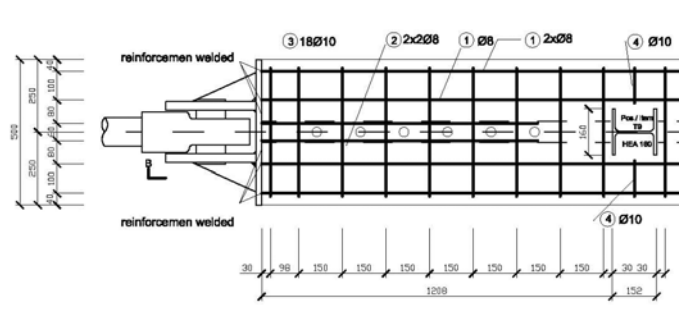


Figure 4-50: Layout of the test specimen

The shear studs were designed with a diameter of 19 mm to ensure a full shear connection and to minimize the number of studs. The length of the shear studs was chosen with $l = 75$ mm to have enough concrete cover at the top of the slab and to fulfil the requirement according EC 4-1-1 § 6.6.5 [70] that the distance between the lower layer of reinforcement and the lower fibre of the stud's head was at least 30 mm.

4.4.2.3 Test setup

In Figure 4-51 and Figure 4-52 the test station with the two hydraulic jacks and a test specimen is shown. The hydraulic jacks were operating deformation controlled. The vertical hydraulic jack could apply a maximum force of 2.5 MN, the horizontal jack was able to apply a maximum force of 1.0 MN. The used loading velocity for the tests was 1mm/min. By increasing force and deformation by the vertical hydraulic jack a bending moment was applied to the testing specimen. The deformation of the testing body was increased nearly up to the ultimate moment of the joint $M_{j,u}$ then the vertical jack was stopped (see Figure 4-51). So for the second stage of the testing procedure the vertical jack was arrested by fixing the imposed deformation and not by keeping the vertical loading on a fixed value.

In the second step of the loading procedure the horizontal jack applied a tensile force leading to a decreasing moment exposure of the joint. The tensile force was increased until failure of the test specimen (see Figure 4-52).

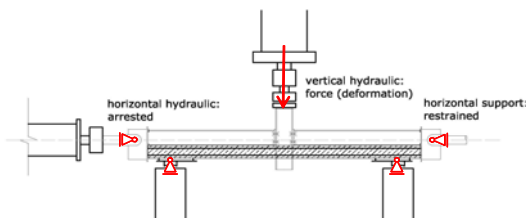


Figure 4-51: Load step 1 (corresponds to stage II Figure 4-46)

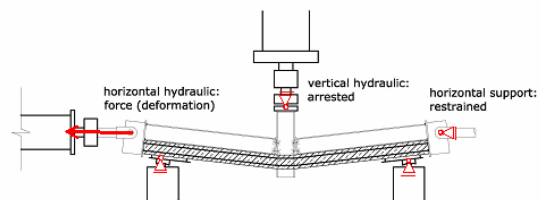


Figure 4-52: Load step 2 (corresponds to stage III Figure 4-47)

4.4.2.4 Material characteristics

The behaviour of the total joint primarily depends on the behaviour of the collapsing components. For the composite joint tests nearly all joint components are stressed up to yielding so the actual strength of each component is important for the overall joint behaviour. In the following the yield strength and the tensile strength of steel components as well as the mean cylinder compressive strength of the concrete determined at the University of Stuttgart are given.

IPE 140:	$f_y \approx 430 \text{ N/mm}^2$	$f_u \approx 550 \text{ N/mm}^2$
HEA 160:	$f_y \approx 390 \text{ N/mm}^2$	$f_u \approx 520 \text{ N/mm}^2$
endplate:	$f_y \approx 570 \text{ N/mm}^2$	$f_u \approx 660 \text{ N/mm}^2$
bolts :	$f_y \approx 735 \text{ N/mm}^2$	$f_u \approx 918 \text{ N/mm}^2$

reinforcement: $f_y \approx 540 \text{ N/mm}^2$ $f_u \approx 660 \text{ N/mm}^2$

concrete: $f_{cm,cyl} = 0.805 f_{cm,cube} = 0.805 \times 30 \text{ N/mm}^2 = 24,15 \text{ N/mm}^2$

4.4.2.5 Properties of the joints

The joints have been designed in order to ensure an overall ductile behaviour of the joint also with account of over-strength effects. The joint configuration is described in Figure 4-53 and Figure 4-54.

For the preliminary analysis of the joints a possible over-strength of 35% (value proposed for seismic design in EC 8 [71]) was assumed for all components with steel grade S 355. In the internal report of the University Liège about the “Experimental test simulating the event loss of a column in a composite building” [11] a comparison about the influence of over-strength depending on different components is shown.

In Table 4-3 the moment resistance of the composite joints according to the procedure of the component method in EC4 [70] and EC3 [69] have been computed. For the initial state the yield strength $f_y = 355 \text{ N/mm}^2$ and the tensile strength $f_u = 510 \text{ N/mm}^2$ corresponding to the standard have been used. For the second state the values f_y and f_u according the tensile tests mentioned in the chapter above have been used.

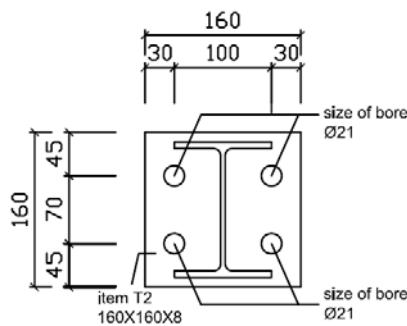


Figure 4-53: Geometrical properties of the endplate

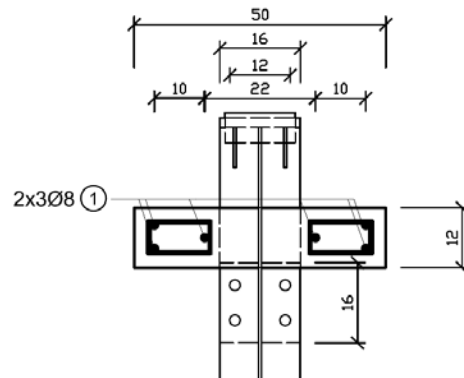


Figure 4-54: Geometrical dimensions of the composite joint

As already mentioned in § 4.3.2.2 the weakest component of the internal joint under hogging moment is the beam flange in compression for material properties according to standard as well as for the actual properties.

Table 4-3: Bearing capacities of the joints (hogging moment) acc. EC 4 Part 1-1

	Overstrength	$M_{e,R}$ [kNm]	$M_{pl,R}$ [kNm]	M_u [kNm]	Failure mode
Initial state	no	27.1	40.5	55.8	BFC
2° state	all	33.4	50.1	60.5	BFC

The joints under sagging moment include the component “Concrete under compression” which is not defined until now in the EC4. To estimate the maximal bearing capacity the procedure to compute the theoretical capacity M_{pl} was derived from computation of M_{pl} of a composite girder under sagging moment. First the maximum acceptable tension force of the steel components, including the bottom layer of the reinforcement is determined, next the height of the compression zone x_{pl} is calculated and afterwards the single inner lever arms of each tension component could be identified. The used compressive strength of the component concrete slab under compression for the calculation, the mean cylinder compressive strength is considered. In Table 4-4 the calculated values for the moment bearing

capacity under sagging are presented. The initial state shows again the values considering all strength according to the standard and the 2° state reflect the actual material properties.

Table 4-4: Bearing capacities of the joints (sagging moment) acc. EC 4 Part 1-1

	Overstrength	$M_{e,R}^+$ [kNm]	$M_{pl,R}^+$ [kNm]	M_u^+ [kNm]	Failure mode
Initial state	no	36.9	54.8	-	CC
2° state	all	43.8	65,3	-	CC

4.4.2.6 Results of the joints under pure bending exposure

A. HOGGING MOMENT

For the composite joint tests under hogging moment, the first cracks started from the lower corners of the column flange and ran diagonally to the edge of the slab as visible in Figure 4-56. By increasing the load, some further cracks developed in the distance of the stirrups on both sides of the column, this is illustrated by Figure 4-55. But the crack width of the diagonal cracks at the column flanges became by far the largest of all cracks. The curve of the rotation capacity for the joints under hogging bending moment (negative moment), see Figure 4-57 has an elastic, initial stiffness up to $M_j \approx 18$ kNm. At this point the first cracks at the lower fibre of the concrete slab appeared and the cross-section came more flexible. This resulted in a decrease of the stiffness which led to a bend in the curve. In the following the curve goes linearly up to $M_j \approx 40$ kNm. From there a yielding of the first components started and the curve came flat.



Figure 4-55: Crack distribution in the distance of the stirrups

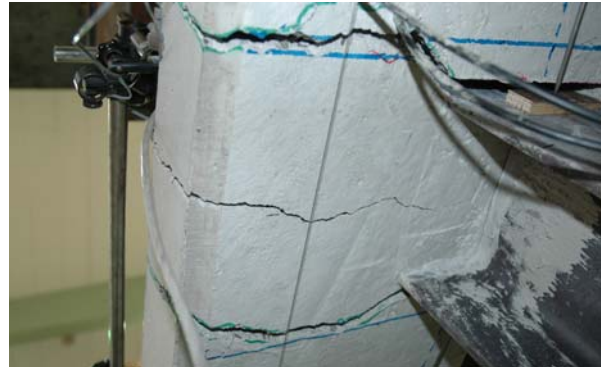


Figure 4-56: Two big cracks at the corner of the column profile

All test specimens V1-V3 showed similar M-phi-curves which was due to the fact that the material characteristics for each component in the different tests are the same. The first test specimen under hogging moment V1 aimed at the evaluation of the real moment bearing capacity. Due to that reason the available rotation capacity of V1 differ a little bit from V2 and V3 (see Figure 4-57).

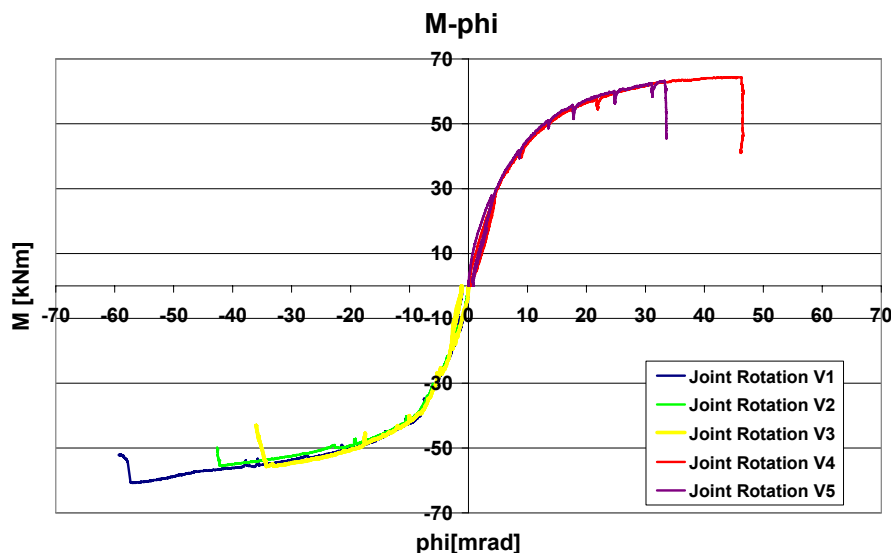


Figure 4-57: M-phi-curves for the “pure” joint rotation

horizontal loading.

B. SAGGING MOMENT

Whereas the behaviour of the joint rotation for hogging moment was mainly influenced by the steel components (including the rebars) the behaviour of the joint rotation for sagging bending moment depends on the effect of crumbling of the concrete at the upper surface of the slab, as presented in Figure 4-58. Just before reaching a horizontal tangent of the curve the concrete at the upper surface began spalling and that was also the reason for the limitation of the bearing capacity, see Figure 4-59. At the two tests under sagging moment it turned out that the concrete slab under compression could not carry the strong compressive strain which was determined by the sharp bend from the joint rotation. The test specimen V4 aimed again at the evaluation of the real moment bearing capacity under sagging moment. For the test specimen V5 the vertical jack was stopped by beginning of the effect of crumbling at the concrete surface that is the explanation of the different rotation capacities of both tests.



Figure 4-58: Crack distribution and deformation behaviour for sagging moment

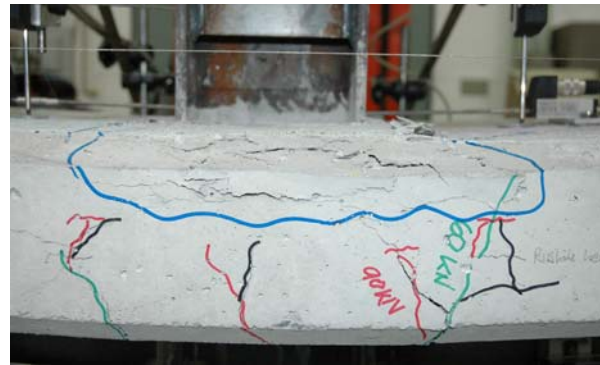


Figure 4-59: Crumbling of the concrete in column section

The test specimens under sagging moment have an initial stiffness a bit greater than for hogging moment. The curve of the rotation capacity for sagging moment starts with an elastic initial stiffness up to $M_j \approx 28$ kNm. At this point the first small cracks appeared at the lower fibre of the concrete slab and the next part of the M-phi-curve is curvilinear. The continual curvilinearity stays until reaching the limit load.

4.4.2.7 Results of the M-N-interaction

The interaction between the moment and normal-force exposure of the joint during the test procedure was calculated as followed:

- During the first step the tests specimen was under pure bending exposure. A vertical load was applied by the vertical jack and due to the symmetry of the test specimen the vertical support reactions were assumed to be $V/2$. The lever arm between endplate and vertical support was 924 mm as illustrated in Figure 4-60.

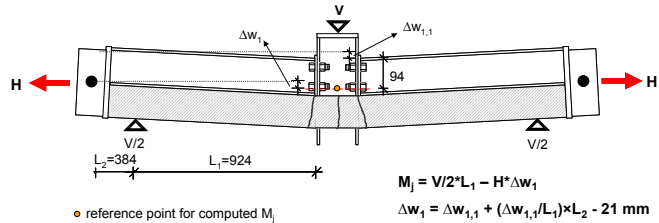
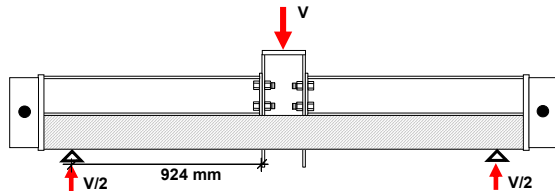


Figure 4-60: Bearing reactions for the first state of the loading procedure

Figure 4-61: Bearing reactions for the second state of the loading procedure(hogging)

- For the second step of the loading procedure the vertical jack was arrested with the certain deflection and the horizontal loading began to start by the horizontal jack. The horizontal tension force caused an additional joint moment which counteracted in opposite direction of the joint moment caused by the vertical jack. The inner lever arm of the H-force depended on the choice of the reference point, the location of the load application point and of the deflection of the test specimen. All geometrical values for the calculation of additional joint moment due to the horizontal tensile force are given exemplary for hogging state in Figure 4-61.

For the computation of the joint moment for sagging moment it had to be considered that the test specimen was upside down in comparison to hogging moment.

The M-N-curves in Figure 4-62 for positive and negative moment are in good agreement with the theoretical curve calculated in § 5.3.4.2. The M-N-curves for positive moment change at the end into negative moment and meet the M-N-curves for negative moment at the same level.

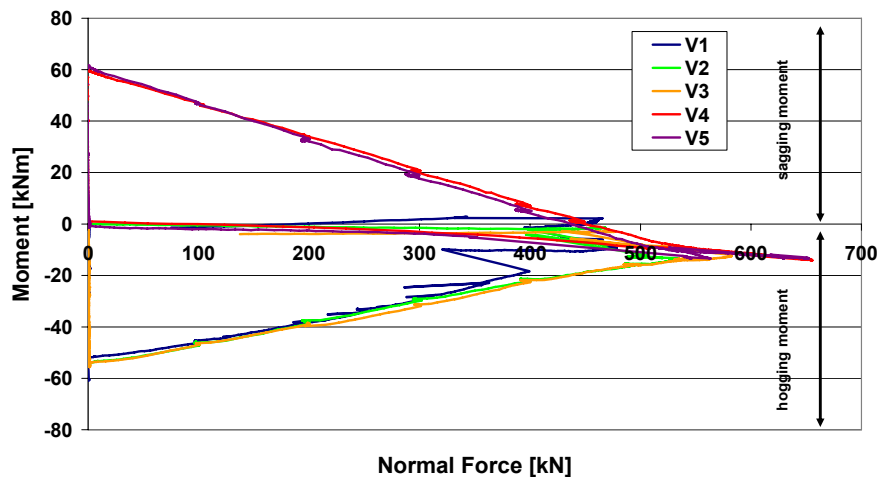


Figure 4-62: Computed M-N-curves of the composite joint tests

because by starting the horizontal loading fracture of one rebar already happened and so only five rebars have been available for the M-N-interaction. Before reaching the maximum horizontal tension force the second and third rebar ruptured during test V1. For the tests V2 and V3 rupture of the rebars occurred not before reaching the ultimate tension force. That's the explanation of the different behaviour of the curve V1 in comparison to V2 and V3 (Figure 4-62). So the top tension force for V2 and V3 was about 100 kN more than for V1 which corresponds to bearing capacity of 3 Ø 8mm rebars

For hogging moment the initial conditions by starting the biaxial loading were the following: the concrete slab was under tension and more or less totally utilised, the upper flange of the steel beam and the upper bolt row were under compression. The M-N-curves for hogging moment looks very similar for the tests V2 and V3 (see Figure 4-62). The curve of test V1 differed a bit

($1.5 \text{ cm}^2 \times 66 \text{ kN/cm}^2 \approx 100 \text{ kN}$). At the end failure of all rebars occurred (as illustrated in Figure 4-63) whereas the pure steel joint was still able to carry a remarkable load. In Figure 4-63 the highly ductile behaviour of the steel components of the joint are well illustrated as well as the different deformation behaviour of the endplate and the column flange in the Figure 4-63 bottom right.



Figure 4-63: Test specimen V1 after failure under M-N exposure (hogging)

For sagging moment the initial conditions by starting the horizontal tension loading differed from hogging moment. The compression zone of the concrete slab was over nearly the half height of the slab and the lower bolts were under tension. Because the ultimate joint moment was limited by the bearing capacity of the concrete under compression all components which were able to carry tension load were still available when starting the biaxial loading. So both curves V4 and V5 had nearly the same behaviour and the same ultimate horizontal tension load. As visible in Figure 4-62 the joint moment changed at the end of the test from positive into negative. This was also confirmed by the failure mode observed during the test. The failure mode was rupture of all rebars in the concrete slab and in the test V5 an additional fracture of one upper bolt occurred in Figure 4-64 down left. For the test under sagging bending moment and tension the overall ductile behaviour of the pure steel part of the joint is visible and also the component column web in tension was clearly activated and yielding occurred as the Luders's bands in Figure 4-64 indicated.



Figure 4-64: Test specimen V4 after failure under M-N exposure (sagging)

The photo top left in Figure 4-64 shows the failure of the concrete slab including the rebars and the rupture of one of the upper bolts is visible in the photo down left. This supports the findings of the computed M-N-curves that just before collapse the moment changed into opposite and the tension stressing under biaxial loading was maximum at the upper part of the joint.

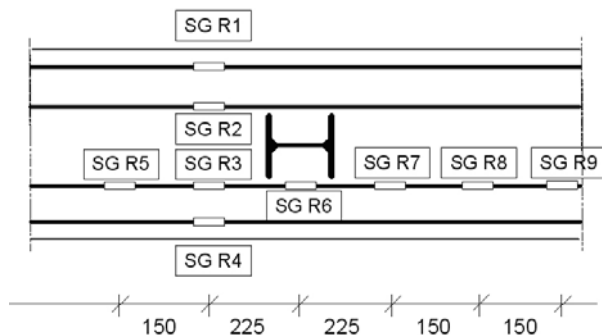


Figure 4-65: Arrangement of strain gauges on rebars for test V1

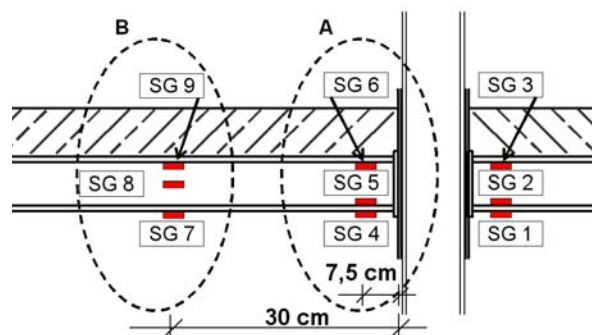


Figure 4-66: Arrangement of strain gauges on IPE 140 for tests V1-V5

To observe the development of the stress distribution during the test and to confirm the activation of the membrane effect strain gauges were glued on the steel beams at two positions. For hogging moment strain gauges were also glued on rebars in the concrete slab.

In Figure 4-65 the locations of the strain gauges on the longitudinal rebars are shown. In Figure 4-66 the location of the strain gauges on the beam profile are illustrated. The location of SG R8 corresponded to the location of SG 7 to SG 9. The position of SG R5 corresponded not totally with the level of SG 4 to SG 6 because afterwards SG 4 to SG 6 were shifted closer to the endplate to be able to record the buckling of the beam flange in compression.

The strain gauges were glued on both sides of the joint directly beside the endplate and on one side of the beam also in a certain distance to the endplate where a linear stress distribution was assumed. These strain gauges aimed also to compute the moment and the beam flexion in this position.

The diagrams of the stress distribution in Figure 4-67 to Figure 4-68 show the initial behaviour under pure bending exposure and then the change under combined bending and tension and at the end under more or less pure tension exposure. The used strain gauges were only able to record strains up to 1.7%. So the strain gauges on the rebars had broken down very early (for stress values of about 550 N/mm^2 which corresponds with $f_{y,\text{rebar}}$), that means only a small elongation of the rebars could be measured. The values of the strain gauges on the rebars also strongly depended on the cracks in the concrete slab. If the crack appeared directly in the position of the strain gauge the measured value was much more than in an uncracked spot. The strain gauges at the beam IPE 140 profile reached maximal stress values of about 440 N/mm^2 which corresponded with $f_{y,\text{IPE}}$.

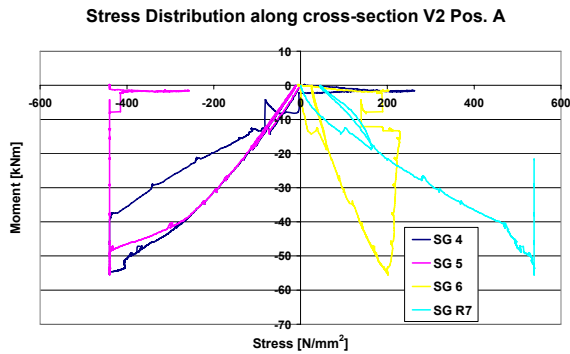


Figure 4-67: Stress Distribution V2 (Pos. A)

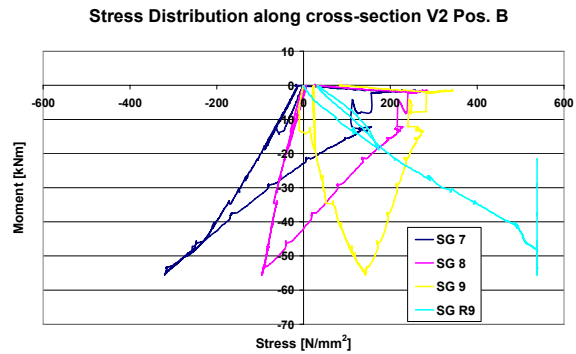


Figure 4-68: Stress Distribution V2 (Pos. B)

For the tests under hogging moment and tension (exemplary V2) the compressive stress in the external flange of the steel beam (Pos. A) came up to the yield strength. During the test buckling of the beam flange under compression was observed which confirmed the measurement. When starting the application of the additional tension force the stress changed gradually into tension stress, see SG 4 in Figure 4-67. For Pos. B the stress distribution across the cross-section had been assumed as linear because of the distance of Pos. B to the endplate. This is totally confirmed by the diagram in Figure 4-68.

For the joints under sagging moment and tension strain gauges had only been glued on the steel beam. The compressive stress in the concrete slab could so not be measured. The stress distribution in Pos. A shows that for pure bending state the stress at the bottom flange SG 4 was maximum. By applying the additional tensile force there was for a while no further increase of the stress in the IPE profile, because the whole tension force was first transferred by the reinforcement. When the joint moment changed from positive into negative moment, the upper flange of the IPE profile was stressed by additional tension and the bottom flange got compression stress due to the negative bending moment. The response of the strain gauges confirmed this quite well as illustrated in Figure 4-69 and Figure 4-70.

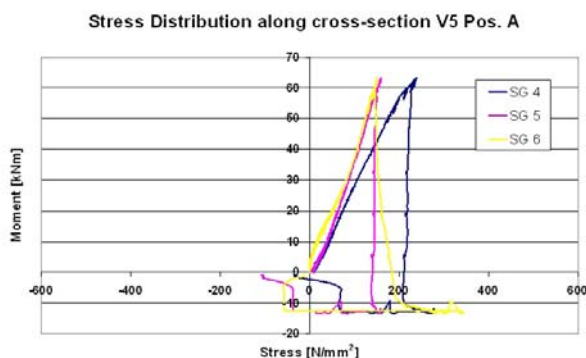


Figure 4-69: Stress Distribution V5 (Pos. A)

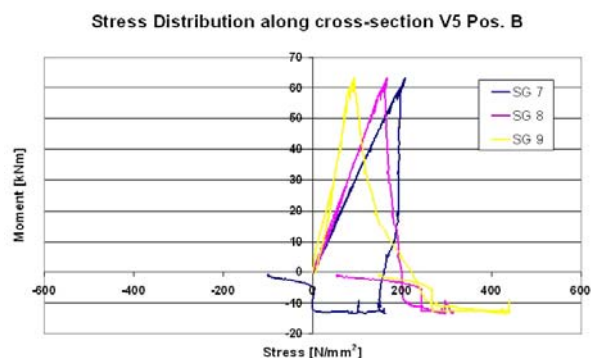


Figure 4-70: Stress Distribution V5 (Pos. B)

The value of SG 6 at the upper beam flange (Pos. A) in Figure 4-69 increased at the end of the test, also SG 9 (Pos. B) in Figure 4-70. This corresponded very well with the observed failure mode during the test. Rupture of the reinforcement and of one upper bolt happened. The diagram in Figure 4-69 also

visualize that both bolt rows, the lower and upper ones had more or less the same utilisation, because of the capability of plastic redistribution of the endplate the stress in SG 5 and SG 6 were nearly the same.

4.4.2.8 Conclusions

As mentioned in § 4.4.2.1 the most important outcome of the composite joint tests are the results of the M- Φ and M-N-behaviour. So the composite joint tests have been successful. The curves of the joints for M- Φ and M-N-interaction could be recorded and the behaviour of the joints by following the curve from pure bending exposure to pure tension exposure could be studied. Although especially the endplate had clear over-strength the overall ductile behaviour of the joints could be guaranteed due to an efficient ductility design of the joints. By comparing the results of the component deformation measured for the joint tests with them of the corresponding component tests (given in [21]) a quite good consistency was detected. Also the comparison to the substructure test shows a good agreement. The results (M- Φ and M-N-interaction) of the joint tests have been used to model the joint behaviour for recalculating the substructure tests and the results of the calculation correspond very well with the tests results.

It could be stated that both, composite joint tests, as well as the substructure test showed the ability of the composite joints to undergo large rotations and to change the internal load combination from pure bending state to a combined bending and tension exposure. Failure was mainly induced by the concrete slab: for the hogging moment joints by increased cracks and final rupture of the reinforcement, for the sagging moment joints by crushing of the concrete and decreasing of the concrete compression zone. However the pure steel connection was still able to carry a remarkable amount of load.

The results of the composite joint have been also used to validate the analytical model in § 5.3.4.

4.4.3 Steel joint tests

4.4.3.1 General

The background of these pure steel joint tests was to check the ductility criterion according to EN1993-1-8 [69]. In previous tests conducted in Stuttgart by Kuhlmann/Schäfer [83] brittle failure of the bolts had been observed although the ductility criterion according to EN 1993-1-8 was not violated. In these former composite joint tests the component “reinforcement in tension” developed as highly ductile tension bar had been designed as weakest component. The bolts were clearly oversized but nevertheless a rupture of the bolts happened before the failure of the component RFT could occur. It was assumed that the brittle bolt failure occurred due to bending exposure of the bolts.



Figure 4-71: Unexpected brittle bolt failure in previous test conducted in Stuttgart [83]

This bending exposure seems to depend on the distance between the flange and the web of the beam on one side and the bolt on the other side. To receive a more reliable criterion in order to prevent premature brittle failure modes these tests were conducted. The longitudinal dimensions of the testing body and the principal test set-up can be taken from Figure 4-73. Within the tests two different parameters have been investigated. The thickness of the endplate and the arrangement of the bolts were varied. The bending tests on pure steel joints included a number of 6 tests. For further information see [23].

4.4.3.2 Design and dimensions of the steel joint test specimens

The beams of the testing specimen consisted of IPE 500 profiles, while for the column an HEB 300 profile was used. The bolts were M20 of grade 10.9. The endplate dimensions and the thicknesses were varied. The endplate thickness was in a range of 6 mm to 16 mm and the arrangement of the bolts had been changed according to Figure 4-72. All steel elements consisted of S355. At the location of the vertical support for the beams stiffeners had been welded at the web to avoid local failure due to concentrated load application.

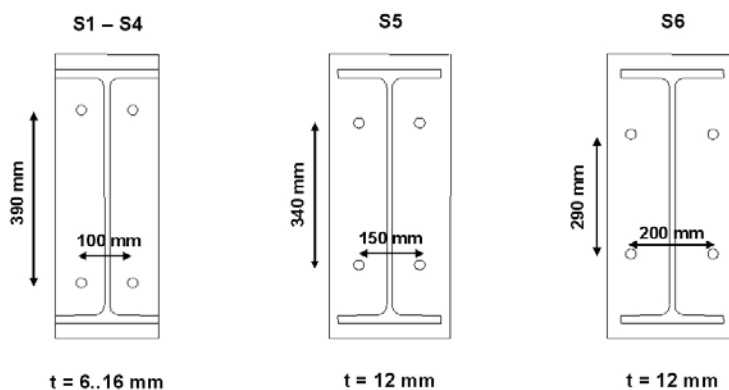


Figure 4-72: Overview of the test specimens S1- S6

changed. In the first test series S1-S4 the endplate thickness had been changed from 6 mm up to 16 mm. The critical value acc. the ductility criterion was close by 12 mm. So for endplate thickness thinner than 12 mm a clear underestimation of the bearing capacity acc. to the EN 1993-1-8 [69] was supposed. The second series S1-S5-S6 the arrangement of the bolts had been changed in a way that the horizontal distance between the beam web and the bolts and the vertical distance between the beams flange and the bolts were increased.

The design of the test specimens came after the aspect to provoke all the three possible failure modes for the component “endplate in bending”. The layout of the endplate and bolts was designed according the nominal values of the strength.

4.4.3.3 Test setup

In Figure 4-73 the test station with the arrangement of the hydraulic jack is shown. The hydraulic jacks were operating deformation controlled. The vertical hydraulic jack can apply a maximum force of 2.5 MN. The used loading velocity for the tests was 1 mm/min. By increasing force and deformation by the vertical hydraulic jack a moment was applied to the testing specimen. The deformation of the testing body was increased up to the failure of the joint. The distance between the axis of the joint and the axis of the vertical support was 2000 mm. The support was a roller bearing to ensure no restraining at the beams ends.

The dimensions of the column profile had been chosen intentionally higher to ensure that the column profiles remained elastic and therefore to reduce the number of parameters which influence the joint behaviour. The base test specimen was test S1 with an endplate thickness of $t_p = 12$ mm. One test series included the variation of the endplate thickness within a range of 6 mm to 16 mm and for the second test series the bolt arrangement and the projection of the endplate were

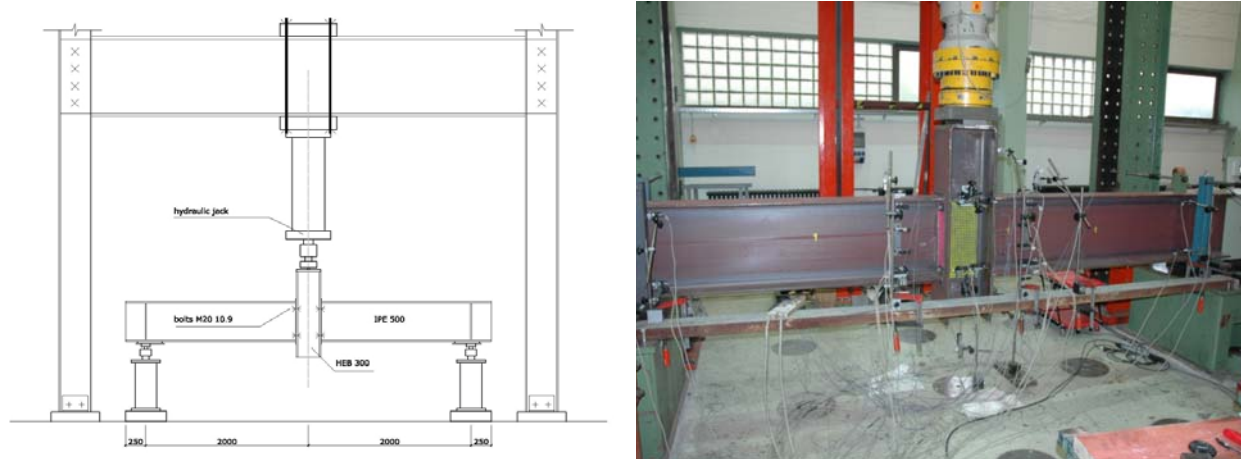


Figure 4-73: View on the test setup

The column pieces and the beams with welded on endplates had been prefabricated by Arcelor. In the laboratory of USTUTT the test specimens had only been screwed. The bolts M20 10.9 were prestressed by a torque of about 400 Nm which corresponds to $0.75 M_{\max}$ of the allowable torque.

4.4.3.4 Material characteristics

The behaviour of the total joint primarily depended on the behaviour of the collapsing components. For the components which were not stressed up to the yield strength the values of tensile strength and the elongation at failure were more or less insignificant. The decisive components of the joint were the endplate and the bolts. The steel beam as well as the columns remained more or less elastic. All material characteristics were determined by tensile tests at the University of Stuttgart and are given in [23].

4.4.3.5 Test results

The dimensions of the column profiles were chosen in such a way that the behaviour remained elastic for all tests performed. The variation of the endplate thickness was chosen to get all possible failure modes of the component endplate in bending (mode 1 to mode 3). The bending tests at the pure steel joints with thin endplates showed that for endplate thickness smaller than required by the ductility criterion additional bearing capacity could be activated due to membrane effects. Also the arrangement of the bolts had great influence of the deformation behaviour and bearing capacity of the joints. By increasing the vertical distance between the beam flange and the bolts and the horizontal distance between the beam web and the bolts the endplate becomes more deformable.

The load history and the resulting deformation behaviour depending on the failure mode of the endplate during the test are exemplary given for the test specimens with different behaviour respectively.

The test S1 with intended and also observed failure mode 2 is shown in Figure 4-74. For the load step $50\% M_{j,u}$ there was nearly no visible deformation for the endplate observable. By reaching $80\% M_{j,u}$ the lower edge of the endplate was lifting off the column flange and also between the upper and lower bolt row there was a small gap between endplate and column. But at all the deformations of the endplate were relatively small. Just before collapse there was some small additional increase of the endplate deformations as visible in Figure 4-74 down left but the total deformations remained relatively small. The final collapse of the joint occurred by failure of a bolt due to collapse of the thread, because of the used galvanized bolts.

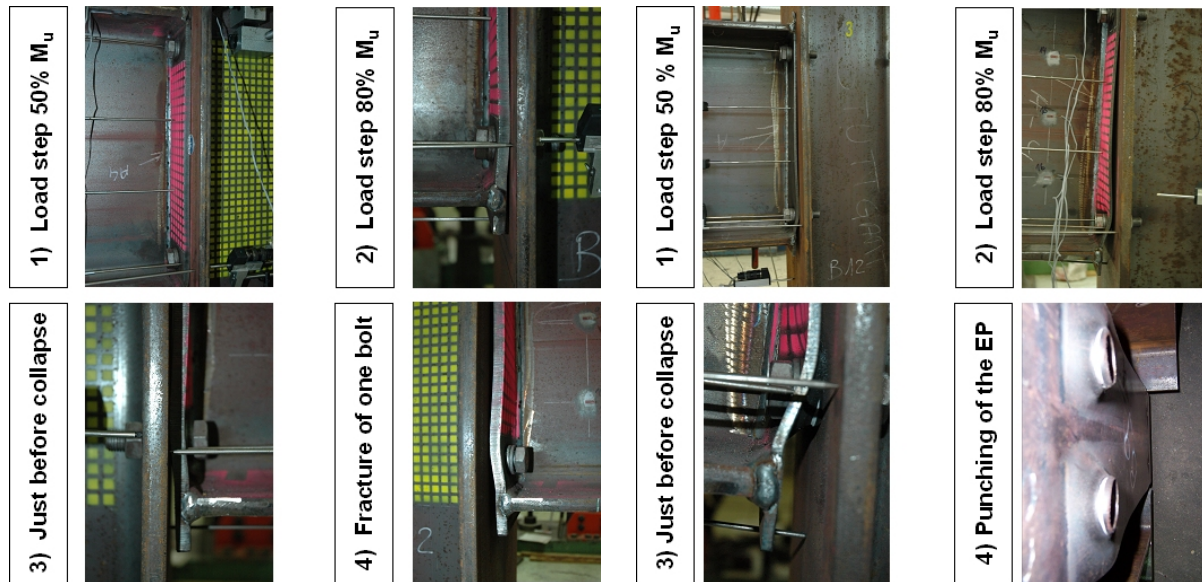


Figure 4-74: Development of the endplate deformation of test S1

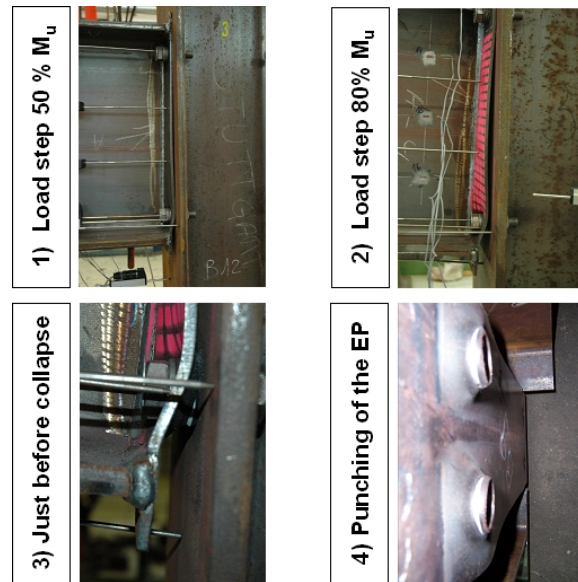


Figure 4-75: Development of the endplate deformation of test S3

The test S3 with intended as well as observed failure mode 1 is illustrated in Figure 4-75. Already for low loading clearly visible deformations of the endplate could be observed especially in the zone at the lower bolts. These deformations around the lower bolts developed to a cone-shaped deformation for further increasing of the load. At the end failure of the endplate due to punching occurred as shown in the lower photos of Figure 4-75.

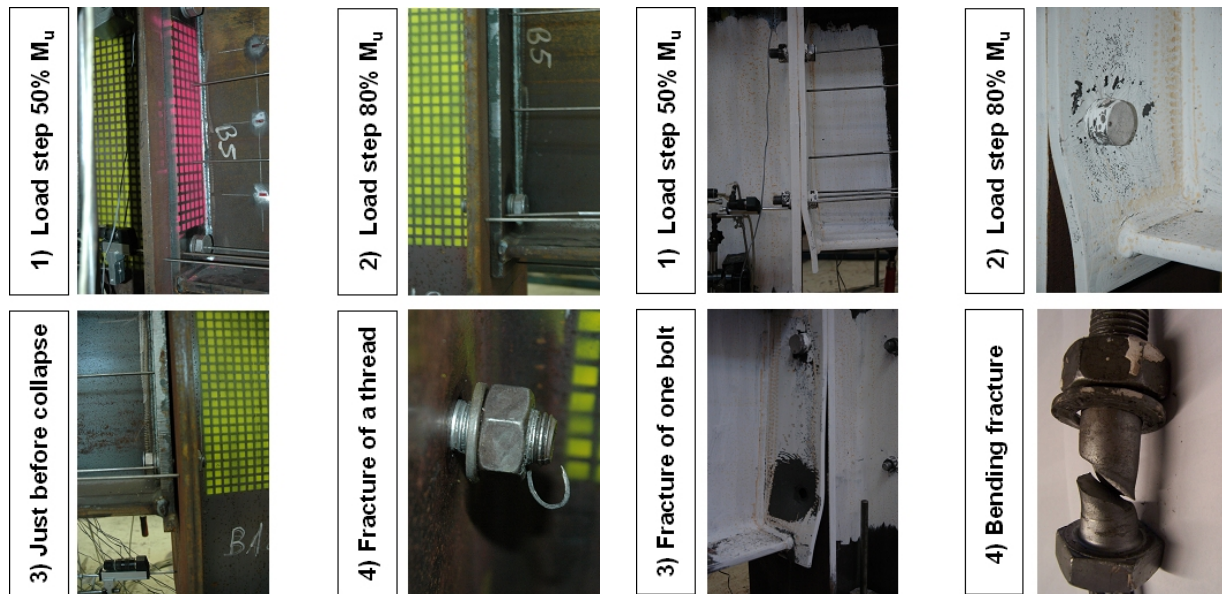


Figure 4-76: Development of the endplate deformation of test S4

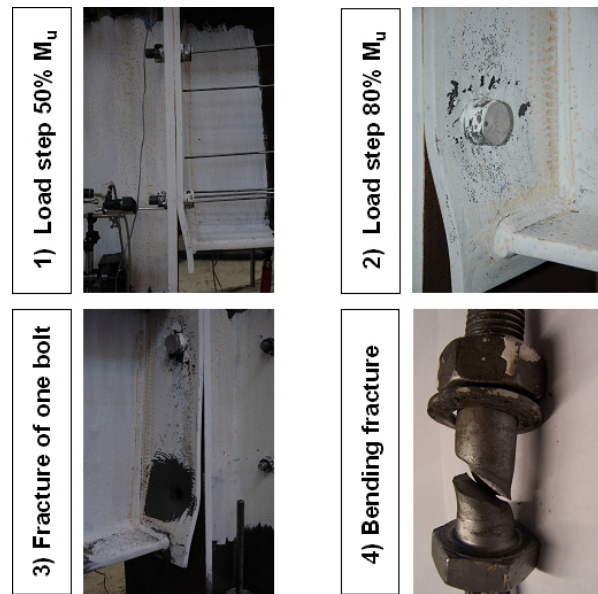


Figure 4-77: Development of the endplate deformation of test S6

The test S4 with the intended and observed failure mode 3, failure of the bolts before reaching plastic hinges in the endplate is presented in Figure 4-76. It is obvious that up to 80 % M_{ju} there was no visible deformation of the endplate. Just before the end of the test a really small lifting of the endplate was observed, but the endplate remained nearly elastic. However brittle bolt failure occurred without any advance notice by visible deformations at the joint.

The test S6 has as the test S1 an intended as well as observed failure mode 2. The difference between these two tests was that in test S6 due to the varied bolt arrangement the deformability of the endplate was improved (see Figure 4-77) leading to an additional bending stress of the bolts. For test S1 the bolts were mainly stressed in tension resulting in a failure of the thread of the bolt. In test S6 high deformed

endplate caused a mixed tension and bending exposure to the bolts. This results in fracture of the bolt at the shaft as shown down right in Figure 4-77.

Table 4-5: Overview about the bearing capacity of the steel joints tests

Ref. No.	endplate thickness t_p [mm]	intended failure mode	$M_{j,u}^-$ factorized [kNm]	actual failure mode	$M_{j,u}^-$ test	$M_{j,u, test} / M_{j,u}$
S 1	12	EPB+BT	181,0	EPB+BT	243,92	1,35
S 2	9	EPB + BT	168,5	EPB+BT	243,08	1,44
S 3	6	EPB	47,3	EPB	121,32	2,56
S 4	16	BT	230,1	BT	229,71	1,00
S 5	12	EPB+BT	148,7	EPB+BT	208,38	1,40
S 6	12	EPB+BT	129,0	EPB+BT	199,65	1,55

A. Results of the test series with changed endplate thickness

Within this sub-series the test specimens S1-S4 were tested. All test specimens had the same bolt arrangement and bolt size, only the endplate thickness changed. The basis test specimen was S1 with $t_p = 12$ mm, which corresponded to the ductility criterion acc. EN 1993-1-8 [69] by considering the nominal material characteristics. S2 and S3 with endplate thickness $t_p = 8$ mm and $t_p = 6$ mm should show the failure mode 1 when considering the nominal material values and S4 with $t_p = 16$ mm was assumed to have failure mode 3.

The change of the endplate thickness influences the rotation capacity and the bearing capacity of the joint, as visible in Figure 4-78.

The tests specimen S1 showed an elastic behaviour up to a moment of 100 kNm, afterwards the curve had a more plastic behaviour because the component EPB started to yield. So a redistribution of forces within the endplate took place which led to an activation of the upper bolt row. Due to this activation of the upper bolts the bearing capacity could be increased a little bit. By comparing the calculated bearing capacity according to EN 1993-1-8 with the tested bearing capacity for S1, as shown in Table 4-5, the ratio between $M_{u, test} / M_{u, cal}$ is 1.35. The higher bearing capacity in the tests could be explained with an additional ΔM caused by the upper bolt row and additional membrane forces in the endplate. Both effects have been not considered in the calculation acc the component method in EN 1993-1-8. The test specimen S2 with a planned endplate thickness of $t_p = 8$ mm had an actual thickness of $t_p = 9.1$ mm and much over-strength of f_y . This resulted in a similar bearing capacity as S1 but at the same time a more ductile behaviour. The deviation of $M_{u, test}$ and $M_{u, cal}$ for S2 is 44%, a bit more than for S1 because of the thinner endplate which led to higher formation of membrane effects. Both test specimens S1 and S2 showed at the end a failure mode 2, combined failure of the endplate and bolts. The jump of the curve S2 at a value of about 100 kNm resulted of an operator error. The loading velocity was abruptly increased and due to this fact the start of the plastic behaviour of the test specimen S2 could not be recorded in detail.

The tests specimen S3 with a very thin endplate of $t_p = 6$ mm had only a very small elastic range with reduced initial stiffness. The bearing capacity was also very low, only half of the tests values of S1 and S2. The failure mode for test S3 was as expected, mode 3, punching of the endplate.

By comparing $M_{u, test} / M_{u, cal}$ of S3 in Table 4-5 an underestimation of the calculated bearing capacity of ~ 2.5 times is visible. This is due to the fact that the load-carrying effect of the very thin endplate of S3 is mainly influenced by the membrane effect. This membrane effect is not covered by the formulas in EN 1993-1-8.

The last test specimen within this series was S4 with an endplate thickness higher than required by the ductility criterion acc. EN 1993-1-8. The thicker endplate causes a more or less elastic behaviour of the endplate which resulted in nearly totally elastic behaviour of the M-phi-curve. The bearing capacity of S4 is less than S1 and S2 because no redistribution in the endplate occurred and so the upper bolts were not activated for tension. The ratio $M_{u, \text{test}}/M_{u, \text{cal}}$ is 1.0 and that shows that the formulas in EN 1993-1-8 work very well for an elastic behaviour of the endplate.

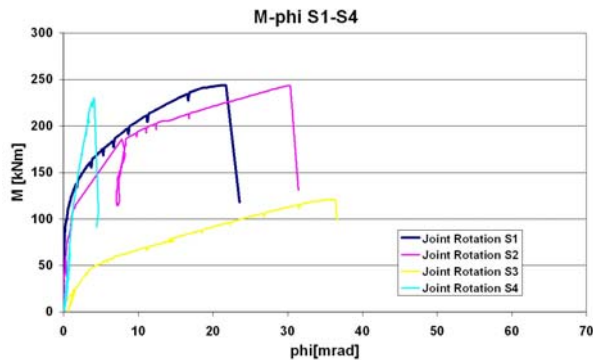


Figure 4-78: Moment-phi curves of S1-S4

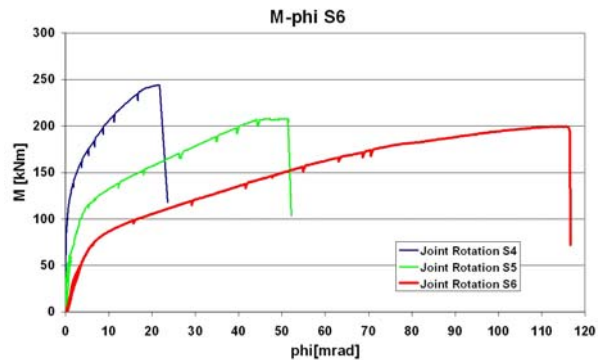


Figure 4-79: Moment-phi curves of S1-S5-S6

B. Results of the test series with changed bolt arrangement

The second sub-series investigated the influence of the bolt arrangement on the rotation capacity and bearing capacity. The test specimens within this series were S1 as basis specimen and S5 and S6 with an increasing horizontal and vertical distance of the bolts, see Figure 4-72. The diagonal transition of the lower bolts as well as the upper bolts led to the following effects:

By increasing the horizontal distance between the bolts and the beam web the model of the T-stub became more flexible because the length “m” (acc. EN 1993-1-8 chapter 6.2 [69]) was increased.

By increasing the vertical distance between the beam flange and the lower bolts the inner lever arm of the lower bolts was decreased which leads to a decrease of the moment bearing capacity.

By increasing the distance of the beam flange and the upper bolts the inner lever arm for the upper bolts was increased which led to increase of the contribution of the upper bolts which contributed also to the moment bearing capacity. The bearing capacity of the test S5 in comparison to S1 was about 85%, but simultaneously the rotation capacity was about 200% of S1. The bearing capacity of S6 was about 82% of S1 but the rotation capacity increased at the same time up to 500% of S1, as presented in Figure 4-79

Because of this additional deformability of the endplate the membrane effect increased from S1 to S6 which is also clearly visible by comparing $M_{u, \text{test}}$ and $M_{u, \text{cal}}$ in Table 4-5. Another effect of the deformable endplate was that the lower bolts got additional bending stresses which led to a bending rupture of a bolt in the test S6.

Table 4-6: Comparison of the bearing capacities and rotations of the joints S1-S5-S6

Test specimen	S1	S5	S6
Bearing capacity	100 %	85,5 %	82 %
Rotation capacity	100 %	~ 220 %	~ 500 %

The large deformations of the endplate resulted in an additional bearing effect of the endplate. This effect was the membrane effect which was developing mainly in horizontal direction between the two bolts in one row. But by decreasing the vertical distance between the upper and lower bolts further membrane effects in vertical direction were possible. So a biaxial membrane condition could develop from the large deformations of the endplate. So the varied bolt arrangement of S5 and S6 resulted in a

decrease of bearing capacity and clear increase of ductility as shown in Table 4-6. Due to the membrane effect the decrease of bearing capacity was relatively limited.

4.4.3.6 Evaluation of the test results

To evaluate the tests results of the of the steel joint test the component deformations were analysed furthermore they were compared with corresponding T-stub tests performed in Trento and in addition a recalculation of the tests with Finite Elements was performed.

A. Comparison of the component deformations

To check if the measured component deformations and the measured rotations are in good correspondence values for the deformations of the tensile components derived from the rotation were determined. This check is done for each of the three failure mode so as an example the tests S1, S4 are illustrated here:

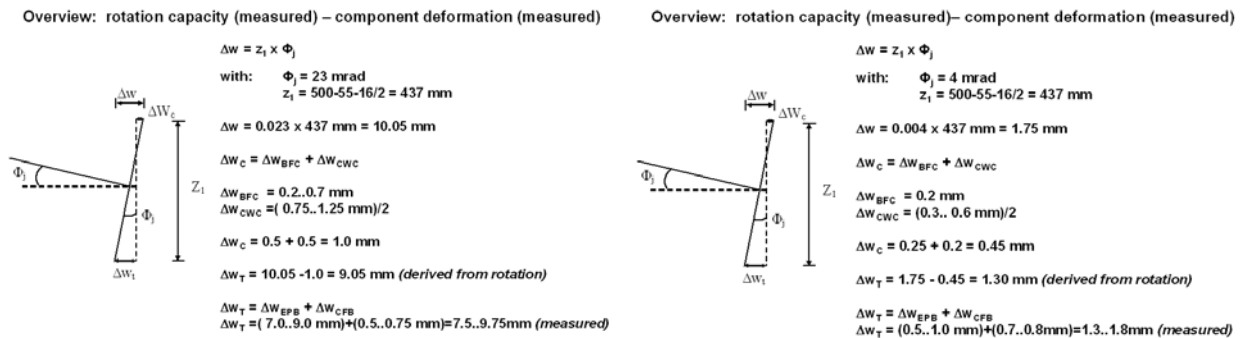


Figure 4-80: Check of the rotation capacity and the component deformations of test S1

Figure 4-81: Check of the rotation capacity and the component deformations of test S4

For the test S1 (Figure 4-80) and test S4 (Figure 4-81) the comparison of the measured component deformations and the deformations derived from the rotation are in good agreement. This was valid as well for all other tests. The main conclusions resulting from the evaluation of the component deformations are the following:

- The decisive component to get (high) rotation capacity within these tests was the component “endplate in bending”. As clearly visible in Figure 4-80 the total deformation in the tension zone Δw_T existed more or less only by the endplate deformation. For the test S4 nearly no endplate deformation was measured resulting in minimum joint rotation.
- To influence the deformability of the component EPB the adjustment of the bolts depending on the endplate is decisive.
- At the one hand the ratio of bolt diameter to the endplate thickness and on the other hand the arrangement of the bolts at the endplate are crucial parameters to influence the ductility as well as the bearing capacity.

B. Comparison with the T-stub tests performed in Trento

Within this RFCS-Research - Project a large number of component tests have been performed at the University of Trento [6]. Among others there has been T-stub tests for the endplate thickness $t_p=12 \text{ mm}$ with varied bolt arrangement. This varied bolt arrangement corresponds to the tests S1 – S5 – S6. These T-stub tests have been performed with and without stiffener. For this comparison only the tests with stiffener are chosen because the stiffener in the T-stub tests corresponds to the beam flange in the joint tests. In Table 4-7 the relative bearing and deformation capacities of the T-stub test are listed. So an attempt is made to compare the joint test results (Table 4-6) with the T-stub test results qualitatively. The comparison is based on the values of the transducer TR05 in Figure 4-82 which measured the endplate deformation close to the bolts.

Table 4-7: Comparison of the bearing capacities and deformations of the T-stub tests 6bab-6bb-6bc

T-stub test specimen	6bab	6bb	6bc
Corresponding steel joint test	S1	S5	S6
Bearing capacity	100 %	81,5 %	76,8 %
Deformability	100 %	~ 210%	~ 310 %

In Figure 4-82 the arrangement of the transducers at the T-stub are exemplary given for test 6bab, for the two other tests the arrangement was more or less similar. In Figure 4-83 the measured deformations of TR 05 depending on the load are presented.

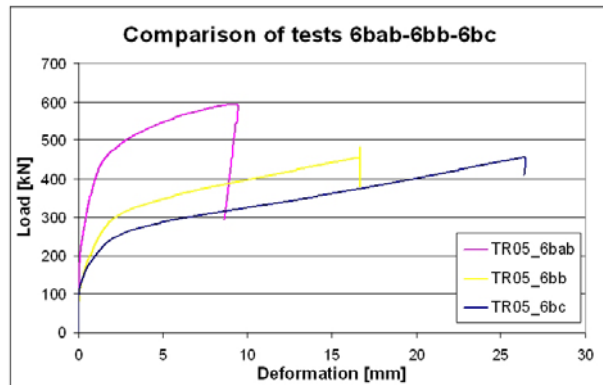
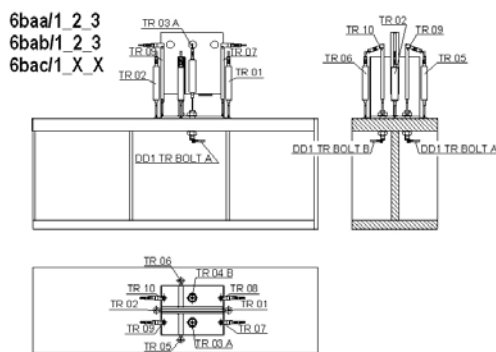


Figure 4-82: Transducer arrangement of T-stub test 6bab

Figure 4-83: Measured curves of the T-stubs 6bab, 6bb, 6bc

By comparing the joint tests with the T-stub tests layout it is obviously that membrane effects in the T-stub are possible only in uniaxial direction whereas the joint configuration allows a biaxial membrane condition. That influences of course the bearing capacity and rotation capacity. So it is logical that the T-stub specimens with varied bolt arrangement have less relative bearing capacity in comparison to the corresponding joint tests. But the deviation is not too much. Also the increase of ductility is less for the T-stubs, see Table 4-6 and Table 4-7. Especially for the test 6bc the increase of the ductility is only ~310 % compared to joint test S6 with an increase of ductility by ~500 %. This difference may be explained by comparing the bearing capacity of 6bc and S6. As test load of 6bc has a decrease to 76,8 % of 6bab but the bearing capacity of test S6 decreases only to 82 % of S1, the value of ductility for S6 at the same level of bearing capacity than 6bc has to be considered. So by reading the ductility for curve S6 the value: $0.768 \times 243 \text{ kNm} = 186 \text{ kNm}$ (see Figure 4-79) resulting in an increase of ductility by ~340% in comparison to S1 could be determined. This value fits much better to the T-stub test 6bc.

It could be stated that the results of the joint test and T-stub tests match qualitatively very well. The influence of the varied bolt arrangement is the same for the bearing capacity as well as for ductility.

C. Recalculation of the steel joint tests

The results of the numerical simulation showed a good agreement to the test results. In Figure 4-84 and Figure 4-85 a comparison of the numerical results and the tests results e. g. for S1 is given and it is clearly visible that there is only a small deviation of the experimentally and numerically calculated curve. This was valid for all tests, the maximum deviation observed between FE and experimental results came up to 10% which is sufficient accurate.

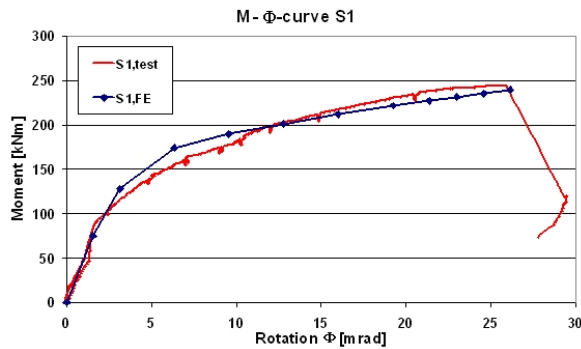


Figure 4-84: validation of the numerical model

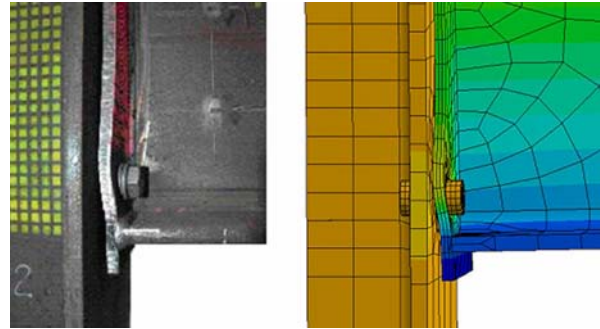


Figure 4-85: Comparison of deformed shape: experimental - numerical

The Main aim of the steel joint tests was to investigate the ductility criterion according EN 1993-1-8 [69] and to determine parameters influencing the load bearing behaviour of the endplate. An advantage of the numerical simulations is that stress and strain distribution at any location can be plotted. By calibrating and validating the Finite-Element-Model at the test results the numerical simulations become a good tool to determine these parameters in an effective way. The numerical simulations enabled the visualizing of the membrane effect in the endplate.

In Figure 4-86 cuttings of the endplate with stress distribution in plane direction are shown and the membrane effect for thin endplates is clearly visible. (Blue colour indicates compression stresses, green and turquoise colour shows tension stresses)

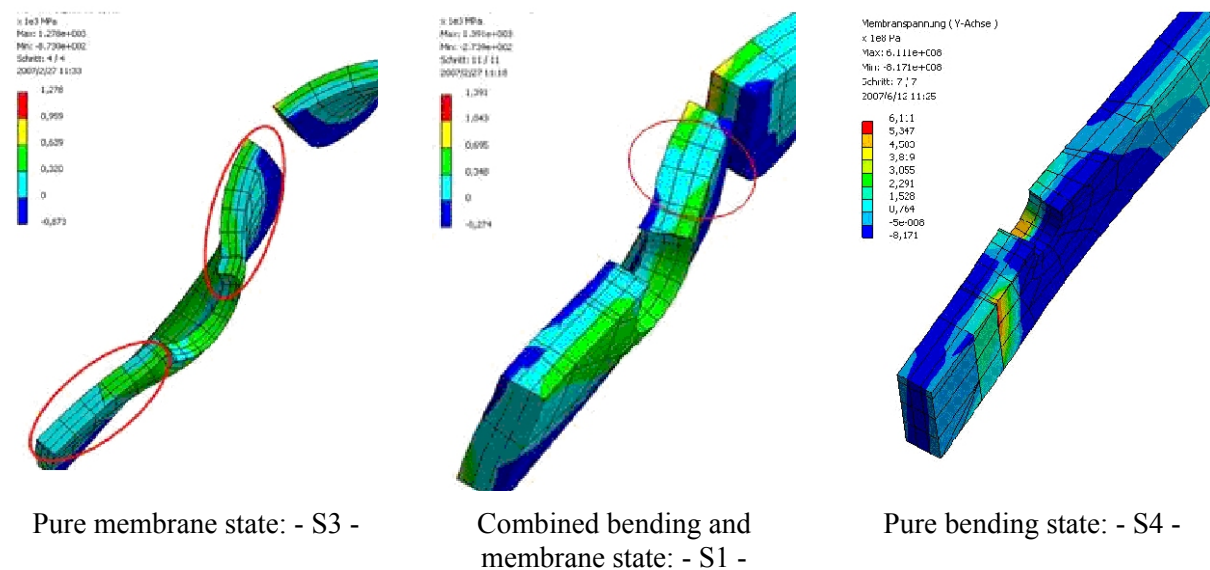


Figure 4-86: Localisation of membrane effects within the endplate

This is a short overview about the investigations executed for the steel joints concerning the activation and influence of membrane forces in the endplate of bolted joint connections. Within the work of the diploma thesis [17] further parameters to improve the ductility and at the same time keep a respectable resistance of the joint have been investigated. A more detailed report about the numerical investigations is also given in the report about the experimental tests on steel joints [23].

4.4.3.7 Conclusions

A crucial finding of these tests was that due to an increase of the endplate deformations additional membrane forces in the endplate could be activated leading to much more bearing resistance as calculated according to the component method. These membrane effects could only be activated completely if the resistance of the bolts was sufficient. Therefore the bolts have to be oversized in comparison to the design according to the component method. The deformability of the endplate causes

even an additional effect to the bolts. Due to the highly deformed endplate the bolts were additionally stressed by bending. Especially for the test S6 this additionally bending exposure of the bolts was observed. For test S6 rupture of a bolt in the shaft due to bending and tension exposure occurred. So the assumptions of the former tests of Schäfer [83], [96] that the premature brittle bolt failure is caused by additional bearing effects in the endplate and the bolts are furthermore additionally stressed by bending could fully be confirmed. The comparison with the component tests performed in Trento [6] showed good correspondence so the Trento test could confirm the findings of the steel joint tests performed in Stuttgart. A short overview about requirements for ductile joints derived from the investigations on steel joint as well as on composite joints is given in § 4.6.

4.5 Component tests

4.5.1 General

This section describes the main features and the results of the experimental study carried out at the University of Trento (Department of Mechanical and Structural Engineering) on steel and concrete beam-to-column joint components. The study comprises tests on:

- full-scale reinforced concrete specimens;
- unstiffened and stiffened T-Stub specimens simulating the column and the end-plate components;
- connections.

Tests were planned so as to enable the characterization of the components response in the field of large displacements, when significant tensile forces are building up in the floor system. The specimens configuration was consistent with the tests carried out on the sub-structure (§ 4.3) and on the joint sub-assemblages (§ 4.4).

Due to reason of clearness this section is shared in three parts each one of them devoted to one of the main typologies of tests performed: § 4.5.2 is dedicated to the tests on concrete specimens, § 4.5.3 summarises the tests on T-stub specimens, and § 4.5.4 focuses on the connection.

A detailed report about the component test is given in [6].

4.5.2 Experimental study on concrete specimens

4.5.2.1 General

The main aspects in determining the deformation capacity of reinforced concrete in tension concerns the evaluation of the stiffening effect of concrete which affects the deformation of the bare rebars. In all the stages (uncracked, crack formation, stabilised cracking and post-yielding stages) concrete provides a stiffening contribution to the reinforcement [92]. After the cracking phase this effects (the well-known tension stiffening effect) assumes a central role due to its influence on the overall ductility.

In steel and concrete composite joints the available deformation capacity and hence the ability to redistribute action effects depend on the deformation capacity of its basic components. The deformation capacity of the slab, which is a key component of composite joints, depends on the geometry of the connection and primarily on the strain of the embedded rebars. Despite simplified relationships are available to predict the behaviour of concrete in tension, recent researches pointed out the need of additional studies [83]. In order to improve the knowledge on this specific topic, in the framework of this project, tensile tests on reinforced concrete elements were designed.

4.5.2.2 Layout of the specimens

The experimental program of reinforced concrete components consisted of pure tensile tests on:

- slab specimens characterised by dimensions and reinforcement layout strictly related to the sub-structure object of the research project (§ 4.3). The main features of the specimens, named RCSL, are presented in Figure 4-87. The reinforcement ratios characterising the specimens are 0.838% (sec. A-A in Figure 4-87), 0.739% (sec. C-C in Figure 4-87) and 0.503% (sec. B-B in Figure 4-87). A total of five tests were performed. The sensitivity of these tests suggested to perform a preliminary test to set the test procedure and check the test set-up: specimen RCSL1 was used at this aim.
- specimens with square cross section (Figure 4-88) (nominal side dimension of 220 mm) characterised by two reinforcement ratios $\rho_{11} = 0.415\%$ (specimens named RCRR1) and $\rho_{12} = 0.831\%$ (specimens labelled as RCRR2). For each reinforcement ratio, three specimens were considered. The limited data available in literature on tension stiffening suggested this second series of tests in order to investigate the influence of the reinforcement ratio on such a phenomena.

The design assumed concrete C25/30 and steel B450C for the reinforcement. The tests were performed applying a tension force to the specimens, which were located in vertical position under a counter frame. The connection between specimens, the counter frame and the strong floor of the laboratory was realized by using Gewi-rebars (Figure 4-87 and Figure 4-88) which were overlapped and welded to the longitudinal reinforcement. The specimens were cast on formworks realized by means of steel profiles specially designed to allow for moving the specimens and rotating them into the vertical position without crack initiation. The specimens, cast inside the laboratory, were maintained in moist conditions for 7 days after the cast to avoid cracks due to shrinkage. The time of curing ranged from a minimum of 86 days (specimen RCRR1) to a maximum of 154 days (specimen RCRR1-3).

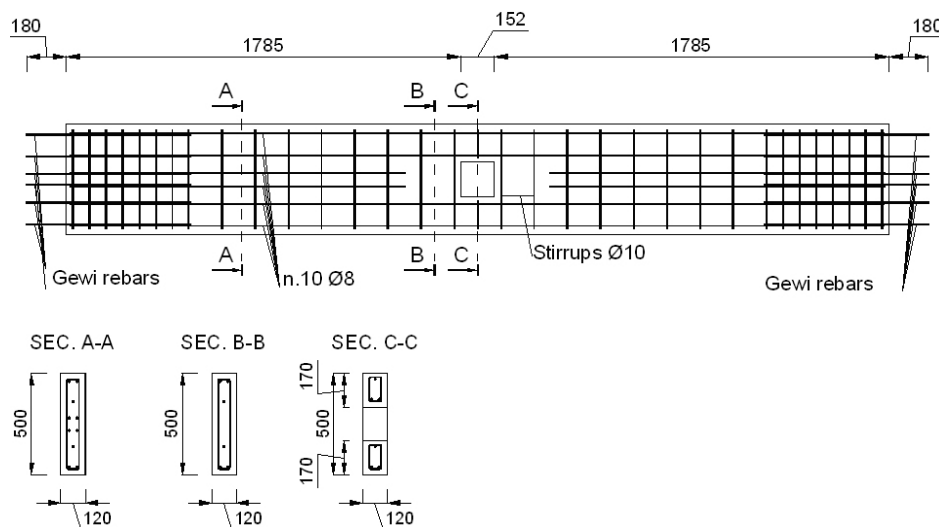


Figure 4-87: Geometrical configuration for specimens RCSL (measures in mm)

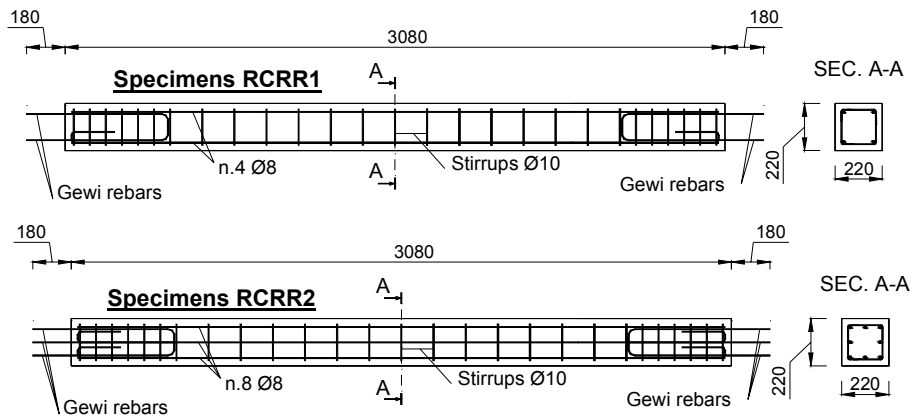


Figure 4-88: Geometrical configuration for specimens RCRR (measures in mm)

Specimens were first connected to the strong floor of the laboratory and then rotated into the vertical position and connected to the actuator. Hinged restrain conditions were realized at both the end of the specimens. The formworks were removed after the complete connection of the specimens to the tests set-up.

4.5.2.3 The tests

The tests carried out under displacement control condition comprised of a series of loading-unloading cycles up to the collapse of the specimen so as to follow the evolution of the cracks. The load was applied via a MTS hydraulic jack with a maximum capacity in tension of 640 kN.

The specimens' elongation was measured with displacement transducers characterised by different gage lengths. In specimens RSCL the maximum gage length was of 2688 mm (nominal value) and the minimum of 300 mm (nominal value). For specimens RCRR1 and RCRR2 the maximum and the minimum gage lengths were of 2175 mm and 450 mm respectively (nominal values). This allows registering both the overall and the local response of the specimens. Furthermore, with the aim to reveal asymmetric behaviours, displacements were measured on the slabs (specimens RSCL) on two opposite sides (Figure 4-89) and on all the four sides on the specimens with square cross section (specimens RCRR1 and RCRR2) (Figure 4-90). All the transducers were applied so as to capture the deformation of the central area between the end zones where longitudinal and Gewi rebars overlap. The width of notional cracks was also measured during some tests by means of strain gage transducers.

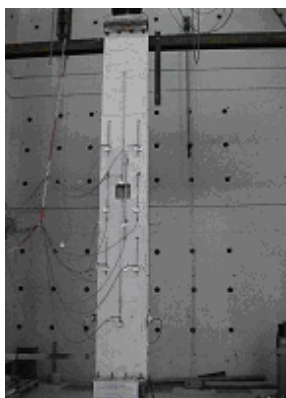


Figure 4-89: Transducers set-up for specimen RSCL

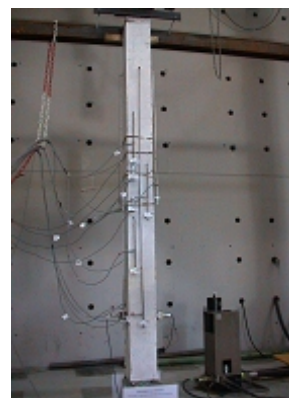
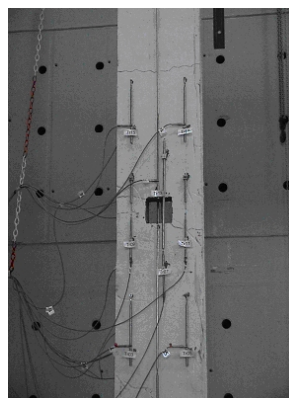


Figure 4-90: Transducers set-up for specimen RCRR

4.5.2.4 Material properties

In order to characterise the concrete specimens, tests on both hardened concrete and rebars were performed. As to the concrete properties, during the casting phase 8 concrete cubes and 10 cylinders were taken. Compression tests on cubes and splitting tests on cylinders were performed at the time at the tensile tests on the full-scale specimens (specimens RCSL and RCRR) so as to determine the average strength properties which correspond to the actual strength of concrete. The mean average cube compressive strength (R_m) was of 38.68 MPa while the mean value of tensile splitting strength (f_{ctm}) was of 3.31 MPa. As to the mechanical properties of rebars, the attention was focused only on longitudinal reinforcement. At this aim, eight tensile tests were performed. The average values of the test results are summarised Figure 4-91.

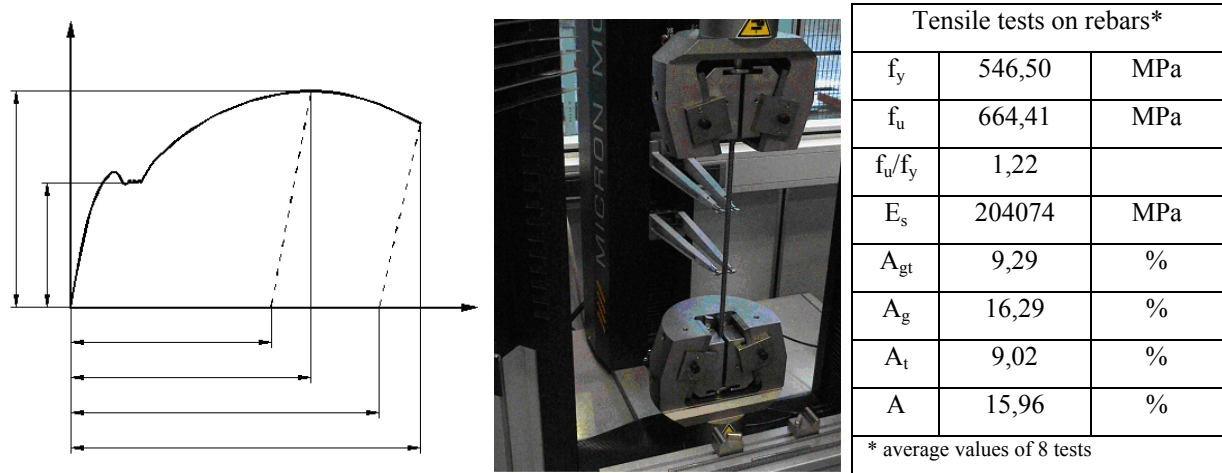


Figure 4-91: Results of the tensile tests on rebars.

As a general comment to the material properties it should be remarked that results agree with the requirements prescribed by standards for concrete C25/30 and rebars B450C.

4.5.2.5 Test results

The different geometry and reinforcement layout which characterised the two typologies of specimens (specimens RCSL and RCRR1-RCRR2), resulted in a quite different behaviour. Specimens RCSL exhibited a more complex response due to the geometric and the mechanical discontinuity caused by the central hole and by the non continuous reinforcement in the central area, which also resulted in a lower resistance. As expected, the first crack in these specimens formed in the weak central area (Figure 4-92 on the left). In specimens RCRR1 and RCRR2 the regularity of the geometry and of the rebars configuration, induced the opening of the first crack in a generic section of the specimens (Figure 4-93 on the left). Following load increments resulted a spreading of the cracks. After the attainment of a stabilized crack configuration, following load increments resulted in the increase of the cracks' width, phenomenon emphasized by the yielding of the longitudinal rebars. In all the tests, the final cracks pattern was characterised by a great regularity with cracks located approximately in correspondence of each stirrups. The attainment of the ultimate conditions was caused by the collapse of the longitudinal rebars.

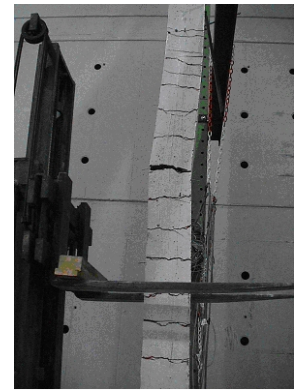
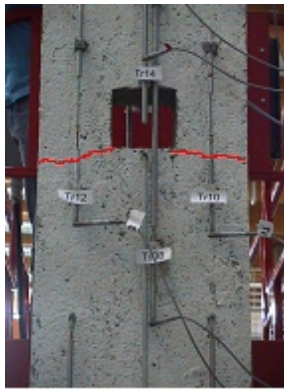


Figure 4-92: Crack path for specimen RCSL

Figure 4-93: Crack path for specimen RCRR

The results of the tests in terms of first cracking and of collapse load are summarised in Table 4-8. By considering results of each group of tests, it can be noted:

- a moderate dispersion of the first cracking loads, consequence of the uncertainty which characterise the tensile resistance of concrete;
- a negligible influence of the reinforcement ratio on the first cracking load of specimens RCRR1 and RCRR2. Despite specimens RCRR2 had a reinforcement ratio twice than that of RCRR1 specimens, both considered values are quite low and not able to affected the response of the specimens in the stage I (uncracked stage);
- the negligible dispersion of the collapse loads. In ultimate conditions the specimens response is affected by the strength of the bare rebars, which are characterised by a limited dispersion;
- a higher first cracking load in specimen RCSL1 if compared with the response of the remaining RCSL specimens. This can be explained by considering that specimen RCSL1 was cast without the central hole and as a consequence the resistant area of concrete of the weaker section increased.

Table 4-8: Test results for reinforced concrete specimens

ID Specimen		Load/kN	
		First cracking	Maximum
Specimens RCSL (size 500x120x3722 mm)			
RCSL1	99,684	211,344	
RCSL2	75,588	212,724	
RCSL3	66,960	218,184	
RCSL4	64,572	207,864	
RCSL5	50,592	211,356	
Specimens RCRR (size 220x220x3080 mm)			
$\rho_{11} = 0,415\%$	RCRR1-1	55,872	138,012
	RCRR1-2	57,000	137,556
	RCRR1-3	57,432	139,032
$\rho_{12} = 0,831\%$	RCRR2-1	67,212	266,328
	RCRR2-2	58,968	273,000
	RCRR2-3	53,472	267,228

The deformation capacity of the specimen was measured by the transducers displacements which, as previously mentioned, were located so as to capture both the overall and the local response. Curves in Figure 4-94 and Figure 4-95 show typical overall responses for the slabs and for the specimens with square cross-section. Curves are related to displacements measured by the transducers with the longer gage length applied on different sides of the specimens. It can be observed a general good agreement between curves. This trend, observed in all the tests, reveals an “overall symmetry” of behaviour. As a comment to results, it can be observed that displacements related to long gage lengths are influenced in a negligible way by local effects such as lack of homogeneity of the material, local eccentricity of load due to tolerances on the geometry of the specimens (rebars covers, section’s dimensions) and opening of cracks. This fact can be pointed out by considering the responses of transducers characterised by shorter gage length which differently from the longer gage lengths, show a scatter of the results. In Figure 4-96, which refers to transducers with a gage length of 300 mm it can be noted that despite the tensile force applied, some transducers measured displacements in the opposite direction with respect to the force. This can be the result of local load eccentricities, whose influence is more significant for low levels of load. Curves are also affected by the opening of the cracks which causes a sudden increase of the displacement at the same load level. The aforementioned effects became more evident as the gage length decreases.

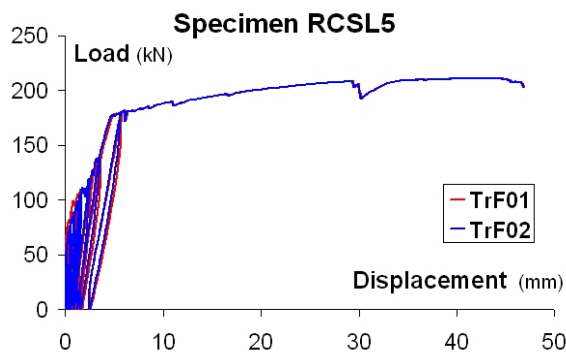


Figure 4-94: Overall response of specimen RCSL5 (gage length 2687mm)

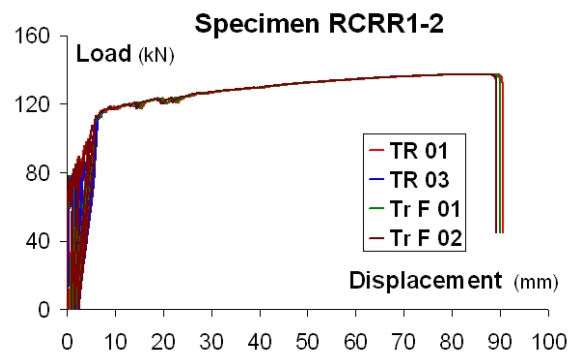


Figure 4-95: Overall response of specimen RCRR1-2 (gage length 2175 mm)

The effect of the central hole on the deformation capacity of slabs was pointed out by comparing the response of transducers characterised by the same gage length located in the central area and far from this area. The more flexible behaviour of the central zone results in an increment of approximately 100% in terms of displacements. The specimens with square cross section (specimens RCRR1 and RCRR2) showed a quite regular behaviour in terms of load-displacement curves also considering the responses of the transducers with the shorter gage lengths. The comparison of results related to specimens RCRR1 and RCRR2 presented in Figure 4-97 allowed a first appraisal on the influence of the reinforcement ratio on the experimental responses. It can be noted the influence of the reinforcement ratio on the collapse load, while the effect on the first cracking load and on the ultimate deformation capacity is negligible.

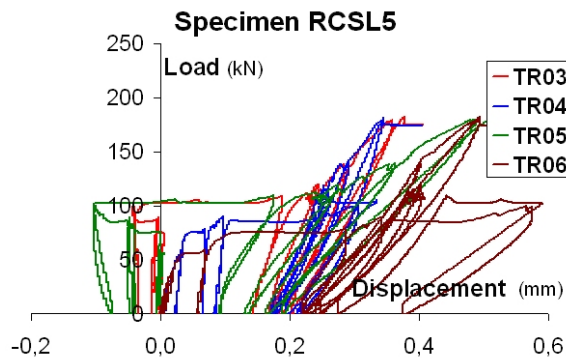


Figure 4-96: Transducers response (gage length 300 mm)

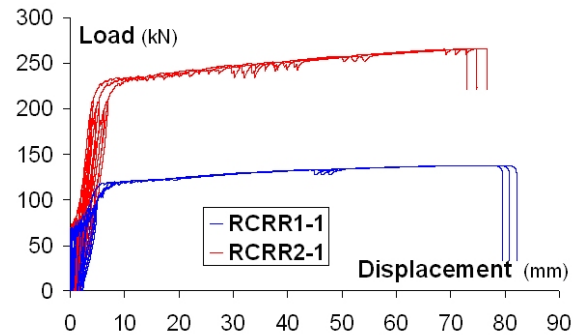


Figure 4-97: Effect of reinforcement ratio (gage length 2175 mm)

4.5.2.6 Tension stiffening effect

In order to quantify tension stiffening effect of concrete on the specimens overall ductility the deformation capacity of the concrete specimens was compared to that of the bare rebars. The analysis focused the attention on the behaviour at the maximum loading condition and at collapse.

The deformation capacity of the concrete specimens was determined from the experimental load-displacement curves associated with the longer gage length, which allowed collecting the displacements associated to the maximum and to the collapse loads. Results allowed evaluating the average elongation of the specimens. Table 4-9 which compare the responses of the concrete specimen and that of the rebars, refer to both the total and the non proportional elongations associated with the maximum load and the collapse load (Figure 4-91).

Table 4-9: Comparison between deformation capacities of concrete specimens and of bare rebars.

ID specimen	Average deformation capacity			
	Maximum load		Ultimate load	
	$A_{gt,m}$ /‰	$A_{g,m}$ /‰	$A_{t,m}$ /‰	$A_{,m}$ /‰
RCSL2	1,73	1,39	1,84	1,50
RCSL3	1,81	1,45	1,91	1,58
RCSL4	1,30	0,96	1,37	1,05
RCSL5	1,59	1,25	1,74	1,41
Average values	1,61	1,26	1,72	1,39
RCRR1-1	3,58	3,26	3,73	3,41
RCRR1-2	3,98	3,66	4,12	3,80
RCRR1-3	3,93	3,61	4,08	3,76
Average values	3,83	3,51	3,98	3,66
RCRR2-1	3,39	3,12	3,42	3,15
RCRR2-2	5,14	4,81	5,32	4,99
RCRR2-3	3,55	3,23	3,58	3,26
Average values	4,03	3,72	4,11	3,80
Bare rebars	9,29	9,02	16,29	15,96

Results show:

- the limited deformation capacity of specimens RCSL if compared to specimens RCRR;
- with the exception of specimen RCRR2-2, specimens RCRR1 and RCRR2 exhibit a similar behaviour despite their different reinforcement ratio;
- the non negligible contribution of the stiffening effect of concrete. This effect in specimens RCSL appears more significant than for specimens RCRR. Focusing the attention on the deformation capacity at maximum load, the average percentage total elongation of specimens RCSL is in fact only 17% than that of the bare rebars. It becomes respectively 39% and 43% in case of specimens RCRR1 and RCRR2.

The limited deformation capacity exhibited by the slabs is confirmed by the comparison of test results with data available in literature. Figure 4-98 compares the deformation of the reinforced concrete specimens with the corresponding deformation of the bare rebars at the maximum load. It can be noted that the specimens RCRR (blue symbols), show a good agreement with the data available in the literature, while, for specimens RCSL (red symbols), a remarkably higher tension stiffening is observed. A similar trend is pointed out in Figure 4-99 which compares the deformation capacity of the concrete specimens at the maximum load with the “hardening capacity” of the embedded rebars expressed in terms of the ratio f_u/f_y (Figure 4-91).

The slabs' behaviour can be explained by considering the geometry and reinforcement layout of these specimens. The reduced thickness (120 mm), the presence of a central hole to simulate the position of the column and the non uniform distribution of longitudinal rebars along the specimen (Figure 4-87) could affect the mechanisms of forces transmission between steel and concrete, so explaining the experimental outcomes.

4.5.2.7 Conclusions

This section refers to an experimental study on full-scale concrete specimens subject to pure tension, which was performed in order to get an appraisal of the influence of tension stiffening on the deformation capacity of steel and concrete composite joints. At this aim 11 tensile tests were carried out on two typologies of specimens. In analysis of tests results, a great attention is devoted to the overall behaviour of the specimens. The comparison between the deformation capacity of the specimens and that of the bare rebars allows in fact evaluating the stiffening effect of concrete in between the cracks.

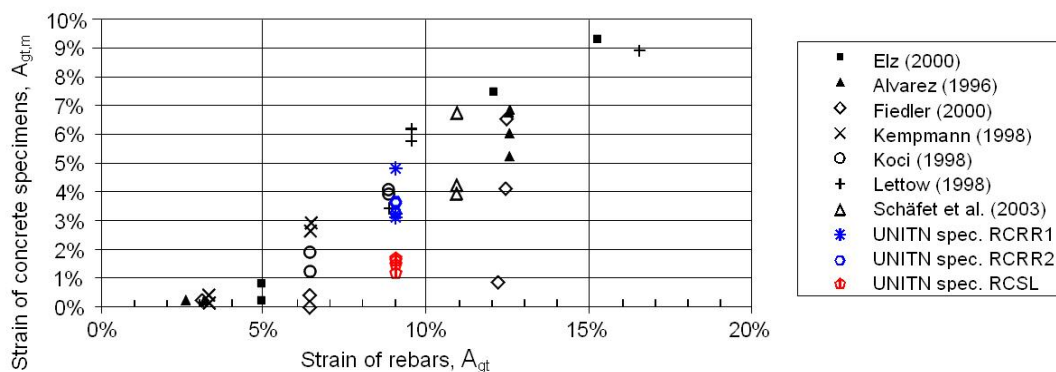


Figure 4-98: Comparison between concrete specimens and rebars depending on maximum strain of rebars

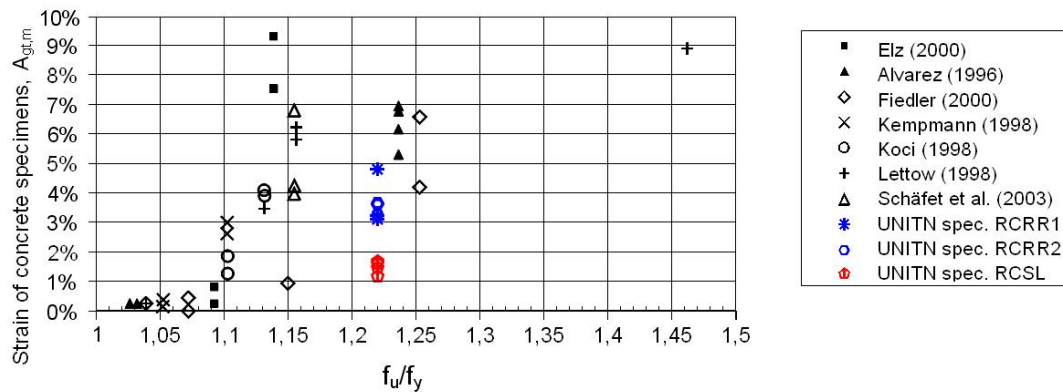


Figure 4-99: Comparison between concrete specimens and rebars depending on strength ratio of rebars

The test results point out the non negligible stiffening effects of concrete in all the stages which characterise the behaviour of a reinforced concrete specimen under pure tension. Focusing the attention on the response at the ultimate conditions, it was found that the concrete can reduce the deformation capacity of steel from a minimum of 57% to a maximum of 83%. The comparison between tests results and data available in literature suggests the need of additional studies focused on the influence on tension stiffening of the sectional geometry and of the layout of the reinforcement.

4.5.3 Experimental tests on T-stubs

4.5.3.1 General

The rotation capacity of a steel connection depends on the deformation capacity of the less ductile component. In beam-to-column bolted joint connections a significant part of the inelastic rotation is provided by the column flange and by the end-plate. The most efficient model of these joint components is represented by the “equivalent T-stub”. This model was validated by many studies [80], [107] and incorporated in the Eurocode 3 [69]. The force-displacement curves of T-stubs can hence be used to have a design approximation of such an important source of plastic rotation of beam-to-column bolted joints. An insight of the deformation capacity of end-plate joints may be achieved by studying the response of T-stub elements. At this aim, a total of 95 tests in the field of large displacements were planned in order to investigate some critical aspects. The experimental study comprised of:

- unstiffened T-stub specimens simulating the column and the end-plate components. In detail, it were performed:
- 39 tests under pure tension on T-stubs specimens characterised by different lengths in order to have an appraisal of the recommendations in the Eurocode 3 [69] for the effective T-stub length;
- 16 tests under different combinations of axial (N) and force shear (V) aiming at determining the interaction N-V domain.
- stiffened T-stub specimens under tension (40 tests), designed in order to get an appraisal of the influence of stiffeners on the T-stub performance.

Specimens were designed so that consistency with the reference composite frame considered in this research project (§ 4.3) and with the steel joint configurations analyzed at the University of Stuttgart (§ 4.4) was achieved. Further details are given in [6].

4.5.3.2 Layout of the specimen

The study was carried out on the joint configurations showed in Figure 4-100. The design of the specimens' geometry was performed in accordance with the EN 1993-1-8 [69], with the purpose of

evaluating the effective lengths and the collapse mode for the column flange and the end-plate in the tension zone.

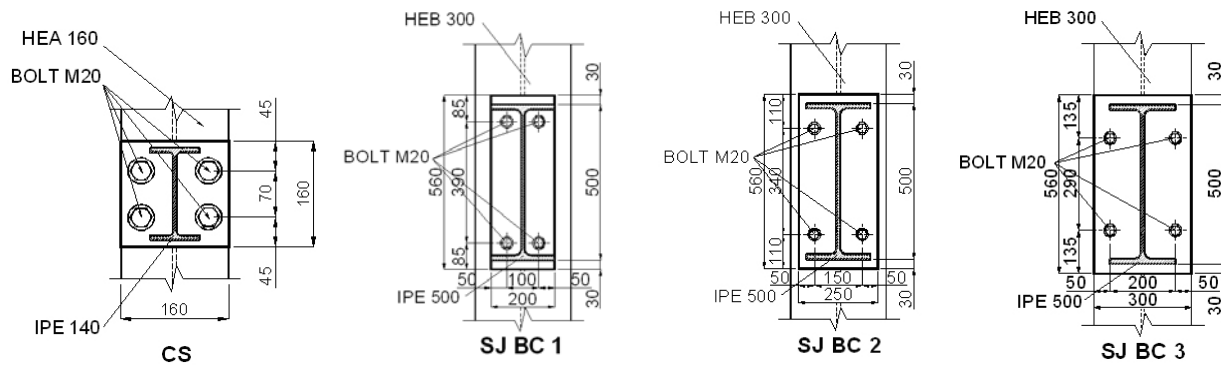


Figure 4-100: Joint configurations. (measures in mm)

For all the joint configurations, T-stubs simulating the column flange and the end-plate were hence considered. T-stub specimens with length equal or greater than the estimated effective length were designed.

For the CS joint a total of 10 T-stub configurations were tested. Column and end-plate T-stubs were characterised by the same geometry as to the length and the stiffener position. Unstiffened T-stubs had a length of 80 or 256mm. The shorter length is directly related to the actual geometry of the connection. All stiffened T-stubs had a length of 256mm; three locations of the transverse stiffener relative to the bolts were selected (i.e., 28, 56 and 84mm). Stiffeners were 8mm thick.

For the SJ joints, 16 T-stub configurations were tested. The length of the column T-stubs was of 170, 285 and 354mm for the SJ BC1, SJ BC2 and SJ BC 3 joints, respectively. The end plate T-stubs had a length of 254mm (SJBC1 joint), 353mm (SJ BC2 joint) and 443mm (SJ BC 3 joint). In stiffened T-stubs of both the column and the end-plate the position of the stiffener relative to the bolts was of 39, 64 and 89mm for the SJ BC1, SJ BC2 and SJ BC3 joint, respectively. The thickness of the stiffener was of 16mm (i.e., the beam flange thickness). For the SJ BC1 joint three different end-plate thicknesses were considered: 8, 12 and 16mm.

In the design of the specimens, the nominal strength of the structural steel (S355) and of the bolts (class 8.8 and 10.9 for the CS and SJ joints) were used to ensure a ductile collapse mode. Some changes in the collapse mode were caused by the difference between the nominal and the actual material properties.

4.5.3.3 T-stub tests under tension

The first series of T-stubs tests (79 tests) were under pure tension. They were carried out by connecting the flange of the specimen to a rigid support. The load was applied through the web so as the force is aligned to the bolts connecting the flange to the rigid support.

In order to evaluate the influence of the preload of the bolts on the T-stub performance, tests were carried out with different levels of preload. In particular, the snug tight condition and a preload force of 125kN (corresponding to a torque moment of 350 Nm) were adopted for the T-stubs of the CS joint. Similarly, for the T-stubs of the SJ joints the snug tight condition, a preload force of 125kN (corresponding to a torque moment of 400 Nm) and a preload force of 170kN were selected. The torque moment values were consistent with the bolt preload adopted during the tests on the composite structure and on the steel joints.

The transducers' set-ups were designed so that the main sources of deformation were measured for each test configuration Figure 4-101. Flange displacements at different locations and displacements of the bolts head were recorded. Furthermore, in order to investigate the prying effect, in some tests the bolt shank elongation was also measured. In these cases, the measure of the bolt's elongation was used also to check the level of the preload.

All the tests were carried out under displacement control. The loading process comprises of a preliminary cycle up to approximately 10% of the estimated collapse load and a subsequent cycle up to collapse.



Figure 4-101: Typical transducers' set-up for tension tests on T-stubs.

4.5.3.4 T-stub tests under axial and shear force

In order to investigate the response of T-stubs under different combination of axial and shear force the testing apparatus presented in Figure 4-102 was designed. The connection between the upper and the lower 'rigid parts' of the apparatus is realised by the T-stub specimen, which is bolted to both parts. This testing system is connected to the strong floor of the Laboratory and to a hydraulic actuator. The axis of application of the applied load passes through the bolt line at the interface between the T-stub flange and upper part of the apparatus (Figure 4-102). The testing apparatus can be connected at different locations, so rotating the load line with respect to the T-stub of an angle α . Such a rotation allows effective application of different combinations of axial and shears force. In particular, the values of 0° , 15° , 30° , 45° , 60° and 75° were explored for the angle α . The condition of $\alpha = 0^\circ$ corresponds to the case of pure shear. The M20class 8.8 bolts, connecting the T-stub flange to the end fixture, were preloaded with a torque moment of 350Nm. During the tests, the flange displacement components in the direction parallel and perpendicular to the flange were measured (Figure 4-102). The tests were carried out under displacement control. The loading process comprises of a preliminary cycle up to approximately 10% of the estimated collapse load and a subsequent cycle up to the collapse condition.

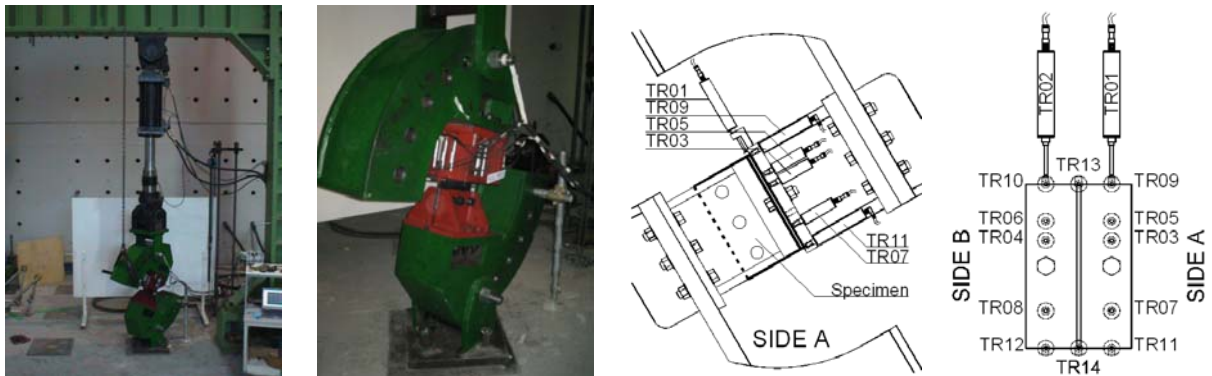


Figure 4-102: Testing apparatus and transducers' set-up for tests on T-stubs under axial and shear force.

4.5.3.5 Material properties

In order to evaluate the tests results, the mechanical properties of the steel components were obtained. Material properties, but the end plate of the CS joint, were determined by the University of Stuttgart. As to the end-plate of the CS joint, five tensile tests were performed at the University of Trento: the average value was 413MPa for the yield strength, and 551MPa for the ultimate strength.

Tensile tests on the bolts were also performed. The experimental curves were interpolated via polynomial functions. The average value of the collapse load was of 229kN and 280kN for bolts M20 class 8.8 and bolts M20 class 10.9, respectively.

4.5.3.6 Test results of the tension tests

A total of 79 tensile tests on T-stub specimens were performed. In detail, 43 tests relate to the CS joint and 36 tests relate to the SJ joints. Tests were carried out up to collapse. The average values of the collapse loads are collected in Table 4-10 and Table 4-11. The nominal length and the effective length are also listed in the tables. The large amount of data does not allow to refer in an extensive way about the results. In the following the main outcomes of the study are summarised:

- T-stubs of the CS joint showed remarkable flange displacements which involved the entire end-plate/column flange. On the opposite side T-stubs of the SJ joints, but for the end-plate T-stub 8mm thick, showed quite limited flange displacements which were mostly concentrated near the bolts;
- Collapse loads quite higher than those evaluated via the procedure of the EN 1993-1-8 [69] were obtained. It should be mentioned that the Eurocode approach is based on simplified relationships which neglects effects such as the hardening of materials, the membrane effect and the interaction between bending and shear, which on the contrary remarkably affect the T-stubs response in the plastic range;
- Load-flange displacement curves were characterised by a remarkable hardening effect due to the material hardening and the membrane action which develops when large flange displacements occur. The establishment of a criterion for evaluating the load associated with the yielding of the flange was hence required;
- T-stubs responses appears quite sensitive to the presence of stiffeners and in particular to the stiffeners' position. As an example, in the case of the end-plate T-stubs of the CS joint the increase of the collapse load of stiffened specimens was in the range of 16.9% to 30.8%. As to the T-stub ductility, results show a negative effect of stiffeners when they are located close to the bolt.
- Endplate thickness affects remarkably the stiffness, the strength and the collapse mode of T-stubs. In the case of the SJ BC1 joint, an increase of 4 mm of the flange thickness resulted in an increase of the collapse load of 32% for both the stiffened and the unstiffened configuration;
- The non negligible influence of the bolt preload on the initial stiffens of T-stubs was confirmed. The ductility may be affected as well;

Table 4-10: Test results for the CS joints.

END-PLATE T-STUBS					COLUMN T-STUBS				
ID specimen	n° test	Length		Collapse load kN	ID specimen	n° test	Length		Collapse load kN
		Nominal mm	Effective mm				Nominal mm	Effective mm	
UNSTIFFENED T-STUBS									
1BA	5	80	256	200,42	1CA	5	80	178	230,52
1BB	4	256	256	281,86	1CB	5	256	178	285,73
STIFFENED T-STUBS									
2BA	4	256	210	368,54	2CA	4	256	210	382,90
2BB	4	256	179	357,59	2CB	4	256	179	347,77
2BC	4	256	175	329,44	2CC	4	256	175	314,86

Table 4-11: Test results for the SJ joints.

END-PLATE T-STUBS						COLUMN T-STUBS				
Joint Type	ID specimen	n° test	Length		Collapse load kN	ID specimen	n° test	Length		Collapse load kN
			Nominal mm	Effective mm				Nominal mm	Effective mm	
UNSTIFFENED T-STUBS										
SJ BC1	5BAA	3	254	254	327,36	5CA	2	170	144/217	600,10
	5BAB	3	254	254	431,16					
	5BAC	2	254	254	576,16					
SJ BC2	5BB	3	353	353	371,27	5CB	1	285	285	568,36
SJ BC3	5BC	3	443	443	339,39	5CC	3	354	354	507,47
STIFFENED T-STUBS										
SJ BC1	6BAA	3	254	246	449,84	6CA	1	170	144/183	589,00
	6BAB	3	254	246	592,08					
	6BAC	1	254	246	612,52					
SJ BC2	6BB	3	353	346	460,72	6CB	1	285	301/307	602,80
SJ BC3	6BC	3	443	443	453,12	6CC	1	354	361	567,12

An analysis of the deformed shapes at collapse (contour lines and slope contour lines) was performed with the aim of checking the reliability of the Eurocode approach:

- in case of the CS joint, the agreement was satisfactory for both the unstiffened and stiffened T-stubs;
- in the case of unstiffened T-stub of the SJ joints, the agreement was satisfactory, but in one case for which the collapse was in mode 3 instead of 1;
- in the case of stiffened T-stubs of the SJ joints, the premature failure of the bolts due to the significant bending caused by the local deformation of the flange prevented activation of the expected mode 1, and collapse was hence in mode 3;

An additional study of specimens characterised by collapse mode 1 was carried out aiming at investigating the validity of the Eurocode 3 [69] approach. Despite the uncertainty on the evaluation of force associated with the yielding of the flange, on the location of the plastic hinges in the web area and on the location of the prying forces, the results of the analysis pointed out a rather good agreement between experimental and numerical outcomes. Results pointed out also the need of further research work focused on the influence of the distance between the stiffener and the bolts on the value of the effective length.

4.5.3.7 Test results of the tests under tension and shear force

Tests were planned for the CS joint configuration: the T-stub specimens of the column were 256mm long, the specimens of the end-plate were 80mm long. Despite the preliminary evaluation on the end-plate T-stubs indicated the bearing resistance of the flange as the governing failure mode, the specimens failed by premature collapse of the web. For this reason test data are reported only for the column T-stub.

For all the 16 column tests collapse was achieved by bolt fracture after a significant flange deformation. Different responses were observed for the bolts and the flange as function of inclination angle α (Figure 4-103). In all the tests, a remarkable bearing deformation of the holes occurred (Figure 4-103). A “flange mechanism” was activated with the development of non negligible plastic deformations, but for the pure shear tests ($\alpha=0^\circ$), (Figure 4-103). Higher the tensile force components higher the flange deformation.

The average collapse loads associated with each test angle are gathered in Table 4-12, where the applied force's components in the parallel and the perpendicular direction with respect to the flange are reported. The value associated with $\alpha=90^\circ$ is the pure tension resistance (see § 4.5.3.6). The experimental axial-shear force domain is presented in Figure 4-103. The interaction between the axial and the shear force appears to be non negligible. However, the number of tests is too limited to draw definite conclusions. At this aim additional tests on different T-stub configuration would be necessary.

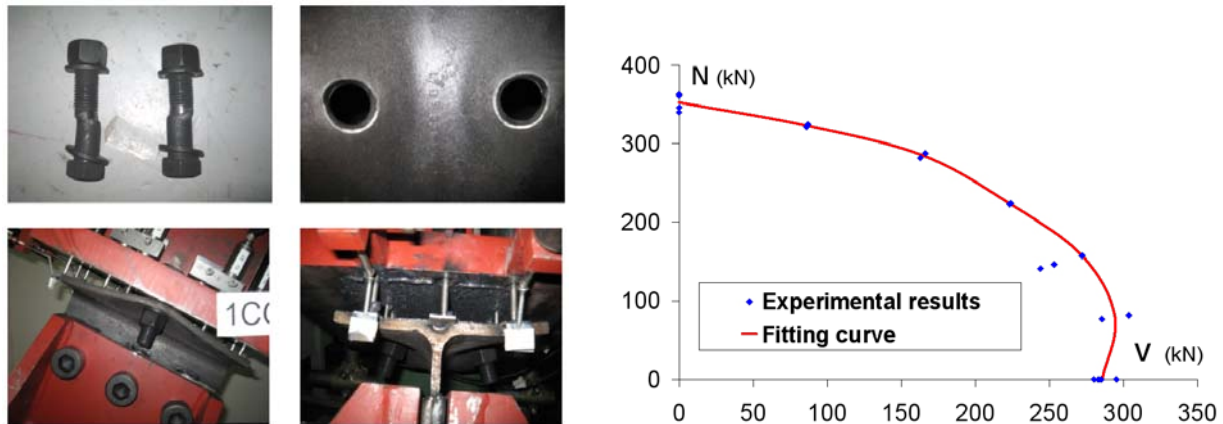


Figure 4-103: Bolts' and flange deformations (on the left) and N-V domain (on the right) for column T-stub specimens of length 256mm.

4.5.3.8 Conclusions

The key outcomes of study of the response of T-stubs under pure tension and under different combination of axial and shear force have been presented. Specimens were related to four steel joint configurations: the CS joint used in the reference composite frame of the research project and the SJ joints tested at the University of Stuttgart. The SJ joints were characterised by different end-plate layout and thickness, and bolt-to-web locations. A total of 79 tension tests were carried out on both stiffened and unstiffened T-stubs representative of the end-plates and of the columns. The tests under axial and shear force were performed only on the column T-stubs of the CS joint (16 tests).

Tensile tests allowed at investigating different aspects such as the influence of the presence of stiffeners and of their location, of the end-plate thickness and of the preload of the bolts. The experimental response confirmed the remarkable deformation capacity of specimens consequent to the hardening of the material and the activation of a membrane action. The "T-stub" approach proposed by the Eurocode [69] neglects such important contributions, which can be considered as a reserve of strength and deformation capacity, contributing to fulfil the ductility requirements for joints in the case of exceptional loading conditions (robust systems). Criteria aiming at the evaluation of the performance of T-stub in the large displacements field are not provided by the Eurocode [69], and in effect are outside its scope. This requires the definition of adequate methods enabling control of the main parameters affecting the ultimate strength and ductility of T-stubs.

Table 4-12: Test's results for column T-stub specimens under axial and shear force.

Angle of test	n° test performed	Collapse load kN	Axial component kN	Shear component kN
0°	4	352,55	0,00	352,55
15°	2	334,40	86,55	323,01
30°	2	329,20	164,60	285,10
45°	2	316,08	223,50	223,50
60°	4	314,44	272,31	157,22
75°	2	305,00	294,61	78,94
90°	5	285,73	285,73	0,00

Besides the case of collapse due to bolt failure, the T-stub approach proposed by the Eurocode [69] is based on the development of complete or partial flange plastic mechanisms. This clear distinction among the different modes leads to simpler design. However, the analysis of tests results clearly indicated that there is a sort of transition between the different modes, and 'mixed' modes can develop. Moreover, the flange yielding condition can not be accurately identified, and the definition of a criterion for its evaluation was required. The analysis of tests results was combined with the study of the deformed shapes at collapse (contour lines and slope contour lines), and showed a satisfactory agreement between the tests results and the Eurocode approach in the case of the CS joint, with reference to collapse mode and yielding load. A similar remark can be done for the unstiffened T-stub of the SJ joints, but for one case for which the collapse was in mode 3 instead of 1. Stiffened T-stubs collapsed by premature failure of the bolts due the significant bending caused by the local deformation of the flange. The activation of the expected mode 1 was hence prevented, and collapse was in mode 3. These results suggest the need of further studies focused on some specific aspects of the T-stub behaviour and collapse mechanism, such as the effect of the stiffeners and of the bolt-to-web location.

The studies on T-stubs were completed by a series of tests under different combination of axial and shear force. A total of 16 tests on the column T-stub of the CS joint were carried out. All tests showed the development of significant plastic flange deformation. Different responses were observed for the bolts and the flange depending on the ratio between the shear and axial force. Test results allowed a first appraisal of the N-V domain, which shows a non negligible interaction between axial and shear force. However, the number of tests is too limited to draw definite conclusions. At this aim, additional tests on different T-stub configuration would be necessary.

4.5.4 Test on the connection

4.5.4.1 General

A further series of tests were planned aimed at "bridging" the T-stub to the complete steel connection response. A total of 14 tests were carried out on the CS steel joint configuration of the reference composite frame. Three specimen configurations were selected:

- End-plate T-stub connected to the column (3 tests);
- Full steel connection on rigid support (5 tests);
- Full steel connection on the column (complete joint, 6 tests).

For the first configuration, tests under pure tension were planned, while for the other configurations tests were performed under different combinations of axial (N) and shear force (V).

4.5.4.2 Layout of the specimens

END-PLATE T-STUB CONNECTED TO THE COLUMN

The column stub, a rolled section HEA 160, had a nominal length of 1 m; the end-plate T-stub was 80mm long and had a flange 8mm thick. The T-stub was bolted to the column flange at mid-length by means of two bolts M20 class 8.8. The column stub was connected to a counter frame so as to reproduce the ideal restraint conditions of hinges at the end.

FULL STEEL CONNECTION ON RIGID SUPPORT

The specimens were composed by a beam stub (steel profile IPE 140) of nominal length of 950mm welded to a square end-plate with a side of 160mm and a thickness of 8mm. The connection comprises of 4 bolts M20 class 8.8. Specimens were connected to a rigid support. The load was applied to the free end of the beam. The distance between the point of application of the load and the rigid support was of 845mm.

FULL STEEL CONNECTION ON COLUMN (COMPLETE JOINT)

Specimens were composed by a column stub (a HEA160) of nominal length of 1000 mm and by of beam stub (an IPE 140) of nominal length of 958 m. The beam stub is connected through a square end-plate of side 160 mm and 8 mm thick and 4 bolts M20 class 8.8. The column was “hinged” to the counter frame at the ends. The load was applied to the free end of the beam. The nominal distance of the point of load application with respect to the column was of 850mm.

4.5.4.3 The tests

For the first configuration three tension tests were performed, while for the second and the third configuration tests in tension and under different combinations of axial (N) and shear force (V) were carried out. A total of five tests were performed for the connection on rigid support: one under pure tension and four under shear and tension. As to the complete joint, six specimens were tested: two under pure tension and four under shear and tension. In detail, two tests were carried out for each of the two combinations of shear and axial force considered. The following procedure was adopted. At the beginning of the tests, a relative inclination between beam and actuator was present (Figure 4-104a). As soon as the load is applied, a rotation of the beam occurs leading to a progressive alignment between the actuator and the beam (Figure 4-104b).

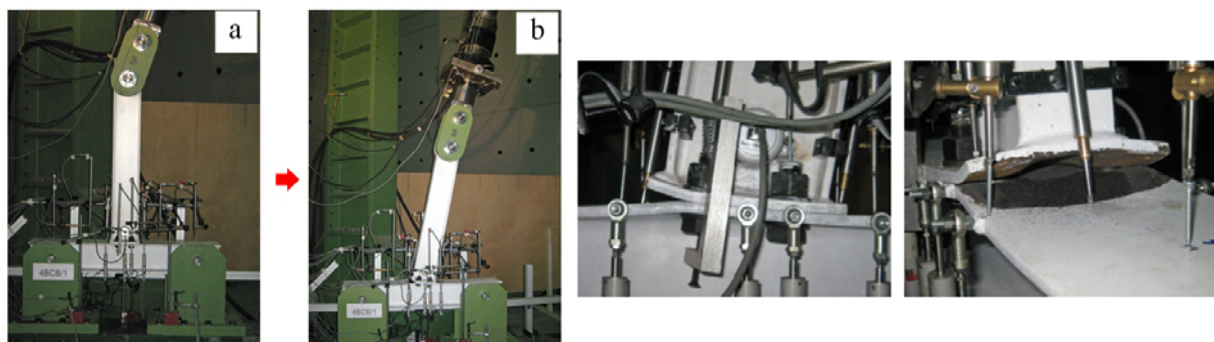


Figure 4-104: Test on the complete joint – Initial beam-to-actuator angle of 20°

At collapse, a complete beam-to-actuator alignment was achieved when compatible with the rotation capacity of the connection. It should be mentioned that a bending moment is also applied to the connection due to the particular test set-up. However, this moment which depends on the relative beam-to-actuator angle, varies with a law similar to that which characterise the connection response in a real frame when a column is failing. The initial values of beam-to-actuator angle were 11° and 20° for the connections on rigid support and of 12° and 20° for the complete joint. Specific measurement set-ups were designed in order to get the main sources of deformation. In the case of end-plate T-stub connected to the column, the deformation of the flanges of the column, the relative displacement of the upper and lower column flanges, the displacement of the flange of the T-stub and, finally, the displacements of the head of the bolts were measured. In the tests on the connection on rigid support

and on the complete joints, the attention was focused on the end-plate displacements which were measured in different locations. Besides, the displacements of the head of the bolts and the bolt shank elongation were measured for the connections tests. In the tests on the complete joints, the displacements of the upper flange and the relative displacements between the upper and the lower flange of the column were also measured. The inclination of both the beam and the actuator were monitored by clinometers.

All the tests were carried out under displacement control conditions. The loading process comprises of a preliminary cycle up to approximately 30 kN, and a subsequent cycle up to collapse.

4.5.4.4 Test results

END-PLATE T-STUB CONNECTED TO THE COLUMN

The tests were characterised by a similar response in terms of collapse load and ultimate displacement of the T-stub flange. The collapse was caused, in all the tests, by the failure of the bolts, which were subject to significant bending due to the high deformation of both the column and the T-stub flanges. Cracks at the flange-to-web welds initiated just before attainment of the collapse. The collapse loads are collected in Figure 4-105. For comparison purposes, in the last column of the table in Figure 4-105 the average value of the collapse load obtained from the tension tests on the end-plate T-stub connected to a rigid support is presented (§ 4.5.3.6). It is apparent that the column flange deformation leads to a reduction of about 10.4% in average of the ultimate load. The deformation of the column affects all the T-stub response as shown by Figure 4-106, where the load-displacement curves for the flange of the “same” T-stub tested on rigid support and on the column are plotted. The preloading torque is the same in both cases. The specimens’ responses show a quite similar trend. It should be noted that here is not a significant difference in terms of ductility.

Specimens	Collapse load kN	Tension tests on end plate T-stub kN
3A/1	178,20	200,42
3A/2	179,16	
3A/3	181,16	

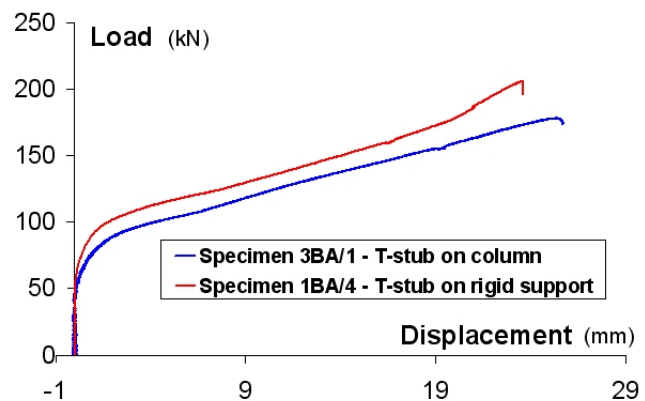


Figure 4-105: Test's results for end-plate T-stub on rigid support.

Figure 4-106: Comparison between end-plate T-stub on column and on rigid support.

FULL STEEL CONNECTION ON RIGID SUPPORT

The experimental response in all the tests was characterised by a remarkable inelastic deformation of the end-plate. As a consequence, bolts were subject to significant bending. In tests under shear and axial force, the complete alignment between beam and actuator was attained only for the specimens with an initial beam-to-actuator angle of 11° . Test results in terms of collapse forces are presented in Table 4-13 which compares the response associated to the three tests configurations considered. In the table the actual inclination angle of the actuator at the beginning of the tests (MTS angle) is given. The force's components (axial and shear force) at the ultimate condition were computed with respect the longitudinal axis of the beam in the deformed position. Table 4-13 points out the remarkable influence of the combined action of shear, axial force and bending moment. If the tension test is assumed as reference, an initial inclination angle of approximately 11° results in a decrease of the ultimate load of 16.2%. In the case of an inclination angle of 20° , the reduction in strength increased to 43.7%.

A comparison between the experimental load capacity of the end-plate T-stub and of the full connection on rigid support in tension is presented in Figure 4-107. In accordance to the Eurocode approach, the values of the ultimate load of T-stubs, both stiffened and unstiffened, with a length equal to the effective length are presented (§ 4.5.3.6). If the interaction between the bolt rows is disregarded, and the connection ultimate capacity is approximated as two times the end-plate T-stub maximum load, the T-stubs would in any case overestimate the strength of the connection. This overestimation is of 5.6 % and of 38.1% if the unstiffened or the stiffened T-stubs are considered. These differences depend on the lack of capability of the T-stub tests to reproduce correctly the interaction effect between the bolt rows (Figure 4-108).

Table 4-13: Test's results for the connection on rigid support.

Specimen	Actual MTS initial angle deg	Maximum applied load kN	Axial component kN	Shear component kN	Bending moment kNm
4BA/2	0°	533,84	533,84	0	0
4BB/3/11°	11°,10	453,48	453,48	-0,63	-0,54
4BB/4/11°	10°,98	441,56	441,56	1,95	1,66
4BB/1/20°	19°,51	293,64	293,30	14,14	12,00
4BB/2/20°	19°,34	307,96	307,82	9,17	7,78

Specimen	Tensile test on	Maximum load kN
4BA/2	Connection on rigid support	533,84
1BB	Unstiffend end-plate	281,86
2BA	Stiffened end-plate	368,54

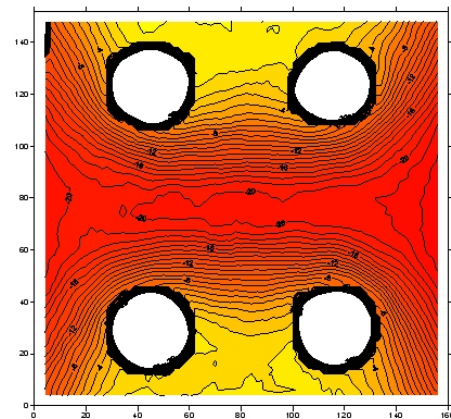


Figure 4-107: Comparison between connection on rigid support and T-stub responses.

Figure 4-108: Contour map at collapse for connection on rigid support.

FULL STEEL CONNECTION ON THE COLUMN (COMPLETE JOINT)

Large deformations of both the column and the end-plate developed before collapse (Figure 4-104) which was caused by bolt fracturing. In the tests under a combination of axial and shear force, cracks on beam to end-plate weld initiated near to collapse. The collapse loads for the three tests configurations are presented in Table 4-14. The inclination angle of the actuator at the beginning of the test (MTS angle) is also reported. The applied force's components (axial and shear forces) associated with the ultimate condition were computed with respect the longitudinal axis of the beam in the deformed position. Modest inclination angles (11°) do not affect the resistance capacity. If the angle increases (20°) a remarkable reduction in strength is observed (21.5%). The influence of the inclination angle seems to be rather different than in the case of rigid support. The comparison between results in Table 4-13 and Table 4-14 allows an appraisal on the influence of the column deformability on the connection response. If the response of the connection on rigid support is assumed as the reference one, the results in Table 4-14 point out that the influence of the column deformation on the connection performance is

negligible when an initial inclination angle of 20° is considered. Strength reduction of 15.5% and 29% occurred in case of inclination angle of 11° and tension force, respectively.

Table 4-14: Test's results for the complete joints.

Specimen	Actual MTS initial angle deg	Maximum load kN	Axial component kN	Shear component kN	Bending moment kNm
4BCA/1	0°	375,52	375,52	0	0
4BCA/2	0°	382,16	382,16	0	0
4BCB/3/ 12°	$11^\circ, 70$	372,64	372,63	3,14	2,67
4BCB/4/ 12°	12°	383,52	383,42	8,83	7,50
4BCB/1/ 20°	20°	274,68	274,35	13,38	11,46
4BCB/2/ 20°	19°	319,88	319,83	5,58	4,75

As to the load-displacement history of the end-plate, the influence of column deformation depends on the beam-to-actuator angle.

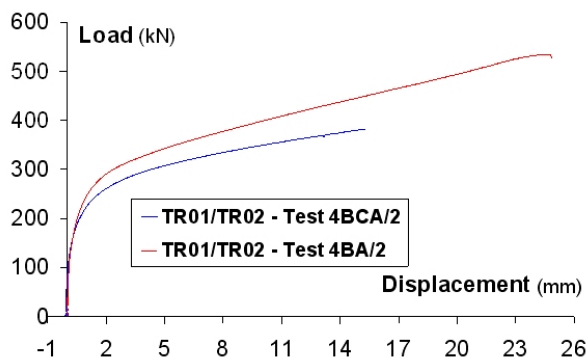


Figure 4-109: Comparison between connection on rigid support and on the column.

Figure 4-109 compares the response of specimens 4BCA/2 (test on complete joint) and 4BA/2 (full connection on rigid support) subject to pure tension. The displacements of the end-plate associated to test 4BCA/2 were “cleaned” of the displacement of the column flange. Transducers in both the tests were located in the same position. The influence of the column flange deformation on stiffness, ductility and strength is apparent. When the inclination angle increases, the influence on the deformation capacity tends to reduce, and the complete joint to become stiffer than the connection on rigid support.

4.5.4.5 Conclusions

This section refers to an experimental study of the connection of the steel joint of the reference composite frame analysed by the research project. Following the approach of the component method three different specimen configurations were considered. Tests were performed on the end-plate T-stub connected to the column, on the full steel connection on rigid support and on the column. Pure tension tests were carried out on the T-stubs, while tests under tension and under two different combination of axial and shear force were performed on the connection. An initial relative angle between the beam and the actuator enables different combinations of axial and shear force.

Tests allowed an appraisal of the influence of the column deformability on the T-stub and on the connection responses. If the rigid support condition is assumed as the reference one, both the T-stub and the connection were adversely affected by the column deformation: the collapse load decreases of 10% for the T-stub, and of 15.5% and 29% for the connection, depending on the load conditions. The stiffness and the ductility are also significantly influenced.

As to the loading condition, the response of the connection on rigid support is remarkably affected. If the tension test is assumed as reference, an initial inclination angle of about 11° results in a decrease of the ultimate load of 16.2%. In the case of an inclination angle of 20° , the reduction in strength increased to 43.7%. In the case of connection on column, the effect of the initial loading condition appears

negligible in case of modest initial beam-to-actuator inclination angle. If the angle increases (20°) a remarkable reduction in strength is observed (21.5%).

4.6 Summary and conclusions of the experimental results

Progressive failure of the whole structure caused by local damage (e. g. failure of a column caused by a vehicle impact, explosion, fire, earthquake) can be prevented by robust design. Taking profit from the inherent ductile behaviour of steel, this project analysed the requirements for joints by following the strategy “alternate load path method” by activating membrane effects in the structure due to catenary action. A catenary action for redistribution of internal forces within a structural system requires large deformations of the structure. Large deformations demand for ductile joints.

The composite joint tests as well as the substructure test demonstrated that the previous concept to strengthen the joints in order to achieve that the plastic hinges are placed in the beams is not a necessary condition for activation of catenary action in a frame structure. It is also possible to place the plastic hinges into the joints by designing partial-strength joints with sufficient ductility. The component tests completed the experimental tests by investigating how to influence the resistance and ductility of single components with simple modifications.

An important finding of the experimental investigations is that all single relevant components of the joints have to be chosen such that for the transition from pure bending state to a combined bending and tension exposure the weakest component in each case is always ductile. To avoid that components with brittle failure mode in a bolted endplate connection cause premature brittle failure of the whole joint such components as the bolts have to be “oversized”. To determine the size of the bolts also over-strength effects of the structural steel as well as membrane effects in the endplate or column flange have to be considered for the joint design. Until now the component method in EN 1993-1-8 [69] does not consider any of these effects.

To be able to undergo from pure bending exposure to a pure tension exposure first it has to be ensured that sufficient rotation deformability of the joints is available. So large deformations to activate membrane forces in the structure could develop which lead to biaxial loading of the joints. For the components of the joint which are under compression for the state of pure bending the loading gradually change from compression into tension by additional loading of the joint by membrane forces. So these components have a lot of plastic reserves in comparison to the tension components which are already strongly utilized for pure bending state when starting with biaxial loading of the joint. This means the compression components should be preferred as weakest components by designing a ductile joint for M-N-interaction.

The tension components have to provide sufficient deformation capacity because they are already highly stressed under pure bending and have to have reserves for the additional tension exposure. Within the component tests the tension components like the reinforcement in tension, endplate in bending or column flange in bending have been investigated aiming to improve the deformation capacity of these components.

Main aim was to define requirements for ductile joint solutions which support the ductile behaviour of the steel and which are able to utilize the immense plastic reserves for exceptional loading. Therefore ductile joint solutions should be made available for practical design which need no additional elements, don't cause any significant extra costs and which are realizable without any difficulty.

Some requirements for single components and some general design criteria derived from the experimental test results to ensure a highly ductile behaviour of the joints are presented in Table 4-15.

Table 4-15: Requirements for joint components to ensure a ductile joint behaviour.

COMPONENT	REQUIREMENTS
reinforcement in tension (RFT)	<ul style="list-style-type: none"> the ductility of the tension bar in the concrete slab can be improved by extending the tension bar due to an increase of the distance of the first shear stud to the endplate; the ductility of the reinforcement can be improved by choosing B 450 C ($f_u/f_y > 1.3$) instead of BSt 500 S (B) ($f_u/f_y > 1.08$)
endplate in bending (EPB) + column flange in bending (CFB)	<ul style="list-style-type: none"> it is advantageous when both components have nearly the same resistance acc. the definition in EN 1993-1-8, that means in usual cases the same steel grade as well as the same thickness, so both may contribute similarly to the joint deformation; the resistance of these components have to be smaller than the resistance of the bolts (considering over-strength and membrane effects for both components); the ductility may be improved by increasing the vertical distance from the bolts to the beam flange and horizontal distance from the bolts to the beam web for composite joints the deformability of both components have to be sufficient to activate the tension bar in the concrete slab completely
bolts in tension (BT)	<ul style="list-style-type: none"> the bolts have to be oversized in such a way that all over-strength effects as well as membrane effects in all designed ductile components are covered
beam flange in compression (BFC)	<ul style="list-style-type: none"> the beam flange in compression tends to be designed as weakest component of the joint due to the fact that buckling of the flange is a quite ductile failure and under biaxial loading the stress changed into tension so for additional normal tension force the beam flange is still fully functional
concrete slab in compression (CC)	<ul style="list-style-type: none"> the concrete slab in compression for joints under sagging moment fails due to the sharp bend from the joint rotation and the resulting high compressive strain at the upper concrete surface; the crushing of the concrete is important to enable also a ductile behaviour for sagging moment but the influence of the concrete compressive strength to the crushing effect seems to be of minor importance

5 NUMERICAL AND ANALYTICAL STUDIES

5.1 General

The main objectives of the numerical and analytical studies are detection of the parameters influencing robustness (parameter study) and optimisation and idealisation of the joints to obtain robust structures. In order to achieve robust structures the joint geometry has to be optimised. The required deformation of the joints (only analysis) has to be compared with the available deformation (test results and analysis). The different Finite Element softwares are an important tool to determine the response of the structural system for a huge amount of various scenarios and to find out the needed requirements of the joints and members to resist the relevant exceptional event.

In the framework of the project “Robust structures by joint ductility” different parametric studies have to be carried out. The influence of single members (for example the behaviour of joints, the stiffness of beams, the dimensions of the structure, etc.) on the global behaviour of the structure in terms of robustness, can be determined by modifying single properties of a complex structure.

The FEM numerical simulations are basis to understand how the structure and its constitutive elements behave and how the redistribution of forces takes place in the unaffected part of the frame. In this process, a special attention is devoted to the study of the loading sequence inside the joints. As a result of these FEM numerical simulations and associated parametrical studies, simplified behavioural models are developed and validated; these ones progressively lead to analytical models, from which requirements to be satisfied by the structural system and by the joints are derived. The analytical formulas enable the designer the determination of design criteria in a simple and economic way.

5.2 Validation of the numerical tools

5.2.1 Introduction

Within the project, different numerical tools are used to investigate the behaviour of steel and composite structures subjected to an exceptional action. The present section is dedicated to the validation of these numerical tools.

In a first step, the Finite Element software FINELG developed at Liège University has been validated (§ 5.2.2). This validation has been performed with the substructure test (§ 4.3); indeed, the tested substructure has been modelled with FINELG and the so-obtained numerical results have been compared to the experimental results.

Then, to validate the other software, two benchmark studies associated to two different exceptional situations have been performed:

- The first one is a benchmark study simulating the loss of a column in a steel structure (§ 5.2.3).
- The second one is a benchmark study simulating the loss of a bracing in a composite structure (§ 5.2.4).

To provide the results of the benchmark study simulating the loss of a column, a separate document including the benchmark results of the University of Stuttgart (UStutt), the University of Liege (ULg) and PSP Aachen (PSP) are given as an annex to the final report [36].

5.2.2 Validation of FINELG with the experimental tests

As mentioned previously, the behaviour of the tested substructure has been predicted through the software FINELG, FE software developed at the University of Liège.

The mechanical and the geometrical properties which have been introduced in the numerical modelling are the ones measured at the Argenco laboratory (§ 4.3.4.2 and § 4.3.4.3). Also, the behaviour of the substructure composite joints which have been implemented is the one observed through the isolated joint tests performed at the University of Stuttgart (§ 4.4.2). The load path defined in the numerical simulation is exactly the one followed during the test (§ 4.3.4.4).

The difficulty of the modelling is to introduce the actual behaviour of the joints within the simulation; indeed, the combined interactions within the joints between the axial load and the bending moment (“M-N”) and between the bending stiffness and the axial stiffness have to be reflected within the numerical simulation, as these interactions widely influence the development of the catenary action within the modelled structure. In the actual Finite Element codes, no Finite Element permits to model such combined interactions.

Within the present study, two different solutions have been investigated:

- The first one consists in modelling the joint behaviour with a rotational spring only. So, there is no M-N and no axial and bending stiffness interactions introduced in the modelling.
- The second one consists in modelling the joint behaviour through equivalent double-T beam elements exhibiting the same M-N resistance as the joint one. Also, the bending stiffnesses of the equivalent beams have been calibrated to exhibit the bending stiffnesses of the joints. In total, two equivalent double-T beams have been defined: one to model the behaviour of the joint under hogging moment and one to model the behaviour of the joint under sagging moment (see Figure 5-1 and Figure 5-2). With this solution, the M-N interaction resistance curve is taken into account but not the one between the bending and axial stiffnesses; indeed, if the elongation of the double-T beams, when the plastic hinges are formed, is compared to the joint one experimentally determined, it is observed that the equivalent beams are less stiff than the joints. Accordingly, the lateral restraint at the substructure extremities has been artificially increased to compensate this lack of axial stiffness within the beams.

The comparison between the so-obtained results and the experimental one are given in Figure 5-3. It can be seen that with the two solutions, the obtained results are not satisfactory, except for the modelling with the equivalent double-T sections up to a deflection of 475 mm, i.e. when significant membrane forces appear in the system. It is associated to the fact that none of the proposed solutions permits to model accurately the actual behaviour of the joints. Additional researches are requested to improve the numerical modelling of the behaviour of joints with account of the different interactions appearing when catenary action develops in a structure.

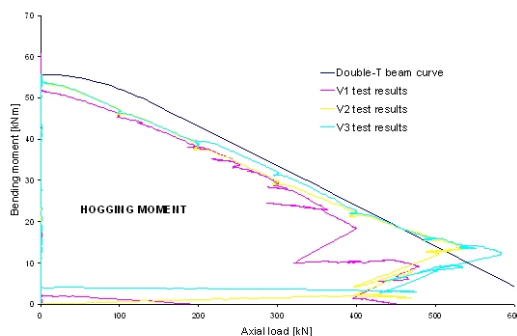


Figure 5-1: Comparison of the M-N interaction curves – hogging moment

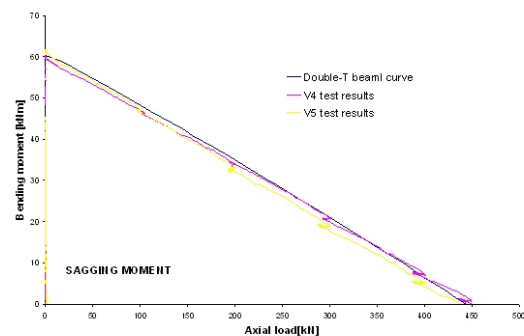


Figure 5-2: Comparison of the M-N interaction curves – sagging moment

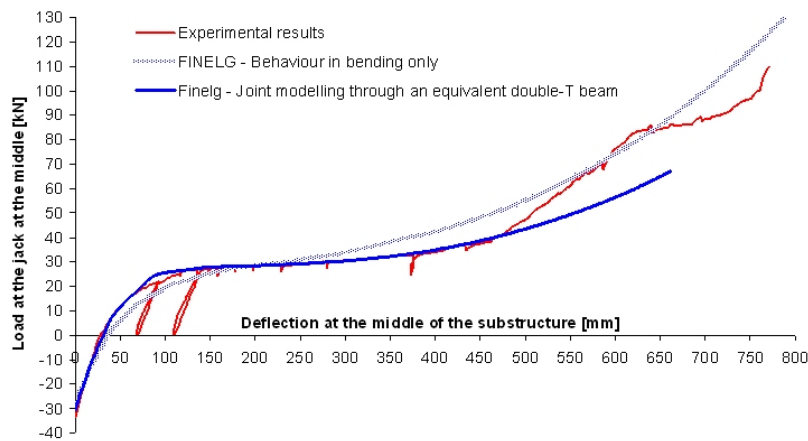


Figure 5-3: Comparison between the numerical predictions and the experimental results

5.2.3 Benchmarking of other software - loss of a column

5.2.3.1 General

In the framework of the project “Robust structures by joint ductility” different parametric studies have been carried out. The influence of single members (for example the behaviour of joints, the stiffness of beams, the dimensions of the structure, etc.) on the global behaviour of the structure in terms of robustness can be determined by modifying single properties of a complex structure. Facing the huge effort of test series, a reliable Finite Element (FE) modelling seems to be essential to detect the effects of single properties on the robust behaviour of a various number of structures. In order to calibrate the FE software of all involved project partners, benchmark models were introduced. The substructure of benchmark model 1 was tested in the laboratory of the university Liege. Therefore the dimensions of this model were limited due to the laboratory facilities. In order to reduce the computation time and the number of affecting parameters, a pure steel benchmark model was also introduced in this project. The dimensions of benchmark model 3 are those ones of a realistic office building. All effects that influence the robustness can be studied at benchmark model 3 in an efficient way. In the annex of this report [36] all the activities are summarized and the results are used as a reference to calibrate any further software package. For simulation of the structure ULg uses the FE software FINELG [73], PSP the software ABAQUS [39] and UStutt the FE program ANSYS [40]. To provide the results of the benchmark 3 activities, a separate document [36] including the benchmark results of the University of Stuttgart (UStutt), the University of Liege (ULg) and PSP Aachen (PSP) is given in the annex to this document.

5.2.3.2 Description of the structure benchmark model 3

A 2D steel frame was designed according to EN 1993-1-1 [68]. The loads were taken as recommended in EN 1991-1-1 [64]. The frame has 7 bays and 6 storeys. The span of the beams is 8.00 m and the height of the storeys is 3.50 m. The out of plane distance between the frames is 5.00m. The column bases are fully fixed (all degrees of freedom fixed) and the joints are assumed as rigid and full strength joints. The system has no further bracings.

5.2.3.3 Results

In a collapse analysis the design loads were increased until the collapse of the structure. The load factor referring to the design loads (with safety factors) and the horizontal displacement at the top of the structure were measured.

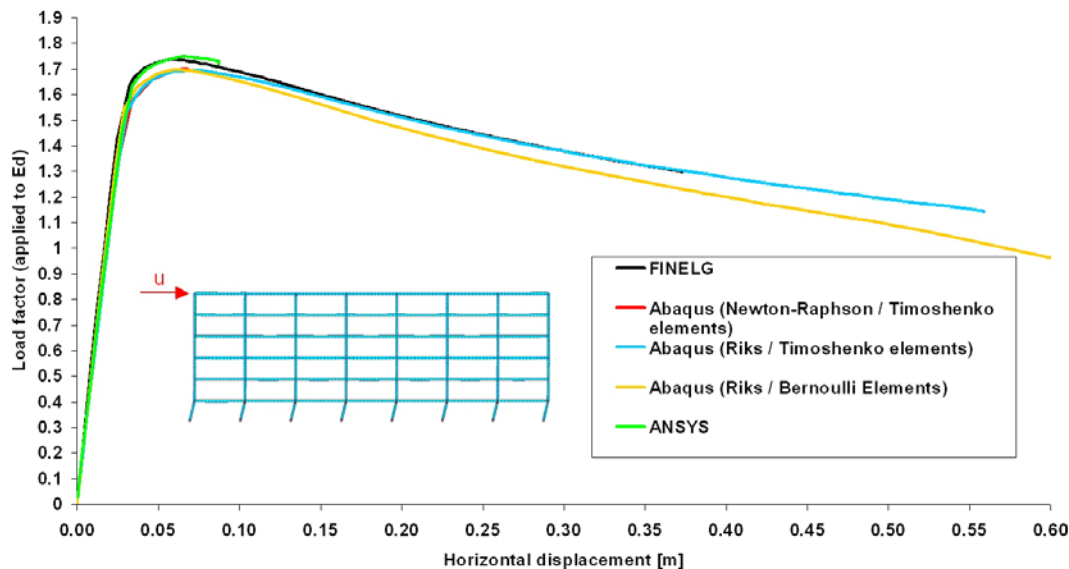


Figure 5-4: Comparison of collapse analysis of benchmark model 3

As it can be seen from Figure 5-4, every FE programs give nearly the same results during the elastic load path and the fully plastified load path. Only when the structure starts yielding, and a redistribution of internal forces takes place, the FE programs give slightly different results.

The results of several other calculations are compared in the benchmark annex, and a good agreement of the FE results can be determined in all calculations.

5.2.4 Benchmarking of other software - loss of a bracing

5.2.4.1 General

As already mentioned in § 5.2.3 it is really important to calibrate the various FE-software to ensure accurate and realistic results of the performed numerical simulations. For the benchmark model 2 “loss off a bracing” a framed composite structure of a car park was introduced. More details about the structural system including all dimensions are given in § 5.2.4.2 and § 5.4. The partners involved in this benchmark model 2 are Ulg with the software FINELG and UStutt with the software SOFISTIK. The software SOFISTIK was used by UStutt because it is well suitable to model and calculate composite structures, also large structures with adequate computation time. So UStutt decided to use SOFISTIK for this numerical study. FINELG was also used for benchmark model 1 and 3 and as result calibrated at the substructure test. So this benchmarking aim at the validation of the program SOFISTIK to be able to do further numerical studies with this software. A complete overview about the activity of the investigation loss of a bracing is given in [24].

5.2.4.2 Description of the structure benchmark model 2

The structure for benchmark model 2 is a 2D framed composite structure designed according EN 1994-1-1 [70] and EN 1993 -1-1 [68]. The applied loads were taken from EN 1991-1-1 [64] and EN 1991-1-4 [65]. The frame has 3 bays and 3 storeys, the span of the beams is 16.0 m and the storey height is 3.50 m. The connecting joints between columns and beams are assumed as semi-rigid ones and the column base are hinged. Bracings are arranged in one bay over the total height and they have to brace a number of 5 frames. Further description is following in § 5.4.2.

5.2.4.3 Results

In a first analysis the collapse resistance of the undamaged structure was determined by increasing all applied loads proportionally. The analysis was performed with characteristic values for all affected loads as well as for all material resistances.

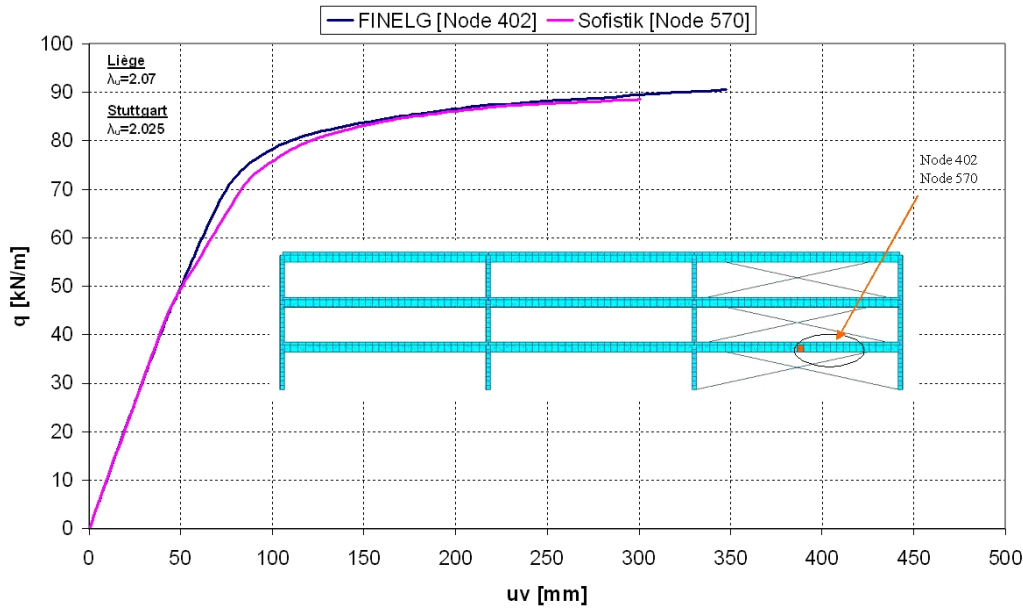


Figure 5-5: Comparison of collapse analysis of benchmark model 2

Both FE programs FINELG and SOFISTIK are in good agreement as presented in Figure 5-5 only when parts of the structure starts yielding some small deviations of both curves exist. Also for the damaged structure both software correspond well.

5.2.5 Conclusions

Through the comparison between the numerical results and the test results, the difficulty to model the actual behaviour of structural joints subjected to bending moments and axial loads has been demonstrated. Therefore a new FE element able to simulate the behaviour of these joints has to be developed. But the development of such a Finite Element would be a project in itself.

Then, two benchmark studies have been performed. The first one was dedicated to the validation of the numerical tools to simulate the response of steel structures subjected to the exceptional event “loss of a column”. Through this study, the three FE software used by the different partners (i.e. FINELG, ABAQUS and ANSYS) were validated; indeed, the same predictions were obtained through these different software. The second study was dedicated to the validation of the numerical tools to simulate the response of framed composite structures caused by the “Loss of a bracing”. Therefore the software program SOFISTIK was additionally validated and has shown good correspondence in comparison with FINELG.

5.3 Investigations on the event “Loss of a column”

5.3.1 Introduction

In the present section, the numerical and analytical investigations related to the exceptional event “loss of a column” are presented.

In § 5.3.2, the numerical investigations performed on 2D and 3D structures are first detailed; the latter are performed with one of the validated software presented in the previous section. The objective is to investigate the behaviour of these structures as a consequence to the loss of a column, the development of the catenary action and the redistributions of the loads within the structure.

Then, in order to develop simplified analytical methods to predict the response of a structure caused by to the loss of a column, a simplified substructure modelling has been defined. The validation of this

modelling and parametrical studies aiming at highlighting the parameters to be considered in the analytical methods are presented § 5.3.3.

Finally, the developed simplified analytical models are described in § 5.3.4 and also in separate design guidelines [34].

5.3.2 Numerical studies of 2D and 3D structures

5.3.2.1 Introduction

In the framework of this project the behaviour of steel and composite structures in exceptional failure scenarios, e.g. the loss of a column, were studied. For that purpose a steel structure with realistic dimensions was chosen and different failure scenarios were simulated.

In a first parametric study, the redistribution of internal forces and the appearing deformations and rotations at a 2-D frame were determined, to understand the behaviour of the structure and to highlight general phenomena, that can be observed for the failure of every internal column. The failure of the columns was simulated under different external loads. In a first simulation only the main loads, the loads in vertical direction, were applied. To detect the sensitivity of the structure concerning horizontal loads, wind loads were added in a second study. In a third 2-D study the failure of every internal column was simulated under exceptional Eurocode-load combinations. In a second step the failure of selected columns was simulated in a 3-D steel structure, to check, if the conclusions derived by the 2-D simulations can be transferred to 3-D structures directly. All dynamic effects were neglected in all simulations.

The main intention of these analyses is to highlight requirements in terms of deformation and rotation capacity that should be fulfilled by the joints and other structural elements, when a similar building is designed. To fulfil the requirements means, that a building that can be compared to the structure that was studied here, should behave “robust” in the case of a column collapse, even if it is not designed for this case. An abstract of the parametric studies on the event loss of a column is given in the next chapters. The whole simulation activities are summarized in the annex “Parametric studies: loss of a column” of this report, see [37].

5.3.2.2 Investigations on a 2D-system

A 2-D steel frame was designed according to EN 1993-1-1 [68]. The loads were taken as recommended in EN 1991-1-1 [64]. The frame has 7 bays and 6 storeys. The span of the beams is 8.00 [m] and the height of the storeys is 3.50[m]. The out of plane distance between the frames is 5[m]. The column bases are fully fixed (all degrees of freedom fixed) and the joints are assumed as rigid and full strength joints. The system has no further bracings. The structure is the same one as “Benchmark model 3” used for benchmarking of the software (see Benchmark document of this project [36]).

For denotation every column row of the 2-D frame is specified by a letter (A to H). The storey serially numbered by 0 to 5. Using this code every single column can be identified by the combination of the specific letter and number directly, as demonstrated for column C-1 in Figure 5-6.

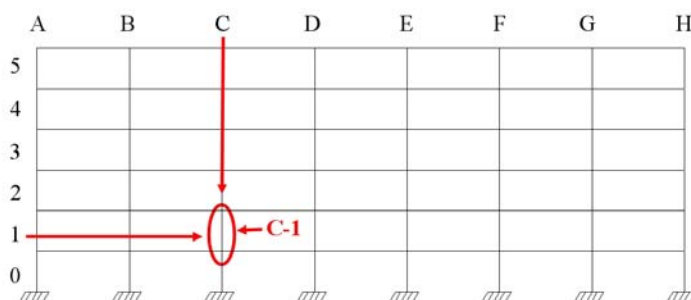


Figure 5-6: Denotation code of columns

A. Parameter study under full vertical loads

In the first parameter study at the 2-D Steel structure the failure of every internal column under full vertical loads was performed out and several data were monitored.

This simulation is a three step procedure:

- First step: The external vertical loads were applied on the intact structure.
- Second step: The failure of the given column was simulated by removing this column “slowly” until the axial forces in this specific column were zero. That means that all dynamic effects were neglected in this simulation.
- Third step: The external loads were increased proportionally until the steel structure collapses.

The applied vertical loads in this parametric study were permanent-, living- and snow loads. These vertical loads were applied simultaneously in step 1 without any safety or combination factors as given in Equation (5.1). In step 3 all loads were increased simultaneously.

$$E_K = 1.0 (22.05 + 18.60) + 1.0 \times 21.00 + 1.0 \times 3.35 \left[\frac{kN}{m} \right] \quad (5.1)$$

Equation (5.1): Load case vertical loads (22.05 / 18.60: Permanent load; 21.00: Living load; 3.35: Snow loads)

Results:

As described in chapter A the vertical loads were applied in step 1, a single column was removed in step 2 and the external load was increased until the structure collapses in step 3.

In Table 5-1 the load factors of the external loads that lead to a collapse in step 3 are given for the failure of any column. That means that 100[%] of the external loads given in equation (5.1) are applied in step 1. In step 2 for example the column C-1 was removed and in step 3 the external loads were increased proportionally from 100[%] to 111[%]. The “collapse” factors of this structure under vertical loads are summarized in Table 5-1 for every internal column. The denotation of the columns is in accordance with Figure 5-6 in § 5.3.2.2.

Table 5-1: “Collapse” factor

		Load factor [%]							
		Column row							
		A	B	C	D	E	F	G	H
Storey number	5	-	165	148	222	222	148	165	-
	4	-	141	128	163	163	128	141	-
	3	-	121	122	125	125	122	121	-
	2	-	113	119	120	120	119	113	-
	1	-	109	111	119	119	111	109	-
	0	-	102	103	117	117	103	102	-

The first conclusion of the results given in Table 5-1 are, that all “collapse” factors are higher than 100[%]. That means, that the given 2-D structure can stand the failure of any column under full vertical loads and the loads can even be increased after the failure of a column.

The matrix of Table 5-1 is symmetric in relation to the vertical axis of reflection, because there are only symmetric vertical loads acting.

Generally the collapse factor for inner columns (Row E, D, E, F) is higher than the collapse factor for more external rows (B and G). This result was expected, because the horizontal stiffness of the

remaining, not directly affected structure (k-factor) is higher for internal columns. That means, that membrane forces can develop in the beam, and the internal loads can be redistributed easily.

Another trend is the increasing collapse factor of the columns in the in the upper storeys, because in this storeys less forces have to be redistributed.

The failure mechanisms of the columns in the lower storeys are governed by local failures in the direct affected area of the frame. The failure mechanisms of some columns in the upper storeys are governed by buckling effects in the lowest storey. The phenomena will be explained in the annex “Parametric studies: loss of a column” of this report.

B. Parameter study under full vertical and horizontal loads

In a second parametric study the 2-D steel structure under full vertical loads and additional wind loads was computed and analysed. Permanent-, living-, snow- and wind loads were applied on the structure. These loads are vertical and horizontal loads and they were applied without safety factors in the combination of Equation (5.2).

In this study is the influence of wind loads can be analysed, because the vertical loads are identical with those that were applied in the previous parametric study.

The calculations including wind loads were performed for every internal column of the structure, but the simulation was stopped at the end of step 2. That means the column was fully removed but the external loads were not increased to cause the collapse of the structure. The failure of a single column did not cause a collapse of the whole system.

For this simulation the M- ϕ curve and the M-N curve for failure of column C-0 are illustrated below exemplarily. Those curves can be directly compared to the curves under vertical loads only.

$$E_K = 1.0 (22.05 + 18.60) + 1.0 \times 21.00 + 1.0 \times 3.35 + 1.0 (4.40 + 2.75) \left[\frac{kN}{m} \right] \quad (5.2)$$

Equation (5.2): Load case vertical and horizontal loads (22.05 / 18.60: Permanent load; 21.00: Living load; 3.35: Snow loads; 4.40 / 2.75: wind loads at the sides)

M- ϕ behaviour:

The M- ϕ behaviour of the external joint during the failure of column C-0 under vertical and wind loads is given in Figure 5-7. In this study the vertical and horizontal loads were not increased after the failure of the column, as explained in chapter B. The “load history” curve (vertical displacement versus standardised normal forces in the removed column) stops at 100 [%]. The M- ϕ curve can be observed for every moment until the column has failed. The failure of the column did not cause a collapse of the system.

The characteristic changes in the gradient of the “load history” curve are similar than in the simulation without wind loads. That indicates that plastic hinges develop at the external joints and later at the internal joints of the directly affected beam. The additional wind has no relevant influence on the load history curve. The shape of the M- ϕ curve doesn’t change at all, because it depends on the shape of the beam section and the assumed material law.

When the column has totally failed the bending moment increases up to approx. 654[kNm] with a rotation of 0.039[rad] and a vertical displacement of 0.32[m]. These values are nearly identical to those ones of the calculation without wind. The influence of additional wind loads seems to be not relevant.

M- N behaviour:

Additional wind loads acting on the structure induce additional normal forces in the horizontal beams. Thus an influence on the M-N distribution of internal loads was expected. The diagrams in Figure 5-8 show, that the influence can be neglected more or less.

When the column C-0 has failed totally the normal forces in beam is 122[kN] while the bending-moment is 654[kNm] and the vertical-displacement at the middle of the affected beam 0.32[m].

Compared to 120[kN] normal force and 656[kNm] bending moment in the simulation without wind the difference is low.

As more results of the parameter study activities are calculated, a separate document [37] is prepared as an annex of this report. In this annex the M- N and M- ϕ curves for other column failures under these loads are given.

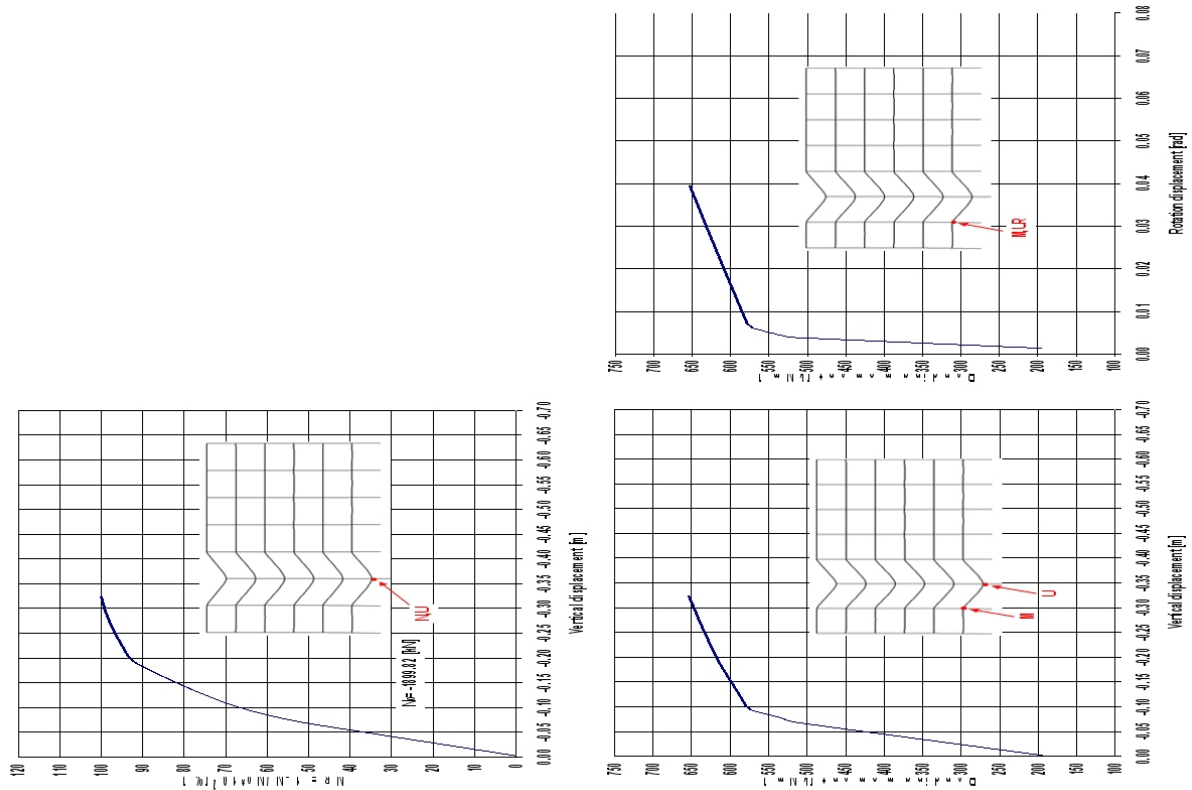


Figure 5-7: M- ϕ interaction of loss a column C-0

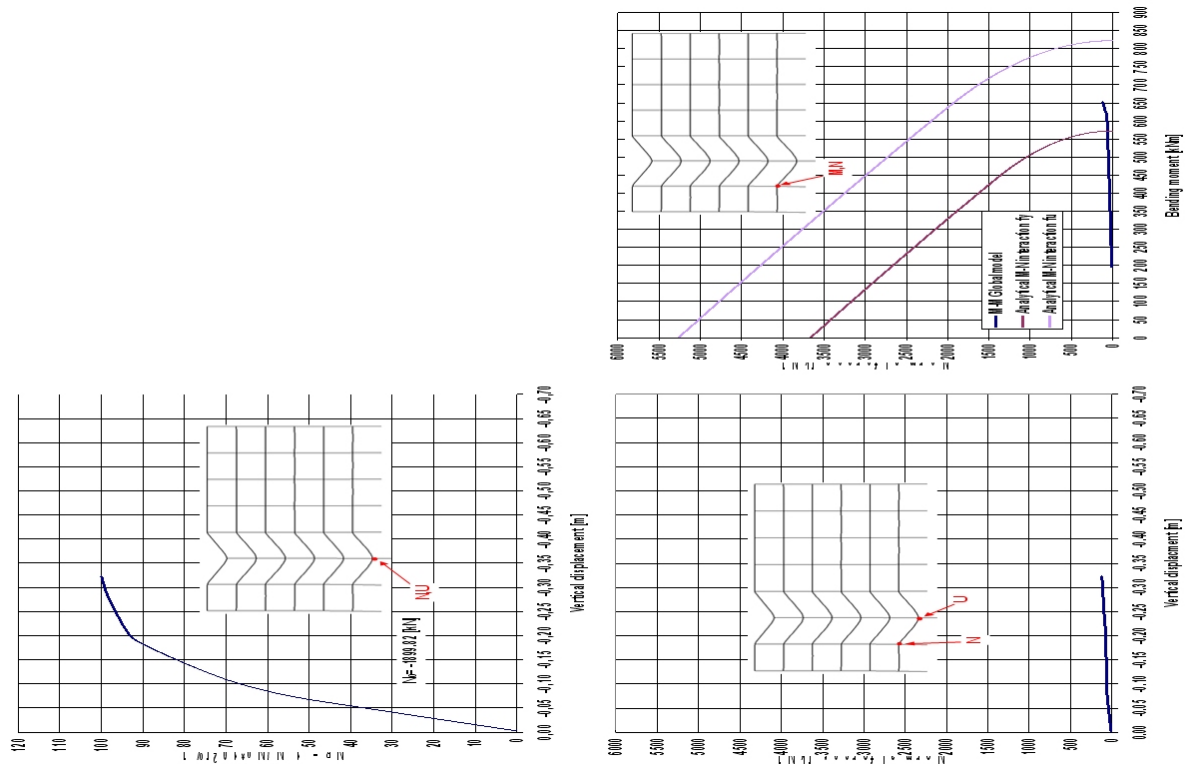


Figure 5-8: M-N interaction of loss a column C-0

C. Parameter study under exceptional Eurocode-load combinations

Further studies of the 2-D steel structure under exceptional Eurocode-load combinations were performed. This calculation is used to examine the plastic behaviour of the structure assuming that the column failure is an exceptional event and the applied loads can be reduced in accordance to the design loads of Eurocode-0. As in the previous calculations the failure of every single internal column was simulated, but the external loads were not increased proportionally up to the collapse of the structure afterwards.

The general equation for exceptional load combinations is given below. The combination factors ψ are taken as recommended in EN 1990 [63]. The combination factors can differ depending on the national Annexes.

Using the Eurocode rules, these loads lead to three different loads case combinations that have to be considered.

$$\sum_j \gamma_{GA,j} \times G_{k,j} + A_d + \psi_{1,1} \times Q_{k,1} + \sum_{i>1} \psi_{2,i} \times Q_{k,i} \quad (5.3)$$

Equation (5.3): Exceptional design combination

Table 5-2: Load case combinations

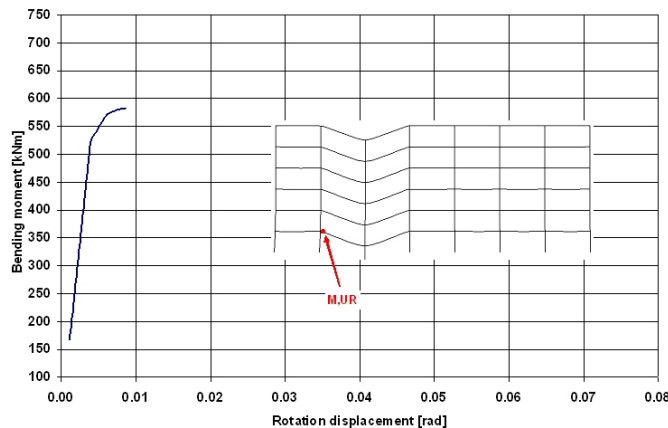
<u>Load case combination 1</u>	<u>Load case combination 2</u>	<u>Load case combination 3</u>
Predominant load = live load	Predominant load = snow load	Predominant load = wind load
$E_d = 1.0 \times 40.65 +$ $0.5 \times 21.00 +$ $0.0 \times 3.35 +$ 0.0×7.15	$E_d = 1.0 \times 40.65 +$ $0.2 \times 3.35 +$ $0.3 \times 21.00 +$ 0.0×7.15	$E_d = 1.0 \times 40.65 +$ $0.2 \times 7.15 +$ $0.3 \times 21.00 +$ 0.0×3.35
40.65: Permanent load; 21.00: Living load; 3.35: Snow loads; 7.15: wind loads at the sides		

Load case combination 1 and 2 (in Table 5-2) lead to vertical loads only. Load case combination 2 is not relevant, because the sum of the vertical loads is lower than in LCC 1. Load case combination 3 leads to quite small vertical loads and additional horizontal loads.

The structure gives a non elastic response to the applied loads when the loss of a column is simulated, accordingly the deformation and rotation will not decrease proportionally to the applied loads. To get information about the required rotation capacity of the joints when the loss of a column appears under an exceptional load case combination, two further parametric studies with loads according to load case combination 1 and 3 were performed.

M- ϕ behaviour:

The M- ϕ curve of column failure C-0 in the third study under the loads of the load case combination-1 (LCC-1) is given in Figure 5-9.

**Figure 5-9: M-N interaction of loss a column C-0**

D. Conclusions 2D modelling

During the failure simulation of column C-0 you can see that the external joints of the beams in the area above the affected column begin to yield simultaneously (for load distribution see annex “Parametric studies: Loss of a column”). Plastic hinges begin to develop at the edges of the beams. The loads on most upper beam are small in comparison to the loads in the other storeys. This leads to less deformations and the yielding in the most upper beam appears later. On the other hand side the less deformed most upper beam resists the horizontal deformation of the remaining structure. Hence compression forces in the most upper beam develop. This compression forces indicate, that an “arch-effect” is going to develop. In a structure with different dimensions (more storeys) the appearance of such an “arch-effect” may be detected more clearly.

Various simulations of other column failures confirm that the influence of horizontal wind loads can be neglected for this structure.

On the other hand side the influence of the applied external vertical load is high. Considering this structure the reduction of vertical loads on a regular storey from 43.05[kN/m] (full vertical loads) to

32.55[kN/m] (vertical loads according to LCC1) leads to a reduction of the appearing deformation from 0.32[m] to 0.11[m]. Under the relevant load case combinations according to EC-0 the plastic hinges at the external joints of the direct affected beam just began to develop. A clear redistribution of bending moment to normal forces was not detected under EC-loads at all.

The bending moments, normal forces and rotations at the edge of the direct affected beam are summarized in Table 5-3 as well as the vertical deformation in the middle of the beam. These values appeared, when the simulation of column C-0 failure was completed (end of step 2).

The maximal displacements and rotations of the C-0 column failure do cover the results of most of the other column failure simulations. As documented in the Annex, the failure of column B-0 under full vertical loads leads to a rotation of 0.044[rad] which is quite close to 0.040[rad] from the C-0 column failure. The detailed load deformation curves are given in the annex “Parametric studies: loss of a column”.

To check if the 2-D results, with all their non-linear effects, can be transferred to a usual 3-D structure, several 3-D simulations were performed. These results of these calculations are given in the next chapters.

Table 5-3: Internal loads and deformations under different loads when the simulation of loss of column C-0 was completed.

Parameter studies	Bending-moment	Normal-forces	Rotation-displacement	Vertical-displacement
	M [kNm]	N [kN]	φ [rad]	U [m]
Under full vertical loads	655.60	120.23	0.040	0.32
Under full vertical- and wind loads	653.53	121.79	0.039	0.32
under exceptional EC-load combination LCC-1	582.25	79.66	0.009	0.11
under exceptional EC-load combination LCC-3	542.99	64.28	0.005	0.09

5.3.2.3 Investigation on a 3D-system

A. Description structure

For reduction of calculation time, the frame that was used in the 2-D analysis was reduced from 7 bays to 4 bays. Thus the main frame of the 3-D structure has 4 bays and 6 storeys. The span of the beams is 8.00[m] and the height of the storeys is 3.50[m] (see Figure 5-10). The out of plane distance between the frames (secondary beams) is 5[m].

The column bases are fully fixed (all degrees of freedom fixed) and the in plane joints of the main frame are assumed as rigid and full strength joints. The joints of the secondary beams of the 3-D structure are assumed as bending-moment hinges. The 3-D structure is braced in the y-z plane (see Figure 5-10).

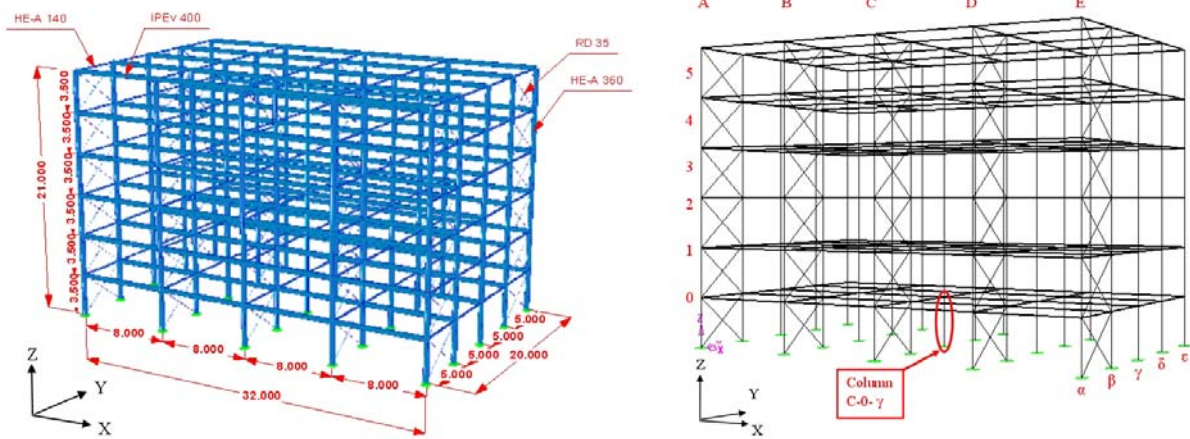


Figure 5-10: 3-D structure and denotation

For the design of the secondary beams and the bracings an additional loads case has to be taken into account. The additional load, wind in the y-direction of the 3-D. The wind compression on the 3-D structure is 7.04[kN/m] in the centre of the building and 3.52[kN/m] at the edge of the 3-D structure.

The wind suction in the centre of the building is 4.4[kN/m] and the wind suction at the edge is 2.20[kN/m]. The wind loads in y-direction act simultaneously. The loads were taken as recommended in EN 1991-1-1 [64].

All other loads cases for design are equal to those ones applied to the 2-D structure as documented in § 5.3.2.2 sub-chapter A.

A design for the secondary beams and the bracings was performed under the relevant load case combinations the in accordance to EN 1993-1-1 [68]. The linear calculation was carried out with the material S355J0. The partial safety factors were 1.50 for variable loads and 1.35 for permanent loads. In a linear calculation a critical load factor referring to the design loads of $\eta = 6.32$ was obtained. Using the definition in Eurocode the 3-D structure is sway, thus second order effects should not be neglected in design. In a second order calculation stresses and deformations of the structure with the chosen profiles were checked.

The following member section was obtained in the design:

Columns:	HE-A 360 Steel S355 Class 1 $A = 143 \text{ cm}^2$ $I_y = 33090 \text{ cm}^4$ $I_z = 7890 \text{ cm}^4$	Beams:	IPEv 400 Steel S355 Class 1 $A = 107 \text{ cm}^2$ $I_y = 30140 \text{ cm}^4$ $I_z = 1770 \text{ cm}^4$
Secondary beams:	HE-A 140 Steel S355 Class 1 $A = 31.4 \text{ cm}^2$ $I_y = 1030 \text{ cm}^4$ $I_z = 389 \text{ cm}^4$	Bracing:	RD 35 Steel S355 $A = 9.62 \text{ cm}^2$ $I_y = 7.37 \text{ cm}^4$

B. First failure simulation of an internal column under vertical loads

In this chapter the first results of an internal column failure simulation are presented.

The failure of column C-0- γ according (denotation see Figure 5-10) was simulated under 1.0 times characteristic vertical loads. That means that the loads are the same than in the first parametric study of the 2-D model.

The Abaqus/CAE model was braced asymmetric. During the computation the 3-D structure collapsed, even before the simulation of the column failure was finished. The appearing deformation when the normal forces in column C-0- γ were reduced to 93[%] of the initial force is given in Figure 5-11. The beams, especially the most upper one, seem to buckle about the weak axis. As detected in the 2-D calculation compression forces develop in the most upper beam. The asymmetric bracing induces a deformation in direction of the weak axis and the column failure causes a deformation in direction of the strong axis. This deformation of the most upper beam under compression forces could lead to a buckling collapse of the most upper beam, which was not designed to resist high compression forces.

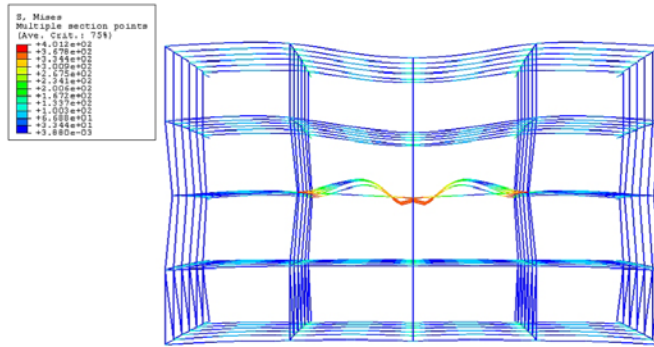


Figure 5-11: Top view on the collapsed structure (93 % of column failure C-0- γ simulated); illustrated with a deformation scale factor of 100

Several curves given in the annex “Parametric studies: loss of a column” as well as Figure 5-11 indicate buckling phenomena in the top beam.

To check, if the buckling is a fault of the numerical modelling of the complex 3-D structure, a simplified model of the most upper IPEv 400 beam under the given deformations and loads, that were obtained at the collapse of the structure, was computed.

The most upper beam was isolated and the boundary conditions were simplified as demonstrated in Figure 5-12 and Figure 5-13. Then in a first step the horizontal and vertical displacements obtained in the calculation of the whole model were applied at the bearing in the middle of the 16[m] beam, and afterwards the compression forces were added as external loads in a second step. The applied deformations and loads are summarized in Figure 5-13.

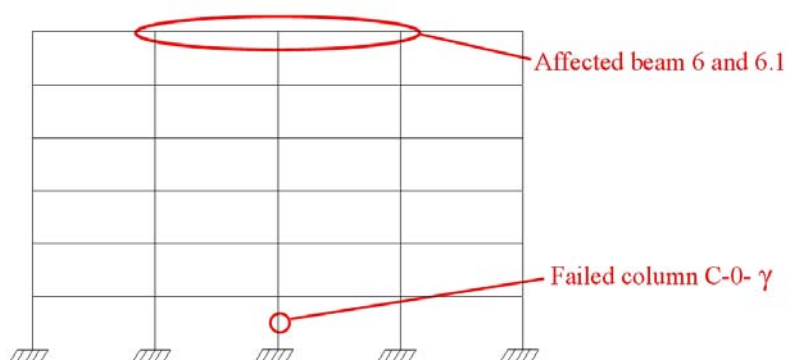


Figure 5-12: Middle frame of the global 3-D structure

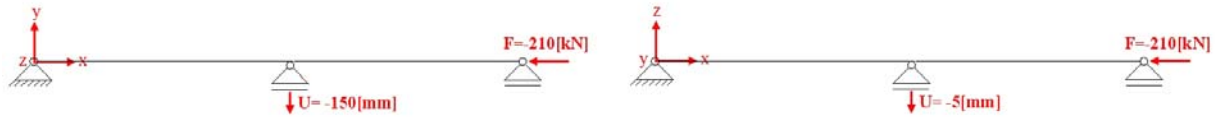


Figure 5-13: Front view and top view of the reduced model of the beam 6 and beam 6.1.

To get a better illustration of the internal stress distribution and to take also torsional buckling into account, the calculation of the simplified “buckling” model was performed with shell elements instead of beam elements. The behaviour of such a beam is different, but the simulation will demonstrate, if there is the possibility that buckling under the given loads and deformations occurs.

In Figure 5-14 you can see the mises-stresses und the vertical- and horizontal displacement of -150[mm] and -5[mm] and the compression forces of 210[kN] (step 2 of the non linear calculation is finished).

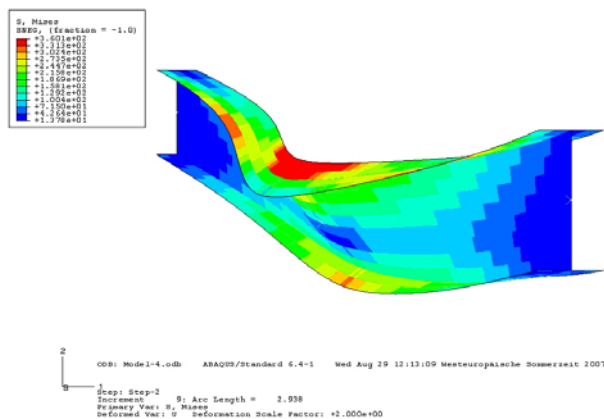


Figure 5-14: Mises-stresses after the second step of the calculation (displacement + compression); illustrated with deformation scale factor 2

C. Conclusions of 3D modelling

The first calculations of a column failure in the ground floor of a 3-D structure indicate, that this specific structure collapses caused by a buckling of the most upper horizontal beam. For further calculations the numerical model should be checked carefully, but some first simulations have confirmed, that the appearance of buckling phenomena about the weak axis has to be observed in a real 3-D structure.

The parametric study on the 2-D structure indicates as well, that compression forces in the most upper beam can not be neglected.

It is obvious that the further simulations on a 3-D model lead to a better understanding of the stability phenomena that have to be considered in a robust design.

Additional information of the 3-D structure is given in the annex “Parametric studies: “Loss of a column”.

5.3.3 Numerical studies of the simplified substructure

5.3.3.1 General

Through parametrical studies performed on thousands of frames [88], it has been shown that the membrane forces developing in the beams of the storey just above the loss column are significantly more important than the ones developing in the other beams, as illustrated in Figure 5-15.

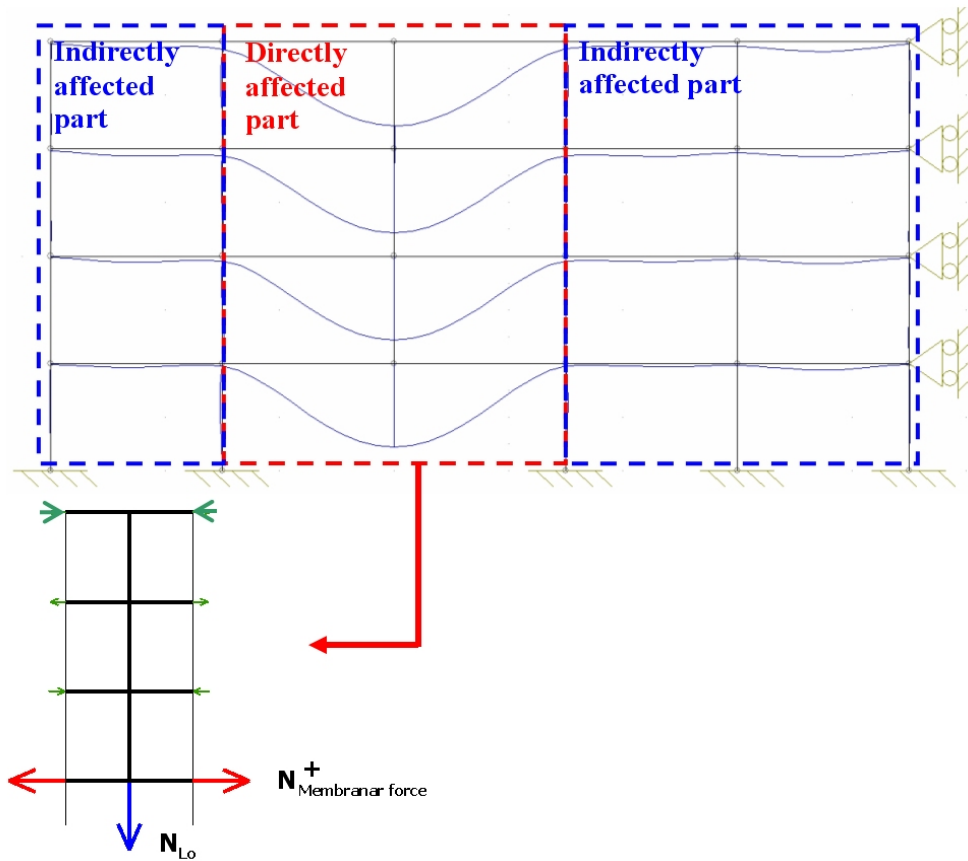


Figure 5-15: Distribution of the membrane forces developing in the directly affected part

Consequently, it is decided to investigate the behaviour of this storey only and to extract this storey from the frame to define a simplified subsystem, as illustrated in Figure 5-16, which will simulate with a sufficient accuracy the behaviour of the directly affected part, i.e. the part of the structure just above the loss column.

To be able to isolate the subsystem, different parameters have to be defined:

- The lateral restraint K which represents the lateral stiffness of the indirectly affected part when the membrane forces develop in the directly affected part;
- The resistance F_{Rd} of the indirectly affected part, i.e. the maximum horizontal load coming from the directly affected part that the indirectly affected part can sustain;
- The loads p and Q that the system has to support.

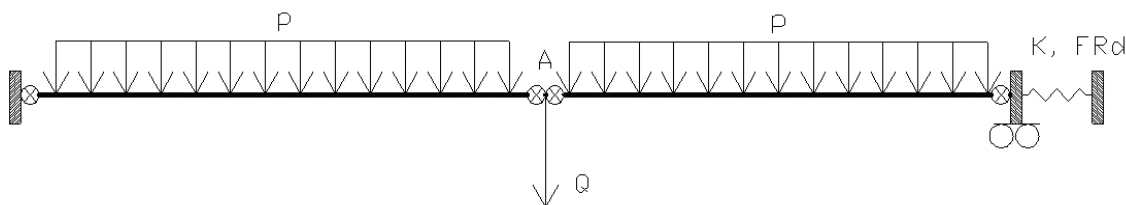


Figure 5-16: Extracted subsystem

The beams and the joints are the ones met in the bottom storey of the directly affected part. The uniformly distributed load p is the load applied to the structure just before the column loss and is assumed to be constant.

The parameters K and F_{Rd} are properties of the indirectly affected part which will influence the development of the membrane forces in the beams. Analytical methods aiming at predicting the values of these parameters have been developed and validated (see § 5.3.4).

In a first paragraph (§ 5.3.3.2), the validation of this simplified substructure modelling is presented. Then, in § 5.3.3.3, parametrical studies aiming at identifying the parameters influencing the answer of the simplified substructure are presented.

The details about the numerical investigations performed on the simplified substructure are available in annex documents [10], [38].

5.3.3.2 Validation of the simplified substructure modelling

A. Introduction

When a column fails in the global structure, many effects appear in the two beams which had been supported by the column (see Figure 5-17). Therefore a substructure consisting of two elements (IPEv400 according to the sections used in the global model) is defined. A substructure is a subset of beams and/or elements of the global structure (see Figure 5-18).

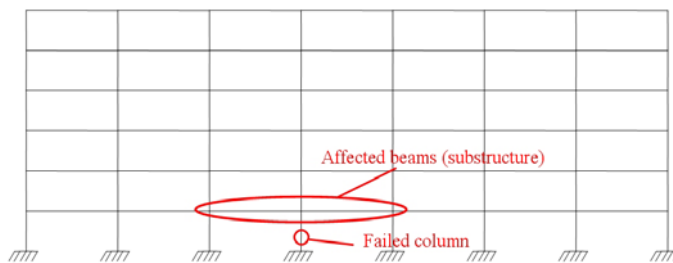


Figure 5-17: Global model



Figure 5-18: Affected beams of the global model

Figure 5-19: Simplified substructure model

To reflect the mechanical behaviour of the global structure, the rest of the structure is replaced by springs, which are placed at the points where the substructure is in contact with the global structure. By using non-linear springs, this system can reflect the exact behaviour of the global system.

The rotational and vertical degrees of freedom can be neglected, as the vertical and rotational stiffness at the joints at both sides of the substructure approach to infinite.

A further simplification consists of replacing the horizontal springs at both sides of the substructure (k_1 and k_2) by one single horizontal spring (k_{eq}) with an equivalent stiffness at one side and fix the horizontal degree of freedom at the other side.

The axial forces from the upper and the lower column have opposite directions and only the difference acts directly upon the submodel. All this simplifications lead to the simplified substructure given in Figure 5-19.

B. Deriving the equivalent spring stiffness

Calculations modelling the whole structure lead to horizontal forces and different horizontal displacements at the two ends of the affected beams.

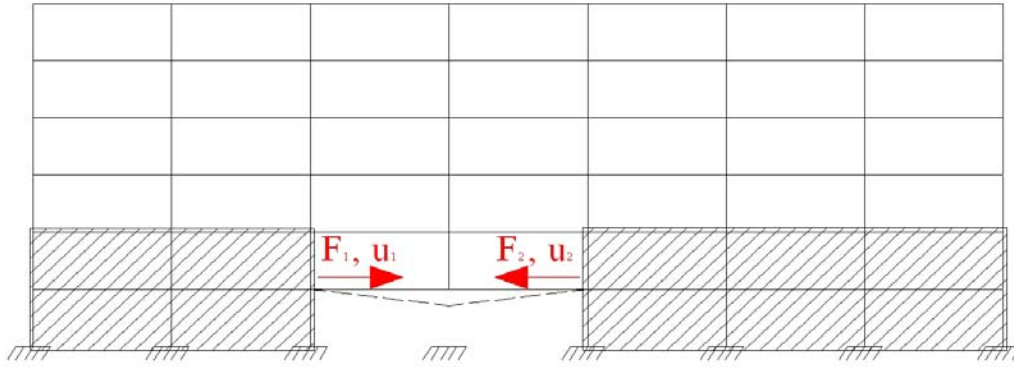


Figure 5-20: Global model

To derive a value for the equivalent spring stiffness, that represents the horizontal stiffness of the remaining structure (given in Figure 5-20), a calculation on the global model was performed in 3 steps:

1. The uniform loads were distributed on the intact structure
2. The relevant column was “removed” until the forces in the column were zero
3. The column was replaced by an axial tension force until the global system collapses

The non-linear force-displacement curves for the lateral springs k_1 and k_2 during these three steps, as well as the one for the equivalent non-linear spring k_{eq} are given in the following diagram. For k_{eq} the stiffness of k_1 and k_2 are combined.

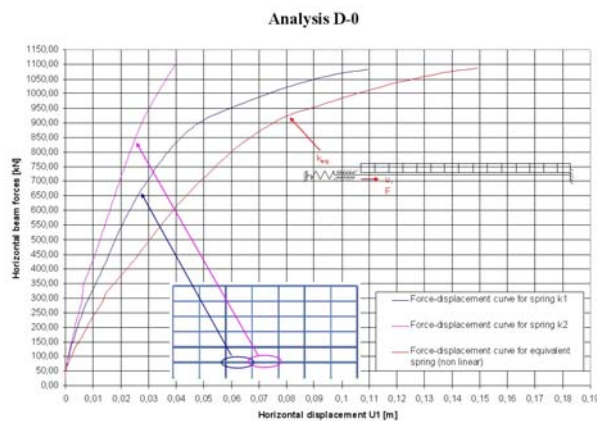


Figure 5-21: Spring force-displacement curves

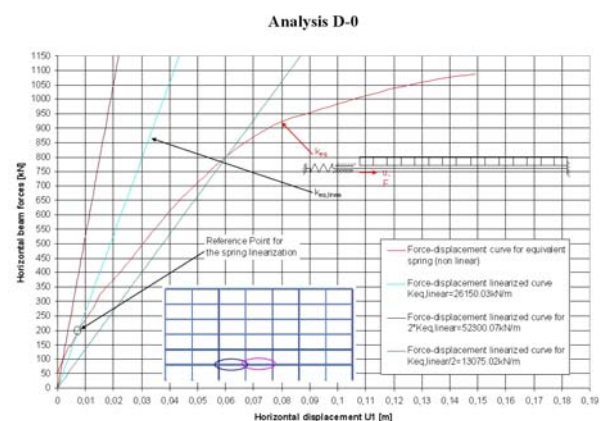


Figure 5-22: Simplification of the spring behaviour

A further simplification of the model can be made by assuming a linear behaviour of the horizontal spring according to Figure 5-22. This linearization is done by choosing one reference point of the force-displacement curve. The chosen point is the one where the lower column has disappeared from the static system (zero forces in the lower column). The resulting spring stiffness is shown in the following Figure 5-22. In order to check the validity of this assumption and the influence of the linear stiffness on the results, additional calculations have been carried out with the half and the double of the spring stiffness.

C. Applied loads

The permanent and live loads that were applied on the substructure are identical with those ones applied on the corresponding floor of the global model. Additionally two concentrated forces that represent the axial loads of the upper and the lower column act on the substructure as given in Figure 5-23. These two concentrated forces are applied at the same location. They have opposite directions and different amplitude. Only the difference of this two forces acts as an external force on the substructure. This

resulting force F_{res} is given in Figure 5-24. The distribution of the axial forces of the upper and lower column of the global model during these three steps is well as the difference of those two forces F_{res} . In the substructure simulations this F_{res} was applied on the model. For validation purposes a substructure calculation with two independent concentrated external forces representing the two “original” axial column forces was performed. This simulation led to the same results than the simulation with a resulting force.

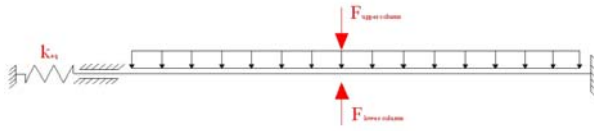


Figure 5-23: Loads of the upper and the lower column during collapse simulation

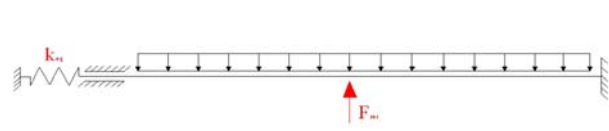


Figure 5-24: Resulting loads acting on the substructure

Usually the external force F_{res} was applied in 5 steps on the substructure. Even applying the maximal resulting force in one step had not much influence on the results of the substructure simulations.

D. Conclusions of numerical calculations of a simplified substructure

As visualized in Figure 5-25 the results of the global model simulations and the substructure simulations are in very good agreement.

When the vertical displacements at the middle of the affected beams are plotted against the F_{res} forces (Figure 5-25), the curves begin to spread after the lower column is removed completely. The behaviour of the substructure in load step 3 (failed column is replaced by tension forces) depends on the linear stiffness of the equivalent springs placed at the edge of the substructure.

That means that the main effects of the global model behaviour can be reproduced by calculating a substructure with proper boundary conditions.

The development of axial beam forces in the substructure is also quite similar, to those one appearing in the global model. It can be observed, that those curves are more sensitive to the stiffness of the equivalent linear springs of the substructure. The curves begin to spread, when the horizontal forces of the intersection point of the linear spring behaviour and the non-linear behaviour of the global model is reached.

Several other results of different substructure calculations are given in the internal report “Calibration of the simplified substructure” [38]. All calculations confirm, that the main effects of the global model behaviour can be reproduced by calculating a substructure with proper boundary conditions.

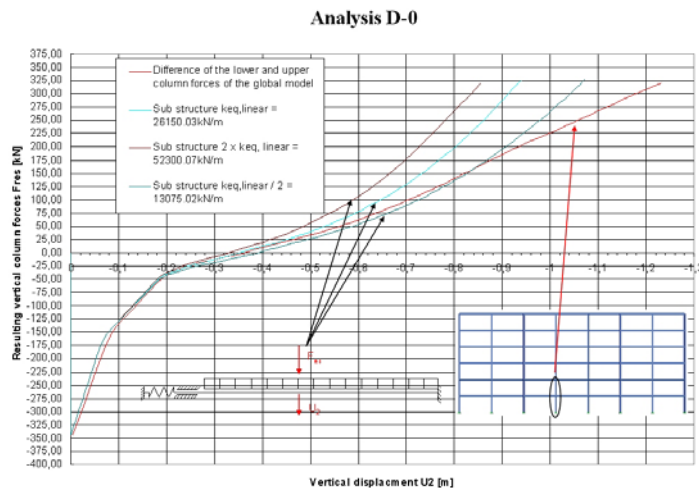


Figure 5-25: Deformation of the global model and the substructure

5.3.3.3 Parametrical studies on the simplified substructure

A. Introduction

In order to understand how the various parameters influence the response of the simplified substructure, an eleven-level parametric study has been first carried out. The main results are presented in the present paragraph. In the latter, additional parametrical studies are also presented to investigate with more details the influence of some “key” parameters on the simplified substructure response and in particular, on the development of the catenary action:

- Variation of the lateral restraint K ;
- Variation of the beam cross-section A and;
- Variation of the beam inertia I .

Remark: in all the investigated models, the resistance F_{Rd} of the horizontal spring (see Figure 5-16) is assumed to be equal to the axial resistance of the beam.

B. Parametrical studies

As previously mentioned, an eleven-level parametric study is first carried out to understand how the various parameters influence the response of the simplified substructure. The different studied levels are illustrated in Figure 5-26 and their main properties are summarised in Table 5-4.

The main parameters considered in this eleven-level approach are the following ones:

- The beam response: the stiffness of the beams in bending (EI) and under axial force (EA) are varied, as well as the yield strength f_y of the constitutive material; a high value of EI allows to simulate “rigid” beams, while the adoption of high values of f_y enables to simulate a fully elastic response of the beam elements.
- The K restraint: the importance of the membrane effects in the beam increases with the K values, while the beam transverse displacements at failure decrease. For high values of K high tying forces are obtained at beam ends, while demand in terms of rotational capacity is requested at beam ends when large displacements occur in the beam, i.e. for low values of K .
- The resistance properties of the beam end sections: no connection is assumed to act at beam ends; so possible plastic hinges develop in the beam itself for an axial force equal to $N_{pl,Rd}$ (tension resistance of the beam), for a bending moment equal to $M_{pl,Rd}$ (bending resistance of the beam cross-section) or under a combination of bending moment and axial forces. In the

parametric study, no interaction between axial forces and bending moments is first contemplated (Level 1 to 7); then a non-linear interaction resistance curve characterising the beam cross-section is considered (Level 7 to 11).

Also, additional parametrical studies are performed to vary “key parameters” identified through the “eleven-level” parametrical study. The starting points for these parametrical studies are Level 1 (i.e. “Rigid system”) and/or Level 9 (i.e. “Bi-encased beam”). For these two levels, the parameters which are varied are:

- the stiffness of the horizontal spring K ($K \in]\infty; 3000 \text{ kN} / \text{m}]$);
- the beam cross section A_b ($A_b \in]\infty; 0.125 A_{IPE200}]$) and;
- the beam moment of inertia I_b ($I_b \in]\infty; 0.25 I_{IPE200}]$).

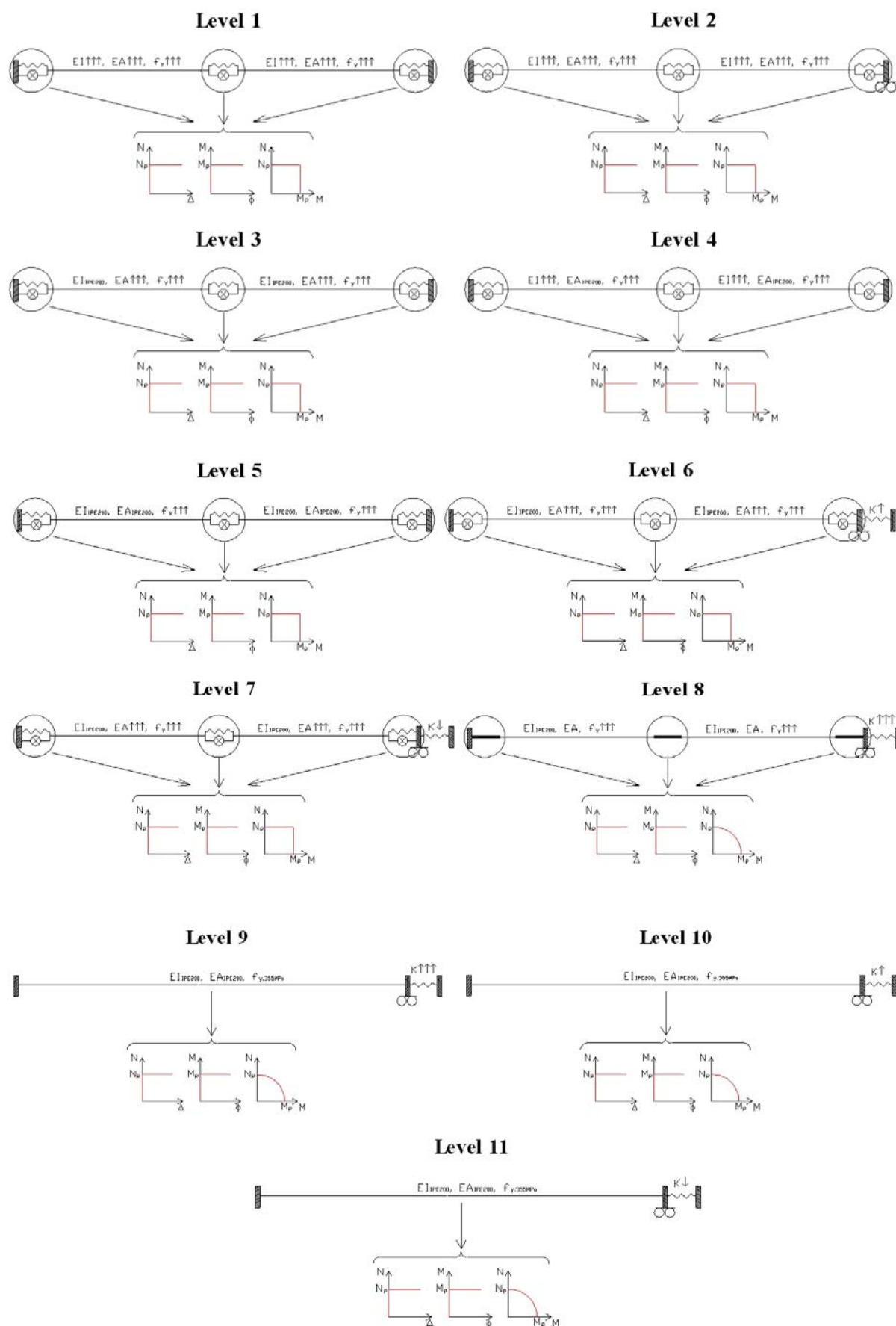


Figure 5-26: The eleven levels of the parametric study

Table 5-4: Main properties of the studied levels

Level	L_{beams} [m]	EI	EA	$f_{y,beams}$ [MPa]	K [kN/m]	$M-N$ interaction
Level 1	4	∞	∞	∞	∞	-
Level 2	4	∞	∞	∞	0	-
Level 3	4	IPE200	∞	∞	∞	-
Level 4	4	∞	IPE200	∞	∞	-
Level 5	4	IPE200	IPE200	∞	∞	-
Level 6	4	IPE200	∞	∞	900000	-
Level 7	4	IPE200	∞	∞	10	-
Level 8	4	IPE200	IPE200	∞	∞	IPE200_355Mpa
Level 9	4	IPE200	IPE200	355	∞	IPE200_355Mpa
Level 10	4	IPE200	IPE200	355	900000	IPE200_355Mpa
Level 11	4	IPE200	IPE200	355	10000	IPE200_355Mpa

Full non-linear 2-D numerical analyses are performed through the validated software FINELG [73], with due account of geometrical and material non linearities. The beams are modelled by means of plane 2-D beam elements with three nodes. As a 2-D numerical analysis is performed, the out-of-plane buckling phenomena as lateral-torsional buckling are not taken into account in the computations.

In order to not restrict the development of the catenary action in the numerical modelling, the plastic strain limitations have been deactivated in the software. So, it is assumed that the different members of the simplified subsystem have an infinite ductility. In conclusion, the collapse of the subsystem is assumed to be achieved when the axial forces in the system reach the resistance F_{Rd} of the horizontal spring or the axial resistance of the beam $N_{pl,Rd}$. For level 9 to 11, the steel beams are assumed to have an elastic limit equal to 355 Mpa; in these cases, the steel material is modelled through an elastic-perfectly plastic law. In the other levels, the steel beams are assumed to be perfectly elastic ones.

The applied uniformly distributed load is increased until collapse of the system which corresponds to the achievement of the axial plastic resistance of the translational springs or of the beam (N_{pl}) in the present cases. Some of the obtained results for the additional parametrical studies are illustrated from Figure 5-27 to Figure 5-29; more details are available in [10].

The main results obtained through the performed parametrical studies are summarised here below:

- The maximum applied load which can be reached depends of the value of K . It increases with decreasing values of K . The needs in terms of ductility increase also when the K value is decreasing (see Figure 5-27).
- The development of the catenary action depends on the relative values of the axial beam stiffness EA/L and the stiffness of the spring K . In practical situations, it has been shown that the influence of the axial beam stiffness may be neglected (see Figure 5-28).
- The influence of the bending stiffness EI/L on the development of the catenary action may be neglected (see Figure 5-29).
- The $M-N$ interaction and the localised elongation associated to the catenary actions at the plastic hinge level have a significant influence on the beam response and in particular, on the vertical displacement measured at mid-span of the simplified substructure.

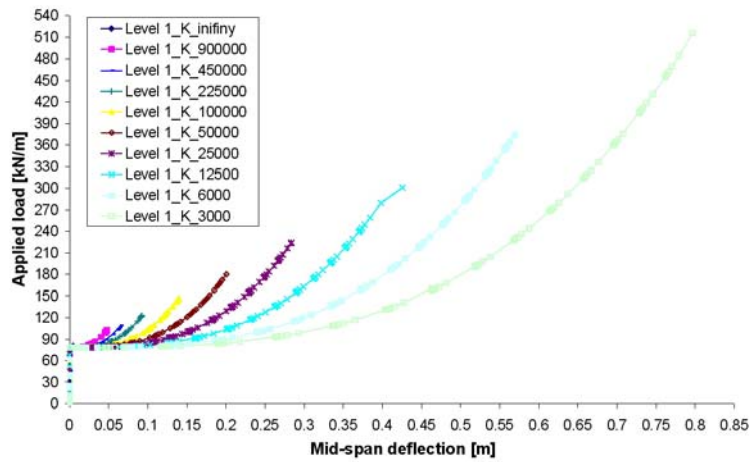


Figure 5-27: Variation of K – Results for “Level 1” subsystem – Mid-span deflection vs. applied load curve

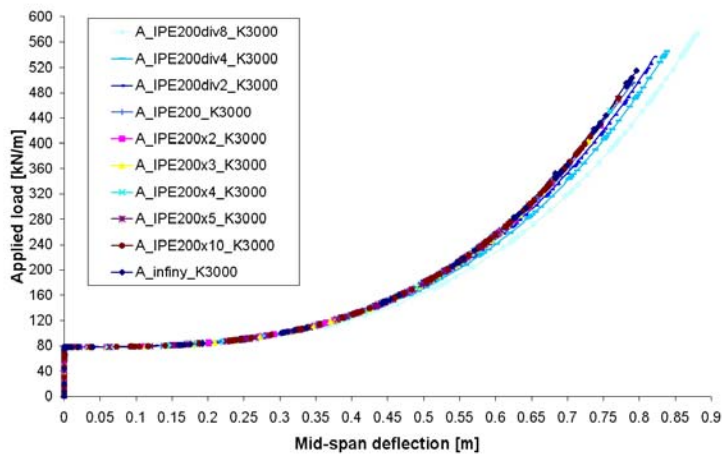


Figure 5-28: Variation of A – Results for “Level 1” subsystem with $K = 3000 \text{ kN/m}$ – Mid-span deflection vs. applied load c

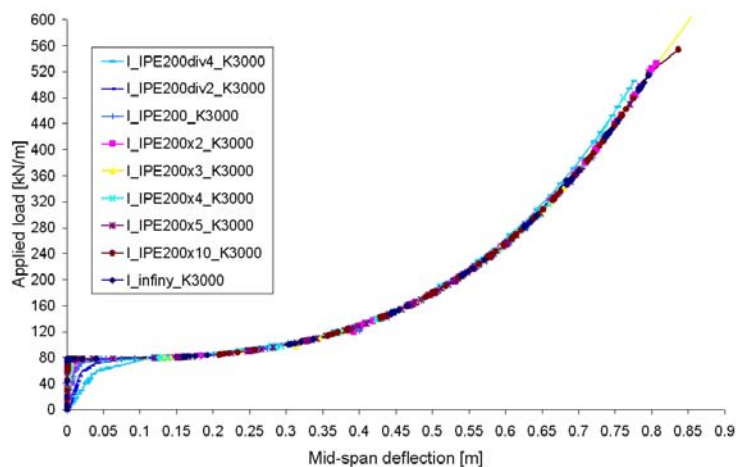


Figure 5-29: Variation of I – Results for “Level 9” subsystem with $K = 3000 \text{ kN/m}$ – Mid-span deflection vs. applied load curve

C. Conclusions

Through the performed parametrical studies, the parameters to be considered in the analytical model to predict the simplified substructure response have been identified. These parameters are:

- the lateral restraint simulated by the horizontal spring with a stiffness “K”;
- the M-N interaction at the plastic hinge level (developing in the beams or in the partial-strength joints);
- the plastic elongation of the plastic hinge associated to the development of the catenary action.

On the other side, it has been demonstrated that it is not requested to take into account of the bending stiffness “EI/L” and the axial stiffness “EA/L” of the beams to predict with a good accuracy the development of the catenary actions.

5.3.4 Development of analytical methods to predict the development of the membrane forces

5.3.4.1 Introduction

In the present paragraph, the analytical methods dedicated to the prediction of the development of the catenary action in a structure are described.

As mentioned in the previous paragraph, different parameters have to be taken into account within the analytical method; in particular, the M-N interaction at the plastic hinge level has to be included. Accordingly, an analytical method to predict the M-N interaction resistance curve of beam-to-column joints is first presented in § 5.3.4.2. This method is based on an analytical procedure developed for steel joints [52]; within the project, the latter has been extended to composite joints and validated through comparisons to the experimental tests.

Then, the analytical procedure to predict the development of the membrane forces within the substructure model is presented and validated through comparison to the experimental test results in § 5.3.4.3. Further information according the analytical method are also given in [34], [57].

5.3.4.2 Analytical prediction of the M-N interaction resistance curve of composite joints

A. Introduction

Through the substructure test presented in § 4.3.4, it was shown that the joints, when big deflection appears in a structure further to the loss of a column, are subjected to combined bending moments and tensile loads.

Accordingly, tests in isolation were performed at the University of Stuttgart on the substructure composite joint configuration in order to obtain the bending moment – tensile load resistance curves of the latter when subjected to sagging and hogging moments; the obtained results are presented in § 4.4.2.

At the University of Liège, analytical developments have been performed in order to be able to predict the resistance curve of composite joints subjected to combined M and N interaction.

The presence of axial loads in the beams has an influence on the rotational stiffness, the resistance moment and rotation capacity of the joints. As the analytical method proposed in the Eurocodes, i.e. the component method, is dedicated to the characterisation of the joint subjected to bending moment only, the proposed field of application is limited to joints in which the axial force N_{Ed} acting in the joint remains lower than 5 % of the axial design resistance of the connected beam $N_{pl,Rd}$:

$$\frac{N_{Ed}}{N_{pl,Rd}} < 0.05 \quad (5.4)$$

Under this limit in equation (5.4), it is assumed that the rotational response of the joints is not significantly affected by the axial loads. This limitation is a fully arbitrary one and is not at all scientifically justified. It has also to be underline that this criteria only depends of the applied axial load N_{Ed} and of the plastic resistance of the beam $N_{pl,Rd}$ which is quite surprising as what is considered here is the influence of the applied axial load on the joint response.

If the criterion given here above is not satisfied, it is recommended in the Eurocodes to consider that the interaction resistance diagram is defined by the polygon linking the four points corresponding respectively to the hogging and sagging bending resistances in absence of axial force and to the tension and compression axial resistances in absence of bending.

In a previous study [52], it was illustrated that the proposed method is quite questionable. So, in the PhD thesis of F. Cerfontaine [52], an improved design procedure, based on the component method concept, has been developed to predict the response of ductile and non-ductile steel joints subjected to combine axial loads and bending moments.

Within the project, two main activities have been conducted at the University of Liège:

- The component method has been applied to the substructure joint configuration to predict the response of the latter subjected to bending moments only (hogging and sagging).
- The design procedure developed by F. Cerfontaine for steel joints has been extended to composite joints and validated through comparisons to the experimental test results.

These activities are summarised here below. The properties of the materials which have been considered in the analytical computations are the ones obtained through experimental tests (coupon tests for the steel materials and cube tests for the concrete) in order to be able to compare the analytical predictions to the experimental results.

More details about these investigations are available in the PhD thesis of Jean-François Demonceau [57].

B. Behaviour of the composite joint subjected to bending moments

The comparison between the analytical prediction and the experimental results obtained for the joint subjected to hogging moment is presented in Figure 5-30 and in Table 5-5. The analytically determined collapse mode is “beam flange in compression” (for the resistance and ultimate bending moment) which is in line with what was identified during the experimental test.

From the comparison, it can be observed that the initial stiffness (compared to the unloading-reloading branch) and the resistant moment are in good agreement with the experimental test while the ultimate moment and the post-limit stiffness are underestimated; indeed, a difference of 10 % exists between the “experimental” ultimate moment and the “analytical” one.

One phenomenon which could explain this difference observed for the post-limit stiffness is the development of membrane forces in the components “end-plate in bending” and “column flange in bending”, phenomenon which is not actually covered by the component method. Indeed, the tested specimen is composed of a thin end-plate (thickness of 8 mm) and a thin column flange (thickness of 9 mm) which deformed significantly at the end of the test; these deformations can then lead to the development of membrane forces within these components (see Figure 5-31) which can increase the resistance and the stiffness of the latter.

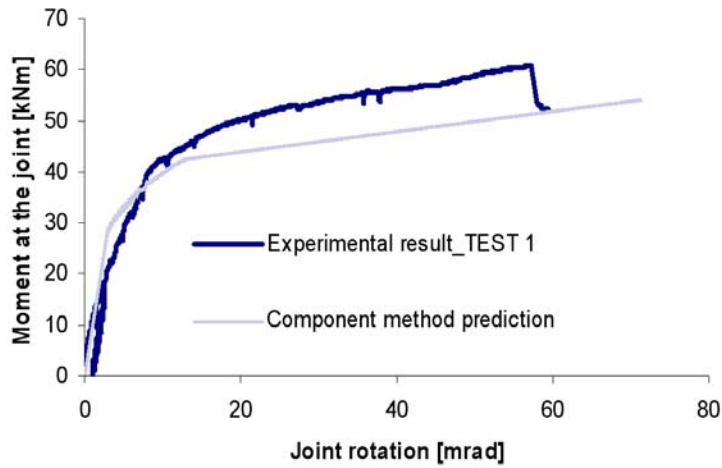


Figure 5-30: Comparison between the analytical prediction and the experimental results – hogging moment

Table 5-5: Key values obtained experimentally and through the new prediction approach

	Exp. results	Component method results
$S_{j,mi}$ [kNm/rad]	± 9530	9850
M_u [kNm]	60,6	54,07
ϕ_u [rad]	0,062	0,071

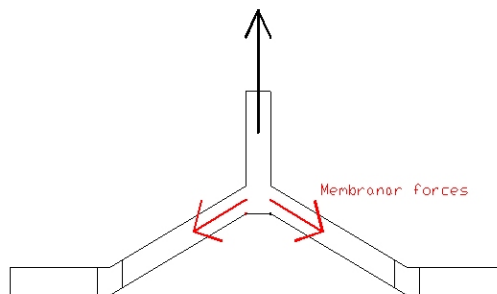
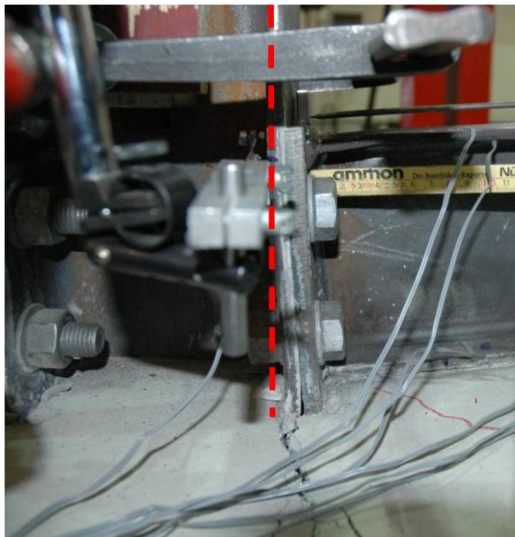


Figure 5-31: Deformation of the end-plate and the column flange at the end of the bending test

The comparison between the component method prediction and the experimental result for the joint subjected to sagging moment is given in Figure 5-32 and Table 5-6.

The component method as actually proposed in the Eurocodes is not yet able to predict the behaviour of composite joints subjected to sagging moment. Indeed, no method is available to characterise one of the

activated components which is “concrete slab in compression”. In [57], an analytical method to characterise this new component is proposed and validated; this method is used herein to characterise the studied joint.

Through the comparison, it can be observed that a good agreement is obtained between the analytical and the experimental results for $S_{j,ini}$ and the resistance and ultimate bending moments while the post-elastic stiffness is widely under-estimated which is confirmed by the over-estimated value of Φ_u (see Table 5-6). The analytically determined collapse mode for the resistance and ultimate bending moment is “column flange in bending” which is in full agreement with the experimental observation. The difference on the value of the ultimate moment is equal to 3 %.

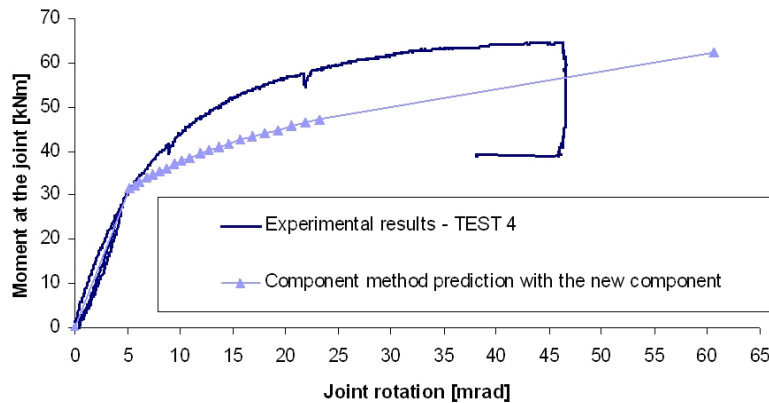


Figure 5-32 Comparison between the component method prediction and the experimental test result

Table 5-6: Key values obtained experimentally and through the new prediction approach

	Exp. results	Component method results
$S_{j,ini}$ [kNm/rad]	± 6400	6061
M_u [kNm]	64,5	62,4
ϕ_u [rad]	0,047	0,062

Remark: for the computation of the ultimate moment M_u , the resistance of the concrete which has been used is the actual resistance obtained through cylinder compression test + 8 Mpa as recommended in EN 1992 [67].

As for the joint subjected to hogging moment, the difference observed for the post-elastic stiffness can be explain by the development of membrane forces in the components “column flange in bending”, phenomenon which is not actually covered by the component method and the characterisation of this component (see Figure 5-31). The effects of these membrane forces on the joint response is more important under sagging moment than under hogging moment because, under sagging moment, the component “column flange in bending” is directly involved in the collapse mode which leads to an important deformation of the latter.

The non-linear part of the analytical behavioural curve of a joint is computed through a formula influenced by a shape factor ψ . The value proposed in the codes for a joint with a bolted end-plate is 2,7, if this value is modified in order to take into account implicitly of the additional stiffness coming from the development the membrane forces within the component “column flange in bending” (for instance, $\psi = 1$), a better accuracy between the analytical prediction and the experimental results can be obtained, as illustrated in Figure 5-33.

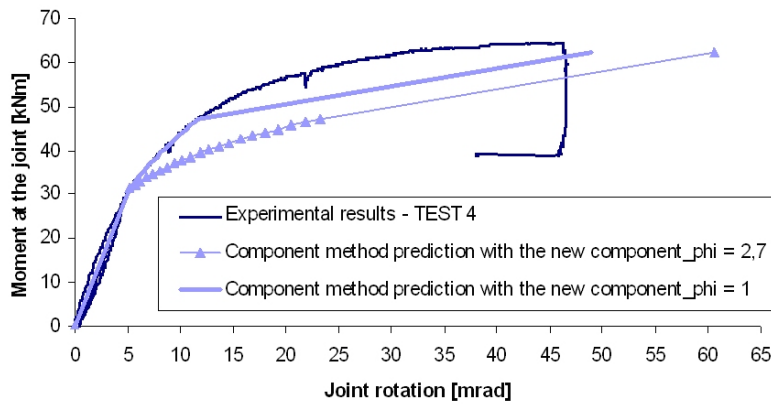


Figure 5-33 Comparison between the component method prediction and the experimental test result

C. Behaviour of the composite joint subjected to combined bending moments and tensile loads

As previously mentioned, the analytical procedure presented in [52] and developed by F. Cerfontaine is applicable to steel joints only.

In different references, it is demonstrated that the component method can be easily applied to composite joint configurations to predict their behaviour under bending moments. The particularity of composite joint configurations is the fact that two main additional components are activated: the slab rebars in tension and the concrete slab in compression. As the analytical procedure presented in [52] is based on the component method concept, the latter is easily extended to composite joint configurations by including the behaviour of the two additional components into the procedure. More details about this extension of the method are available in [57].

The comparison of the obtained analytical results to the experimental test results (see § 4.4.2) is presented in Figure 5-34. On the latter, it can be observed that two analytical curves are reported:

- One named “plastic interaction curve” which is computed with the elastic resistance stresses of the materials and;
- One named “ultimate interaction curve” which is computed with the ultimate resistance stresses of the materials.

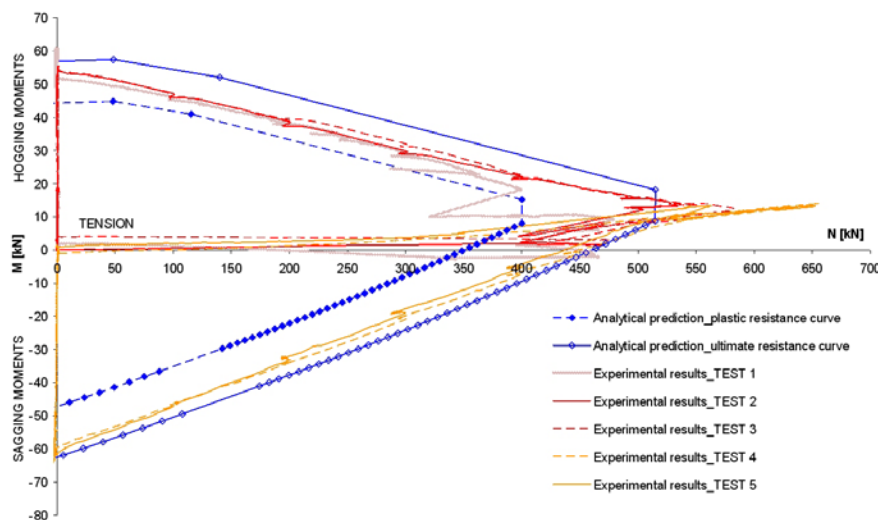


Figure 5-34 Comparison of the resistance interaction curves

Remark: TEST $i = V_i$ as reported in § 4.4.2.

According to Figure 5-34, the computed analytical curves are in very good agreement with the experimental results. Indeed, the experimental curves are between the plastic and ultimate analytical resistance curves which are in line with the loading sequence followed during the tests.

In the hogging moment zone, it can be observed that for very small values of tensile loads, the experimental curve is close to the ultimate analytical one which is logical, as a bending moment close to the ultimate resistance bending moment of the joint is applied to the tested specimen before applying the tensile load. Then, when the tensile load is increasing, the experimental curve first deviates from the ultimate analytical one to finally come back close to the ultimate analytical curve. This phenomenon can be explained by the fact that, to pass from the ultimate hogging moment to the ultimate tensile resistant load, different components are activated; indeed, the component which is associated to the ultimate hogging moment is “beam flange in compression” while the one associated to the ultimate tensile load is the component “column flange in bending”.

This phenomenon is not observed in the sagging moment zone; indeed, as shown in Figure 5-34, the experimental curve is close to the ultimate analytical one from the pure bending to the ultimate tensile load. Again, it is in agreement with the component activated from the pure bending to the ultimate tensile load which is the same in the present case, i.e. the component “column flange in bending”.

With the analytical procedure, it can be seen that, for the maximum tensile load, different values of the bending moments can be associated. This is possible due to the fact that the bolt row resistances are associated to a group effect; indeed, to pass from point A to point E of Figure 5-34, there is a redistribution of loads between the bolt rows involved in the group effect, redistribution of loads which does not affect the value of the tension load, as the sum of the bolt row loads is always equal to the group resistance ($= 236.7 \text{ kN}$), but affects the value of the bending moments, as the sum of the products “ ” are not constant during the redistribution. This phenomenon is illustrated in Figure 5-35 where the distribution of the loads between the bolt rows at point A and point E of Figure 5-34 is given.

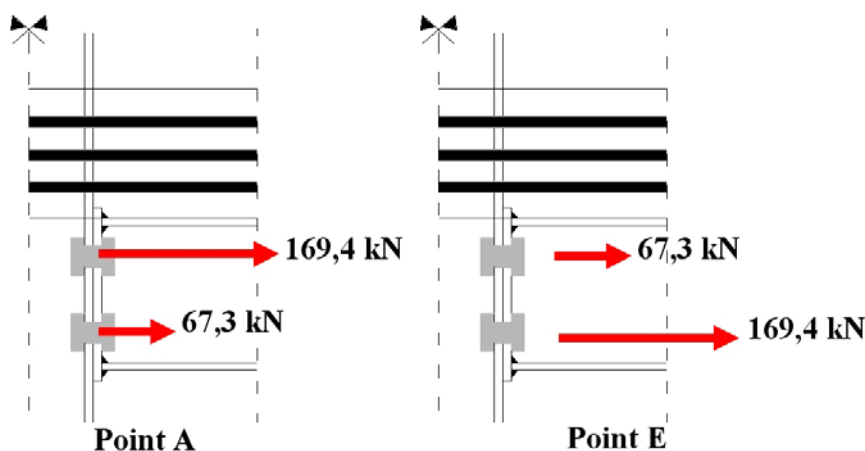


Figure 5-35 Distribution of the loads within the bolt rows at point A and point E of Figure 114

Also, in Figure 5-34, it is shown that the maximum tensile load which can be supported by the joint is underestimated by the analytical procedure. This difference can be justified by the fact that the proposed analytical procedure does not take into account of the presence of membrane forces within the components “column flange in bending” and “end-plate in bending” which develops when big deformations of these components are observed, i.e. when high tensile loads are applied to the joint. This phenomenon was already identified when investigating the behaviour of these joints subjected to bending moments.

5.3.4.3 Analytical procedure to predict the development of the membrane forces in a structure

In § 5.3.3, it was shown that it is possible to extract a simplified substructure able to reproduce the global response of a frame further to a column loss. Within the project, an analytical procedure able to predict the response of the simplified substructure when the membrane forces appear in the system has been developed and validated. The main results are summarised here below.

The objective with the analytical procedure is to predict the behaviour in the post-plastic domain, i.e. after the formation of the beam plastic mechanism in the system; accordingly, the analytical model is based on a rigid-plastic analysis. Also, as the deformations of the substructure are significant and influence its response, a second-order analysis is conducted.

The substructure to be investigated is presented in Figure 5-36 with the definition of some parameters which have to be considered in the analytical procedure (most of them have been identified through the parametrical studies presented in § 5.3.3.3):

- p is the (constant) uniformly distributed load applied on the storey modelled by the simplified substructure;
- L is the total initial length of the simplified substructure;
- Δ_Q is the vertical displacement at the load application point;
- δ_K is the deformation of the horizontal spring simulating the lateral restraint coming from the indirectly affected part;
- δ_{N1} and δ_{N2} are the plastic elongations at each plastic hinges;
- θ is the rotation at the plastic hinges at the beam extremities.

In addition, the axial and bending resistances at the plastic hinges N_{Rd1} and M_{Rd1} for the plastic hinges 1 and 4 and N_{Rd2} and M_{Rd2} for the plastic hinges 2 and 3 have also to be taken into account (it is assumed that the two plastic hinges 1 and 4 and the two plastic hinges 2 and 3 (see Figure 5-36) have respectively the same resistance interaction curves).

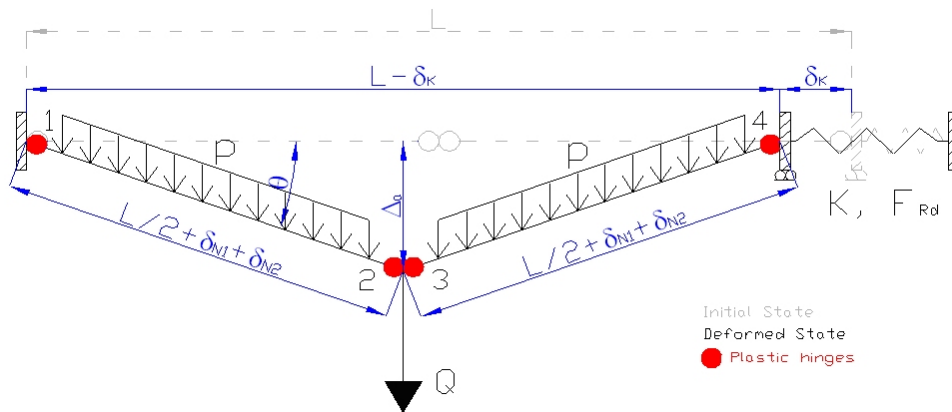


Figure 5-36 Substructure to be investigated and definition of the main parameters

In Figure 5-36, it can be observed that the concentrated load Q associated to the column loss is assumed to be applied at the middle of the simplified substructure, i.e. it is assumed that the beam spans each side of the loss column are equal. However, the developed theory can be easily extended to situations where these spans are not equal.

In order to be able to predict the response of the simplified substructure, the parameters K and F_{Rd} have to be known; these parameters depend of the properties of the indirectly affected part (see Figure 5-15). Within the PhD of Luu Nguyen Nam Hai [88], analytical procedures have been defined to predict these properties.

The developed method has been applied to the tested substructure configuration. The properties of the plastic hinges which have been considered are in fact the properties of the composite joints experimentally determined at the University of Stuttgart (relation between N_{Rd1} and M_{Rd1} and N_{Rd2} and M_{Rd2} and the plastic elongation of the hinges δ_{N1} and δ_{N2}). The so-obtained results are presented in Figure 5-37.

Two analytical curves are reported on this figure: one for which the uniformly applied load p is taken into account and one for which this load is neglected. It can be observed that exactly the same results are obtained for the analytical predictions. It is due to the fact that, when the plastic mechanism is formed, only the concentrated load Q is varying. The advantage of neglecting p is the simplification of the analytical formulas to be applied within the developed procedure.

Also, it can be observed in Figure 5-37 that a very good agreement is obtained between the analytical prediction and the experimental one what validates the developed analytical procedure.

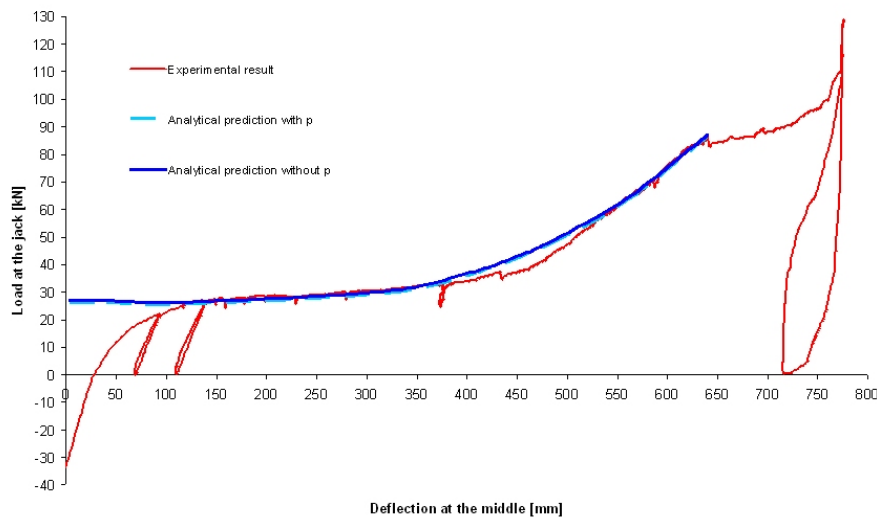


Figure 5-37 Comparison between the analytical predictions and the experimental result

5.3.4.4 Conclusions

Within the present paragraph, the analytical developments performed at the University of Liège have been described.

An analytical procedure dedicated to the prediction of the behaviour of composite joints subjected to combined bending moments and axial loads has been developed and validated within the project.

Also, a simplified analytical method allowing the prediction of the development of the membrane forces and of the frame response further to the loss of a column has been developed and validated through comparison to the substructure experimental test results. This simplified method is based on a rigid-plastic - second-order analysis and takes into account of the M-N interaction acting at the plastic hinge level.

5.4 Investigations on the event “Loss of a bracing”

5.4.1 General

The numerical studies shall explain the global behaviour of the structure when local failure of a bracing occurs and determines the remaining bearing capacity of the damaged structure, as well as the alternate load paths. The value of robustness is reflected by the global behaviour when modifying the initial structure and is expressed by the value of collapse resistance (limit load factor).

Aim of the numerical simulation of the event “loss of a bracing” in a car park frame is to study the redistribution of the internal forces within the structure when fracture of a bracing happened. A really important question concerning the requirements when the event “loss of a column” occurs is the required joint rotations and the minimum required joint resistance to ensure collapse resistance of the structure. For the car park frame it has been also decided to use a composite structure and not a pure steel frame because in practice the executed car park frames are mainly composite structures. In order to achieve an economically efficient structure joints at the inner column are designed as semi-rigid ones which have more bearing capacity than pure steel joints and the concrete slab with its huge ratio of dead load is also integrated into the load-bearing structure.

More detailed information is given in [24].

5.4.2 Dimensions and properties of the car park frame

The design of the braced frame for a car park using composite beams and steel columns is done with practically orientated dimensions and profiles. The inner joints should be designed as composite joints, while the edge joints are pure steel joints because it is difficult to ensure an anchorage of the reinforcement at the edge columns in an economic way. All joints are considered as semi-rigid joints with bilinear behaviour. At the footing all columns have hinged bearings. This leads to a main span of the frame of 16 m, a storeys height of 3.5 m, as given in Figure 5-38. The distance of the frames in transversal direction amounts to 5.0 m, see Figure 5-39.

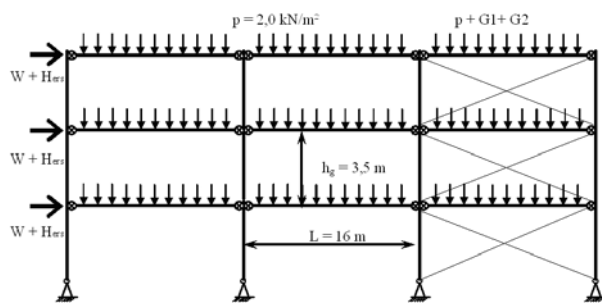


Figure 5-38: Main dimensions and loads of the main frame

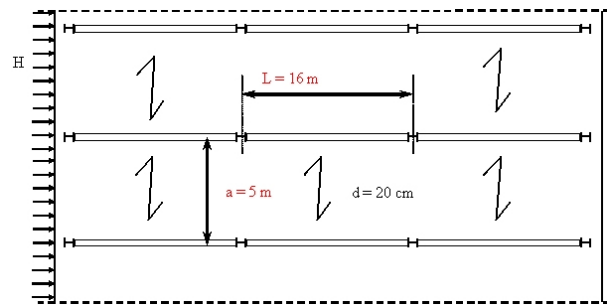


Figure 5-39: Main dimension of the structure in transversal direction

The structure shall be braced in both directions. Secondary beams are connecting the frames to each other. It's also assumed that one bracing has to stiffen 5 frames. The cross sections are designed in such a way that the degree of utilization ranges between 90% and 105 % of $M_{el,Rd}$. [$M_{el,Rd}$ is the moment under which the bottom flange of the girder reaches $f_{y,Rd}$.]

The thickness of the concrete slab is chosen to be 20 cm. The effective width b_{eff} is determined as well as internal forces according to EN 1994-1-1, 5.4 [70]. The number and design of the headed studs are taken in that way that a rigid connection between steel girder and the concrete slab can be assumed.

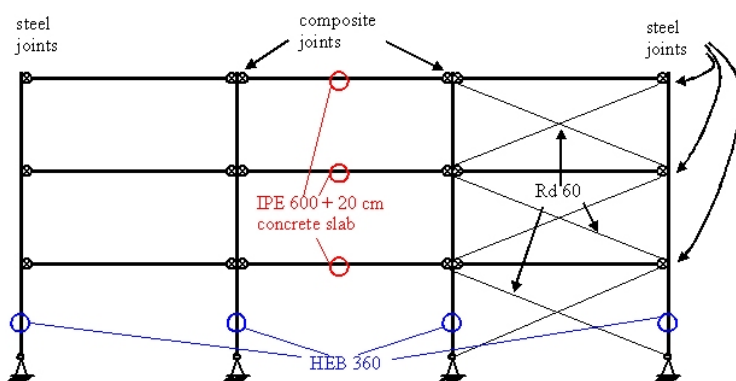


Figure 5-40: Cross-sections of the members

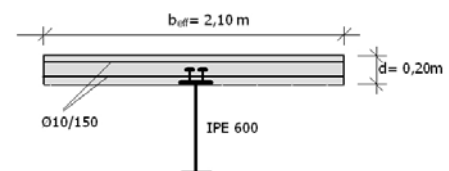


Figure 5-41: Cross-section of the composite beam over total length

The column bases are perfectly hinged. Internal joints are regarded as composite joints, while external joints are assumed to be pure steel connection as the reinforcement there is not able to transfer any forces into the column. The joints are designed in that way that they are according to EN 1993-1-8, 5.2 [69] classified as semi rigid and partial strength joints.

The moment resistance and the axial resistance as well as the initial stiffness of the joints are calculated according to EN 1993-1-8 [69] and ECCS doc. 109 (1999) [60]. The joint configuration is realized by a bolted endplate connection with four bolts M27 grad 8.8 and the longitudinal reinforcement in the concrete slab are rebars $\varnothing 10$ each 150 mm.

Table 5-7: Resistance of the composite beams and composite joints

members location	resistance on design level		resistance on characteristic level	
	$M_{pl,j,Rd}$	$M_{pl,Rd}$	$M_{pl,j}$	M_{pl}
inner	590 kNm	1569 kNm	687 kNm	2507 kNm
external	270 kNm	1332 kNm	297 kNm	1477 kNm

The materials are used as follows: concrete is of grade C25/30, reinforcing material B 450C is used with $f_{y,k} = 450 \text{ N/mm}^2$, the concrete cover is assumed to 3 cm (top + bottom), steel profiles consist of grade S355 and for the bracings round steel with $\varnothing = 6 \text{ cm}$ S 355 is used too.

For the design of the braced frame only bilinear relation between M - Φ_j of the joints is assumed.

5.4.3 Applied loads at the car park

The dead load of the construction consists of the dead load of the concrete slab as well as of the steel beams as illustrated in Figure 5-42:

$$g_1 = 5.0 \text{ m} \times 0.20 \text{ m} \times 25 \text{ kN/m}^3 + 1.224 \text{ kN/m} = 26.224 \text{ kN/m}$$

Also a superimposed dead load (covering) $g_2 = 1.5 \text{ kN/m}^2$ is considered:

$$g_2 = 5.0 \text{ m} \times 1.5 \text{ kN/m}^2 = 7.5 \text{ kN/m}$$

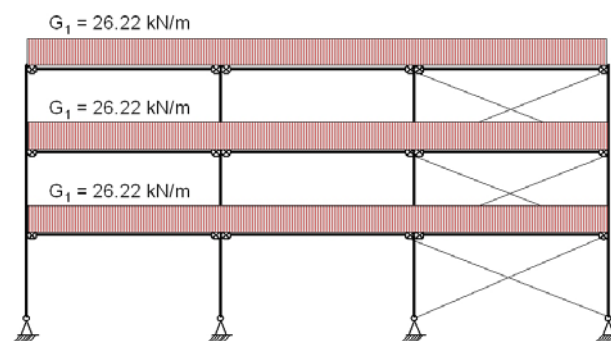


Figure 5-42: Dead Load

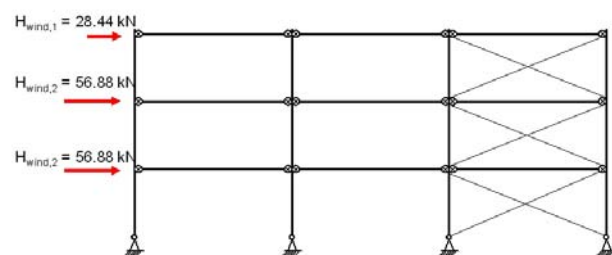


Figure 5-43: Wind Load

Vertical live loads on the storeys are considered according category F acc. to EN 1991-1-1 [64] as line loads on the beams:

$$p^* = 2.0 \text{ kN/m}^2$$

$$p = 5.0 \text{ m} \times 2.0 \text{ kN/m}^2 = 10 \text{ kN/m}$$

The wind loads on the lateral surfaces of the car park frame have been taken into account acc. EN1991-1-4 [65] with the assumption that the wind load is acting over the whole wall area neglecting the openings. The distributed load resulting from the design load of EN 1991-1-4 [65] is:

$$w = 0.65 \text{ kN/m}^2$$

The distributed load is summarized to single loads acting on the level of the beams of each storey, see Figure 5-43:

$$\text{Level +3.50 m \& 7.00m:} \quad H_{\text{Wind } 2} = 3.5\text{m} \times 25.0\text{m} \times 0.65 \text{ kN/m}^2 = 56.88 \text{ kN}$$

$$\text{Level +10.5 m:} \quad H_{\text{Wind } 1} = 3.5\text{m}/2 \times 25.0\text{m} \times 0.65 \text{ kN/m}^2 = 28.44 \text{ kN}$$

Imperfections and misalignments of the columns are taken into account according to EN 1994-1-1, 5.3.2.2 and 5.3.2.3 [70], with reference to EN 1993-1-1, 5.3.2. [68].

The dummy load due to imperfection resulting from dead load is calculated to:

$$H_{\text{imp},1} = \Phi * N = 0.00244 * (26.22 + 7.5 \text{ kN/m}) * 5.0 * 48.0\text{m} = 19.75 \text{ kN}$$

The dummy load due to imperfection caused by live load is:

$$H_{\text{imp},2} = \Phi * N = 0.00244 * 10.0 \text{ kN/m} * 5.0 * 48.0\text{m} = 5.85 \text{ kN}$$

All loads given here are presented without design factors. The design factors are taken into account according to EN 1990 [63] and have only been used for the calculation for ULS and SLS.

5.4.4 Procedure of the numerical simulation

As already mentioned in § 5.4.2 the composite frame was designed practically orientated for ULS and SLS, so that the degree of utilization in midspan ranged between 90% and 105 % of $M_{\text{el,Rd}}$. For this calculation the bracings were fully in function the frame structure was considered as non-sway frame (see Figure 5-44). Based on this the dimensions of the members were determined. The next step was to change from “design level” into “characteristic level”, that means no factorised loads were assumed and the material resistance was calculated with factor 1.0. For this system all loads were increased proportionally up to failure of the system. So the limit load factor as well as the failure mode for the undamaged system was determined. The next calculation procedure was the scenario “loss of a diagonal bracing”. It was started by replacing the internal force of the bracing by an external force and reducing this force stepwise from 100% to 0%. When the bracing was completely failed, the structural system in this storey had changed from non-sway frame to a “partial” sway frame (as presented in Figure 5-45). Of course in the upper storeys the bracings still existed and they had the effect of a stiff panel. Then the collapse resistance of the damaged system was calculated by determining the limit load factor after loss of the bracing. Therefore all loads are increased proportionally until failure of the frame. Resulting of this also the failure mode of the damaged structure was given. Now the analyses of the undamaged and damaged frame were compared and changes of the overall behaviour of the structure and of the internal forces in the members were investigated. The final step investigated how the redistribution of forces within the structural system took place.

A really important question concerning the requirements when the event “loss of a column” occurred was the required joint rotations and the minimum required joint resistance to ensure collapse resistance of the structure.

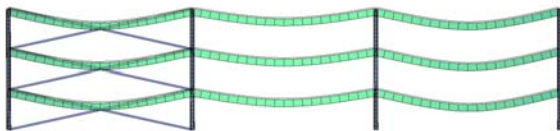


Figure 5-44: Calculation of the fully functional structure

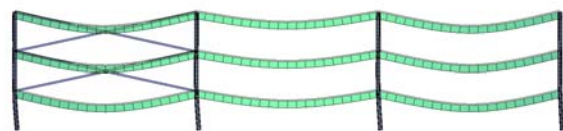


Figure 5-45: Calculation of the damaged structure

5.4.5 Numerical simulations for “Loss of a bracing”

5.4.5.1 Calculation of the undamaged frame structure

All characteristic loads have been increased proportionally to determine the limit load factor of the car park frame. That means the loading was proportionally increased until collapse of the structural system. This calculation was done without any safety factors for loads, as well as for the materials as explained in § 5.2.4 and aimed on the validation of the FE - tools.

The failure mode of the undamaged structure was a plastic beam mechanism of the coloured beams in the first storey in Figure 5-5. The plastic zone developed first in the beam of the first storey where the bracing were located. This was due to the fact that the normal compression force in this beam was maximal because of the bracings. Resulting of second order effects an additional moment was caused by the beam deflection and the compression force.

The calculations with the two different softwares FINELG [73] and SOFISTIK [100] corresponded very well as shown in Table 5-8. Just when the beams started yielding a small deviation of both analyses was visible.

Table 5-8: Comparison of the limit load factors of the undamaged system

	FINELG	SOFISTIK	Deviation [%]
Limit load factor	2.07	2.025	~ 2%

5.4.5.2 Calculation for “Loss of a bracing”

In a second analysis the limit load factor of the damaged frame was calculated. Again all characteristic loads were increased proportionally until collapse of the structure. For the calculation of the damaged structure the failure mode changed into a plastic panel mechanism. The limit load factor was as consequence also less than for the undamaged structure. That was due to the reason that the non-sway frame became a “partial” sway frame (in the bottom storey) and additional moments resulting of second order effects increased the bending exposure in the columns in the level of the first storey. The limit load factor of the damaged structure was still quite high because the remaining bracings in the upper storeys braced the whole frame structure for lateral loading.

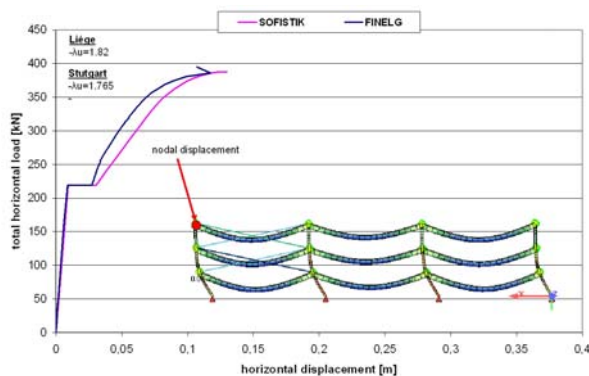


Figure 5-46: Analysis of the limit load factors of the damaged system (horizontal load)

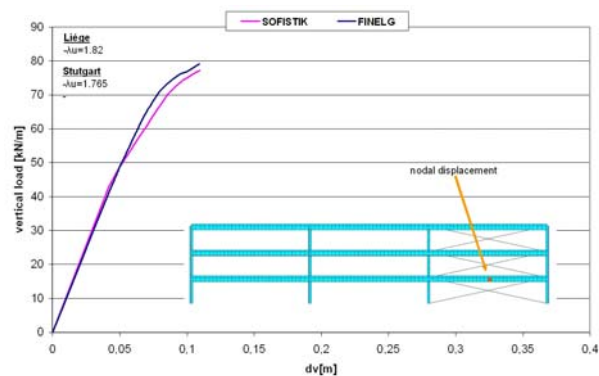


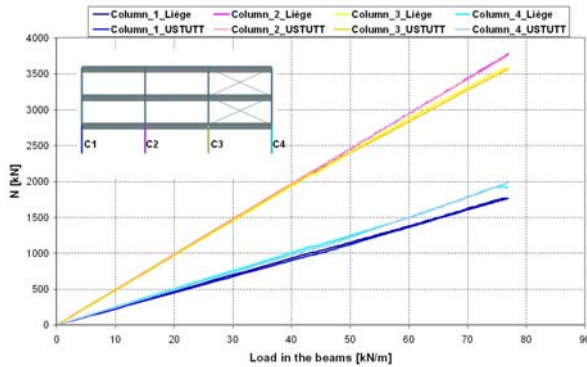
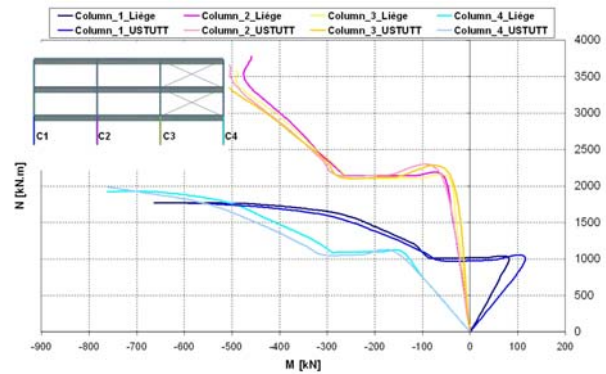
Figure 5-47: Analysis of the limit load factors of the damaged system (vertical load)

In Figure 5-46 and Figure 5-47 the load-displacement curves of the damaged frame are given and they show a quite good correspondence for the limit load factor (see Table 5-9) but some deviation of both curves exists after failure of the bracing. But it could be noticed that the results of FINELG [73] and SOFISTIK [100] were quite good in line and due to the fact that FINELG has been validated at the substructure it could be assumed that the results are reasonably correct that means the real behaviour of the structure was more or less reproduced.

Table 5-9: Comparison of the limit load factors of the damaged system

	FINELG	SOFISTIK	Deviation [%]
Limit load factor	1.82	1.765	~ 3.5 %

A comparison of the normal forces in the columns presented in Figure 5-48 as well as the M-N-interaction in the columns given in Figure 5-49 shows also a very good agreement of the results of both softwares FINELG and SOFISTIK.

**Figure 5-48: Comparison of the normal force diagram in the columns (damaged system)****Figure 5-49: Comparison of the M-N-interaction in the columns (damaged system)**

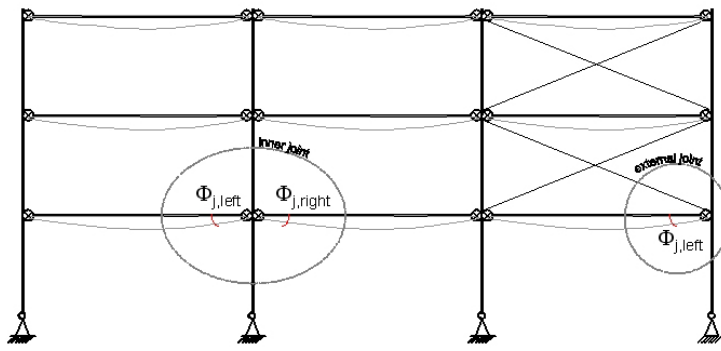
Regarding the required joint rotations of the inner and external joints of the composite frame the following maximum values, given in Table 5-10 were observed in the numerical simulation with SOFISTIK. The values were measured for the time step just before collapse of the car park frame. The decisive inner joint as well as the external joint with the maximal values of Φ_j is illustrated in Figure 5-50. The development of the required joint rotations during the whole scenario, loss of a bracing and afterwards further increase of all loads until collapse of the frame, is illustrated in Figure 5-51 and Figure 5-52.

It is clearly visible that at the right side of the inner joint a reduction of the beam restraint took place to activate the frame effect with the column which led to a quite small required joint rotation, whereas at the left side of the joint the required rotation was about 30 mrad. A detail consideration of the inclination of the beam and its influence on the columns declination especially in sway-frames are given in § 5.4.6.2.

For the external joint (pure steel joint assumed) the determined required joint rotation was more than 30 mrad. Figure 5-51 and Figure 5-52 show also that for the event loss of a bracing with a load factor 1.0 the required joint rotations were relatively small (≈ 10 mrad) due to the fact that the remaining bracings in the upper storey avoid a large horizontal transition of the frame.

Table 5-10: Joint rotations at the inner and external joints just before collapse of the frame

	$M_{j, \text{left}}$ [kNm]	$\Phi_{j, \text{left}}$ [kNm]	$M_{j, \text{right}}$ [mrad]	$\Phi_{j, \text{right}}$ [mrad]
inner joint	686.,0	27.70	486.1	3.20
external joint	297.0	33.20	-	-



For the calculated values in Table 5-10 the lateral loading of the car park frame was acting at the left side in Figure 5-50. So the horizontal transition of the upper storey occurred in the direction of the right side. Taken this into account the values for the joint moments and joint rotations in Table 5-10 were calculated.

Figure 5-50: Location of the calculated Φ_j in Table 5-10

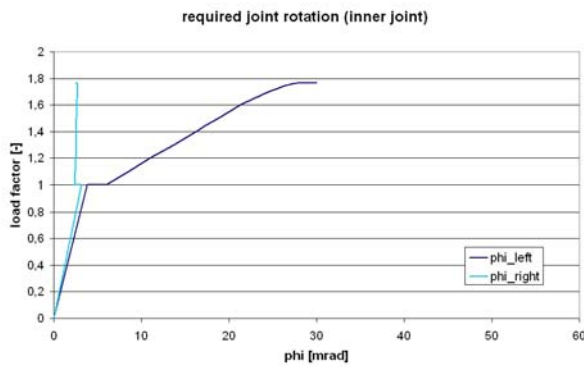


Figure 5-51: Required joint rotation inner composite joint

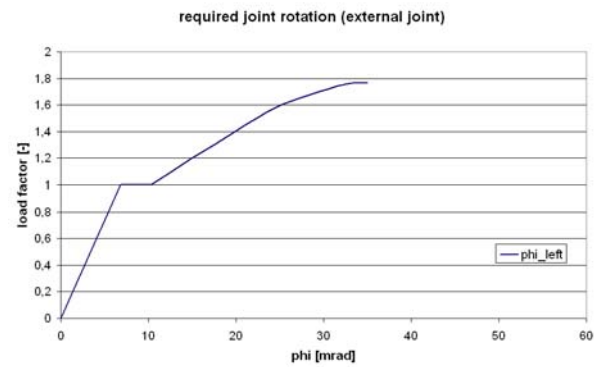


Figure 5-52: Required joint rotation external steel joint

5.4.6 Further parametrical studies for the car park frame

5.4.6.1 Introduction

Within this chapter some further critical limit states of the car park frame were additionally investigated regarding the event loss of a bracing. First the behaviour of a pure sway-frame was analysed, next the event loss of one bracing with different joint properties was calculated and at last the influence of the size of the column profile to the collapse resistance was investigated.

5.4.6.2 Examination of the car park as pure sway-frame

So starting with reflecting on the car park as sway-frame: investigations on sway-frames by Schäfer [83], [96] and Lahmeyer [84] showed that the inclination of the beam α decisively influence the declination of the column ψ . The inclination of the beam, i.e. the rotation at support of the beam, depends mainly on the utilization of the beam in span. If the beam stays in a range of $M_{beam} < 1.1 M_{el,R}$ the curvature of the composite beam has relatively small values which results in a moderate beam inclination and leads to only less column declination.

As visualised in Figure 5-53, the declination of the column is mainly dependent on the inclination of the beam close to the connection:

$$\psi = \alpha_R - \Phi_{j,R} \quad (5.5)$$

with:

α_R inclination of the beam at its left support in Figure 5-53 [mrad]

$\Phi_{j,R}$ rotation of the right joint in Figure 5-53 [mrad]

The highest rotation occurs on the left joint and is composed of:

$$\Phi_{j,req} = \alpha_R + \alpha_L - \Phi_{j,R} \quad (5.6)$$

with:

α_L inclination of the beam at its support on the right side in Figure 5-53 [mrad]

$\Phi_{j,req}$ required rotation in Figure 5-53 [mrad]

whereas the elastic rotation of the right joint may be neglected.

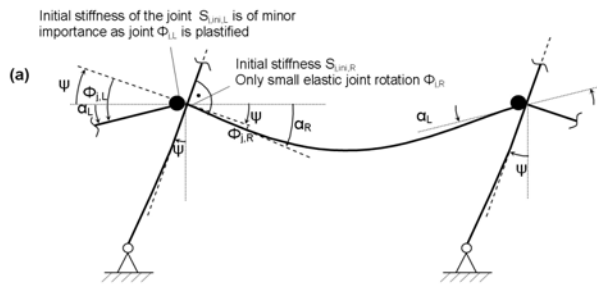


Figure 5-53: Joint rotations extract of a composite sway-frame with partial-strength joints

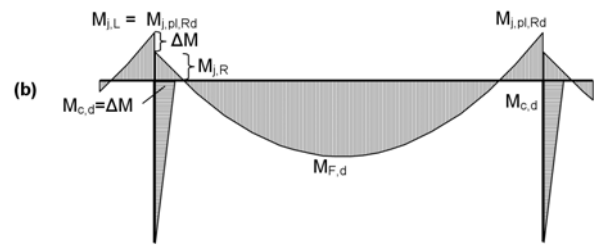


Figure 5-54: Moment distribution extract of a composite sway-frame with partial-strength joints

Additional load leads to a plastification of the composite beam in the sagging moment area, which leads to a disproportionate curvature of the composite beam resulting in high inclinations α of the beams at the supports (composite joint), see Figure 5-53. As the required rotation $\Phi_{j,req}$ of the joint depends mainly on the sum of the inclinations α of the beam, see equation (5.5), the required rotation $\Phi_{j,req}$ is strongly increasing.

The declination of the column Ψ is effected by the high inclination α_R of the beam. Thus, additional horizontal forces due to second order effects occur. Finally the structural system collapses before the plastic moment M_{pl} of the composite beam is achieved in the sagging moment area. That is due to the fact that the moment ΔM in Figure 5-54, needed for stabilization of the frame, further increases leading also to a disproportionate increase of the utilisation of the steel column. The here described effects are in close correlation as illustrated in Figure 5-55.

The effects of plasticity are only detected by the more realistic plastic zone theory for the plastic hinge theory, a higher ultimate load is calculated as prior partial plastification of the beam in the sagging moment area is not covered which would lead to an overestimation of the collapse resistance.

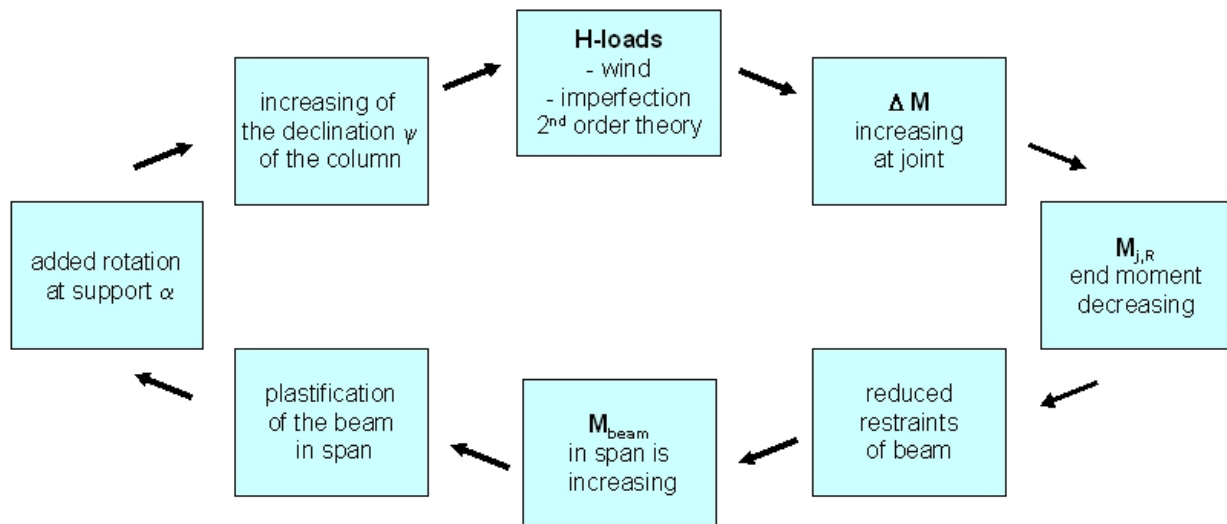


Figure 5-55: Development of plastic panel mechanism of sway frames with semi-rigid joints

So for functional and economical aspects sway frames with semi-rigid joints and without bracings are worthwhile but under the aspect of robustness the application of bracings is useful. Even if one of the bracings fails the collapse resistance of the frame is quite good. The probability that the bracings in all storeys fail without any damage of the other structural members is low.

5.4.6.3 Examination of different joint characteristics for the car park frame

Next the influence of the joint property was investigated when the bracings in the upper storey are still fully functional. Therefore the used joint characteristic in § 5.4.2 was assumed as basic value and different joint characteristics with higher and smaller resistance (M_{pl}) were considered for the analysis of the event loss of a bracing. The initial stiffness was changed as well respectively but for the assumed bilinear behaviour it was of minor importance concerning the joint rotation at limit state.

Figure 5-56 the horizontal transition of the node at the upper edge of the frame is illustrated in dependence on the load factor (vertical + lateral loading). Also for a relatively small restraint (10% $M_{pl,beam}$) of the composite beams the decrease of the limit load factor was minimal. Not until reaching a nearly perfect hinged joint the failure mechanism changed into a plastic beam mechanism and at the same time a drop of the limit load factor occurred.

This calculation demonstrated that if the bracings in the upper storeys remained functional the joint capacity M_{pl} was of minor importance.

Due to the change of the restraints of the beams at the columns the vertical deflection of the beams in midspan was changing as shown in Figure 5-57.

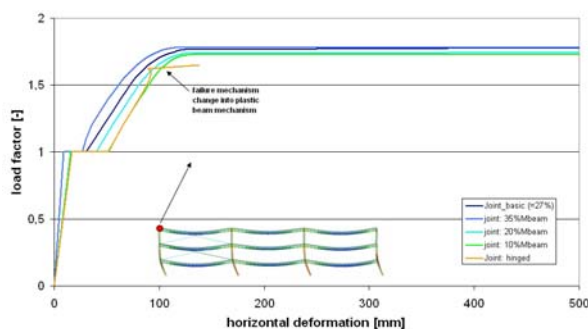


Figure 5-56: Influence of the capacity M_{pl} of the joint to the limit load factor

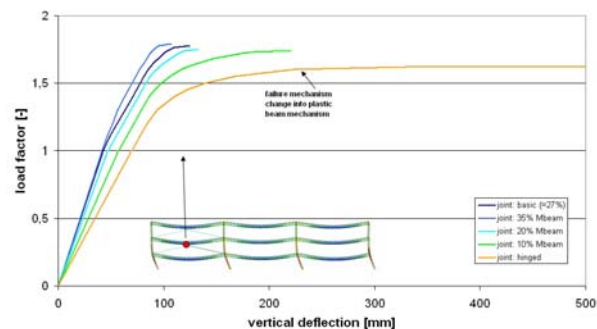


Figure 5-57: Influence of the capacity M_{pl} of the joint to the limit load factor

5.4.6.4 Examination of the size of the column profile

Another additional investigation done was how the size of the column profile is influencing the collapse resistance of the frame. Therefore the used column profile described in § 5.4.2 was considered as basic value, the type of the profile HEB remains the same only the size of the profile was changed. In Figure 5-58 the horizontal deformation of the node at the upper edge of the frame is given independence of the limit load factor. The decrease of the limit load factor by downsizing the column profile is clearly visible. Due to the fact that the failure mechanism for the basic profile was already a plastic panel mechanism the downsizing of the column profile decisively influenced the limit load factor. For increasing the size of the profile to a HEB 400 the failure mechanism changed into a plastic beam mechanism.

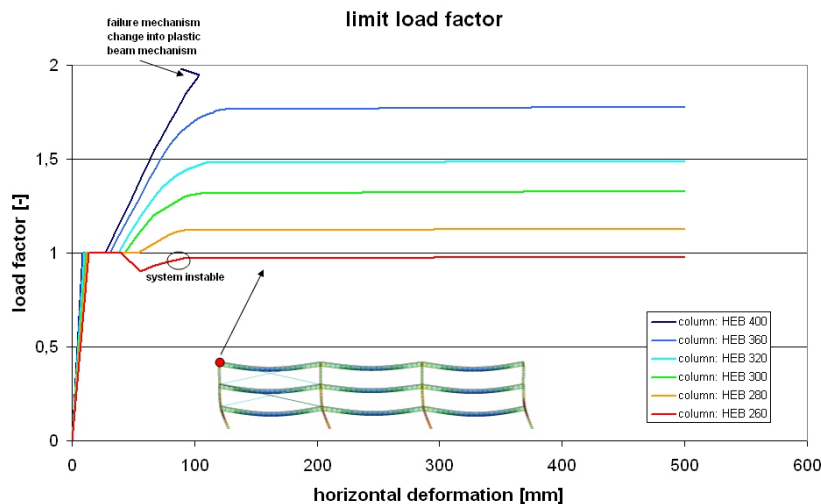


Figure 5-58: Influence of the column profile to the limit load factor

e.g. HEB 360 to HEB 300 the limit load factor of the damaged structure was reduced to a value of about ~1.30. By reducing the profile to a HEB 280 the limit load factor was only by ~1.10. For further downsizing of the column profile a collapse resistance of the car park after failure of a bracing existed no longer as shown in Figure 5-58.

So for column profiles which are relatively intensively utilized already in the state of serviceability (undamaged structure) the exceptional event “loss of a bracing” might lead to a progressive collapse of the whole car park. Additional investigations on the influence of the column profile demonstrated that the limit load factor of such a frame structure depends significantly on the size of the column profile. By decreasing the size of the profile from

5.4.7 Conclusions

The investigations of the exceptional event “loss of a bracing” point out that failure of a bracing in composite frame with semi-rigid beam-to-column connections does not directly lead to a collapse of the whole structure. The damaged structure is still able to carry a load which corresponds to more than 1.7 times of the characteristic loading. The requirements of the joint rotation capacity after failure of a bracing are reaching maximal values of about 10 mrad. For further increase of the loading until collapse of the frame maximal joint rotations of about 30-40 mrad were calculated. Resulting of this the failure mode by reaching the limit load factor is no failure of the joint but a plastic panel mechanism of the columns. A plastic zone in the columns in the level of the first storey occurred, the horizontal deformations increase which leads to stability failure.

The load path in all members during the failure of the bracing and also afterwards for further increase of the loading could be followed. The redistribution of forces within the structural system was determined. Within the parametrical study different members of the frame have been investigate concerning their influence of the collapse resistance. Further conclusions are following in § 6.3.

5.5 Investigation on the event “Fire”

In order to verify whether the case of a localised fire may be reduced to one of the basic events such as “loss of a column” or “loss of a bracing” for a practical example the calculation of a situation under fire

is performed. The calculation was made for the project Transpolis in Belgium. On the next figures (Figure 5-59 and Figure 5-60) the general view of the building and a description of the bearing façades.

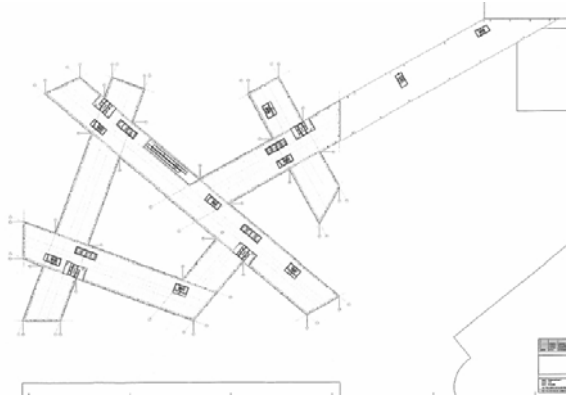


Figure 5-59: Transpolis-General view

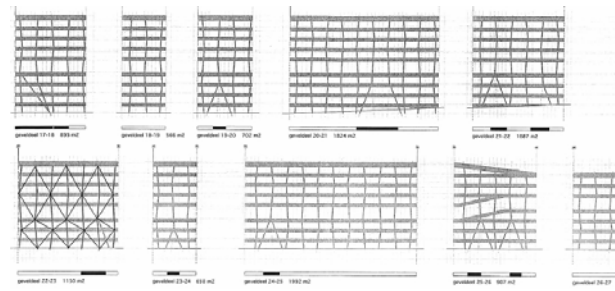


Figure 5-60: Transpolis-Detail

The structural system is composed of prestressed hollow core slab of 14m span bearing from one façade to the other. On each façade, the hollow core slab is supported by integrated steel profiles. An example of a section is given in Figure 5-61. The columns are composed of different HD sections depending on the location. Figure 5-62 shows the section of the heated column.

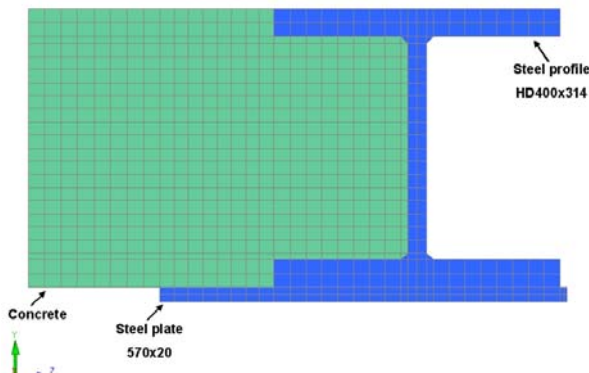


Figure 5-61: Thermal analysis - Beam HD400x314

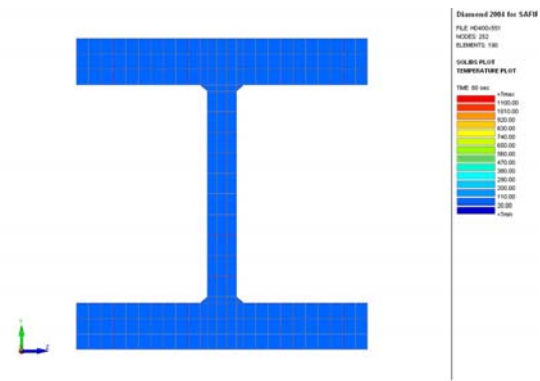


Figure 5-62: Thermal analysis - Column HD400x551

A part of the bearing façade was simulated using the Finite Element software SAFIR [74]. Hereafter, the Figure 5-63 shows the structural system with the accidental combination load.

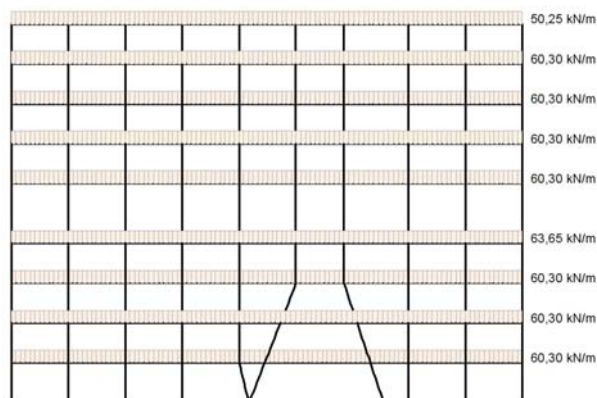


Figure 5-63: Loading of the structure (Transpolis)

The localised fire was applied on one of the column of the ground floor (see Figure 5-64). In a first step, the length of the column increases due to the thermal expansion and push the structure upwards (Figure 5-65).

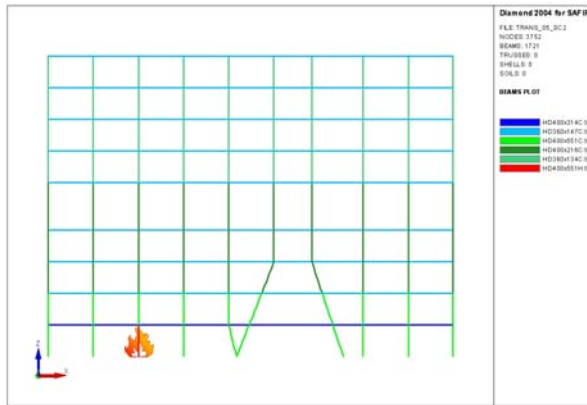


Figure 5-64: Geometry of the structural system

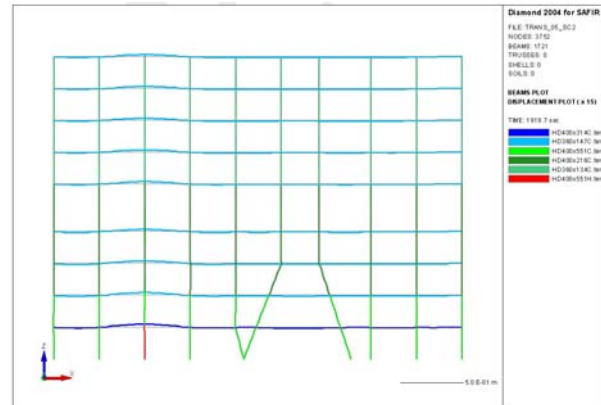


Figure 5-65: Deformation of the Structure after 1920 seconds of fire

In a second step, the column buckles due to the loss of bearing capacity. The load is redistributed in the rest of the structure and the global stability of the building is ensured (see deformed shape in Figure 5-66). The next graph (Figure 5-67) shows the vertical displacement of the top of the column. It can be shown that at the end of the simulation a new equilibrium is found and the structure remains stable.

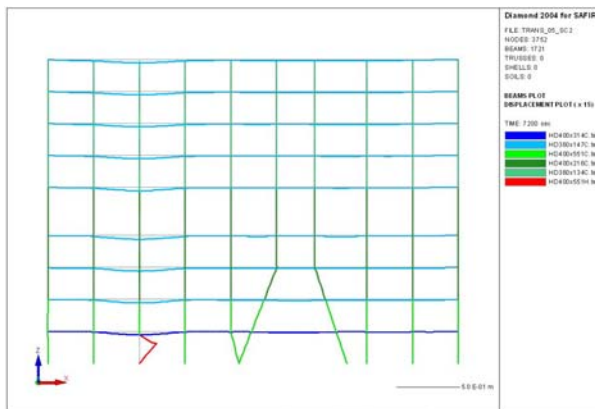


Figure 5-66: Deformation of the structure after 7200 seconds of fire

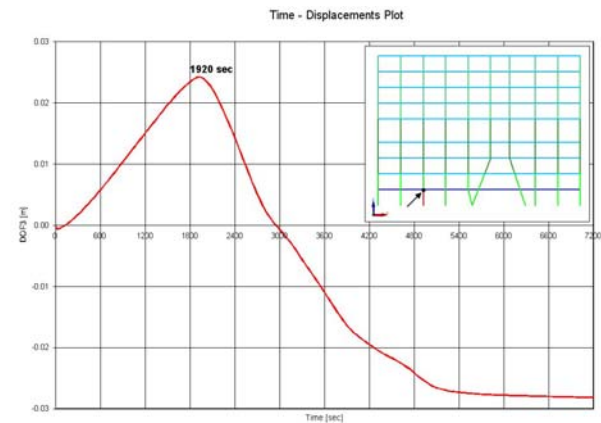


Figure 5-67: Vertical displacement of the node

The conclusion of this calculation is that the structure has sufficient reserves to survive to this event without any over design.

The steel structure was not calculated to be able to bear the loads in case of the loss of a column. This calculation shows the robustness of the steel structure. This calculation shows in addition that thrust may be given to in the calculation made using the natural fire safety concept because even if the fire load is not 100% distributed on the surface, the structure can survive with a concentration of fire load around a column.

5.6 Investigation on the event “Earthquake”

As indicated in § 3.6 the importance of ductility in both seismic and robust design, suggests an accurate analysis of the most important codes and standards concerning the seismic design. Despite the different codes about seismic design available, the analysis was restricted to the AISC document [98], [99] the AS/NZS 1170.0 [44], [45] and EN 1998-1 [71]. The first analysis of the documents highlighted the first

two of them (AISC and AS/NZS 1170.09) adopt basically the same design methodology and detailing rules. Therefore it seemed effective to focus on the comparison of the American Standard (AISC) and EN 1998-1 [71]. In the comparison, the attention was focused on aspects within the scope of this research project. The main aspects appraised for both steel and steel and concrete composite structures refer to the following general areas: basic design concept, seismic classes, limiting material criteria, seismic detailing at element, connections and structural level.

Since the general methodologies of EN 1998-1 (i.e. the capacity design concept) [71] and of the AISC (load and resistance factor design and/or allowable strength design method) [98], [99] differ significantly, no effort has been made to compare them in detail and it has been left to the designer to select the approach i.e. the way in which he wants the system to perform. Nevertheless, the seismic prescriptions and rules adopted by EN 1998-1 [71] are mainly in agreement (in terms of demand of energy dissipation and ductility) with those contained in the codes of other countries like U.S.A. [98], [99], Australia and New Zealand [44], [45].

The extensive study of the above seismic standards enabled to define a set of guidelines which forms a common ground for seismic design. These guidelines have been summarised as:

- Establishing a design concept: The designer is allowed to choose the way the system has to dissipate energy selecting for it a specific Ductility Class by which design factors are derived depending also on the type of the structural system. The greater the factor, the lesser the horizontal design-forces, but also the need for more detailed prescriptions to be followed during the design procedure.
- Deciding what kind of plastic mechanism to adopt and where to place plastic hinges: Dissipative zones must be located inside the system e.g. in beam-to-column joints, in end-parts of beams, in the tensile diagonals, in dissipative links and at the base and top of frames. The non-dissipative areas must be over-designed to prevent brittle failures.
- Having a better knowledge of the selected materials: Restricted classes of materials are set and deemed to be utilised during construction to close the gap between the envisaged and real structural behaviour.
- Paying attention to detail design: It has to be verified that both the single structural element and the structural system possess an amount of ductility in accordance with the design factors adopted in the first step. In several world-wide standards and codes, the sustainability of the ductile behaviour of the system is guaranteed by the adoption of simple rules aiming to the prevention of the early buckling and/or fracture of the steel as well as composite steel and concrete members and components. These detailing rules are based on extensive studies and form the main body of the design requirements and criteria. A brief summary of some of the most important detailing rules are included in § 6.5.

6 DESIGN REQUIREMENTS AND DESIGN CRITERIA

6.1 General

As introduced in § 1 there are many exceptional events and structures which could be considered but only four events have been chosen as model cases within this project.

The event “Loss of a column” was investigated most intensively by experimental tests as well as by numerical simulations. The findings of the experimental and numerical investigations leading to the development of an analytical tool which is able to predict the response of the simplified substructure (§ 5.3.4.3) when the membrane forces appear in the system, see § 6.2. So it is possible to determine e.g. the required rotation capacity for the joints for the event “Loss of a column” at a simplified “two beam system” in order to avoid a complex Finite Element analysis of the whole framed structure. Furthermore the experimental test results enable to define first requirements for the adjustment of single joint components to ensure a highly ductile joint behaviour, i.e. a sufficient available rotations capacity. A description of potential improvements for joint configurations which have subsequently an actual ductile behaviour are given in § 4.6.

The numerical investigations allow the definition of requirements for joints resulting from the response of the structural system. The requirements e.g. the required joint rotation are strongly depending on the particular structural system and boundary conditions like loading, location of the failed column, etc. and resulting of this it is hardly possible to define generally admitted requirements for the required joint rotation resulting from the “Loss of a column”. That is why an analytical method was developed to enable the practical engineer to determine the requirements for the joints due to loss of a column, considering the important boundary conditions, at a simplified system. This design methodology is also separately described in design guidelines, see [34].

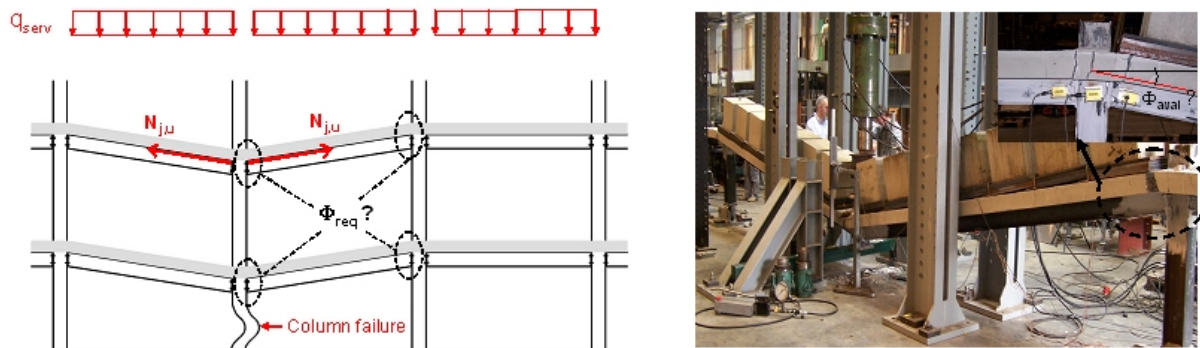


Figure 6-1: Determination of required and available joint rotation e.g. for loss of a column

For the exceptional event “Loss of a bracing” the numerical investigations aimed to define critical values for the required rotation capacity which have to be fulfilled by the joints to allow for redistribution without premature joint failure. These calculations were performed for one type of structure: a typical composite frame of a car park structure, see § 5.4.5 so the determined requirements are still limited to this typical case. In addition former investigations of Schäfer [96] have been taken into account to provide a broader informative basis of requirements. Therefore in § 6.3 some general findings for the event loss of a bracing are summarized.

For “Fire” two states have to be differentiated as illustrated in § 6.4. On one hand localised fire influences only local structural members leading to local failure of members like “Loss of a column” or “Loss of a bracing”. So the local fire may be translated e.g. to the basic events “Loss of a column” or “Loss of a bracing”. This has been shown for a given example in § 5.5. On the other hand a fully engulfed fire is no more a problem of robustness of structure, but a problem of global fire resistance of the building which has to be designed in an independent “hot” design according e.g. to [59] or other investigations and rules.

For the exceptional event “Earthquake” the work was concentrated to collect and to check the most important codes and standards worldwide concerning provisions ensuring a structural ductile behaviour. In the summary in § 6.5 main focus is given to connection requirements of steel as well as of concrete structures. But it has to be kept in mind that the different nature of the actions associated with seismic events or an accidental actions and the consequent different structural behaviour doesn’t allow the extension of the available seismic detailing rules also to robustness without further studies. Certainly, the rules provided by seismic codes may be an interesting reference because the knowledge in seismic design is built up of decades of research in basic principals.

6.2 Conclusions for the event “Loss of a column”

Experimental, numerical and analytical investigations have been performed on the exceptional event “Loss of a column in residential or office buildings”.

A complete experimental test campaign was planned with the objective to fully understand how the membrane forces develop in such frames and how they can affect the behaviour of the structural beam-to-column joints.

In a first step, an experimental test on a substructure was performed. The latter was extracted from a realistic composite frame (design according to Eurocodes) and the test setup was organised so as to have a tested substructure able to reflect the actual behaviour of the global frame from which the latter was extracted. The performed test was successful; indeed, through the latter, it was possible to observe the development of the catenary action within the frame and its effects on the joints. In particular, a very good ductility of the joint was achieved with a maximum observed rotation of 190 mrad.

In a second step, the configuration of the substructure composite joints was tested in isolation at the University of Stuttgart. The objectives of these tests were to characterise the behaviour of these joints subjected under sagging and hogging bending moments with and without tension forces and to obtain the M-N interaction resistance curve. Again, these tests were successful. From the latter, it was possible to confirm the very good ductility of the joints; in particular, it was demonstrated that only ductile components are activated to pass from the behaviour under pure bending to the behaviour under pure tensile load. In addition experimental investigations for steel joints were performed in realistic dimensions to identify failure dependencies especially within the component “endplate in bending” and to optimise the ductility of the joints.

Finally, experimental tests on each components met in the substructure joint configuration were performed at the University of Trento. From the latter, it is possible to understand the influence of each component on the global behaviour of the joint and, in particular, to highlight the effects of the development of the membrane forces within the component in bending (i.e. the column flange and the end-plate in bending) and to identify the non negligible stiffening effects of the concrete for the component “reinforcement in tension”.

From the performed experimental tests, it was possible to validate analytical and numerical tools.

Indeed, numerical investigations were performed on the tested substructure in order to compare the numerical prediction to the experimental results. From this comparison, the difficulty to model the actual behaviour of joints subjected to combined bending moments and axial loads was illustrated. However, it was shown that it is possible to model the behaviour of the joints with equivalent double-T beams if the developed membrane forces within the structure are not too important.

In addition, to complete the validation of the numerical tools, a benchmark study was performed on a steel building frame. The loss of a column was simulated through different software used by the partners involved in the numerical simulations. It was shown that the predictions obtain through these software are in good agreement.

Then, with the so-validated software, numerical analyses were performed on 2D and 3D building structures. Parametrical studies were performed on 2D frames considering different loadings applied to the structure (with or without wind loads, accidental load combination,...). These parametrical studies permitted to observe the redistribution of the loads within the structure and to have an idea on the requested ductility as consequence of the event “Loss of a column” at the structural element level. The

3D simulations allowed including the out-of-plane behaviour of the structural elements; in particular, the risk of a lateral-torsional buckling of structural beams located in the upper storeys of the structure was put into sight.

To develop simplified analytical methods to predict the response of a frame caused by the event “Loss of a column”, the definition of a simplified substructure was proposed. Through 2D numerical analyses, it was shown that it is possible to simulate very accurately the response of a structure through the proposed substructure. In addition, parametrical studies on the substructure were conducted so as to identify the parameters to be included in the developed analytical procedures.

One of the main parameters influencing the response of the simplified substructure is the M-N interaction occurring at the plastic hinge level. Accordingly, an analytical procedure was developed so as to be able to estimate the M-N interaction resistance curve of composite joints. The latter is based on a procedure already developed for steel joints in the PhD thesis of Frederic Cerfontaine [52]. Through comparisons to the results of the experimental tests performed on the substructure and composite joints in isolation, it was shown that the developed method permits to obtain a very accurate prediction of the composite joint behaviour when subjected to combined bending moments and tensile loads. In particular, through the developed procedure, it is possible to determine the components which are activated in the joint to pass from a pure bending loading to a pure tensile loading and, as a result, to know if the activated components are ductile ones, what is very important in the present case.

Finally, an analytical method to predict the development of the catenary action within the so-defined simplified substructure was developed and validated through comparisons to the experimental tests. The developed method is based on a rigid-plastic second-order analysis and permits to accurately predict the response of the simplified substructure.

With the so-obtained substructure response, it is then possible, knowing the maximum concentrated load Q to be supported by the system (what is possible with the analytical procedures presented in the PhD thesis of Luu Nguyen Nam Hai [88]), to predict the maximum vertical displacement associated to the considered column loss (as illustrated in Figure 6-2) and, as a result, the requested rotation capacity at the joint level. This analytical procedure is also included in more detailed in the design handbook [34].

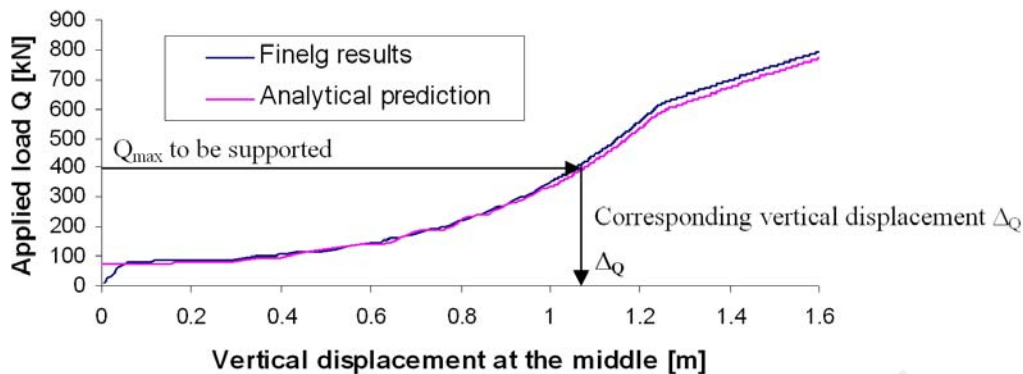


Figure 6-2 Analytical prediction of the simplified subsystem response and determination of the maximum deflection associated to the maximum load to be supported

6.3 Conclusions for the event “Loss of a bracing”

The main conclusion is that the damaged composite frame structure can still resist the 1.0 loading after “Loss of a bracing” of a car park frame without significant problems. This results from the fact that the car park frame with partial-strength joints and additional bracings is a highly redundant structure. The remaining stiff panel effect of the undamaged bracings in the upper storeys still provides a frame effect and in addition the moment resistance of the semi-rigid joints also creates a moment resisting frame. In fact it is known from Schäfer [83], [96], Lahmeyer [84], etc., that semi-rigid joints are also well

applicable in sway-frame structures. However the collapse resistance and the limit load factor depend in these cases decisively on the chosen column profile.

So for column profiles which are relatively intensively utilized already in the state of serviceability (undamaged structure) the exceptional event “Loss of a bracing” might lead to a progressive collapse of the whole car park. The investigations on the event “Loss of a bracing” also showed that the remaining bracings in the upper storeys contribute to a more “robust” behaviour for exceptional horizontal and vertical loading (e.g. extreme wind events, overloading of floor, etc.). A reflection of critical values for maximal requirements for the joints have been done by extracting all bracings of the frame and considering a pure sway-frame, by changing the joint capacities and by downsizing the column profiles.

Investigations on sway-frames by Schäfer [83], [96] and Lahmeyer [96] showed that the inclination of the beam α decisively influences the declination of the column ψ . The inclination of the beam, i.e. the rotation at support of the beam, depends mainly on the utilization of the beam in span. If the beam stays in a range of $M_{\text{beam}} < 1.1 M_{\text{el,R}}$ the curvature of the composite beam has relatively small values which results in a moderate beam inclination and leads to only small column declination as explained in detail in § 5.4.6.2 (Figure 5-53).

The crucial aim within this research project is to define requirements of ductile joints for redundant structure which allow for redistribution in order to allow for a sufficient collapse resistance for certain exceptional events. So in this case the event “Loss of a bracing” was investigated and the requirements for the joints have been observed. The requirements to the joints resulting from the event “Loss of one bracing” were limited to sufficient rotation capacity. The required rotation capacity determined in the numerical calculations was reaching maximum values of about 30-40 mrad. Experimental tests on composite joints (with comparable joints dimensions to the car park) of Schäfer [96] showed that depending on the joint design it is possible to get rotation capacities of 50 mrad and more. This is underlined in the tests conducted within this research project, see report about the composite joint tests under biaxial loading [21] where values of 50-60 mrad were reached experimentally, or [11] the report about the experimental test simulation of “Loss of a column” where joint rotations of about 190 mrad were reached, see also § 4.3.4.6.

In order to evaluate the results it is pointed out that for this simulation of the exceptional event “Loss of a bracing” all affected loads were taken into account with the factor 1.0, which was a rather conservative assumption in comparison to the formulation in EN 1990 [63] for exceptional loading. For accidental design situation additional factors for combination are given in EN 1990 which lead to further reduction of the total loading acting.

Also the material resistance has additional reserves not considered in this investigation because of over-strength effects which are in a range of about 30 % for the structural steel.

It also has to be mentioned that all numerical simulations done for the event “Loss of a bracing” in a car park are static ones. The next step is to consider also dynamic effects within the numerical simulation.

Another aspect is the real three dimensional behaviour of the whole structural system. Especially the actual behaviour of the concrete slab that means e. g. the actual effective width of the concrete slab which influences the stiffness of the composite beam or membrane actions in the slabs and may add further advantageous reserves not considered here.

6.4 Conclusions for the event “Fire”

In case of fire, 2 scenarios have to be differentiated.

Concerning the robustness of steel structures in case of fire, some events may happen but may be “translated” into more basic events. A localised fire for example of a pallets of paper in an office building can locally increase the fire load. If this fire remains localised, only one or two members may be affected by the fire.

If the fire does not remain localised and grows until reaching the flash-over (see Figure 6-3), the problem is no more a problem of robustness of structure but a problem of global fire resistance of the building. All the elements will be heated and will loose their bearing properties.

In these cases reference has been made to other investigations and rules, see e.g. [59], [56], [94].

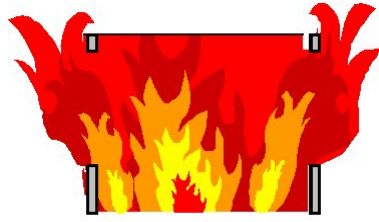
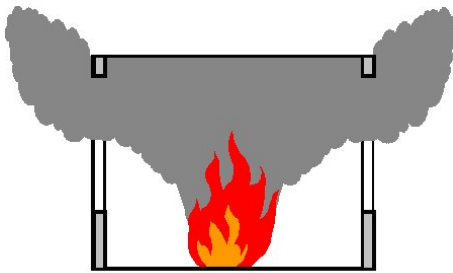


Figure 6-3: Fully engulfed fire

For the calculation of the fire resistance of building, two approaches can be followed the prescriptive approach or the performance based design.

For both, the design assumption for the calculation is the generalised fire that may occur in the building.



In some cases, an unforeseen event may occur (a big pallets of paper start to burn close to a column, a car enter in a low rise building and burn close to a beam, a bracing or a column) which the normal design has not taken that into account. In this case, only one or two elements are affected by the fire (see Figure 6-4).

Figure 6-4: Localised fire

So in the case of such a localised fire, the event “fire” may be translated into basic events such as for example:

- loss of a column in an office or residential building frame;
- loss of a beam in an office or residential building frame;
- loss of a column in an industrial portal frame;
- loss of a bracing in an industrial portal frame;
- loss of a bracing in a car park;

depending on the position of the fire and the nature of the building.

The events “Loss of a column in an office building” and “Loss of a bracing in a car park” have been investigated in the § 5.3 and § 5.4 and summarized in § 6.2 and § 6.3.

6.5 Conclusions for the event “Earthquake”

Upon careful investigation of seismic codes of different countries (§ 5.6), in the following some detailing design rules are collected aiming at ensuring a structural ductile behaviour. It is not practically feasible to summarise all results of such a comparison within the limited space available. It was hence decided to focus on the connection requirements for steel structures and steel and concrete composite structures.

Seismic classes:

The seismic classes are generally categorised as lower, medium and higher ductility class and depends on design factors such as the behaviour factor (EN 1998-1 [71]), or the seismic load reduction factor

(AISC [98], [99]). The greater the factor, the lesser the horizontal design-forces, but also more details to be carefully considered during the detail design procedure. The detailing rules quoted below are for higher ductility class.

Steel structures:

- The structural steels for use in seismic design should be specified based upon their inelastic properties and weld ability with a limit to the minimum yield stress for members expecting inelastic response under the effects of the design earthquake. Minimum yield strength of steel (AISC [98], [99] 345 MPa) and yield to ultimate strength ratio (AISC [98], [99] $1.15 < f_u / f_y < 1.72$ – EN1998-1-1 $1.15 < f_u / f_y < 1.35$) are prescribed.

Composite concrete and steel structures:

- Limits on the minimum and maximum compressive strength of concrete in composite members are specified for the calculation the nominal strength of concrete members (AISC [98], [99] $17 \text{ MPa} < f_c < 69 \text{ MPa}$, EN 1998-1 [71] $C20/25 < f_{ck} < C40/50$).
- The integrity of the concrete slab should be preserved during the earthquake allowing yielding of the structural steel and reinforcement in negative moment regions. In the joint regions seismic rebars shall be provided to govern local spreading of stresses. Figure 6-5 shows the detailing for exterior and interior joint proposed by EN 1998-1 [71].

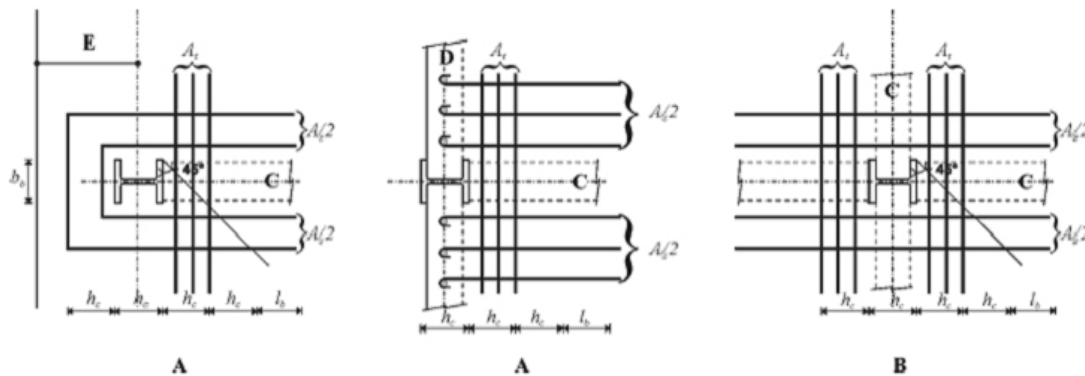


Figure 6-5: Detailing rules for seismic rebars in interior and exterior joints

- Beams intended to behave as composite elements in dissipative zones shall be designed with a minimum degree of shear connection. In EN 1998-1 [71] the ratio between the number of installed studs (N) and the number of studs for full connection (N_f) should be greater than 0.8. The design resistance of connectors in dissipative zones should be reduced by 25% to allow for reverse of loading. This is agreed upon by both codes.
- Coupling beams shall have an embedment length into the reinforced concrete wall sufficient to resist the maximum possible combination of moment and shears generated by the bending and shear strength of the coupling beam. The embedment length l_e shall be taken to begin inside the first layer of confining reinforcement in the wall boundary member. As for EN 1998-1 [71] the embedment length l_e shall not be less than 2 times the height of the coupling beam for higher ductility class (Figure 6-6 on the left).
- When a dissipative steel or composite beam is framing into a reinforced concrete column (Figure 6-6 on the right), vertical column reinforcement with design axial strength equal to the shear strength of the coupling beam should be placed close to the stiffener or face bearing plate adjacent to the dissipative zone. The presence of face bearing plates is required. EN 1998-1 [71] specifies that they should be full depth stiffeners of a combined width not less than $(b_f - 2t)$; their thickness should be not less than $0.75t$ or 8 mm; b_f and t are respectively the beam flange width and the panel web thickness.

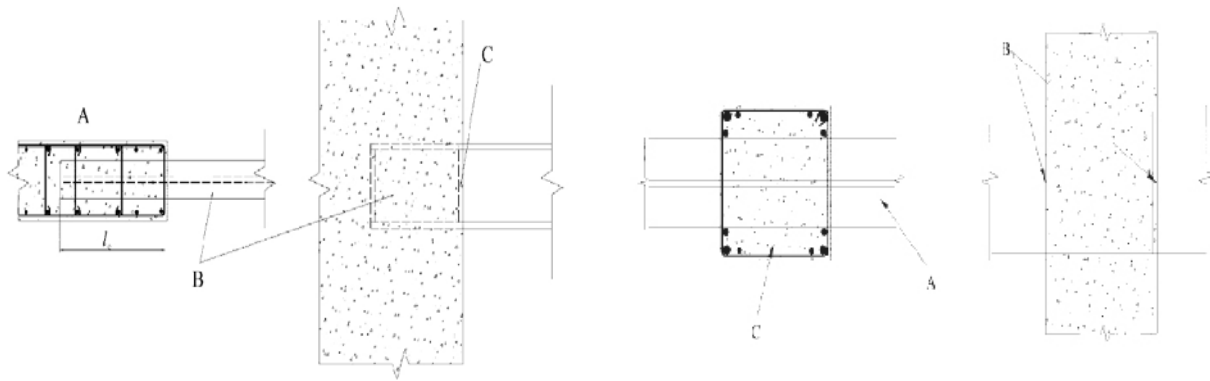


Figure 6-6: Coupling beam framing into a wall (on the left) and beam-to-column connection (on the right)

It should be mentioned that the above listed prescriptions fulfil the necessary ductility requirements for earthquake resistant structures. The different nature of the actions associated with seismic events or an accidental actions and the consequent different structural behaviour doesn't allow the extension of the available seismic detailing rules also to robustness without further studies. Certainly, the rules provided by seismic codes may be an interesting reference. In particular, the detailing rules aiming at enhancing the efficiency of welded details and of the concrete slab in the vicinity of the column seems of interest also when a robust behaviour has to be 'built up'.

7 SUMMARY

This section summarises the conclusions and findings from Chapters 2, 3, 4 and 5.

In Chapter 2 a general overview about the state of the art in the field of robustness is given. Therefore data and information available in literature about the main topics of robustness and how to achieve robustness were collected. In particular the collection was focussed on data of joint ductility as strategy to prevent progressive collapse including causes of progressive collapse, requirements, structural behaviour, etc. The different strategies to prevent progressive collapse were analysed and evaluated. Design rules against progressive collapse and concerning robustness in a huge number of codes have been studied and interpreted regarding the aspect of ductility. Main focus of course was given to the European approach to robustness adopted by EN 1991-1-7 [66]. Furthermore the beam-to-column connections have particularly been investigated because they play a central role in framed structures. Here the knowledge of the plastic rotation/deformation capacity of the beam-to-column joints was of primary importance as well as the possibilities to improve the rotation/deformation capacity. The outcome of the whole work described above is a wide ACCESS-database. The database allows making a quick search by using keywords. This ACCESS-database [1] is included on the annex CD. This may also serve for future research on this topic.

In Chapter 3 the concepts and strategies followed within this research project are presented. The general concept is to derive requirements that a structure should fulfil in addition to those directly resulting from the normal design process and which would provide a certain robustness to the structure, i.e. an ability to resist locally the exceptional loads and ensure a structural integrity to the structure, at least for the time needed to save lives and protect the direct environment. For this it is important to identify so-called key-elements which refer to one or more load bearing members (or sections of a load-bearing structure) that correspond in an initial failure and where the loss of this element may cause, if there are no provisions, a disproportionate collapse.

In order to mitigate such a progressive collapse due to local failure the “alternate load paths” method is adopted. The strategy “alternate load paths” allows local failure because of the redundancy of the load-bearing structure and a possible redistribution of internal forces to the undamaged part of the structure. This may be achieved by the activation of membrane effects within the structural members, for example the activation of a catenary action within a frame structure and the transition from bending state to pure tension exposure. This requires from all the structural members and constitutive joints a high degree of plastic deformability under combined bending, shear and axial forces.

The strategy in terms of concept and procedure followed within the project itself, in particular for the event “Loss of a column”, to define design requirements can be described as follows: firstly experimental tests have been performed (substructure test simulating the event loss of a column, joint and component tests to evaluate the results/behaviour of substructure elements). The test results aimed in addition to validate the numerical tools and afterwards parametrical numerical studies were executed. The numerical studies form the basis for the development of a simplified analytical method. This analytical method allows the practical engineer to predict the membrane forces in the beams and joints as well as to calculate joint requirements in a relatively simple manner.

For the event “loss of a bracing” no experimental investigations were performed, but similar to the procedure described before design guidelines were derived based on systematic numerical studies.

The event “Fire” could mainly be reduced to a local failure of a member such as “Loss of a column” or “Loss of a bracing” in case of a localised fire, for more global events reference has been made to other investigations.

As a second way especially for the event “Earthquake” recommendations are collected and summarized particularly for non-engineered structures that allow for a certain degree of redundancy or over-strength of crucial elements without deriving the details from refined calculations. This procedure follows more the strategy of “direct strength design”.

In Chapter 4 the experimental tests and their evaluation are reported. The experimental test programme has focussed the experimental work on the investigation of one exceptional event: the event “Loss of a

column” in a framed structure. Much effort has been devoted to the definition and the realisation of the testing set-up of the single test series planned in Trento (tests on components in isolation), Stuttgart (tests on joints in isolation) and in Liège (test on substructure) to form a whole chain. The tests in Trento should inform about the behaviour of all single components used in the joint and substructure tests. The tests in Stuttgart should allow to indicate how the selected joints behave when subjected to bending and axial forces and undergo a certain load history and the Liège test interpreted, on the basis of the results of the Stuttgart tests has been used to understand how the structure behaves after the loss of a column and to calibrate the FEM tools used in the numerical studies. Firstly a substructure test was performed at the University of Liège. The tested substructure was extracted from an actual building designed in agreement with the Eurocode 4 and adapted to the dimensions of the laboratory. The simulation of the event “Loss of a column” at the tested substructure was successful, the development of the catenary action in the system was observed and the registered curves confirmed the development of membrane forces in the beams. Also, the composite joints loaded by combined tensile forces and bending moments exhibited a ductile behaviour as expected. The results obtained through this test were used later on to validate the numerical tools.

In addition composite joint tests under biaxial loading were performed at the University of Stuttgart. The joints were identical to the substructure joint configuration and aimed at the determination of the M- Φ behaviour as well as of M-N interaction behaviour. The composite joint tests were also successful and the test results of the composite joint tests, as well as the substructure test showed the ability of the composite joints to undergo large rotations and to change the internal load combination from pure bending state to a combined bending and tension exposure. Failure was mainly induced by the concrete slab: for the hogging moment joints by increased cracks and final rupture of the reinforcement, for the sagging moment joints by crushing of the concrete and decreasing of the concrete compression zone. However the pure steel connection was still able to carry a remarkable amount of load. The results of the composite joint tests have furthermore been used to validate the analytical model. An important finding of the experimental investigations was that all single relevant components of the joints have to be chosen such that for the transition from pure bending state to a combined bending and tension exposure the weakest component in each case is always ductile. For the components of the joint which are under compression for the state of pure bending the loading gradually change from compression into tension by additional loading of the joint by membrane forces. So these components have a lot of plastic reserves in comparison to the tension components which are already strongly utilized for pure bending state when starting with biaxial loading of the joint. This means the compression components should be preferred as weakest components by designing a ductile joint for M-N-interaction. Some requirements for single components and some general design criteria derived from the experimental test results to ensure a highly ductile behaviour of the joints are presented in a Table also given in the design handbook [34].

Also tests on pure steel joints were executed. These tests on larger profiles with realistic dimensions aimed on the check of the ductility criterion according EN 1993-1-8 [69]. And indeed the result of these tests was that the present ductility criterion may be insufficient due to an underestimation of the endplate bearing capacity resulting from over-strength and additional membrane effects. Also the arrangement of the bolts is not covered by the criterion though it is a decisive parameter influencing deformability and membrane effects of the endplate as well as additional bending stresses of the bolts. A crucial finding of these tests also was that due to an increase of the endplate deformations additional membrane forces in the endplate could be activated leading to much more bearing resistance as calculated according to the component method. These membrane effects could only be activated completely if the resistance of the bolts was sufficient. Therefore the bolts have to be oversized in comparison to the design according to the component method.

Furthermore numerous component tests were performed at the University of Trento. All the components were part of the substructure joint configuration. Tests on reinforced concrete specimens investigated the deformation capacity of the concrete slab in tension. Focusing the attention on the response at the ultimate conditions, it was found that the concrete can reduce the deformation capacity of steel from a minimum of 57% to a maximum of 83%. The comparison between tests results and data available in literature suggested the need of additional studies focused on the influence on tension stiffening of the sectional geometry and of the layout of the reinforcement.

Tests on T-stubs for the substructure joint layout as well as of the steel joint tests layout were executed. Tensile tests allowed investigating different aspects such as the influence of the presence of stiffeners and of their location, of the endplate thickness and of the preload of the bolts. The experimental results confirmed the remarkable deformation capacity of specimens as a consequence of the hardening of the material and the activation of a membrane action. The “T-stub” approach proposed by the Eurocode [69] neglects such important contributions, which can be considered as a reserve of strength and deformation capacity, contributing to fulfil the ductility requirements for joints in the case of exceptional loading conditions (robust systems). Criteria aiming at the evaluation of the performance of T-stub in the large displacements field are not provided by the Eurocode, and in effect are outside its scope. This requires the definition of adequate methods enabling control of the main parameters affecting the ultimate strength and ductility of T-stubs. The studies on T-stubs were completed by a series of tests under different combination of axial and shear force. All tests showed the development of significant plastic flange deformation. Different responses were observed for the bolts and the flange depending on the ratio between the shear and axial force. Test results allowed a first appraisal of the N-V domain, which shows a non negligible interaction between axial and shear force. However, the number of tests is too limited to draw definite conclusions. At this aim, additional tests on different T-stub configuration would be necessary.

Test on complete connections were additionally performed. The tests investigated the different behaviour between the endplate T-stub connected to the column and the full steel connection fixed on rigid support or on the column. Pure tension tests were carried out on the T-stubs, while tests under tension and under two different combination of axial and shear force were performed on the connection. An initial relative angle between the beam and the actuator enabled different combinations of axial and shear force. The tests allowed an appraisal of the influence of the column deformability on the T-stub and on the connection responses. The specimens connected to the column showed a clear decrease of the bearing capacity in comparison the one on rigid support. The stiffness and the ductility are also significantly influenced. The tests under combined loading, axial and shear force, due to an initial inclination showed that the reduction of the strength for smaller angles ($< 11^\circ$) decreased moderate but for larger angles ($\geq 20^\circ$) a reduction of the strength to nearly the half strength in comparison to pure tension loading was observed.

In Chapter 5 firstly the parametrical numerical studies investigating the event “Loss of column” in a 2D multi-storey steel frame were presented. The failure simulation of a column showed that the external joints of the beams in the area above the affected column began to yield simultaneously. Plastic hinges began to develop at the edges of the beams. The loads on the most upper beams were small in comparison to the loads in the other storeys. This led to smaller deformations and to a later appearance of the initial yielding in the most upper beams. The smaller deformed most upper beams resisted the horizontal deformation of the remaining structure. Hence compression forces in the most upper beam developed. This compression forces indicate, that an “arch-effect” was going to develop. The influence of horizontal wind loads can be neglected for this structure as confirmed by various simulations of other column failures. In contrast the influence of the applied external vertical load was high. Considering this structure the reduction of vertical loads on a regular storey from full vertical loads to vertical loads according to LCC1 (including reduction factors acc. Eurocode-0) led to a reduction of the appearing deformation to one third. Under the relevant load case combinations according to Eurocode-0 the plastic hinges at the external joints of the direct affected beam just began to develop. A clear redistribution of bending moments to normal forces was not detected under Eurocode-loads at all.

The first calculations of a column failure in the ground floor of a 3-D structure indicated, that this specific structure collapsed caused by a buckling of the most upper horizontal beams. Some first simulations have confirmed that the appearance of buckling phenomena about the weak axis has to be observed in a real 3-D structure. For further 3D-calculations the positive influence of the floor slabs should be included in the model so the buckling of the upper beams could be possibly prevented.

Secondly the parametrical numerical studies were used to develop an analytical tool for the practical engineer to determine the requirements for the affected beams and joints resulting from the event “Loss of a column” at a simple “two-beam-system”. Through the performed parametrical studies, the parameters to be considered in the analytical model to predict the simplified substructure response have been identified. These parameters are the lateral restraint simulated by the horizontal spring with a stiffness “K”; the M-N interaction at the plastic hinge level (developing in the beams or in the partial-

strength joints) and the plastic elongation of the plastic hinge associated to the development of the catenary action.

On the other side, it has been demonstrated that it is not requested to take into account of the bending stiffness “ EI/L ” and the axial stiffness “ EA/L ” of the beams to predict with a good accuracy the development of the catenary actions. The objective with the analytical procedure is to predict the behaviour in the post-plastic domain, i.e. after the formation of the beam plastic mechanism in the system; accordingly, the analytical model is based on a rigid-plastic analysis.

An analytical procedure dedicated to the prediction of the behaviour of composite joints subjected to combined bending moments and axial loads has been developed and validated within the project.

Also, a simplified analytical method allowing the prediction of the development of the membrane forces and of the frame response caused by “Loss of a column” has been developed and validated through comparison to the substructure experimental test results. This simplified method is based on a rigid-plastic - second-order analysis and takes into account of the M-N interaction acting at the plastic hinge level. This analytical method is also presented separately in the design guidelines [34].

The investigations for the exceptional event “Loss of a bracing” of a typical composite car park frame pointed out that failure of a bracing in such a composite frame with semi-rigid beam-to-column connections does not directly lead to a collapse of the whole structure. This results from the fact that the car park frame with partial-strength joints and additional bracings is a highly redundant structure. The remaining stiff panel effect of the undamaged bracings in the upper storeys still provides a frame effect and in addition the moment resistance of the semi-rigid joints also creates a moment resisting frame where the resulting rotation requirements for the joints are not extremely high. Of course the joints have to provide certain ductility for redistribution of forces but in comparison with the event “Loss of a column” the required rotation capacities are considerably less. More decisive for the collapse resistance of the framed structure for the event “Loss of a bracing” is the utilization of the column profiles. So for column profiles which are relatively intensively utilized already in the state of serviceability (undamaged structure) the exceptional event “Loss of a bracing” may lead to a progressive collapse of the whole car park. The investigations also confirmed earlier results on sway-frames that showed that the inclination of the beam α decisively influences the declination of the column ψ . There it was stated that the inclination of the beam, i.e. the rotation at support of the beam, depends mainly on the utilization of the beam in span. If the beam stays in a range of $M_{\text{beam}} < 1.1 M_{\text{el,R}}$ the curvature of the composite beam has relatively small values which results in a moderate beam inclination and leads to only small column declination.

For the event “Fire” it was shown that local fire which is influencing only single members could be substituted into events like “Loss of a column” or “Loss of a bracing”, etc.. Whereas if the fire grows until reaching the flash-over the problem is no more a problem of robustness of the structure but a problem of global fire resistance of the building because all the structural elements are heated and lose their bearing properties. For these cases a real “hot” design has to be realised.

For the exceptional event “Earthquake” a lot of international codes and standards were analysed focusing on detailing design rules and aiming at ensuring a structural ductile behaviour. Some examples for steel and concrete composite structures have been illustrated. Furthermore some knowledge of seismic design was investigated concerning the transferability to robustness. Certainly, the rules provided by seismic codes may be an interesting reference

8 OUTLOOK

The aim of this research project has been to carry out extensive experimental and theoretical investigations on the behaviour of joints (beam-to-column connections) in framed steel or composite structures ensuring a redundant and robust behaviour of the structural system by occurrence of an unforeseen exceptional event. Some exceptional events have been investigated as model cases as summarized in Chapter 7.

The aim of investigations presented here is not so much that it allows already to list design criteria in general for all events and cases which may be thought of but that for a choice of events and especially for the event “Loss of a column” as a prototype an in-depth strategy has been developed and realized up to an implementable analytical method which allows for the determination of joint requirements. That now may be followed for by similar investigations on further events that are characteristic for exceptional scenarios. The concept or strategy developed with this project may thus serve as model guide and is therefore additionally prepared in a design handbook [34].

An important finding of the tests on T-stub was that the experimental results showed a remarkable deformation capacity of specimens as a consequence of the hardening of the material and the activation of a membrane action. But the “T-stub” approach proposed by the Eurocode [69] neglects such important contributions, which can be considered as a reserve of strength and deformation capacity, contributing to fulfil the ductility requirements for joints in the case of exceptional loading conditions (robust systems). Criteria aiming at the evaluation of the performance of T-stub in the large displacements field are not provided by the Eurocode, and in effect are outside its scope. This requires the definition of adequate methods enabling control of the main parameters affecting the ultimate strength and ductility of T-stubs.

Also a reconsideration of the existing ductility criterion according the EN 1993-1-8 [69] seems to be necessary because over-strength effects as well as membrane effects are not yet considered.

An open question is furthermore the influence on tension stiffening of the sectional geometry and of the layout of the reinforcement. The comparison between tests results and data available in literature suggests the need of additional studies because of the variation of the available results.

The numerical simulations showed the difficulty to model the actual behaviour of structural joints subjected to bending moments and axial loads with the available elements in the existing FE softwares. To be able to simulate the behaviour of these joints in a more efficient and accurate way the development of a new FE - element for future activities is necessary.

The research activities in the field of robustness are just at the very beginning, in Europe this research project was one of the first on this topic and could prepare first basics concerning requirements for ductile joints. To be able to define more general requirements, as well as detailing design rules leading to a simplified indirect design method, a continuation and extension of the research work on this topic is necessary in future.

First ideas about a continuation and extension of the research work by a future European research project have been developed. Based on the concept applied in this project and on the results achieved further structures and scenarios have to be investigated. They may finally lead to the definition of a robustness index for any structure which allows the owner to decide on the level of safety and redundancy he wants to apply. The results of this project form the basis to quantify this level and serves as precondition of such an innovative future approach.

TECHNICAL ANNEX A



EUROPEAN COMMISSION
RESEARCH DIRECTORATE-GENERAL

Directorate G – Industrial Technologies
Research Fund for Coal and Steel

WORK PACKAGE DESCRIPTION		WP No	1
Work package Title	Systematic analysis of existing data	Number of man hours²⁹	
WP Leader	5 (Trento)		420
Contractor (s)	1 (Stuttgart)		390
	2 ()		280
	3 (Luxembourg)		160
	4 (Aachen)		140
Total			1.390
1 – Objectives <ul style="list-style-type: none"> • provide overview over existing data concerning the behaviour of structural elements • detect missing data • define conditions for ductile performance 			
2 - Work programme and distribution of tasks with indication of participating contractors <p>Collection and systematic review of existing experimental and analytical force-deformation curves of beams and joints, especially related to ultimate strength and available ductility. The existing data provides information how to construct robust structures and ductile joints. Missing data are detected.</p> <p>All partners contribute to this review in order to profit from the specific knowledge of each partner and to provide each other with the whole existing background information. Partner 5 (Trento) is the leader due to the wide and long continuous research experience being already involved in COST C1 action with particular reference to the behaviour of steel and composite joints from the beginning.</p>			
3 - Interrelation with other work packages (please give WP No) 2, 3, 4, 5, 6, 7 <p>WP1 provides input data for the idealisation of the joints in WP3 and WP6 and on the requirements WP2. The elaboration of the design criteria (WP7) can profit from the already existing knowledge (WP1). Missing knowledge that herewith (WP1) is detected will be gained by testing (WP4).</p>			
4 – Deliverables and milestones <ul style="list-style-type: none"> • data base for the idealisation of the joints in WP3 and WP6 • detection of missing knowledge which has to be gained by testing (WP4) • conditions of ductile behaviour 			



EUROPEAN COMMISSION
RESEARCH DIRECTORATE-GENERAL
Directorate G – Industrial Technologies
Research Fund for Coal and Steel

WORK PACKAGE DESCRIPTION		WP No	2
Work package Title	Requirements	Number of man hours ²⁹	
WP Leader	2 (Liège)	750	
Contractor (s)	1 (Stuttgart)	130	
	3 (Luxembourg)	160	
	4 (Aachen)	420	
	5 (Trento)	272	
Total		1.732	
1 – Objectives			
<ul style="list-style-type: none">determ several accidental impactsidentify different failure modesclassify the requirements for robust structures			
2 - Work programme and distribution of tasks with indication of participating contractors			
<p>The circumstances are summarised under which a collapse of structures occurs. The various accidental impacts are determined. Different failure modes of subsystems (e. g. failure of a column, failure of a beam) are identified and the appropriate requirements are specified. A classification of the requirements for small and severe accidents is conducted. Based on WP 1 and the few existing standards (e. g. BS5950 in U.K) dealing with robustness requirements for robustness are identified.</p> <p>All partners contribute according to their specific knowledge. Main partners are Liège, Aachen and Trento.</p> <p>The partner from Liège has a wide experience, so for example Liège University is chairing the 3-years COST C12 action (involving more than 20 European countries) in which problems of exceptional loading, progressive collapse and robustness are extensively considered ; thus, Liège has been selected as leader of this work package.</p> <p>Aachen has been deeply involved in drafting of the recent new Eurocodes including Basis of Design (EN 1990) which provide general requirements, rules for loading (EN 1991) and applications (e.g. EN 1993 for steel structures). As the Eurocodes are describing the requirement concerning robustness only in a general way (so-called principles) it is essential to establish more detailed rules (so-called application rules) which can be used as a basis for the work of the other WP's. As an outcome of the project such application rules can be of significant help for practitioners.</p> <p>Trento has specific experience concerning structures under earthquake loading and thus gives an important input to this WP.</p>			



EUROPEAN COMMISSION
RESEARCH DIRECTORATE-GENERAL
Directorate G – Industrial Technologies
Research Fund for Coal and Steel

3 - Interrelation with other work packages (please give WP No) 1, 3, 4, 6, 7

The requirements are based on the knowledge of WP1 and define the impact for the system calculation (WP3 and WP6). The ductility requirements affect the design of the tested joints (WP4) and the final development of the design criteria (WP7).

4 – Deliverables and milestones

- classification of failure modes
- identification of the requirements concerning robustness



EUROPEAN COMMISSION
RESEARCH DIRECTORATE-GENERAL
Directorate G – Industrial Technologies
Research Fund for Coal and Steel

WORK PACKAGE DESCRIPTION		WP No	3
Work package Title	System calculation on a simplified level	Number of man hours ²⁹	
WP Leader	1 (Stuttgart)	1.680	
Contractor (s)	2 (Liège)	600	
	4 (Aachen)	420	
	5 (Trento)	420	
Total		3.120	
1 – Objectives			
<ul style="list-style-type: none">• determine the robustness requirements in specific cases• obtain the requirements concerning the ductility of the joints• derive influencing variables and their significance• optimise the structure to behave robust			
2 - Work programme and distribution of tasks with indication of participating contractors			
<p>Typical structures (e. g. office buildings, industrial buildings, parking-lots) with different kind of joints and members (steel / composite) subjected to different failures of subsystems (e. g. Figure 3) are calculated on a simplified level by plastic analysis to obtain the deformations, moments and tying forces in the structural elements, especially within the joints. The failure of a column or of a beam are regarded independent of the cause for the failure (vehicle impact, explosion, fire, earthquake, ...). The behaviour (resistance and stiffness) of the steel joints (Figure 2) is calculated according to e. g. prEN 1993-1-8 , the behaviour of the composite joints according to prEN 1994-1 or the total joint behaviour is estimated from the few known tests, see WP1. Different types and configurations of joints and members are applied and the resulting behaviour of the structure is monitored. The internal forces and deformations in the joint are calculated. Configurations leading to robust structures without global collapse are identified and optimised. Depending on the kind of failure the inherent ductile deformations in the joints are gained that are required by the system.</p> <p>The system calculation is shared among the partners from Stuttgart, Liège, Aachen and Trento. Stuttgart is the leader of the work package due to the experience in plastic calculation of structural systems with high ductile joints and due to the know-how in the optimisation of the ductile joint behaviour.</p> <p>Liège and Aachen have also great experience in structural analysis (computer software Finelg and Dynax) and in the characterisation of joint properties; they are deeply involved in the drafting of prEN 1993 Part 1-1. As far as the design of joints is concerned, they are the main drafters of the component method proposed in the relevant codes such as ENV 1993-1-1 and ECCS Doc. 109, prEN 1993-1-8 and the developer of the computer software COP based on this method.</p>			



EUROPEAN COMMISSION
RESEARCH DIRECTORATE-GENERAL
Directorate G – Industrial Technologies
Research Fund for Coal and Steel

3 - Interrelation with other work packages (please give WP No) 1, 2, 4, 6, 7

The idealisation of the joints is based on the knowledge of WP1, the impact is drawn from WP2. The simplified model (WP3) will be modified and extended to a sophisticated model (WP6). The design criteria (WP7) are partly drawn from the calculation with the simplified model. The dimensioning of the tests (WP4) is based on the calculation results of WP3 in order to ensure a sufficient ductile performance.

4 – Deliverables and milestones

- model of the structural system including the simulation of the joint behaviour
- quantification of the required deformations and the required bearing capacities of the joints to obtain robust structures

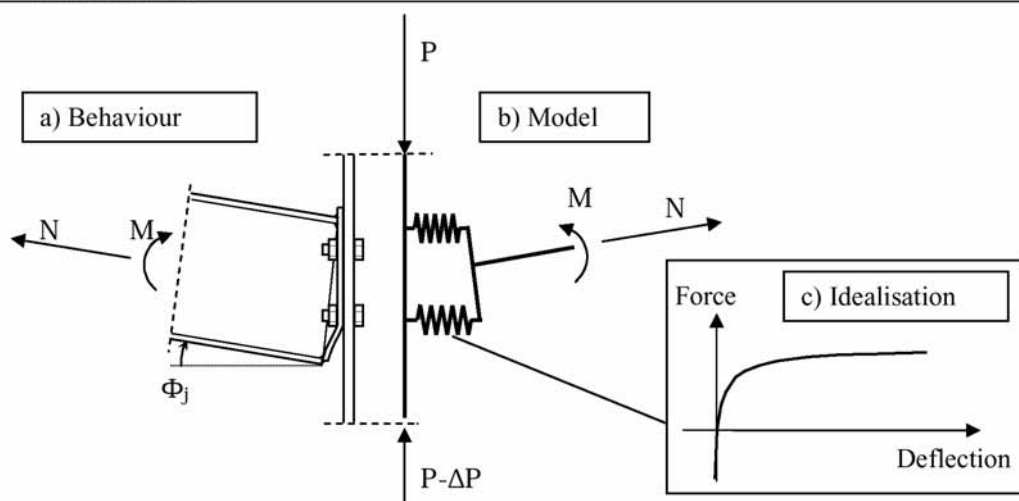


Figure 2: Modelisation of the joint detail

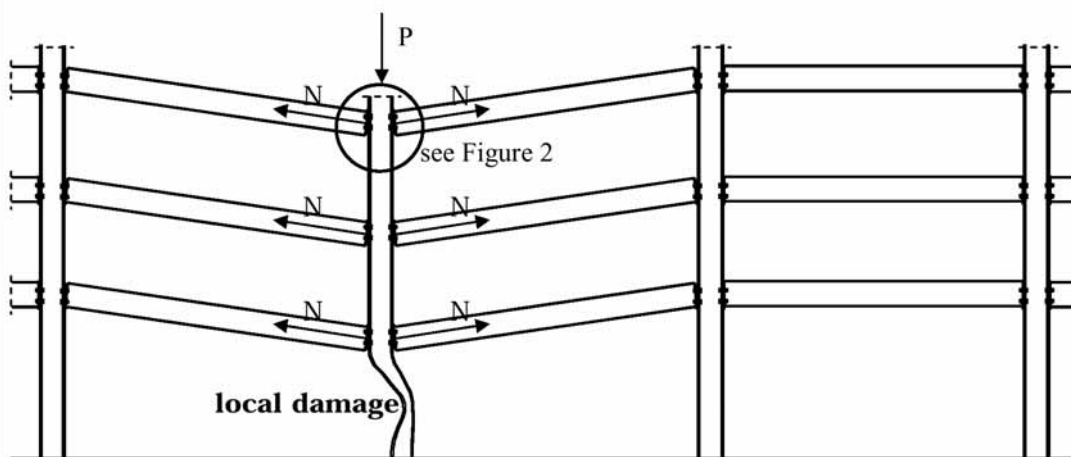


Figure 3: Robust behaviour of the global structure, affected by local accidental failure



EUROPEAN COMMISSION
RESEARCH DIRECTORATE-GENERAL
Directorate G – Industrial Technologies
Research Fund for Coal and Steel

WORK PACKAGE DESCRIPTION		WP No	4
Work package Title	Experimental work	Number of man hours ²⁹	
WP Leader	1 (Stuttgart)	1.810	
Contractor (s)	2 (Liège)	1.200	
	3 (Luxembourg)	160	
	5 (Trento)	1.120	
Total		4.290	
1 – Objectives			
<ul style="list-style-type: none">• observe behaviour of ductile joints (Figure 4a+b) under extreme deformations• monitor the component behaviour (Fig 4c) under extreme deformations• substructure tests (Fig. 4d) with ductile joints to prove its robustness• substructure tests (Fig. 4d) to derive the required ductile deformation.			
2 - Work programme and distribution of tasks with indication of participating contractors			
<p>Experimental studies are performed on selected steel and composite joint solutions that are supposed to be very commonly used due to economical reasons and that are expected, according to WP 3, to be suitable for robust structures. The tests are divided into component tests Figure 4c (Trento) and joint tests Figure 4a and 4b (Stuttgart) and tests on substructures Figure 4d (Liège). The behaviour of the whole joint can be derived by monitoring the behaviour of the single components, compare Figure 2, 4a 4b with Figure 4c. The variation of the components’ geometry leads to numerous different joint solutions. An optimisation of the components’ geometry concerning ductility is conducted. The tests on whole steel and composite joints with optimised components prove the ductile behaviour and quantifies the available ductile deformation inherent in the joint. The specimen are not only subjected to moments (Figure 4b) but also to normal forces (Figure 4a) as there is missing knowledge from joint tests with tying forces. The joint configurations and load parameters are based on the calculations of WP 3. In addition the behaviour of the joints under extreme deformations is monitored and special attention is turned on avoiding brittle failure of the bolts by intelligent design. Two tests on substructures (see Figure 4d) show how the force redistribution develops in the substructure when the failure of one column occurs.</p> <p>The partners Liège, Stuttgart and Trento are experienced in joint testing, Trento has also expert knowledge concerning component tests. So the tests are shared among the partners Stuttgart (joint tests), Liège (substructure tests) and Trento (component tests). The material for the specimens is provided by the industrial partner from Luxembourg.</p>			



EUROPEAN COMMISSION
RESEARCH DIRECTORATE-GENERAL
Directorate G – Industrial Technologies
Research Fund for Coal and Steel

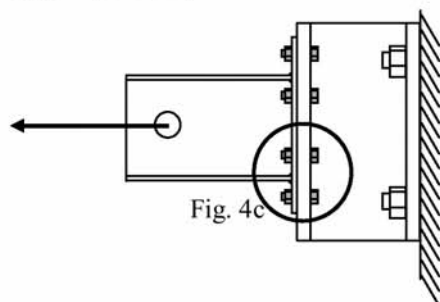
3 - Interrelation with other work packages (please give WP No) 1, 2, 3, 5, 6

The tests cover insufficient knowledge which was detected in WP1. The requirements concerning strength and deformability of the joints are drawn from WP2 and the system calculations WP3. The test results will be later evaluated in WP5 and thus serve as a basis for the idealisation of the joints in the sophisticated calculation model (WP6).

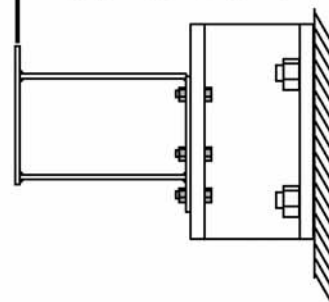
4 – Deliverables and milestones

- tension force-deflection curves and deformability (test Fig. 4a)
- moment-rotation curves and rotational capacity (test Fig. 4b)
- force-deflection curves and deformability (test Fig. 4c)
- required deformations (test Fig 4d)
- prove of robustness (test Fig 4d)

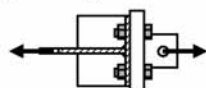
a) joint (tension)



b) joint (bending moment)



c) component (tension)



d) substructure

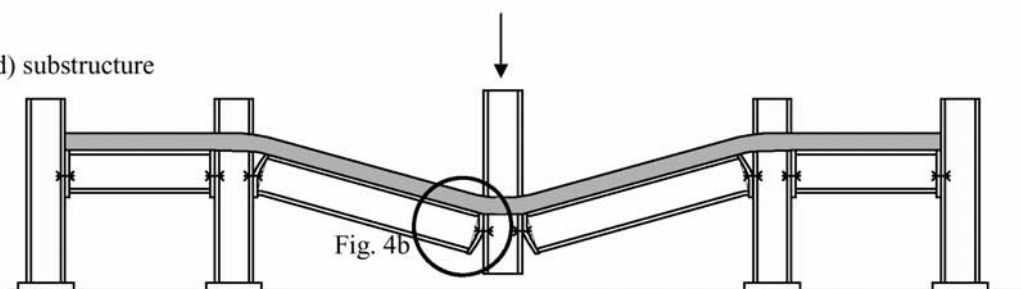


Figure 4: Tests



EUROPEAN COMMISSION
RESEARCH DIRECTORATE-GENERAL
Directorate G – Industrial Technologies
Research Fund for Coal and Steel

WORK PACKAGE DESCRIPTION		WP No	5
Work package Title	Test assessment	Number of man hours ²⁹	
WP Leader	1 (Stuttgart)	780	
Contractor (s)	2 (Liège)	570	
	3 (Luxembourg)	310	
	4 (Aachen)	140	
	5 (Trento)	420	
Total		2.220	
1 – Objectives			
<ul style="list-style-type: none">• analyse the tests• derive the calculation formulae for ultimate strength and deformability of the joints• check if the isolated joint behaves identical to the joints of the substructure• detect the influencing geometric variables (e. g. end plate thickness) on the deformability			
2 - Work programme and distribution of tasks with indication of participating contractors			
<p>The results of the tests are the characteristics (e. g. Figure 2c) of the individual components and the whole M-Φ and/or F-w curves of the entire joint which will be needed for the system calculation on the sophisticated level (WP6). Calculation formulae are derived to calculate the ultimate strength and the ductile deformation of the structural elements. The obtained behaviour of the component tests is integrated in the component model which is verified by the joints tests. Variations of further joint configurations are analysed and the ductility of the joint is optimised (see WP6). The influencing parameters for the ductility of the joint are thus obtained and quantified. The required ductility of the joint is gained by the substructure tests.</p> <p>The test assessment is mainly done by the respective partner Stuttgart Liège and Trento who carried out the tests, see WP4. So Stuttgart is again WP leader. The partners Aachen and Luxembourg are involved in the further processing of the results and therefore contribute to a minor degree.</p>			
3 - Interrelation with other work packages (please give WP No) 1, 4, 6, 7			
<p>The test results gained in WP4 are evaluated on behalf of the knowledge of (WP1) and serve as a basis for the idealisation of the joints in the sophisticated model (WP6). The optimised joints are applied in the system calculations (WP6). The investigated influencing parameters (WP5) for the joints’ ductility give indications for the design criteria (WP7).</p>			
4 – Deliverables and milestones			
<ul style="list-style-type: none">• integration of the component curves in the component model• calculation formulae for ultimate strength and deformability of the joints• influencing parameters on the deformability of the components and of the joints			



EUROPEAN COMMISSION
RESEARCH DIRECTORATE-GENERAL
Directorate G – Industrial Technologies
Research Fund for Coal and Steel

WORK PACKAGE DESCRIPTION		WP No	6
Work package Title	System calculation on a sophisticated level	Number of man hours ²⁹	
WP Leader	4 (Aachen)	1.260	
Contractor (s)	1 (Stuttgart)	1.160	
	2 (Liège)	865	
	5 (Trento)	140	
Total		3.425	
1 – Objectives			
<ul style="list-style-type: none">analyse structural systems more precisely especially concerning robustnessdetect the influencing parameters for robust behaviouroptimise the joint configuration to obtain robust structures			
2 - Work programme and distribution of tasks with indication of participating contractors			
<p>The frame systems are recalculated with ductile structural elements in comparison to normal structures analogous to WP3 but on a sophisticated level including possible second order effects of the frame with the non-linear characteristics of the joints gained in the experimental and numerical studies (WP4 and WP5). The effects of variations of the geometry of the joints on the global behaviour of the structure is analysed and demonstrated. The ductile deformation that is required by the system calculation is compared with the available ductile deformation of the joint gained by the test results (WP4 and WP5).</p> <p>Similar studies have already been successfully performed in Aachen, Stuttgart and Liège to demonstrate the influence of the stiffness and strength of the joint on the global behaviour of the structure. These studies were used as background documentation for the recent generation of the Eurocodes on steel and composite structures mainly drafted by Aachen. Hence, the new studies carried out within this WP will complete the knowledge by studying the influence of the ductility. Main parameters for the studies are different types of frames in combination with different types of joints.</p> <p>Main partners of WP6 are Aachen, Stuttgart and Liège, sharing the work in a similar way as the simplified system calculations (WP3). The partner from Aachen coordinates the WP due to the experience in code writing. Trento contributes to a minor degree.</p>			
3 - Interrelation with other work packages (please give WP No) 1, 2, 3, 4, 5, 7			
<p>The idealisation of the joints is based on the knowledge of WP1, on the test results (WP4) and its evaluation (WP5). The system calculation is derived by modifications from the simplified model (WP3), the impact is gained from WP2. The calculation results are the main input for the design criteria (WP7).</p>			
4 – Deliverables and milestones			
<ul style="list-style-type: none">model of the structural system including the sophisticated simulation of the joint behaviourinfluencing parameters for robust behaviourquantification of various influences on the performance of the system			



EUROPEAN COMMISSION
RESEARCH DIRECTORATE-GENERAL
Directorate G – Industrial Technologies
Research Fund for Coal and Steel

WORK PACKAGE DESCRIPTION		WP No	7
Work package Title	Design criteria	Number of man hours ²⁹	
WP Leader	3 (Luxembourg)	1.082	
Contractor (s)	1 (Stuttgart)	518	
	2 (Liège)	300	
	4 (Aachen)	280	
	5 (Trento)	420	
Total		2.600	
1 – Objectives <ul style="list-style-type: none">• develop design criteria for robust structures• transmit the knowlegde by graphic means• generate handbook for robust design			
2 - Work programme and distribution of tasks with indication of participating contractors <p>Development of simplified design criteria based on WP1 to WP6 to allow the designer to satisfy, in practical situations, the general requirement for robustness expressed in Eurocode 3. The construction criteria are presented in a handbook including technical drawings of ductile joints that are easy for fabrication and erection. Illustrated by these drawings no sophisticated calculations are needed but simple intelligent design, that ensures the easy practical realisation by the designer. Additional pictures of the tests with ductile joints under extreme deformation demonstrate the results of robust design and visually educate the designers mind memorising the important effects of his work on the structural behaviour and structural safety.</p> <p>WP7 is based on the work results of all partners so that each partner is involved in this WP. The partner from Luxembourg is the project leader as he is in close contact to the applicants of steel products and thus is familiar also to the practical and economical requirements. So for the design criteria not only robustness requirements are considered but at the same time practical and economical aspects are taken into account.</p>			
3 - Interrelation with other work packages (please give WP No) 1, 2, 3, 5, 6 <p>The design criteria are gained from the existing knowledge of WP1, the requirements (WP2), the system calculations (WP3 and WP6) and from the assessment of the test results (WP5) in which the ductility of the joints as well as for the substructure has been proved.</p>			
4 – Deliverables and milestones <ul style="list-style-type: none">• design criteria for robust design• handbook for designer• illustrated examples for robust design			